Characterisation of host determinants that influence host-pathogen interaction during infection with *Mycobacterium tuberculosis*

Kaj Maximiliane Kreutzfeldt

A thesis submitted in partial fulfilment of the requirements of the University of Brighton and the University of Sussex for the degree of Doctor of Philosophy

March 2015

Declaration

I declare that the research contained in this thesis, unless otherwise formally indicated within the text, is the original work of the author. The thesis has not been previously submitted to these or any other university for a degree, and does not incorporate any material already submitted for a degree.

_____

Kaj M. Kreutzfeldt

Date:

Abstract

Tuberculosis is endemic in the Gambian population, in which the magnitude of mycobacterial antigen-driven interferon-γ (IFN-γ) response in BCG vaccinated neonates has been linked to regions on the genome that encode the RIP2 kinase, the toll-like receptor 4 adapter protein MD-2 and the NF-κB subunit NF-κB2 by genome-wide linkage analysis.

The receptor interacting protein (RIP2) is an essential kinase downstream of the nucleotide-binding oligomerization domain-containing protein 1 (NOD1) and NOD2, both intracellular pattern-recognition receptors for peptidoglycan moieties that induce activation of NF-κB. To establish the significance of RIP2 kinase during *Mycobacterium tuberculosis* infection, RIP2 was depleted in THP-1-derived macrophages using small interfering RNAs. In the absence of RIP2, THP-1-derived macrophages secreted significantly reduced levels of the pro-inflammatory cytokine IL-1β upon infection with *M. tuberculosis*.

Two missense variations were identified within the kinase domain of *RIPK2* by sequencing 30 DNA samples from a Gambian cohort. Both polymorphisms were predicted to affect protein function. To establish whether these polymorphisms had an impact on RIP2 kinase activity, which may affect downstream signalling, the RIP2 variants were affinity purified and kinase activity measured using an *in vitro* kinase assay. This demonstrated that kinase activity of both RIP2 variants was significantly reduced compared to wild type RIP2. To determine if this reduced kinase activity affected NOD-dependent NF-κB activation, the RIP2 variants were expressed in HEK293 cells depleted of endogenous RIP2. NF-κB activation was measured using an NF-κB reporter assay. Despite the reduced kinase activity the ability of the RIP2 variants to activate NF-κB was unaffected suggesting that RIP2 kinase activity is not required for activation of NF-κB or can be significantly reduced without an impact on NF-κB activation. Loss of RIP2 reduces secretion of IL-1β during *M. tuberculosis* infection. However, despite reduced kinase activity, these RIP2 variants identified in the Gambian population are unlikely to affect NF-κB activation and subsequent immune response to tuberculosis.

Contents

Declaration……. 2
Abstract……. 3
Contents…… 4
Index…….. 5
Index of Figures…… 12
Index of Tables…….. 15
Abbreviations……. 16
Acknowledgements…….. 20

1. Introduction…… 22
2. Material and Methods…… 74
3. Polymorphisms identified in the genes *RIPK2*, *LY96* and *NFKB2* by sequencing DNA samples of Gambian origin……. 100
4. Significance of RIP2 during *M. tuberculosis* infection……. 126
5. Kinase activity of RIP2 variants……. 144
6. Effects of RIP2 variants on downstream signaling of NOD2 …… 170
7. Summary and future work……... 196

References……. 199
Appendix…… 230

Index

Index of Figures **12**

Index of Tables **15**

Abbreviations **16**

Acknowledgments **20**

1. Introduction 22

1.1. Tuberculosis **22**

1.2. *Mycobacterium tuberculosis* **23**

1.3. The immune response to tuberculosis **26**

1.3.1. Innate immune response to tuberculosis **27**

1.3.2. Adaptive immune response to tuberculosis **32**

1.3.2.1. $CD4^+$ T-lymphocytes **32**

1.3.2.2. $CD8^+$ T-lymphocytes **33**

1.3.2.3. γδ T-lymphocytes **34**

1.3.2.4. B-lymphocytes **34**

1.4. Host genetic determinants of susceptibility to *M. tuberculosis* infection **36**

1.4.1. Candidate gene studies **37**

1.4.2. Genome-wide linkage analysis **39**

1.4.3. Genome-wide association studies **40**

1.4.4. Mendelian susceptibility to mycobacterial disease (MSMD) **44**

1.5. Surrogate markers for tuberculosis susceptibility **45**

1.5.1. Cytokine responses as surrogate markers for susceptibility to tuberculosis **46**

1.5.2. Tuberculin skin test reactivity as surrogate marker for susceptibility to tuberculosis **51**

1.5.3. Antigen-specific lymphocyte proliferation as a surrogate marker for susceptibility to tuberculosis **53**

1.6. Genes linked to magnitude of mycobacterial antigen-driven IFN-γ responses of BCG vaccinated newborns 54

1.6.1. Proteins associated with pattern recognition receptors **54**

1.6.1.1. RIP2 ..... **55**

1.6.1.2. RIP2 kinase activity **55**

1.6.1.3. RIP2 kinase activity and RIP2 protein expression **56**

1.6.1.4. RIP2 kinase activity in downstream signalling **58**

1.6.1.5. RIP2 and RIP2 kinase activity in NOD-dependent autophagy **59**

1.6.1.6. RIP2 in the immune response to tuberculosis **59**

1.6.1.7. MD-2 ..... **61**

1.6.1.8. MD-2 during immune response to *M. tuberculosis* **62**

1.6.2. Proteins involved in the regulation of NF-κB activation and the transcription factor NF-κB2 ..... **64**

1.6.2.1. IKK-α, β-TrCP and NF-κB2 (p100/p52) **65**

1.6.2.2. IKK-α, β-TrCP and NF-κB2 in the immune response to tuberculosis **67**

1.6.3. Polymorphisms identified in candidate genes **70**

1.7. Concluding remark 71

1.8. Background and hypothesis 72

1.9. Aims 73

2. Materials and Methods 74

2.1. Common buffers, media and gels 74

2.2. Polymerase chain reaction (PCR) 75

2.3. Agarose gel electrophoresis 79

2.4. SDS-Polyacrylamide gel electrophoresis (SDS-PAGE) 79

2.5. Western blot analysis 79

2.6 Coomassie Stain 80

2.7. Quantification of total protein 80

2.8. Statistical analysis 80

2.9. Study populations 82

2.10. DNA sequencing and sequence analysis 82

2.11. Genotyping 82

2.12. IFN-γ response of BCG vaccinated newborns 83

2.13. Cloning of wild type and variant *RIPK2* 84

2.13.1. Cloning strategy **84**

2.13.2. *E. coli* strain and culture conditions **84**

2.13.3. Transformation of *E. coli* **86**

2.13.4. Extraction of plasmid DNA **86**

2.13.5. DNA extraction **86**

2.13.6. Restriction digestion and ligation **86**

2.13.7. Site directed mutagenesis **87**

2.13.8. Sequencing of DNA constructs **87**

2.14. Cell lines and culture conditions 88

2.15. Transient transfection of cell lines 88

2.15.1. Transfection using chemical reagents **91**

2.15.2. Transfection by electroporation **91**

2.16. Fluorescence microscopy 91

2.17. Luciferase assays 91

2.18. Gene silencing in cell lines 92

2.18.1. Gene silencing in HEK-Blue™ hNOD2 cells **92**

2.18.2. Gene silencing in THP-1 cells **93**

2.19. Cell viability assays 93

2.20. Stimulation of NOD pathways 94

2.21. Quanti Blue™ assay 94

2.22. Protein purification 94

2.22.1. Affinity purification of RIP2 by immobilised metal chelate chromatography **95**

2.22.2. Affinity purification by immunoprecipitation **95**

2.22.3. Affinity purification using immobilized anti-V5 antibody **96**

2.22.4. Buffer exchange and concentration **96**

2.22.5. Quantification of purified RIP2 ..... **96**

2.23. Kinase assay 97

2.24. *M. tuberculosis* strains and culture conditions 97

2.25. Infection of THP-1 cells with *M. tuberculosis* 97

2.26. Enzyme-linked immunosorbent assay (ELISA) 98

2.27. *M. tuberculosis* viable counting 99

3 Polymorphisms identified in the genes *RIPK2*, *LY96* and *NFKB2* by sequencing DNA samples of Gambian origin 100

3.1. Introduction 100

3.2. Results 103

3.2.1. Polymorphisms identified among *RIPK2*, *LY96* and *NFKB2* **103**

3.2.2. Polymorphisms in *RIPK2* **103**

3.2.3. Polymorphisms in *LY96* **105**

3.2.4. Polymorphisms in *NFKB2* **107**

3.2.5. Distribution of alleles and genotypes in the Gambian population **107**

3.2.6. Comparison of IFN-γ responses by genotype **112**

3.3. Discussion 118

3.3.1. Polymorphisms identified among *RIPK2*, *LY96* and *NFKB2* **118**

3.3.2. Distribution of alleles and genotypes in the Gambian population **121**

3.3.3. Comparison of IFN-γ responses of different genotypes **123**

3.3.4 Selection of polymorphisms for further study..... **124**

4 Significance of RIP2 during *M. tuberculosis* infection **126**

4.1 Introduction **126**

4.2 Results **128**

4.2.1 Infection of THP-1 cells with *M. tuberculosis* H37Rv **128**

4.2.2 Knock down of RIP2 ..... **129**

4.2.3 Survival of electroporated THP-1 cells **129**

4.2.4 Absence of RIP2 does not affect *M. tuberculosis* or macrophage survival during infection..... **134**

4.2.5 RIP2 regulates induction of IL-1β during infection with *M. tuberculosis* **134**

4.3 Discussion **137**

4.3.1 Absence of RIP2 does not affect *M. tuberculosis* or macrophage survival during infection..... **138**

4.3.2 RIP2 regulates induction of IL-1β but not TNF or type I interferons during infection with *M. tuberculosis* **139**

4.3.3 Significance of IL-1β during *M. tuberculosis* infection..... **141**

4.3.4 Effect of electroporation on cytokine responses **142**

5. Kinase activity of RIP2 variants **144**

5.1. Introduction **144**

5.2. Results **146**

5.2.1. Expression of recombinant RIP2 ..... **146**

5.2.2. Affinity purification of RIP2 with C-terminal HIS-tag **146**

5.2.3. Affinity purification of C-terminally V5-tagged RIP2 by immunoprecipitation **146**

5.2.4. Affinity purification using anti-V5 agarose and 0.2M glycine **149**

5.2.5. Kinase activity of purified RIP2 ..... **152**

5.2.6. Affinity purification using anti-V5 agarose and V5-peptide **156**

5.2.7. Affinity purification of N-terminally HIS-tagged RIP2 ..... **156**

5.2.8. Generation and purification of RIP2 kinase variants **158**

5.2.9. Effect of variants RIP2 I259T and RIP2 L268V on kinase activity of RIP2 compared to wild type **158**

5.3. Discussion **165**

5.3.1. Expression and purification of RIP2 ..... **165**

5.3.2. RIP2 variants display reduced kinase activity **167**

6. Effects of RIP2 variants on downstream signalling of NOD2 ..... **170**

6.1. Introduction **170**

6.2. Results **172**

6.2.1. Stimulation of NOD2 signalling pathways in THP-1 Blue™ cells **172**

6.2.2. Transient transfection of THP-1 cells **172**

6.2.3. Nucleofection of THP-1 cells **175**

6.2.4. Stimulation of HEK-Blue™ hNOD2 cells with MDP **178**

6.2.5. Expression of RIP2 in HEK-Blue™ hNOD2 cells **178**

6.2.6. Stability of RIP2 variants **180**

6.2.7. Depletion of endogenous RIP2 in HEK-Blue™ hNOD2 cells **180**

6.2.8. Transfection with wild type and variant recombinant RIP2 restores NOD2-mediated NF-κB/AP-1 SEAP reporter activation in RIP2-depleted cells **185**

6.3. Discussion **189**

6.3.1. Stimulation of NOD2 signalling pathways in THP-1 Blue™ cells **189**

6.3.2. Transient transfection of THP-1 cells **190**

6.3.3. Study of RIP2 variants in HEK-Blue™ hNOD2 cells **192**

6.3.4. Kinase deficient RIP2 variants do not affect NOD-dependent activation of SEAP reporter **193**

7. Summary and future work 196

8. References **199**

9. Appendix **230**

9.1. Plasmid maps **230**

9.2. Polymorphisms identified in *RIPK2, LY96* and *NFKB2* **242**

Index of Figures

1. Introduction

1.1 Schematic representation of the mycobacterial cell wall……..... 25

1.2 RIP2 and the NOD signalling pathways……... 57

1.3 MD-2 and the TLR4 signalling pathway……..... 63

1.4 IKK-α, β-TrCP and NF-κB2 (p100/p52) as part of the canonical and non-canonical NF-κB signalling pathways……..... 69

3. Polymorphisms identified in the genes *RIPK2*, *LY96* and *NFKB2* by sequencing DNA samples of Gambian origin

3.1 Schematic representation of polymorphisms identified in *RIPK2*/RIP2…… 104

3.2 Schematic representation of polymorphisms identified in *LY96*… 106

3.3 Schematic representation of polymorphisms identified in *NFKB2*.. 108

3.4 Distribution of alleles in the Gambian population…… 110

3.5 Distribution of genotypes in the Gambian population…… 111

3.6 IFN-γ responses of PPD stimulated PBMCs from BCG-vaccinated newborns genotyped for six polymorphisms……... 113

3.7 IFN-γ responses of PPD stimulated whole blood from BCG-vaccinated newborns genotyped for six polymorphisms ……. 115

3.8 IFN-γ responses of killed *M. tuberculosis* stimulated PBMCs from BCG-vaccinated newborns genotyped for six polymorphisms……. 116

3.9 IFN-γ responses of killed *M. tuberculosis* stimulated whole blood from BCG-vaccinated newborns genotyped for six polymorphisms…….. 117

4. Significance of RIP2 during *M. tuberculosis* infection

4.1 Infection of THP-1 cells with *M. tuberculosis* decreases macrophage viability……. 130

4.2 *M. tuberculosis* infected THP-1 cells secrete IL-1β, TNF and IP-10 131

4.3 Gene knock-down of *RIPK2* in THP-1 cells…… 132

4.4 Gene knock-down of *RIPK2* does not result in significant cell death…….. 133

4.5 RIP2-deficiency has no effect on the viability of *M. tuberculosis* or macrophages…… 135
4.6 *RIPK2* gene knock-down results in decreased secretion of IL-1β but not TNF and IP-10 from *M. tuberculosis* infected THP-1-derived macrophages……..... 136

5. Kinase activity of RIP2 variants
5.1 Expression of recombinant RIP2 in HEK293T …… 147
5.2 Recombinant RIP2 cannot be purified via a C-terminal HIS-tag…. 148
5.3 Recombinant RIP2 cannot be purified by immunoprecipitation … 150
5.4 Recombinant RIP2 cannot be affinity purified using anti-v5 agarose……. 151
5.5 Recombinant RIP2 can be purified by affinity chromatography using anti- V5 agarose in a two-step process…….. 153
5.6 Quantification of recombinant RIP2 purified using anti-V5 agarose 154
5.7 Recombinant RIP2 purified using anti-V5 agarose is not kinase active…… 155
5.8 Recombinant RIP2 cannot be released from anti-V5 agarose competition with a V5-peptide……... 157
5.9 Recombinant RIP2 can be purified using metal chelate chromatography via an N-terminal HIS-tag…….. 159
5.10 Recombinant RIP2 I259T can be purified using metal chelate chromatography via an N-terminal HIS-tag……... 160
5.11 Recombinant RIP2 L268V can be purified using metal chelate chromatography via an N-terminal HIS-tag……... 161
5.12 Relative quantification of wild type and variant RIP2 recombinant protein …….. 162
5.13 RIP2 variants have reduced kinase activity…… 163

6. Effects of RIP2 variants on downstream signalling of NOD2
6.1 THP-1 cells respond synergistically to co-stimulation with MDP and LPS…… 173

6.2 THP-1 cells cannot be effectively transfected with plasmid DNA by chemical transfection…… 174
6.3 THP-1 cells cannot efficiently be transfected with plasmid DNA by chemical transfection and do not respond to R-848 stimulation after transfection…… 176
6.4 THP-1 cells cannot be transfected with plasmid DNA by electroporation…… 177
6.5 HEK-Blue™ hNOD2 cells respond in a dose-dependent manner to stimulation with MDP…… 179
6.6 Recombinant RIP2 and endogenous RIP2 are expressed equally in HEK cells…….. 181
6.7 Recombinant wild type and variant RIP2 are expressed at equal levels in HEK cells…….. 182
6.8 Endogenously expressed RIP2 is significantly knocked down 48h/72h after transfection of HEK-Blue™ hNOD2 cells with *RIPK2* siRNA…… 183
6.9 Depletion of RIP2 in HEK-Blue™ hNOD2 cells results in reduced response to MDP…… 184
6.10 Overview of experimental protocol for determination of effect of RIP2 variants in HEK-Blue™ hNOD2 cells …… 187
6.11 Recombinant wild type and variant RIP2 restores NOD2-dependent NF- κB/AP-1 SEAP reporter activation in RIP2 depleted HEK-Blue™ hNOD2 cells…….. 188

9. Appendix

9.1 Schematic representation of pcDNA™6/V5-HIS B…… 230
9.2 Schematic representation of pcDNA6_*RIPK2*wt_V5/HIS……. 231
9.3 Schematic representation of pcDNA6_HIS*RIPK2*wt……. 232
9.4 Schematic representation ofpcDNA6_HIS_*RIPK2*wt…… 233
9.5 Schematic representation of pRL-CMV…….. 234
9.6 Schematic representation of pMAX-GFP …….. 235

Index of Tables

1. Introduction

1.1 Genome-wide and candidate gene linkage analysis investigating tuberculosis…… 42

1.2 Genome-wide association studies investigating tuberculosis… 43

1.3 Genome-wide linkage analysis investigating surrogate markers for tuberculosis…….. 47

2. Materials and Methods

2.1 Commonly used buffers…… 74

2.2 Commonly used media……. 75

2.3 Commonly used Acrylamide gels …… 75

2.4 Oligonucleotides used for sequencing of *LY96* exons…… 76

2.5 Oligonucleotides used for sequencing of *NFKB2* exons……. 77

2.6 Oligonucleotides used for sequencing of *RIPK2* exons…….. 78

2.7 Oligonucleotides used for cloning of *RIPK2* sequences…… 79

2.8 Antibodies used for western blot analysis…… 81

2.9 Plasmids used for *RIPK2* expression……. 85

2.10 Oligonucleotides used for site directed mutagenesis ……. 87

2.11 Reporter plasmids used…… 89

2.12 Transfections and transfection reagents used …….. 90

2.13 Antibodies and standards used for ELISA..…… 99

3. Polymorphisms identified in the genes *RIPK2*, *LY96* and *NFKB2* by sequencing DNA samples of Gambian origin

3.1 Polymorphisms identified in *RIPK2*, *LY96* and *NFKB2*…… 103

3.2 Genotyped polymorphisms…… 109

9. Appendix

9.1 Polymorphisms identified in *RIPK2*……... 242

9.2 Polymorphisms identified in *LY96*…… 248

9.3 Polymorphisms identified in *NFKB2*……..... 249

Abbreviations

ADC	Albumin dextrose complement
Ag85	Antigen 85
AP-1	Activator protein1
ASC	Apoptosis-associated speck-like protein containing CARD
ATG16L1	Autophagy-related protein 16-1
BAFF	B-lymphocyte activating factor
BCG	Bacillus Calmette-Guérin
BMMs	Bone marrow-derived macrophages
BSA	Bovine serum albumin
CARD	Caspase recruitment domain
CD	Cluster of differentiation
CDS	Coding sequence
CF	Culture filtrate
CFP10	Culture filtrate protein 10
Chsp60	*Chlamydia trachomatis* hsp 60
CI	Confidence interval
CLR	C-type lectin receptors
CR	Complement receptor
CREB	cAMP response element-binding protein
DAI	DNA-dependent activator of IFN-regulatory factors
DDX41	DEAD-box polypeptide 41
Dectin-1	Dendritic cell associated C-type lectin 1
DTH	Delayed type hypersensitivity
eDNA	Extracellular DNA
ELISA	Enzyme-linked immunosorbent assay
ERK	Extracellular signal-regulated kinase
ESAT-6	Early secretory antigenic 6kDa
ESX-1	ESAT-6 secretion system
FBS	Foetal bovine serum
GFP	Green fluorescent protein
GWAS	Genome-wide association study
GWLA	Genome-wide linkage analysis
HEK	Human embryonic kidney
HIS	Polyhistidine
HIV	Human immunodeficiency virus
HRP	Horseradish peroxidase
hsp	Heat shock protein
ie-DAP	D-glutamyl-meso-diaminopimelic acid
IFI16	Interferon inducible protein-16
IgG	Immunoglobulin G
IKK	Inhibitor of nuclear factor κB kinase
IL	Interleukin

IP-10	Interferon-γ inducing protein 10
IRF	Interferon regulatory factor
IκB	Inhibitor of κB
IRAK	Interleukin-1 receptor-associated kinase
JNK	c-Jun N-terminal kinase
KASPTM	Kompetetive Allele Specific PCR
KMTB	Killed *M. tuberculosis*
LB	Luria-Bertani
LM	Lipomannan
LPS	Lipopolysaccharide
LTβR	Lymphotoxin-β receptor
LUBAC	Linear ubiquitin chain assembly complex
ManLAM	Mannose-capped lipoarabinomannan
MAP	Mitogen activated kinase
MBP	Myelin basic protein
MCL	C-type lectin domain family 4 member D
MCP-1	Monocyte chemotactic protein 1
MD-2	Myeloid differentiation 2
MDP	Muramyl dipeptide
MDR-TB	Multi-drug resistant tuberculosis
MHC	Major histocompatibility complex
Mincle	Macrophage-inducible C-type lectin
MOI	Mutiplicity of infection
MPI	Mannosyl-phosphatidyl-myo-inositol
MR	Mannose receptor
mRNA	messenger RNA
MSMD	Mendelian susceptibility to mycobacterial disease
MyD88	Myeloid differentiation primary response gene 88
NEMO	NF-κB essential modulator
NF-κB	Nuclear factor kappa-light-chain-enhancer of activated B cells
NIK	NF-κB inducing kinase
NK	Natural killer
NLR	NOD-like receptor
NLRP3	NACHT, LRR and PYD domains-containing protein 3
NO	Nitric oxide
NOD	Nucleotide-binding oligomerisation domain
NOS	Nitric oxide synthase
NRAMP1	Natural resistance associated macrophage protein
OADC	Oleic acid albumin dextrose complement
PAMPS	Pathogen associated molecular patterns
PBMCs	Peripheral blood mononuclear cells
PBS	Phosphate buffered saline
PBS-T	Phosphate buffered saline-Tween

PCR	Polymerase chain reaction
PIM	Phosphatidyl-myo-inositol mannoside
PMA	Phorbol 12-myristate 13-acetate
PPD	Purified protein derivative
PRR	Pathogen recognition receptor
PVDF	Polyvenylidene difluoride
RD1	Region of difference 1
RIP1	Receptor-interacting protein kinase1
RIP2	Receptor-interacting protein kinase 2
RT	Room temperature
SCF	Skp, Cullin, F-box containing complex
SD	Standard deviation
SDS	Sdium dodecyl sulphate
SDS-PAGE	SDS-Polyacrylamide gel electrophoresis
SEM	Standard error of the mean
SEAP	Secreted embryonic alkaline phophatase
siRNA	small interfering RNA
SNP	Single nucleotide polymorphism
SRE	Serum response element
STAT1	Signal transducers of transcription 1
TAB	TAK binding protein
TAK	TGF-β-activated kinase
TBE	Tris borate EDTA
TBK1	TANK-binding kinase 1
TBS	Tris buffered saline
TBS-T	Tris buffered saline- Tween
TCR	T-cell receptor
TDM	Trehalose dimycolate
TIR	Toll-interleukin 1 receptor
TIRAP	Toll-interleukin 1 receptor (TIR) domain containing adapter protein
TLR	Toll-like receptor
TNF	Tumor necrosis factor
TNFR	TNF receptor
TRAF	TNF receptor associated factor
TRAM	TRIF-related adapter molecule
TRIF	TIR domain-containing adapter protein inducing IFN-β
TST	Tuberculin skin test
UTR	Untranslated region
v/v	Volume/ volume
w/v	Weight / volume
wt	Wild type
XDR-TB	Extensively drug resistant tuberculosis

β-TrCP	F-box/WD repeat-containing protein 1A/ β-transducin repeat containing E3 ubiquitin protein ligase

Acknowledgments

I would like to thank my supervisors Prof. Melanie Newport, Dr. Sandra Sacre and Dr. Simon Waddell for giving me the opportunity to do this PhD, their direction and guidance.

A big thank you to Dr. Lisa Mullen for her help, support and encouragement during this time. Furthermore, I would like to thank Dr. Chris Finan and Dr. David Thomas, for their assistance with bioinformatics and Dr. Helen Stewart for her help with microscopy. Finally, I would like to thank Francesca, Giselle, Georgie, Lamia, Laura H, Laura W, Manuela, Marina, Matt G, Matt S, Paola, Ryan, Sonia and Sophie for their advice and friendship during this time.

I would like to thank the National Centre for the Replacement, Refinement & Reduction of Animals in Research for funding this project.

"Is this [*RIPK2*] famous?"

1. Introduction

1.1. Tuberculosis

In 2013 approximately 1.5 million people died from tuberculosis. This makes *Mycobacterium tuberculosis,* the causative agent of tuberculosis, the second leading cause of mortality globally due to a single infectious agent. Approximately 2 billion individuals worldwide are thought to be infected with *M. tuberculosis* and despite numbers of cases declining over the years there were an estimated 9 million new cases in 2013. Over 80% of the world tuberculosis burden is born by 22 countries in South-East Asia, the Western Pacific region and sub-Saharan Africa (WHO, 2014).

Even though the pathogen is able to persist within the human host, only 3-10% of infected individuals develop active disease over the course of their lifetime. However, the risk of developing active disease is substantially increased (5-10% per life year) in individuals infected with the human immunodeficiency virus (HIV) (Ottenhoff, 2012). Of the 9 million new tuberculosis cases in 2013, about 13% of individuals were co-infected with HIV and almost 25% of tuberculosis deaths occurred in this population (WHO, 2014).

M. tuberculosis can affect virtually any part of the human body and can causes meningitis and disseminated disease. However, infection more commonly results in pulmonary disease and is subsequently transmitted almost exclusively by airborne droplets (Sharma *et al*., 2012; Thwaites *et al*., 2013; Turner and Bothamley, 2014). This makes control of the disease challenging as it spreads easily in overcrowded environments, making individuals living in impoverished conditions, homeless people, migrants and refugees particularly vulnerable (Sulis *et al*., 2014). Subsequently, some of the most susceptible individuals also have limited or no access to treatment, which is problematic as the long treatment regimen required for tuberculosis, usually consists of 2-4 drugs (ethambutol, isoniazid, pyrazinamide and rifampicin) given for at least 6 months (Sulis *et al*., 2014; WHO, 2010). Additionally, the long antibiotic course required, also frequently leads to poor patient compliance, which is one factor that has contributed to the emergence of multi-drug resistant tuberculosis (MDR-TB) and extensively drug resistant

tuberculosis (XDR-TB) strains in recent years (Heyckendorf *et al*., 2014; WHO, 2010). About 480,000 individuals developed MDR-TB in 2013 of which an estimated 9% also had XDR-TB (WHO, 2014).

To date, the *M. bovis* Bacillus Calmette-Guérin (BCG) vaccine, introduced in 1921, is the only vaccine that has proven effective against tuberculosis (Netea and van Crevel, 2014). This live attenuated vaccine was developed through continuous passage of *M. bovis*, the causative agent of tuberculosis in cattle, *in vitro* (1929). Attenuation of BCG was attributed to the loss of a region on the genome termed region of difference 1 (RD1) encoding several important virulence factors, including the early secretory antigenic 6kDa (ESAT-6) and culture filtrate protein 10 (CFP10) (Behr *et al*., 1999). BCG protects against the more severe disseminated forms of tuberculosis observed in children, such as meningitis and miliary tuberculosis (Rodrigues *et al*., 1993). However, efficacy of this vaccine against pulmonary tuberculosis varies greatly (0-80%) (Abubakar *et al*., 2013; Fine, 1995). Nevertheless, a recent meta-analysis showed that BCG is about 19% effective (risk ratio 81%, 95% confidence interval (CI) 71-92%) in protecting against infection in children (Roy *et al*., 2014). Additionally, this vaccine is not considered safe to be given to HIV^+ individuals due to the increased risk of disseminated BCG infection (WHO, 2014).

1.2. *Mycobacterium tuberculosis*

The causative agent of tuberculosis is the rod-shaped, acid fast bacterium *M. tuberculosis* (Kaufmann, 2001). First identified by Robert Koch in 1882, *M. tuberculosis* is an intracellular pathogen that predominantly targets macrophages (Kaufmann, 2001; Koch, 1882). Characteristics of *M. tuberculosis* include slow growth rate and a unique cell wall, which both contribute to the chronic nature of tuberculosis infection and are responsible for the complex long-term antibiotic regimens required for treatment (Kaufmann, 2001). The bacterium possesses a thick waxy hydrophobic cell wall consisting of long chain fatty acids, glycolipids and other components, which facilitate survival in the hostile environment inside the macrophage phagosome (Figure 1.1) (Torrelles and Schlesinger, 2010). This hydrophobic

cell wall results in slow nutrient uptake and is responsible for the slow replication rate of the organism (Kaufmann, 2001; Kleinnijenhuis *et al*., 2011). The internal portion of the mycobacterial cell wall, between the internal plasma membrane and mycolic acid layer, consists of peptidoglycan, arabinogalactan and phosphatidyl-myo-inositol mannosides (PIMs). PIMs can be divided into higher and lower order PIMs, depending on their mannose content (lower order PIMs containing 1-4 mannose residues and higher order PIMs containing 5 or 6 mannose residues). The external portion of the mycobacterial cell wall consists mostly of mycolic acids. In addition, the cell wall contains lipomannan (LM), mannose-capped lipoarabinomannan (ManLAM), trehalose dimycolate (TDM) and mannoglycoproteins (Torrelles and Schlesinger, 2010). PIMs, LM and ManLAM are thought to be anchored to the cell membrane through a shared mannosyl-phosphatidyl-myo-inositol domain (MPI) (Hunter and Brennan, 1990). A capsule consisting of polysaccharides and proteins surrounds the mycobacterial cell wall (Torrelles and Schlesinger, 2010). Even though lipids expressed on the cell surface mask the underlying pathogen associated structures and limit recognition, all these cell wall components provide targets for detection by innate immune cells (Cambier *et al*., 2014). Furthermore, another major virulence factor expressed by *M. tuberculosis,* but not attenuated members of the *M. tuberculosis* complex, is the early secretory antigenic target 6 (ESAT-6) system 1 (ESX-1) locus which encodes a type VII secretion system. ESX-1 is involved in the secretion of, among other secreted factors, ESAT-6 and culture filtrate protein 10 (CFP-10), which are potent antigens resulting in high numbers of antigen specific T-lymphocytes (Li *et al*., 2011a; Simeone *et al*., 2009).

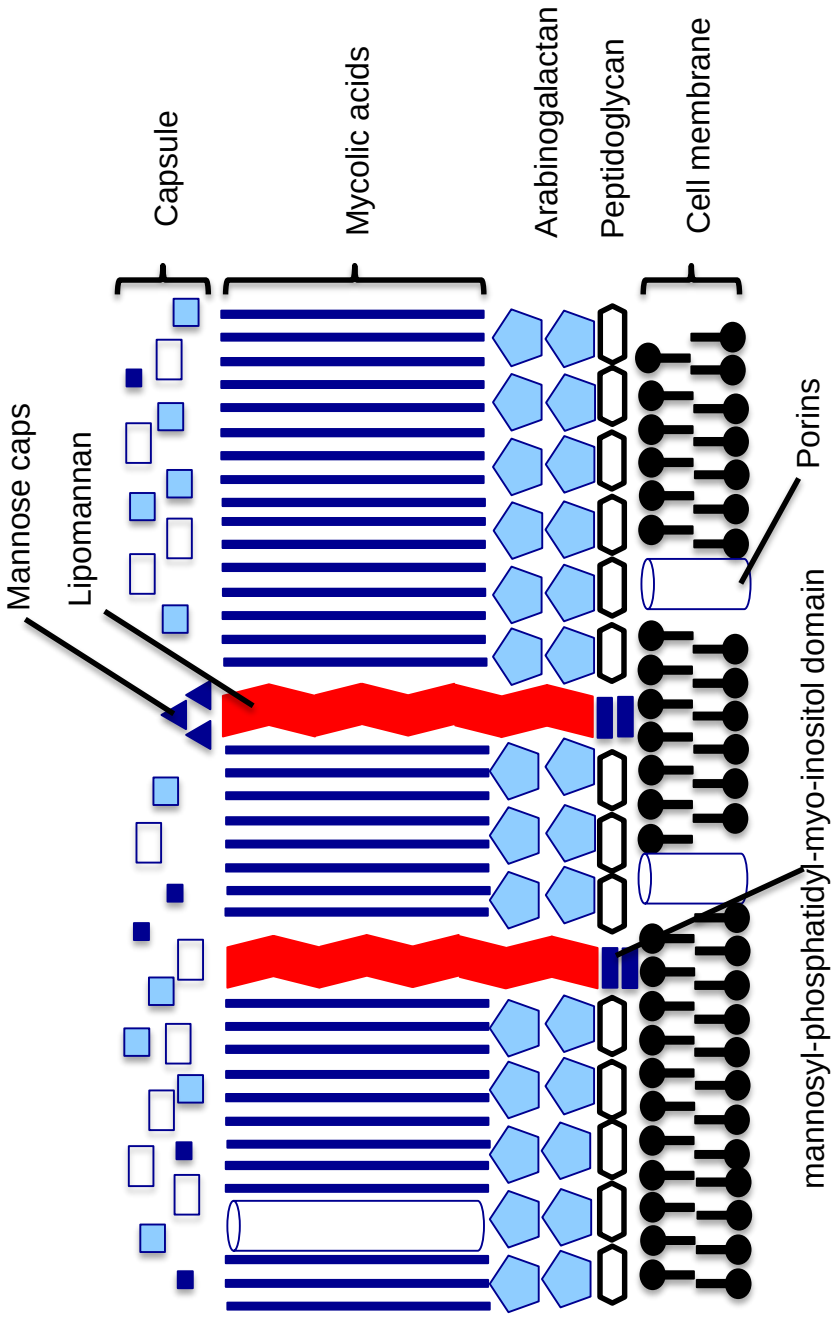

Figure 1.1 Schematic representation of the mycobacterial cell wall

1.3. The immune response to tuberculosis

The immune response in mammals relies on two powerful effectors: the innate and the adaptive immune system. The innate immune response provides the first line of defense against invading pathogens such as *M. tuberculosis* and is permanently in place to be able to respond to infection immediately. The innate immune system is comprised of phagocytic cells and natural killer (NK) cells, and the cytokines released by these cell populations. Additionally, blood proteins such as complement, and physical barriers such as epithelia are also considered components of the innate immune system. To respond efficiently to pathogenic assault, the innate immune system has to be able to detect a wide variety of different infectious agents. This is achieved by non-specific recognition of conserved pathogen associated molecular patterns (PAMPs) by pattern recognition receptors (PRRs) (Mogensen, 2009).

Two important characteristics of the adaptive immune system are its specificity and its ability to 'remember', meaning that it responds more efficiently to an antigen it has encountered before. The adaptive immune system consists of cell mediated immunity and humoral immunity. Whereas humoral immunity depends on B-lymphocytes and predominantly targets extracellular pathogens, cell mediated immunity depends on T-lymphocytes and is required for immune responses against intracellular pathogens such as *M. tuberculosis*. Antigen-specific T-lymphocytes are first activated when antigen presenting cells display antigen to naïve T-lymphocytes on major histocompatibility complex (MHC) class I or II molecules. Whereas MHC class I molecules induce the activation of antigen specific cluster of differentiation (CD) 8^+ cytotoxic T-lymphocytes that are capable of killing infected cells, MHC class II molecules result in activation and proliferation of $CD4^+$ helper T-lymphocytes (Clark and Kupper, 2005). $CD4^+$ helper T-lymphocytes differentiate from naïve T-lymphocytes into effector subsets, distinguishable on the basis of the effector cytokines that they produce. The most studied T-helper subsets are Th1 which produce the effector cytokine IFN-γ and Th2 which secretes the anti-inflammatory cytokines interleukin (IL)-4, IL-5, IL-10 and IL-13. More recently, an additional subset,Th17, which secretes IL-17 was identified (Chang *et al*., 2014). Another population of T-lymphocytes are γδ T-

lymphocytes, which express a distinct T-cell receptor (TCR) and can be $CD4^+$ or $CD8^+$ and subsequently carry out helper or cytotoxic functions (He *et al*., 2014b).

1.3.1. Innate immune response to tuberculosis

As most tuberculosis infections are caused by transmission of airborne droplets, alveolar macrophages resident in the lung are the first innate immune cells that are encountered by *M. tuberculosis* bacilli in a new host (Kleinnijenhuis *et al*., 2011). Alveolar macrophages are the predominant cell type in bronchoalveolar lavage fluid contributing over 90% of the cells present, and they provide the first line of defense against airborne invading pathogens (Reynolds, 1987).

Macrophages possess a diverse range of PRRs, which upon interaction with mycobacterial antigen results in pro-inflammatory responses as well as internalisation of the pathogen. These early immune responses induced by interaction of *M. tuberculosis* bacilli with these receptors are crucial in determining the outcome of infection. However, centuries of co-evolution of humans and *M. tuberculosis* have resulted in both induction of microbicidal processes by the host as well as the induction of processes that allow for survival and proliferation of the pathogen (Kaufmann, 2001).

One important class of PRRs involved in detection of mycobacterial antigen and subsequent induction of pro-inflammatory responses are the toll-like receptors (TLRs). These type I membrane receptors are located either in the plasma membrane or in the endosomal membrane. The cell surface expressed TLRs 1, 2, 4 and 6 have been shown to respond to mycobacterial antigens.

TLR2 has been shown to play a crucial role in controlling *M. tuberculosis* as it is one of the main receptors involved in induction of tumor necrosis factor (TNF). TNF is a critical cytokine in the immune response to tuberculosis that contributes to containment of latent tuberculosis through induction of granuloma formation (Barnes *et al*., 1990; Keane *et al*., 2001). *Tlr2*$^{-/-}$ mice have been shown to be significantly more susceptible to high dose challenges with *M. tuberculosis*. These mice fail to control bacterial growth

during stages of chronic infections and also display defects in granuloma formation (Reiling *et al*., 2002).

TLR2 functions as a homodimer or as a heterodimer in combination with TLR1 or TLR6 facilitating detection of a wide variety of mycobacterial antigens including LAM, LM, PIMs, *M. tuberculosis* heat shock protein (hsp) 60, lipoproteins, TDM and ESAT-6 (Dey and Bishai, 2014). Interaction of TLR2 with most of these ligands results in induction of pro-inflammatory cytokines including TNF, IL-1β, IL-12p70 and IL-6; nitric oxide (NO) and increased cell surface expression of MHC class I and II molecules (Brightbill *et al*., 1999; Byun *et al*., 2012; Prados-Rosales *et al*., 2011). However, interaction of mycobacterial lipoproteins and hsp 60 with TLR2 predominantly activates the anti-inflammatory cytokine IL-10, which suppresses type I interferons and down regulate major histocompatibility complex II antigen processing (Noss *et al*., 2001; Parveen *et al*., 2013; Simmons *et al*., 2010).

Additionally, TLR4 and its adapter protein myeloid differentiation 2 (MD-2) have shown to respond to mycobacterial hsp 60, 65 and 70 and have been shown to contribute to induction of TNF (Bulut *et al*., 2005; Parveen *et al*., 2013).

TLR 8 and 9 are expressed in endosomal membranes and responds to single stranded RNA and CpG DNA, respectively. In the absence of TLR9, mice challenged with *M. tuberculosis* produced reduced levels of IL-12p40 and IFN-γ (Bafica *et al*., 2005; Ito *et al*., 2007). So far, only one study has implicated TLR8 in the immune response to tuberculosis. The receptor was shown to be upregulated in *M. bovis* BCG infected macrophages (Davila *et al*., 2008). TLR7 which is also located in endosomal membranes and responds to single stranded RNA has not been reported to contribute to immune response to tuberculosis, as yet.

Other cell surface receptors that induce pro-inflammatory responses upon detection of mycobacterial antigen belong to the PRR family of C-type lectins (CLRs). These receptors include the dendritic cell associated C-type lectin 1 (Dectin-1), the macrophage-inducible C-type lectin (Mincle) and C-type lectin domain family 4 member D (MCL). Whereas Mincle and MCL have been demonstrated to respond to TDM, the mycobacterial ligand that stimulates

Dectin-1 is as yet unknown (Lee *et al*., 2012; Schoenen *et al*., 2014). Stimulation of all these receptors induces Th1 and Th17 responses (Gringhuis *et al*., 2012; Hattori *et al*., 2014; Ishikawa *et al*., 2009a; Miyake *et al*., 2013; van de Veerdonk *et al*., 2010; Werninghaus *et al*., 2009). Additionally, Dectin-1 has been shown to contribute to the induction of IL-1β during *M. tuberculosis* infection (Gringhuis *et al*., 2012).

Other CLR family members are involved in the internalisation of *M. tuberculosis* by macrophages through phagocytosis. These CLRs include the mannose receptor (MR) and the complement receptors (CR) 1, 3 and 4 (Caron and Hall, 1998; Court *et al*., 2010; Hawkes *et al*., 2010; Kang *et al*., 2005; Melo *et al*., 2000). Mannose receptors are highly expressed on alveolar macrophages and primarily respond to the mycobacterial cell wall components ManLAM and higher order PIMs (Gordon, 2003; Torrelles *et al*., 2006). Interaction of these antigens with MR induces phagocytosis, however subsequent fusion of the phagosome with the lysosome is limited (Kang *et al*., 2005). Both antigens have been shown to prevent acidification of the phagosome by either controlling Ca^{2+} influx into the cytosol or causing fusion with early endosomes instead of lysosomes (Fratti *et al*., 2003; Vergne *et al*., 2003; Vergne *et al*., 2004). Moreover, interaction of mycobacterial antigen not only prevents phagosome lysosome fusion, it also results in induction of anti-inflammatory responses such as production of the Th2 effector cytokines IL-4, IL-10 and IL-13 leading to inhibition of oxidative responses and IL-12 secretion, which favour survival of the pathogen (Chieppa *et al*., 2003; Nigou *et al*., 2001; Pathak *et al*., 2005). Nevertheless, both ManLAM and higher order PIMs have also been shown to be processed in macrophages in order to be presented by CD1 to T-lymphocytes, linking the MR to adaptive T-lymphocyte responses (de la Salle *et al*., 2005; Prigozy *et al*., 1997).

The CR3 also significantly contributes to phagocytosis of *M. tuberculosis* by binding to mycobacteria coated with complement fragments as well as uncoated mycobacterial structures (Schlesinger *et al*., 1990). About 60% of phagocytosis of complement coated bacteria is mediated by CR3 as well as about 50% of phagocytosis of uncoated bacilli (Caron and Hall, 1998; Melo *et al*., 2000). Additionally, scavenger receptors, which respond to low

density lipoproteins, have also been shown to mediate the uptake of *M. tuberculosis* (Hawkes *et al*., 2010). After internalisation of *M. tuberculosis* the bacilli are contained in a membrane bound phagosome (Armstrong and Hart, 1971, 1975). Phagosomes containing *M. tuberculosis* fail to undergo fusion with lysosomes as *M. tuberculosis* actively prevents the maturation of the phagosome and acquisition of the vesicular proton-ATPase responsible for phagosomal acidification (Armstrong and Hart, 1971; Sturgill-Koszycki *et al*., 1994).

Many studies have shown that *M. tuberculosis* inside the macrophage resides within a membrane bound compartment and does not enter the cytosol (Armstrong and Hart, 1971; Wolf *et al*., 2007). However, increasing evidence points towards the bacterium gaining access to the cytosol or at least interacting with the cytosol at some stage after internalisation. Studies found that within 3-4 days up to 25% of bacilli were not surrounded by definite membranes and that the number of bacilli outside of membrane bound compartments increased up to 40% over the course of infection (Armstrong and Hart, 1975; Houben *et al*., 2012).

Evidence for the interaction of the bacilli with the cytosol soon after internalisation comes from reporter assays that utilise the bacteria's lactamase activity to elicit fluorescent signals in the cytosol by means of fluorescence resonance energy transfer based assays (Manzanillo *et al*., 2012; Simeone *et al*., 2012). Interaction of bacteria with the cytosol was shown to depend on the expression of the ESX-1 secretion system (Houben *et al*., 2012; Pandey *et al*., 2009; van der Wel *et al*., 2007). *M. tuberculosis* strains lacking ESX-1 remain within phagosomes and cytosolic receptors do not respond to these strains (Pandey *et al*., 2009; Stanley *et al*., 2007). The virulence factor, ESAT6 which is secreted by *M. tuberculosis* has been shown to possess weak pore-forming abilities and is thought to mediate permeabilisation of the phagosomal membrane (de Jonge *et al*., 2007; Hsu *et al*., 2003). The induced membrane perforation may facilitate the exchange of bacterial components between the phagosome and the cytosol even without translocation of the whole bacteria into the cytosol. This is supported by the fact that cytosolic PRRs become activated within hours after infection with *M. tuberculosis*, despite bacilli being

contained within phagosomes at that point (Manzanillo *et al*., 2012; Mishra *et al*., 2010; Pandey *et al*., 2009; Wong and Jacobs, 2011).

Within the cytosol, the intracellular PRRs nucleotide-binding oligomerisation domain-like receptors (NLRs) NOD1 and NOD2, respond to the peptidoglycan fragments D-glutamyl-meso-diaminopimelic acid (iE-DAP) and muramyl dipeptide (MDP) respectively (Girardin *et al*., 2003a; Inohara *et al*., 2003). NOD2 contributes to the induction of cytokines including TNF, IL-12p40, IL-1β and type I IFN during infection with *M. tuberculosis* (Brooks *et al*., 2011; Gandotra *et al*., 2007; Pandey *et al*., 2009). Another type of NLR that plays a role in the immune response to *M. tuberculosis* is the NACHT, LRR and PYD domain-containing protein 3 (NLRP3) (Mayer-Barber *et al*., 2010). NLRP3 interacts with the adapter protein apoptosis-associated speck-like protein containing CARD (ASC) and pro-caspase 1 to form an inflammasome complex, which is required for processing of precursor forms of the cytokines IL-1β and IL-18 into their active forms (Dorhoi *et al*., 2012). However, other inflammasome complexes, possibly containing caspase 8, have been proposed to contribute to pro-IL-1β processing during *M. tuberculosis* infection as well (Abdalla *et al*., 2012; Gringhuis *et al*., 2012; Mayer-Barber *et al*., 2010; McElvania Tekippe *et al*., 2010).

M. tuberculosis has been shown to deliver extracellular, bacterial DNA (eDNA) from the phagosome into the cytosol in a process that is dependent on the secretion system ESX-1 (Manzanillo *et al*., 2012). Several DNA sensors are present in the cytosol, which include the DEAD-box polypeptide 41 (DDX41), the interferon inducible protein-16 (IFI16) and the DNA-dependent activator of IFN-regulatory factors (DAI) (Parvatiyar *et al*., 2012; Unterholzner *et al*., 2010). Activation of these receptors leads to activation of the transcription factor interferon regulatory factor (IRF) 3 and subsequent induction of type I IFN (Ishikawa *et al*., 2009b; Manzanillo *et al*., 2012). Additionally, stimulation of these signalling pathways by *M. tuberculosis* targets the bacilli for ubiquitination and subsequent autophagy (Watson *et al*., 2012).

Approximately eight days after infection, *M. tuberculosis* bacilli escape from the alveolar macrophage and are taken up by other phagocytic cells

recruited to the site of infection such as dendritic cells, neutrophils and inflammatory monocytes (Wolf *et al*., 2007). Dendritic cells have been shown to carry viable bacteria from the lung to the lung-draining lymph node and the mediastinal lymph node (Chackerian *et al*., 2002; Reiley *et al*., 2008). More recently, a role for inflammatory monocytes has also been proposed in this process (Samstein *et al*., 2013). Subsequently, these cells present mycobacterial antigen to naïve T-lymphocytes resulting in the induction of adaptive immunity (Bhatt *et al*., 2004; Samstein *et al*., 2013).

1.3.2. Adaptive immune response to tuberculosis

The adaptive immune response to tuberculosis is primarily cell mediated and depends on Th1 lymphocytes but also involves $CD8^+$ T-lymphocytes and γδ T-lymphocytes. B-lymphocytes and humoral immunity is thought to be of lesser importance. However, more and more evidence points towards a role for this type of immunity during *M. tuberculosis* infection.

About 10-14 days after infection antigen specific T-lymphocytes are activated through presentation of mycobacterial antigen on MHC class I and II by antigen presenting cells (Chackerian *et al*., 2002; Reiley *et al*., 2008). Activated T-lymphocytes leave the lymph node and migrate to the site of inflammation about 15-18 days after infection where they induce the formation of granulomatous lesions. The granuloma consists of a center of infected macrophages surrounded by a layer of $CD4^+$,$CD8^+$, γδ T-lymphocytes and B-lymphocytes and an outer layer of fibroblasts (Griffiths *et al*., 2010).

1.3.2.1. $CD4^+$ T-lymphocytes

The adaptive immune response to tuberculosis is predominantly mediated by $CD4^+$ Th1 lymphocytes. These cells are crucial in the immune response as they secrete IFN-γ that activates infected macrophages, resulting in induction of microbicidal activity and enhanced expression of MHC class II molecules (Kleinnijenhuis *et al*., 2011). Lack of $CD4^+$ T-lymphocytes or their effector cytokine IFN-γ leads to profound susceptibility to tuberculosis in mice (Caruso *et al*., 1999; Dalton *et al*., 1993; Saunders *et al*., 2002). Similarly, humans carrying mutations in genes involved in the induction of IL-12, which

is required for differentiation of T-lymphocyte progenitors into Th1 lymphocytes, as well as genes required for induction of IFN-γ have been shown to be substantially more susceptible to mycobacterial infection, including *M. tuberculosis* (Bustamante *et al*., 2014; Newport *et al*., 1996). Moreover, individuals deficient in $CD4^+$ T-lymphocytes due to infection with HIV are also severely restricted in their ability to control *M. tuberculosis* infection (Deffur *et al*., 2013).

M. tuberculosis infection has been shown to induce differentiation of Th17 lymphocytes. Th17 lymphocytes contribute to levels of pro-inflammatory cytokines during infection by secretion of IL-17, IL-21 and IL-22. IL-17 has been suggested to contribute to the immune response against *M. tuberculosis* infection. However, γδ T-lymphocytes have been identified as the major producer of IL-17 during infection with *M. tuberculosis*, rather than $CD4^+$ Th17 lymphocytes (Lockhart *et al*., 2006; Peng *et al*., 2008).

Th2 lymphocytes are not thought to contribute to the immune response against tuberculosis and the presence of Th2 effector cytokines IL-4 and IL-13 might even be disadvantageous as they result in inappropriate alternative activation of macrophages (Prezzemolo *et al*., 2014; Rook, 2007).

1.3.2.2. $CD8^+$ T-lymphocytes

$CD8^+$ T-lymphocytes have been shown to be required for successful control of *M. tuberculosis* infection. Mice deficient for β2 microglobulin, which lack $CD8^+$ T-lymphocytes displayed increased susceptibility to infection with *M. tuberculosis* and *M. bovis* BCG relative to wild type mice (Ladel *et al*., 1995; Rolph *et al*., 2001). $CD8^+$ T-lymphocytes are capable of killing *M. tuberculosis* directly through secretion of peforins, granzymes and granulysins as well as contributing to the secretion of IFN-γ and TNF (Caccamo *et al*., 2006; Etna *et al*., 2014; Stenger *et al*., 1998). Furthermore, $CD8^+$ T-lymphocytes also target infected macrophages and other cells presenting mycobacterial antigen on MHC class I molecules and induce apoptosis through Fas-ligand or other cell death receptors (Schaible *et al*., 2003; van der Wel *et al*., 2007; Winau *et al*., 2006).

1.3.2.3. γδ T-lymphocytes

γδ T-lymphocytes have been shown to contribute to the immune response during *M. tuberculosis* infection. Murine as well as macaque infection models have shown that infection with *M. tuberculosis* or *M. bovis* BCG resulted in expansion of γδ T-lymphocyte subsets and influx of these cells into the lung (Dieli *et al*., 2003; Shen *et al*., 2002). γδ T-lymphocytes display cytotoxic activity towards infected macrophages and contribute to secretion of IL-17 and IFN-γ during infection of mice and humans (Dieli *et al*., 2003; Lockhart *et al*., 2006; Peng *et al*., 2008). In mice devoid of IL-17, granuloma formation was shown to be impaired and induction of IFN-γ was reduced suggesting that IL-17 is involved in optimal induction of Th1 responses after challenge with *M. tuberculosis* and *M. bovis* BCG (Gopal *et al*., 2012; Okamoto Yoshida *et al*., 2010; Umemura *et al*., 2007). Mice deficient for the IL-17 receptor subunit A failed to control *M. tuberculosis* during later stages of infection (Freches *et al*., 2013). However, a different study showed that IL-17 is only important in induction of Th1 responses in the absence of IL-12p70 (Khader *et al*., 2005).

1.3.2.4. B-lymphocytes

B-lymphocytes are considered of lesser importance in the immune response to intracellular pathogens such as *M. tuberculosis*. Nevertheless, emerging evidence suggests that B-lymphocytes and humoral immunity are involved in the immune response to tuberculosis. One study by Manglione *et al*. (2007) found that in the absence of B-lymphocytes, mice displayed increased immunopathology, IL-10 levels and neutrophil recruitment to the lung after aerosol challenges with *M. tuberculosis* (Maglione *et al*., 2007). This B-lymphocyte-deficient phenotype could be reversed by transfer of B-lymphocytes. However, the attenuation of the enhanced inflammatory response in recipient mice was thought to be due to immunoglobulins rather than B-lymphocytes directly. Furthermore, high dose aerosol challenges of B-lymphocyte-deficient mice resulted in increased bacterial burden (Maglione *et al*., 2007). A different study, in which B-lymphocyte-deficient mice were infected with a clinical isolate of *M. tuberculosis*, showed that the absence of

B-lymphocytes resulted in reduced granuloma formation, reduced infiltration of lymphocytes and neutrophils into the lung, and a delay in dissemination of bacteria during early infection (Bosio *et al*., 2000). Additionally, B-lymphocytes have been demonstrated to contribute to production of cytokines including IFN-γ (Harris *et al*., 2000).

The FcγR is expressed on macrophages and dendritic cells and binds to the Fc portion of B-lymphocyte secreted immunoglobulin G (IgG) resulting in internalisation of IgG bound antigen (Caron and Hall, 1998). Studies with FcγR-deficient mice demonstrated that in the absence of this receptor mice infected with *M. tuberculosis* displayed increased bacterial burden, immunopathology and mortality rates as well as an increase in IL-10 levels (Maglione *et al*., 2008).

1.4. Host genetic determinants of susceptibility to *M. tuberculosis* infection

Only about 10% of individuals that become infected with *M. tuberculosis* develop active disease, suggesting that most individuals are intrinsically capable of mounting an effective immune response whereas others are not. Some of the first evidence that host genetic determinants contributed to susceptibility to tuberculosis came from a vaccination accident that occurred in Lübeck, Germany in 1928. Instead of vaccinating with BCG, newborn babies were vaccinated with virulent *M. tuberculosis*. Out of the 251 infants, exposed to the virulent mycobacteria, 72 died from or with active tuberculosis, whereas the majority of children survived, suggesting that some individuals intrinsically control tuberculosis infection better than others (Rieder, 2003). That susceptibility to tuberculosis is in part inherited, was corroborated by studies of tuberculosis in monozygous and dizygous twins. Concordance of tuberculosis was shown to be substantially higher in monozygous twins compared to dizygous twins, who only share on average 50% of their genome (Meyer and Thye, 2014).

The differences in susceptibility that have been observed between different populations also adds to the epidemiological evidence that genetic factors contribute to susceptibility to tuberculosis (Motulsky, 1960; Stead *et al*., 1990). These differences are thought to depend on the history of previous exposure to tuberculosis and the subsequent selective pressure the disease had on genes affecting susceptibility to tuberculosis. For example, when the Qu'Apelle Indians were first exposed to tuberculosis in the 1890s the initial mortality from tuberculosis was almost as high as 10% of the total population per year. Over the following 40 years almost half the Indian population succumbed to tuberculosis, but subsequently mortality rates fell to 0.2% suggesting that the surviving individuals were genetically less susceptible to tuberculosis (Motulsky, 1960). To the present day, historic exposure to tuberculosis is thought to affect the susceptibility of different populations. A study investigating incidence of tuberculosis in 25000 residents of nursing homes in Arkansas found that black individuals were twice as likely as white

individuals to become infected with tuberculosis. This difference could not be explained by socio-economic or environmental factors (Stead *et al*., 1990).

Despite substantial evidence suggesting that host genes play an important role in susceptibility to tuberculosis, identifying these genes has proven difficult. This is due to the complexity of susceptibility to tuberculosis, with potentially multiple host genes exerting a small effect (Meyer and Thye, 2014; Newport, 2009). Additionally, environmental factors, co-infection with HIV and the genetics of the pathogen also affect whether and individual develops active tuberculosis (Newport, 2009). Moreover, *M. tuberculosis* lineages found in different geographic regions have been shown to vary significantly in virulence, immunogenicity and also in the clinical phenotypes they cause (Gagneux and Small, 2007).

1.4.1. Candidate gene studies

One frequently used approach to study tuberculosis susceptibility is the study of candidate genes. This approach aims to associate a disease phenotype with usually a bi-allelic polymorphism in a gene, which is probable to be causative of the phenotype. In candidate gene studies the genotype frequencies of a particular mutation are compared between unrelated tuberculosis patients and uninfected controls or between affected and unaffected family members (Meyer and Thye, 2014; Moller and Hoal, 2010). Candidate gene studies have led to the identification of several genes associated with susceptibility to tuberculosis (Bellamy *et al*., 1998; Gong *et al*., 2013; Hawn *et al*., 2006). However, one major disadvantage of this approach is that it requires prior knowledge of the candidate gene's existence and function (Meyer and Thye, 2014; Moller and Hoal, 2010).

One of the most extensively studied genes, which has been significantly associated with susceptibility to pulmonary tuberculosis, is the gene *SLC11A1* (formerly known as *NRAMP1*) (Bellamy *et al*., 1998). *SLC11A1* encodes the natural resistance associated macrophage protein (NRAMP)1, an Fe^{2+}/Mn^{2+} efflux pump that is recruited to the membrane of the phagosome in activated macrophages (Gruenheid *et al*., 1997). This gene was initially identified because of a missense mutation (G169D) in the mouse version of the gene

(*Nramp1*) which resulted in susceptibility to infection with *M. bovis* BCG, though not *M. tuberculosis,* in mice (North *et al*., 1999; Vidal *et al*., 1993). An association study conducted by Bellamy *et al*. (1998) involving smear-positive tuberculosis patients and healthy control subjects in West Africa found an association between 4 polymorphisms in *SLC11A1* and pulmonary tuberculosis (Bellamy *et al*., 1998). Furthermore, susceptibility to tuberculosis was linked to the locus 2q35, which encodes *SLC11A*, in a large Canadian aboriginal family (Greenwood *et al*., 2000). A meta-analysis conducted in 2011 by Li *et al*. including 38 individual studies concluded that *SLC11A1* might play a role in susceptibility to pulmonary tuberculosis (Li *et al*., 2011b).

Another gene that has been studied in several populations, with regard to susceptibility to tuberculosis, is *CCL2* (Gong *et al*., 2013). *CCL2* encodes the monocyte chemotactic protein 1 (MCP-1), which is involved in recruiting monocytes to the site of mycobacterial infection (Serbina *et al*., 2008). One polymorphism -2518G (rs1024611), which leads to increased secretion of MCP-1 upon inflammatory stimuli, has been identified in the promoter region of *CCL2* (Rovin *et al*., 1999). This polymorphism has been studied extensively, but the results have been conflicting (Flores-Villanueva *et al*., 2005; Jamieson *et al*., 2004; Thye *et al*., 2009). The polymorphism was associated with susceptibility to tuberculosis in a Mexican and a Korean population (Flores-Villanueva *et al*., 2005). In contrast, a large study conducted in a Ghanaian population found the polymorphism -2518G to be protective against tuberculosis (Thye *et al*., 2009). No association was observed between the polymorphism and susceptibility to tuberculosis in Russian, Brazilian or South African populations (Jamieson *et al*., 2004; Moller *et al*., 2009; Thye *et al*., 2009). A meta-analysis conducted by Gong *et al*. (2013) came to the conclusion that the -2518G increased risk of tuberculosis in American and Asian, but not African populations (Gong *et al*., 2013).

Another example of a gene that has been associated with susceptibility to tuberculosis is *NOS2A,* which encodes for nitric oxide synthase (NOS) (Moller and Hoal, 2010). Three different NOS are involved in production of NO in humans including inducible NOS, encoded by *NOS2A* (Moller and Hoal, 2010). Various mutations associated with tuberculosis have been identified in

the promoter region of *NOS2A* (Gomez *et al*., 2007; Jamieson *et al*., 2004; Jena *et al*., 2014; Moller *et al*., 2009). The polymorphism -1026G (rs2779249) was associated with susceptibility to tuberculosis in a Brazilian population whereas ten copies of a microsatellite (CCTTT) within the promoter region of *NOS2A* were associated with protection against tuberculosis in two independent studies in a Colombian and an Indian population (Gomez *et al*., 2007; Jamieson *et al*., 2004; Jena *et al*., 2014). A haplotype involving the two polymorphisms -1173C (rs9282799) and -1659T (rs8078340), located within the promoter region of *NOS2A*, was associated with susceptibility to tuberculosis in a South African population. The presence of the major allele of rs9282799 (C) in combination with the minor allele of rs8078340 (T) was observed more frequently in tuberculosis infected individuals relative to healthy controls (Moller *et al*., 2009). The polymorphism rs8078340 affects a predicted transcription factor binding site and in the presence of the T allele of the polymorphism, protein-DNA complex formation was shown to be reduced (Burgner *et al*., 2003). A further 10 polymorphisms in *NOS2A* were associated with tuberculosis in an African-American population, but not a Caucasian population (Velez *et al*., 2009).

Other genes that harbour polymorphisms associated with susceptibility to tuberculosis include the HLA class II gene *HLA-DBQ1; IFNG, encoding* IFN-γ*; VDR,* encoding the vitamin D3 receptor and *TLR2*, encoding the TLR2 receptor (Babb *et al*., 2007; Delgado *et al*., 2006; Thuong *et al*., 2007; Tso *et al*., 2005). Additionally, a polymorphism in the *TIRAP* gene, encoding the TLR adapter protein toll-interleukin 1 receptor (TIR) domain containing adapter protein (TIRAP) was found to be associated with protection against tuberculosis (Khor *et al*., 2007).

1.4.2. Genome-wide linkage analysis

Genome-wide linkage analysis (GWLA) is capable of tracing regions of the genome that are associated with a heritable phenotype by testing for coinheritance of genetic markers in family members that exhibit the phenotype of interest (Moller and Hoal, 2010). The advantage of this approach is that, unlike for candidate gene studies, no prior knowledge of the target gene is

required as the whole genome is scanned (Moller and Hoal, 2010). However, this approach requires precise knowledge of whether the family member is affected, which is not always possible when studying susceptibility to an infectious disease that also requires exposure to the pathogen, and older family members may no longer be alive to include. Furthermore, GWLA is low in power and cannot detect loci on the genome that exert only moderate effect on the phenotype, which would be required for a multifactorial phenotype such as susceptibility to tuberculosis (Moller and Hoal, 2010). Subsequently, GWLA studies for susceptibility to tuberculosis have predominantly identified loci harbouring genes that on biological grounds are unlikely to affect susceptibility to tuberculosis. Furthermore, there is little overlap between the loci identified in the six GWLA conducted to date. Overall, 13 different loci were identified in 6 different populations (12 autosomal and 1 X-linked) (Table 1.1) (Baghdadi *et al*., 2006; Bellamy *et al*., 2000; Cooke *et al*., 2008; Mahasirimongkol *et al*., 2009; Miller *et al*., 2004; Stein *et al*., 2008).

1.4.3. Genome-wide association studies

Genome-wide association studies (GWAS) aim to identify polymorphisms associated with disease phenotype by comparing large numbers of known single nucleotide polymorphisms (SNPs) and copy number variations in affected patients and healthy controls. GWAS studies, like GWLA, have the advantage of no requirement for a prior hypothesis as the entire genome is scanned. Additionally, there is no need for large numbers of affected family members. Nevertheless, large study groups are required and particular attention has to be paid to selection of healthy controls. Healthy control subjects need to be unaffected but representative of the studied patient population. Additionally, their level of exposure to *M. tuberculosis* needs to be considered. The level of exposure of healthy controls is important as absence of infection could be due to reduced genetic susceptibility to infection or insufficient exposure to the pathogen (Meyer and Thye, 2014).

Only five GWAS studies on tuberculosis have been published so far (Table 1.2) (Chimusa *et al*., 2014; Mahasirimongkol *et al*., 2012; Png *et al*., 2012; Thye *et al*., 2012; Thye *et al*., 2010). Three studies demonstrated that

the SNP rs4331426 located in a gene-poor chromosomal region (18q11.2) and rs2057178 located in chromosomal region 11p13, downstream of the gene *WT1*, encoding Wilms tumor 1, are significantly associated with tuberculosis in Ghanaian, Gambian and South African populations (Chimusa *et al*., 2014; Thye *et al*., 2012; Thye *et al*., 2010). A study conducted in Thai and Japanese populations found association between the SNP rs6071980 and tuberculosis. This polymorphism is located within the chromosomal region 20q12 between the two genes *MAFB* and *HSPEP*. *MAFB* encodes the transcription factor MafB involved in differentiation of monocytes to macrophages and the heat shock 10kDa protein, respectively. However, this result was not statistically significant and was only apparent after the results were stratified for the age of the participants (Mahasirimongkol *et al*., 2012).

Population	Phenotype	Chromosomal region	Candidate genes within or in close proximity of locus	Reference
South Africa The Gambia	Tuberculosis	15q11-13 Xq	*CD40LG*, *HERC2*	(Bellamy *et al*., 2000)
Brazil	Tuberculosis	10q26.13 11q12.3 20p12.1	-	(Miller *et al*., 2004)
Morocco	Tuberculosis	8q12-13	-	(Baghdadi *et al*., 2006)
South Africa Malawi	Tuberculosis	6p21-q23 20q13.31-33	*MC3R*, *CTSZ*	(Cooke *et al*., 2008)
Uganda	Tuberculosis	7p22-21 20q13	*IL-6,MC3R*, *CTSZ*	(Stein *et al*., 2008)
Thailand	Tuberculosis	5q23.2-31.2 17p13.3-13.1 20p13-12.3	*GM-CSF*, *IL3*, *IL4*, *IL5*, *IL13, IRF, LEAP2, APBB3, SPK1A, IBD5, CD14, MYBBP1A*	(Mahasirimongkol *et al*., 2009)

Table 1.1 Genome-wide linkage analysis investigating tuberculosis

Population	Phenotype	Chromosomal region	Candidate genes within or in close proximity of locus	Reference
Sub-Saharan African ancestry	Tuberculosis	18q11.2	*GATA6,CTAGE1,RBBP8,CABLES1*	(Thye *et al*., 2010)
Indonesian	Tuberculosis	-	-	(Png *et al*., 2012)
African ancestry	Tuberculosis	11p13	*WT1*	(Thye *et al*., 2012)
Thai and Japanes	Tuberculosis	-	-	(Mahasirimongkol *et al*., 2012)
South African	Tuberculosis	11p13	*WT1*	(Chimusa *et al*., 2014)

Table 1.2 Genome-wide association studies investigating tuberculosis

1.4.4. Mendelian susceptibility to mycobacterial disease (MSMD)

Other studies that have proven informative with regard to susceptibility to tuberculosis are studies of individuals with MSMD (Bustamante *et al*., 2014). MSMD is a rare inherited condition in which individuals are prone to infection with weakly pathogenic mycobacteria such as environmental mycobacteria, *M. bovis* BCG, and also *M. tuberculosis* and *Salmonella* through mutations in genes required for induction or regulation of IFN-γ (Bustamante *et al*., 2014; de Beaucoudrey *et al*., 2010). Even though this condition is rare and cannot account for the prevalence of tuberculosis infection observed in the overall population, the genetic defects leading to MSMD have highlighted the significance of IFN-γ-dependent immunity for control of mycobacterial disease. To date, mutations in nine different genes, seven autosomal and two x-linked, have been identified to cause MSMD (Bustamante *et al*., 2014).

The first gene implicated in MSMD was the *IFNGR1* gene, which encodes the IFN-γ receptor 1. An autosomal recessive mutation was identified in four Maltese children with severe mycobacterial infections. The mutation leads to the expression of a truncated version of the receptor, which lacks the intracellular and membrane binding region, resulting in complete IFN-γ deficiency (Newport *et al*., 1996). To date, 31 different mutations have been observed in the *IFNGR1* gene, all of which lead to complete or partial deficiency of IFN-γ receptor 1 function (Bustamante *et al*., 2014; Jouanguy *et al*., 1996). Additionally, 15 mutations affecting IFN-γ receptor 2 also result in MSMD (Bustamante *et al*., 2014). In the case of both IFN-γ receptors, no receptors or non-functional receptors are expressed on the cell surface, resulting in an abolished or impaired IFN-γ response. Although high levels of IFN-γ are present in the plasma, this subsequently leads to increased susceptibility to mycobacterial infection (Dorman *et al*., 2004; Fieschi *et al*., 2001).

The gene that is most frequently implicated in MSMD is *IL12RB1*, which encodes the IL-12 receptor β1 chain, which forms part of the IL-12 and IL-23 receptor (de Beaucoudrey *et al*., 2010). To date, 78 different mutations have been reported, which usually lead to complete loss of expression of the receptor, resulting in impaired responses to IL-12 (Bustamante *et al*., 2014).

Consequently, patients with these mutations produce only low levels of IFN-γ, increasing their susceptibility to mycobacterial infection (de Beaucoudrey *et al*., 2010; Fieschi *et al*., 2003).

Other genes that have been found to harbour mutations leading to MSMD include *IL12B*, encoding the IL12p40 subunit, which is part of IL-12 and IL-23; *NEMO*, encoding the NF-κB essential modulator (NEMO), which forms part of the nuclear factor kappa-light-chain-enhancer of activated B cells (NF-κB) signal transduction cascade; *STAT1* and *IRF8*, encoding the transcription factors signal transducers of transcription 1 (STAT1) and IRF8 respectively; *CYBB*, encoding the flavocytochrome b_{558} β-chain involved in generation of reactive oxygen species, and *ISG15*, encoding an IFN-induced ubiquitine-like protein (Altare *et al*., 1998; Bustamante *et al*., 2011; Chapgier *et al*., 2006; Filipe-Santos *et al*., 2006; Hambleton *et al*., 2011; Zhang *et al*., 2015).

1.5. Surrogate markers for tuberculosis susceptibility

In order to study genetic susceptibility to tuberculosis in association studies or by linkage analysis, susceptibility to tuberculosis has to be defined as a phenotype (Stein *et al*., 2007). This is difficult as susceptibility to tuberculosis is a complex trait, with severity of disease and the length of the latency period before active disease occurs varying greatly between different patients (Ablasser *et al*., 2009). Additionally, absence of tuberculosis in an individual does not guarantee that the individual is genetically less susceptible to infection, but may be result of insufficient exposure to the pathogen (Newport, 2009). Furthermore, clinical tuberculosis is a very heterogenous phenotype, which complicates the search for genes that predispose to it. Moreover, a number of non-genetic factors can influence the phenotype to different extents in different individuals.

For these reasons, surrogate markers, or phenotypes, have been used to identify host genes that affect susceptibility to infection (Table 1.3) (Newport, 2015; Stein et al., 2003; Stein et al., 2007; Wheeler et al., 2006). For a marker to be suitable as a surrogate for genetic susceptibility to tuberculosis it is essential that the chosen marker is relevant to tuberculosis as well as heritable (Newport, 2015). Suitable markers include quantitative traits, which have a

continuous distribution in the population, such as the magnitude of a cytokine response. The advantage of studying a quantitative trait as a surrogate, as opposed to studying a complex trait such as tuberculosis infection, is that it can be measured more easily and is likely to be influenced by fewer genes, increasing the chance of an informative result (Newport, 2015; Stein et al., 2003).

1.5.1. Cytokine responses as surrogate markers for susceptibility to tuberculosis

The amount of cytokines, such as IFN-γ and TNF, secreted in response to mycobacterial antigens have been used as phenotypic measures in various genome-wide and candidate gene linkage studies (Newport, 2015; Stein et al., 2007; Wheeler et al., 2006). IFN-γ and TNF play essential roles in the immune response to tuberculosis as IFN-γ is required for activation and induction of microbicidal pathways in infected macrophages, and TNF is involved in the induction of granuloma formation during infection with *M. tuberculosis* (Barnes *et al*., 1990; Kaufmann, 2001; Kleinnijenhuis *et al*., 2011). Subsequently, genes that regulate these cytokine responses are likely to affect susceptibility to infection.

Heritability of antigen specific cytokine responses such as the magnitude of mycobacteria-driven IFN-γ have been studied in various populations whereas heritability to TNF responses to mycobacterial antigen have only been addressed in a population from Uganda (Barnes *et al*., 1990; Newport *et al*., 2004; Stein *et al*., 2003). One study conducted by Newport *et al.* (2004) observed significant heritability for the magnitude of IFN-γ response to purified protein derivative (PPD)-RT49 (41%, 95% CI 10-71%) and killed *M. tuberculosis* (39%, 95% CI 3-71%) in a Gambian cohort of BCG-vaccinated neonates. No significant heritability was observed for IFN-γ responses to antigen 85 (Ag85) (3%, 95% CI 0-35%),

Population	Phenotype	Antigen	Chromosomal region	Candidate genes within or in close proximity of locus	Reference
The Gambia	IFN-γ	PPD KMTB	8q13-22 10q23-25 11q23-25	*BTRC*, *CHUK*, *LY96*, *NFKB2*, *RIPK2*	(Newport *et al.* Manuscript in preparation)
Brazil	IFN-γ Antigen specific lymphocyte proliferation Antigen specific IgG Plasma IgE	PPD *M. tuberculosis* soluble antigen M*. leprae* soluble antigen	1q23.3 6p21.2 6q27 17q21	*FCGR3A*, *FCGR2A, FCER1G, PARK2, PARKG, HLA, CCR6, GPR31, DLL1, PSMB1*	(Wheeler *et al*., 2006)
South Africa	TNF	BCG BCG + IFN-γ	1p36 4q32-33 5p15 6q14 7q36 11p15 19q13	*TFN1* locus	(Cobat *et al*., 2013)
Uganda	TNF	*M. tuberculosis* CF	-	*IL10* *IFNGR1* *TNFR1*	(Stein *et al*., 2007)
Uganda	TST	PPD	2q21-24 5p13-5q22	-	(Stein *et al*., 2008)
South Africa	TST Binary and quantitatively	PPD	11p14 5p15	*SLC6A3*	(Cobat *et al*., 2009)
France	TST Binary	PPD	11p15 19q13	*TFN1* locus	(Cobat *et al*., 2015)

Table 1.3 Genome-wide and candidate gene linkage analysis investigating surrogate markers for tuberculosis
PPD, purified protein derivative; KMTB, killed *M. tuberculosis*; CF, culture filtrate; IFN, interferon; TNF, tumor necrosis factor; TST, tuberculin skin test.

short term culture filtrate (CF) (12%, 95% CI 0-46%) and hsp 65 (23%, 95% CI 0-56%). In this study peripheral blood mononuclear cells (PBMCs) were collected from BCG-vaccinated infants five months post vaccination. PBMCs were stimulated with mycobacterial antigens and secreted IFN-γ was measured six days after stimulation (Newport *et al*., 2004).

Another study conducted in a Gambian twin cohort of 12 year old healthy children estimated the IFN-γ response to PPD-RT48 and Ag85 to be (39%, 95% CI 0-68%; 40%, CI 0-86% respectively) heritable (Jepson *et al*., 2001). Cobat *et al*. (2010) demonstrated that heritability of IFN-γ response to PPD, ESAT-6 and live BCG was heritable to 43-58% in siblings of South African origin (Cobat *et al*., 2010).

Studies investigating the heritability of IFN-γ response to mycobacterial antigens in household contacts in Uganda also showed that IFN-γ response was heritable (CF 35%, 95% CI 15.2-54.9%; ESAT6 27%, 95% CI 5.9-48.0% and Ag85B 15%, 95% CI -6.6-36.7%) (Tao *et al*., 2013). However, heritability was reduced if HIV positive individuals were included in the study (Stein *et al*., 2003; Tao *et al*., 2013).

Even though all studies found that IFN-γ responses to mycobacterial antigen were heritable, the heritability values and also the antigens to which responses were heritable varied between different studies. These differences might be due to the study populations in each of the studies or might reflect the different strategies used to estimate the heritability of IFN-γ response to mycobacterial antigen. Two investigations estimated heritability of IFN-γ through twin studies. Comparing similarities between the IFN-γ responses of monozygous and dizygous twin pairs allows the estimation of the contribution of genetics to the trait (Jepson *et al*., 2001; Newport *et al*., 2004). A disadvantage of twin studies is that the extent to which genetics and the shared environment affect a trait cannot be separated. In a study by Newport *et al.* (2004) the effects of the environment on the IFN-γ response to mycobacterial antigen has been minimised as far as possible by studying the twins at a very early age. Furthermore, in this study the exposure of neonates to mycobacterial antigen was ‘normalised’ by vaccinating all infants with an identical dose of the same BCG strain within 24h of birth (as is standard

practice in the Gambia) (Newport *et al*., 2004). Other studies have used whole families, to study the correlation of IFN-γ response of sibling pairs, parents and offspring pairs and also both parents, in order to minimise the impact of shared environmental factors due to co-habitation (Tao *et al*., 2013). Despite variation, all of these studies have shown that there is a genetic component underlying the magnitude of IFN-γ produced in response to mycobacterial antigens, in particular PPD, making IFN-γ a suitable surrogate for genetic susceptibility to tuberculosis.

Heritability of TNF response to mycobacterial antigens has only been studied in a population from Uganda. In this study, cohort TNF responses to *M. tuberculosis* CF were measured in whole blood samples from members of households that had at least one confirmed tuberculosis case. The study found that TNF response to mycobacterial antigen was highly heritable (68%) (Stein *et al*., 2003).

Genome-wide linkage analysis and candidate gene analysis have been conducted using magnitude of mycobacterial antigen driven IFN-γ and TNF as a surrogate phenotype for genetic susceptibility to tuberculosis.

A genome-wide linkage analysis conducted in the Gambian population by Newport *et al.* significantly linked the magnitude of IFN-γ response to PPD-RT49 and killed *M. tuberculosis* to regions on three chromosomes (8q13-22, 10q23-25 and 11q23-25). This study investigated the IFN-γ responses to mycobacterial antigen of 139 dizygous twin pairs at 5 months of age after BCG vaccination at birth, which were previously used to study heritability of IFN-γ responses. The three loci linked to magnitude of mycobacterial antigen-driven IFN-γ responses encoded five genes (*BTRC*, *CHUK*, *LY96*, *NFKB2* and *RIPK2*) that contribute to the regulation of IFN-γ expression (Newport *et al*. manuscript in preparation) (Newport, 2015; Newport et al., 2004).

A genome-wide linkage analysis was performed on IFN-γ data collected as part of a study conducted in Brazil (Miller *et al*., 2004; Wheeler *et al*., 2006). The study included 361 individuals from 37 families with multiple cases of tuberculosis or leprosy. Significant linkage was established between IFN-γ response to PPD and a locus on chromosome 1. This locus encodes various activation markers and receptors of B-lymphocytes, T-lymphocytes and NK

cells as well as the Fc region of IgG and IgE. Furthermore, significant linkage was established between IFN-γ response to mycobacterial antigen and regions on chromosomes 7, 10, 12, 14, 16 and 19. IFN-γ response to *M. leprae* soluble antigen was significantly linked to loci including regions on chromosome 6 that encode HLA class II genes and also within proximity of the gene encoding the E3-ubiquitin protein ligase parkin. Additionally, antigen specific IgG release and total plasma IgE levels were measured in response to mycobacterial antigen. Total IgE levels were significantly linked to a region on chromosome 2, whereas antigen specific IgG was linked to regions on chromosomes 8, 12, 17 and 21 (Wheeler *et al*., 2006).

Two studies have investigated susceptibility to tuberculosis using magnitude of TNF responses to mycobacterial antigen as a surrogate marker (Cobat *et al*., 2013; Stein *et al*., 2007). One of the studies was conducted in South Africa and looked at the TNF response after stimulation with BCG alone or BCG and IFN-γ, in whole blood samples of 392 children of families living in an area where tuberculosis is hyperendemic. The study found significant linkage between magnitude of mycobacteria-driven TNF production and chromosomal region 11p15 now termed TNF locus 1 (*TNF1*). Other loci identified included chromosomal regions 1p36, 4q32, 5p15, 6q14, 7q36 and 19q13 (Cobat *et al*., 2013).

Stein *et al*. (2007 and 2008) investigated the magnitude of TNF produced *ex vivo* by household members of a tuberculosis index case in Uganda in response to stimulation with mycobacterial antigen (Guwatudde *et al*., 2003; Stein *et al*., 2007; Stein *et al*., 2008). Candidate gene linkage analysis was performed involving 12 candidate genes of known importance in TNF production regulation. Significant linkage was established between magnitude of TNF upon stimulation with *M. tuberculosis* CF and three candidate genes. The genes for which linkage was significant included the TNF receptor *TNFR1*, the IFN-γ receptor *IFNGR1*, *IL10* encoding the cytokine IL-10. The same cohort linkage analysis was performed using active tuberculosis as a phenotype opposed to magnitude of TNF production. This analysis identified linkage with the same candidate genes as previously identified using magnitude of TNF production as a phenotype. Additionally, this

analysis identified linkage to genes *TLR2*, *TLR4* and the TNF receptor, *TNFR2*, suggesting that these genes are involved in susceptibility to tuberculosis but not through the regulation of TNF (Stein *et al*., 2007).

When a genome-wide linkage analysis of the same data was performed, magnitude of TNF production was linked to chromosomal region 1p31, which is within proximity of the gene *IL12RB2* encoding the IL-12 receptor β2 and chromosomal region 21q22, in which the gene *IFNGR2*, encoding the IFN-γ receptor 2, is located (Stein *et al*., 2008).

1.5.2. Tuberculin skin test reactivity as surrogate marker for susceptibility to tuberculosis

Another marker that has been used as a surrogate for susceptibility to tuberculosis is the response to the tuberculin skin test (TST) (Cobat *et al*., 2009; Cobat *et al*., 2015; Stein *et al*., 2008). TST involves inoculation of the skin with PPD and measuring the T-lymphocyte-mediated delayed type hypersensitivity (DTH) to mycobacterial antigens (Vukmanovic-Stejic *et al*., 2006). It has been shown that individuals that show no TST response, despite constant high exposure to *M. tuberculosis*, are unlikely to be infected with tuberculosis (2000; Vukmanovic-Stejic *et al*., 2006). Moreover, exposed individuals that remain TST unresponsive are thought to be naturally more resistant to infection, as in these individuals the infection is cleared before T-lymphocyte sensitization occurs (2000). TST reactivity has been shown to be heritable in various populations (Jepson *et al*., 2001; Sepulveda *et al*., 1994). The TST response has been studied as a binary and as a quantitative trait by scoring the result of the TST as positive/negative only or by measuring the diameter of the skin induration, respectively (Cobat *et al*., 2009; Cobat *et al*., 2015; Stein *et al*., 2008).

Reactivity to TST has been studied in various populations with different levels of tuberculosis endemicity (Cobat *et al*., 2009; Cobat *et al*., 2015; Stein *et al*., 2008). The first study published was conducted in Uganda, a country where tuberculosis is endemic. This study included 193 households (803 individuals) of a tuberculosis index case and measured TST reactivity as a binary trait (TST negative or positive). Suggestive significant ($p<10^{-3}$) linkage

was established between a persistently negative tuberculin skin test and chromosomal regions 2q21 -24 and 5p13-5q22 (Stein *et al*., 2008). Additionally, linkage between TST negativity and chromosomal region 2q27, which is within proximity of *SLC11A1* and chromosomal region 8p22, which was previously linked to tuberculosis in a GWLA in a Moroccan population was established (Baghdadi *et al*., 2006; Stein *et al*., 2008).

Two further studies investigated TST reactivity in an area of South Africa hyperendemic for tuberculosis and in an area of France where prevalence of tuberculosis is low. The study conducted in the area of low tuberculosis endemicity included 155 families (540 household contacts of a tuberculosis index case), whereas the study conducted in the area where tuberculosis is hyperendemic included 128 families (536 household contacts, without the requirement of a tuberculosis case in the family) (Cobat *et al*., 2009; Cobat *et al*., 2015). Scoring the TST response as positive or negative, TST reactivity was significantly linked ($p=2.4x10^{-6}$) to chromosomal region 11p14-15 in both populations (Cobat *et al*., 2015). This locus was previously shown to be linked to magnitude of TNF production in response to BCG alone or in combination with IFN-γ in a genome-wide linkage analysis in the South African population and subsequently was termed *TNF1* (Cobat *et al*., 2013). Additionally, when both cohorts were combined there was also suggestive evidence for linkage with a region on chromosome 19q13, which had also been identified to be linked to magnitude of TNF production in response to BCG (Cobat *et al*., 2013; Cobat *et al*., 2015).

Measuring the diameter of the TST response, a quantitative trait, the intensity of TST was significantly linked ($p=9x10^{-6}$) to chromosomal region 5p15 (Cobat *et al*., 2009). Fine mapping of the 5p15 region identified one SNP (rs250682) that was significantly linked to lower intensity of TST response. This SNP was located in the gene *SLC6A3*, which encodes the solute carrier family 6 member 3. This amine transporter is related to SLC11A1 (NRAMP1), which has already been identified to play a role in susceptibility to tuberculosis (Cobat *et al*., 2009; Li *et al*., 2011b).

1.5.3. Antigen-specific lymphocyte proliferation as a surrogate marker for susceptibility to tuberculosis

Another phenotype that has been studied as a marker for genetic susceptibility to tuberculosis is antigen-specific lymphocyte proliferation (Wheeler *et al*., 2006). The frequency of IFN-γ secreting T-lymphocytes antigen-specific for PPD and BCG antigen was shown to be heritable to 53-74% in a South African population (Cobat *et al*., 2010). Proliferation of antigen specific lymphocytes in response to PPD stimulation has been shown to be significantly linked to a region on chromosome 1 in a genome-wide linkage analysis in a population from Brazil (Wheeler *et al*., 2006).

1.6. Genes linked to magnitude of mycobacterial antigen-driven IFN-γ responses of BCG vaccinated newborns

A GWLA conducted by Newport *at al.* described in section 1.5.1, studied IFN-γ responses to PPD and killed *M. tuberculosis* in BCG vaccinated newborns in a Gambian cohort. The study linked IFN-γ responses to three chromosomal loci (8q13-22, 10q23-25 and 11q23-25) (Newport *et al*. manuscript in preparation). Within these loci, two genes (*LY96* and *RIPK2*) were identified encoding proteins (MD-2 and RIP2 respectively) which are expressed in macrophages and dendritic cells and contribute to induction of pro-inflammatory cytokines leading to IFN-γ secretion from T-lymphocytes (Inohara et al., 1998; Newport, 2015; Shimazu et al., 1999). Both genes encode proteins that associate directly with PRRs, which induce activation of the transcription factor NF-κB by the canonical or classical NF-κB pathway (Fitzgerald *et al*., 2004; Philpott *et al*., 2014). Two further genes (*CHUK* and *NFKB2*) were located in the identified loci, encoding proteins inhibitor of nuclear factor κB kinase subunit α (IKK-α) and NF-κB2 respectively, which are part of the non-canonical or alternative NF-κB pathways. They are therefore involved in the regulation of more fundamental immunological processes such as immune cell differentiation and maturation (Sun, 2012). Additionally, one gene (*BTRC*), also located within the identified loci, encoded the F-box/WD repeat-containing protein 1A (β-TrCP) that is involved in the regulation of activation of both the canonical and the non-canonical NF-κB pathways (Scheidereit, 2006; Winston *et al*., 1999).

1.6.1. Proteins associated with pattern recognition receptors

Two genes, *RIPK2* (8q21.3) and *LY96* (8q21.11) encode the proteins receptor interacting kinase 2 (RIP2) and MD-2 also known as lymphocyte antigen 96 (Newport *et al*. manuscript in preparation). RIP2 and MD-2 directly interact with the PRRs NOD1, NOD2 and TLR4 respectively and are essential for either transduction of signals upon receptor activation or ligand sensing by the receptor (Kobayashi *et al*., 2002; Shimazu *et al*., 1999). Activation of these receptors results in activation of NF-κB and induction of pro-inflammatory cytokines (Fitzgerald *et al*., 2004; Philpott *et al*., 2014).

1.6.1.1. RIP2

RIP2 is a kinase that plays an essential role in the downstream signalling of the cytosolic receptors NOD1 and NOD2, which respond to the peptidoglycan fragments iE-DAP and MDP respectively (Girardin *et al*., 2003a; Girardin *et al*., 2003b; Inohara *et al*., 2003). Whereas NOD1 is expressed in a wide variety of cells, expression of NOD2 is restricted to cells of myeloid and lymphoid origin (Philpott *et al*., 2014). Induction of these receptors results in the induction of pro-inflammatory cytokines including TNF, IL-1β, IL-12p40 and IL-6 (Brooks *et al*., 2011; Fritz *et al*., 2005). Additionally, NOD2 is involved in NOD-dependent autophagy (Anand *et al*., 2011; Homer *et al*., 2012).

Upon stimulation, NOD receptors recruit RIP2 to the plasma membrane (Lecine *et al*., 2007). RIP2 directly binds to the NOD receptors through interaction of caspase recruitment domains (CARD), which are present in both NOD and RIP2 (Inohara *et al*., 2000; Ogura *et al*., 2001). Interaction between the NOD receptor and RIP2 results in autophosphorylation of RIP2 and recruitment of ubiquitin ligases including cIAP1, cIAP2, XIAP and Pellino3, which facilitate the attachment of K63-linked ubiquitin chains and the linear ubiquitin chain assembly complex (LUBAC) (Bertrand *et al*., 2009; Damgaard *et al*., 2012; Tigno-Aranjuez *et al*., 2010; Yang *et al*., 2013). The ubiquitin chains are thought to induce proximity between RIP2 and the TAK binding protein 2 (TAB2)/ TAB3/ TGF-β-activated kinase (TAK1) complex as well as the IKK complex consisting of NEMO, IKK-α and IKK-β. Association of these signalling complexes leads to the activation of TAK1, which in turn induces activation of mitogen activated protein (MAP) kinases and subsequent activation of activator protein 1 (AP-1) as well as the activation of IKK-β and subsequent activation of NF-κB, leading to induction of pro-inflammatory cytokines (Figure 1.2) (Hasegawa *et al*., 2008).

1.6.1.2. RIP2 kinase activity

RIP2 was initially identified as a serine/threonine kinase, based on homology (McCarthy *et al*., 1998; Thome *et al*., 1998). Later it was demonstrated that RIP2 was able to auto-phosphorylate on tyrosine residues and subsequently, a phosphorylation site was mapped to Y474. Upon

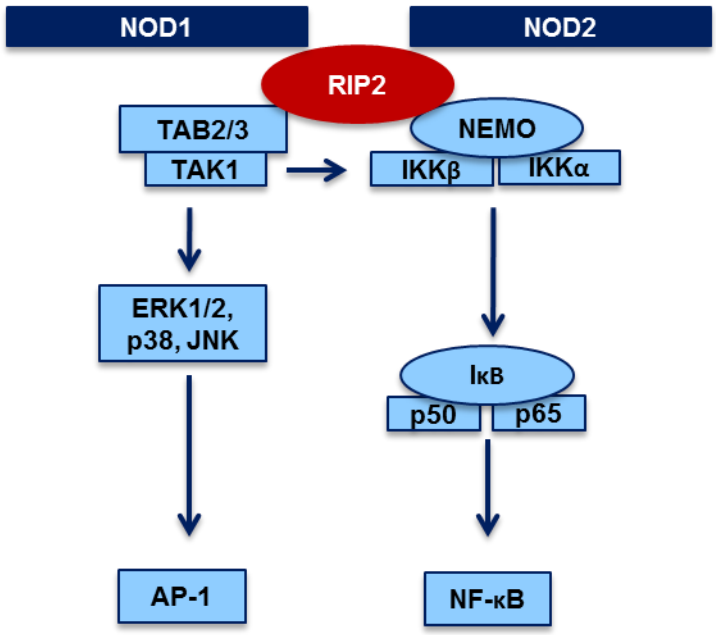

Figure 1.2 RIP2 and the NOD signalling pathways
Stimulation of the cytosolic nucleotide-binding oligomerization domain-containing proteins (NOD) receptors NOD1 and NOD2 results in interaction with the receptor interacting protein 2 (RIP2) inducing down stream signalling through TAK1-binding protein (TAB) and TGFβ-activated kinase (TAK), NF-kappa-B essential modulator (NEMO) and inhibitor of NF-κB kinase (IKK). This leads to activation of the transcription factor nuclear factor kappa-light-chain-enhancer of activated B cells (NF-κB) as well as activation of the mitogen activated protein (MAP) kinases; extracellular signal regulated kinase (ERK), p38 MAP kinase and c-Jun N-terminal kinase (JNK) resulting in activation of the transcription factor activator protein 1 (AP-1). Both transcription factors induce pro-inflammatory cytokines. IκB, Inhibitor of κB.

stimulation of the NOD signalling pathways Y474 becomes phosphorylated, leading to activation of NF-κB. RIP2 mutant Y474F, lacking the tyrosine phosphorylation site, and also the kinase inactive RIP2 mutant K47A both failed to induce tyrosine phosphorylation upon NOD2 stimulation in RIP2 transfected Human embryonic kidney (HEK) 293 cells (Tigno-Aranjuez *et al*., 2010). Additionally, S176 has been identified as an auto-phosphorylation site in a RIP2 construct lacking the CARD domain (Dorsch *et al*., 2006).

1.6.1.3. RIP2 kinase activity and RIP2 protein expression

Various studies have demonstrated that RIP2 kinase activity is essential to maintain the correct level of RIP2 protein expression (Nembrini *et al*., 2009; Windheim *et al*., 2007). RIP2 kinase is rendered inactive by mutation of an essential lysine residue, K47, in the ATP binding site and two conserved aspartic acid residues, D146 and D164, in the kinase domain (McCarthy *et al*., 1998; Thome *et al*., 1998; Windheim *et al*., 2007). All of these mutations have been shown to result in lower expression levels of RIP2 compared to wild type (Hasegawa *et al*., 2008; Lu *et al*., 2005; Nembrini *et al*., 2009; Windheim *et al*., 2007). Inhibition of kinase activity of wild type RIP2 using the kinase inhibitor SB203508 also affected protein stability, further supporting the hypothesis that protein stability of RIP2 can be attributed to lack of kinase activity (Windheim *et al*., 2007). Murine bone marrow derived macrophages expressing only the kinase inactive form of RIP2, which lacks an essential lysine residue in the ATP binding site (K47A and K47R), have been shown to express less RIP2 protein compared to wild type mice, although transcript levels were unaltered (Lu *et al*., 2005; Nembrini *et al*., 2009).

1.6.1.4. RIP2 kinase activity in downstream signalling

Reports regarding the importance of RIP2 kinase activity in downstream signalling are conflicting. Early findings suggested that RIP2 kinase activity was redundant for activation of NF-κB as over- expression of wild type RIP2 and kinase inactive RIP2 mutants equally induced activation of NF-κB and C-Jun N-terminal kinase (JNK) (Eickhoff *et al*., 2004; McCarthy *et al*., 1998; Thome *et al*., 1998). Two studies even found that the kinase dead mutants RIP2 D146A and D164A induced NF-κB and JNK activation more efficiently than wild type RIP2 in transfected HEK293 cells (Eickhoff *et al*., 2004; Windheim *et al*., 2007). Furthermore, over-expression of RIP2 in MCF7 human breast cancer carcinoma cells has been shown to induce extensive apoptosis. This apoptotic activity was independent of the protein's kinase activity as the kinase dead RIP2 variant RIP2 K47A and a truncated version of RIP2 lacking the kinase domain both induced apoptosis (McCarthy *et al*., 1998).

However, in contrast to these data, other studies suggest that RIP2 kinase activity is necessary for optimal NF-κB activation and cytokine responses. Navas *et al.* (1999) demonstrated that a kinase deficient variant of RIP2 D146A showed significantly reduced induction of AP-1 and the serum response element (SRE) promoters (Navas *et al*., 1999). Two studies found that kinase inactive forms of RIP2 mutated on K47 resulted in significantly lower but not completely abolished levels of NF-κB activation (Hasegawa *et al*., 2008; Inohara *et al*., 2000). However, Hasegawa *et al.* (2008) suggested the reduction of NF-κB activation was due to a lower RIP2 expression levels in the absence of kinase activity rather than lack of kinase activity *per se* (Hasegawa *et al*., 2008).

Tigno-Aranjuez *et al*. (2010) demonstrated that in HEK293 cells transiently transfected with a kinase dead RIP2 mutant, RIP2 failed to auto-phosphorylate. Subsequently, NOD2-dependent NF-κB activation was significantly reduced and cytokine responses were impaired (Tigno-Aranjuez *et al*., 2010). In mice expressing RIP2 K47A, stimulation of the NOD pathway also resulted in impaired inflammatory cytokine responses (Nembrini *et al*., 2009). Furthermore, inhibition of RIP2 kinase activity using the RIP2 kinase

inhibitor SB203508, significantly reduced MDP-induced NF-κB activation (Windheim *et al*., 2007).

The E3 ligase ITCH ubiquitinates phosphorylated RIP2 targeting it for inactivation, as in the absence of ITCH NOD-dependent activation of NF-κB and cytokine release is increased (Tao *et al*., 2009; Tigno-Aranjuez *et al*., 2010). Tigno-Aranjuez *et al*. (2010) subsequently hypothesised that phosphorylation of RIP2 might be required for down-regulation of NOD signalling (Tigno-Aranjuez *et al*., 2010). Additionally, RIP2 has been shown to potentiate caspase 8 induced apoptosis in the B-lymphocyte cell line BJAB and play a role in phosphorylation of Bcl10, a protein involved in TCR signalling. Both processes were shown to depend on RIP2 kinase activity (Inohara *et al*., 1998; Ruefli-Brasse *et al*., 2004).

1.6.1.5. RIP2 and RIP2 kinase activity in NOD-dependent autophagy

Upon entry of invasive bacteria into the cytosol, the NLRs NOD1 and NOD2 co-localise to the plasma membrane at the site of bacterial entry and recruit the autophagy-related protein 16-1 (ATG16L1) (Travassos *et al*., 2010). However, this process has been shown to be completely independent of the presence of RIP2. Nevertheless, RIP2 has been shown to contribute to autophagosome formation by NOD receptors (Homer *et al*., 2012; Homer *et al*., 2010). Studies using kinase inhibitors have shown that this process depends on the kinase activity of RIP2 (Homer *et al*., 2012). NOD-dependent autophagy has been shown to play a role in immune responses to intracellular bacterial pathogens such as *Salmonella flexneri* and *Listeria monocytogenes* (Anand *et al*., 2011; Travassos *et al*., 2010).

1.6.1.6. RIP2 in the immune response to tuberculosis

RIP2 kinase is essential for NF-κB activation upon stimulation of NOD1 and the NOD2 and hence plays a central role in the immune responses to *M. tuberculosis* elicited through these two receptors. The NOD1 receptor is thought to play only a minor role in macrophage response to *M. tuberculosis*, as macrophages from *Nod1*$^{-/-}$ mice were shown to produce TNF and IFN-β at similar levels to wild type macrophages (Ferwerda *et al*., 2005; Pandey *et al*.,

2009). Additionally, HEK293T cells expressing NOD1 only induced little activation of NF-κB upon stimulation with *M. tuberculosis* sonicates (Ferwerda *et al*., 2005).

The NOD2 receptor is expressed in cells of myeloid and lymphoid origin and stimulation of the receptor leads to the activation of NF-κB and AP-1 and subsequent secretion of pro-inflammatory cytokines as well as induction of NOD-dependent autophagy (Philpott *et al*., 2014). The NOD2 receptor recognises the peptidoglycan fragment MDP and infection with *M. tuberculosis* has been shown to induce NOD2 signalling in murine and human macrophages (Brooks *et al*., 2011; Inohara *et al*., 2003; Yang *et al*., 2007). The N-glycolylated version of MDP found in *M. tuberculosis* has been shown to be a more potent inducer of NOD2 compared to the acetylated version of MDP present in other bacteria (Coulombe *et al*., 2009). *M. tuberculosis* expressing acetylated MDP opposed to glycolyl-MDP has also been shown to induce significantly reduced levels of TNF (Hansen *et al*., 2014).

So far few studies have focused on immune responses induced by interaction of *M. tuberculosis* with NOD2 in human cells. Brooks *et al*. (2011) found that in human monocyte-derived macrophages depleted of NOD2 by transfection with small interfering RNAs (siRNA), levels of TNF and IL-1β were significantly reduced during infection with *M. tuberculosis* compared to macrophages transfected with scrambled control siRNA (Brooks *et al*., 2011). Indeed, macrophages from *Nod2*$^{-/-}$ mice have also been shown to produce significantly reduced levels of TNF and IL-12p40 when infected with *M. tuberculosis* (Divangahi *et al*., 2008; Gandotra *et al*., 2007; Yang *et al*., 2007). Pandey *et al.* (2009) demonstrated that in the absence of NOD2, *M. tuberculosis* infected murine bone marrow-derived macrophages (BMMs) induced reduced levels of IFN-α/β (mRNA and protein) compared to wild type macrophages (Leber *et al*., 2008; Pandey *et al*., 2009). Furthermore, induction of mRNA of the chemokine C-C motif chemokine 5, which depends on the stimulation of the cell by type I interferons, was almost abrogated (Pandey *et al*., 2009). Additionally, *M. tuberculosis* infected *Nod2*$^{-/-}$ murine BMMs stimulated with IFN-γ produced significantly reduced levels of NO relative to macrophages from wild type mice (Gandotra *et al*., 2007).

The NOD2 receptor synergistically responds to co-stimulation with TLR2 ligands resulting in increased levels of TNF, IL-1β and IL-6 (Ferwerda *et al*., 2005). In contrast, one study found that mRNA levels of TNF from *Nod2*$^{-/-}$ murine BMMs infected with *M. tuberculosis* were indistinguishable from wild type macrophages (Pandey *et al*., 2009). A more recent study found that levels of IFN-β production were unaffected in *M. tuberculosis* infected *Nod2*$^{-/-}$ BMMs (Manzanillo *et al*., 2012). Despite the reduced levels of IL-12p40, TNF, IFN-γ and NO in the absence of NOD2, survival and growth of *M. tuberculosis* was not affected in murine infection models (Divangahi *et al*., 2008; Gandotra *et al*., 2007). However, silencing of NOD2 in human monocyte-derived macrophages has been shown to result in significantly enhanced growth of *M. tuberculosis*, suggesting that there might be a difference in the requirement for NOD2-signalling during *M. tuberculosis* infection between humans and mice (Brooks *et al*., 2011).

NOD2 has been shown to play a role in the induction of autophagy during infection with *S. flexneri* and *L. monocytogenes* in HEK293 and murine BMMs, respectively (Anand *et al*., 2011; Travassos *et al*., 2010). Even though stimulation of NOD2 with synthetic MDP enhances autophagy-mediated clearing of *M. tuberculosis* bacilli in human infected alveolar macrophages, NOD-dependent autophagy has so far not been implicated in control of *M. tuberculosis* infection (Juarez *et al*., 2012).

1.6.1.7. MD-2

MD-2 is an accessory protein that associates with TLR4 (Shimazu *et al*., 1999). The protein has been shown to be essential for ligand binding of the receptor, which detects lipopolysaccharides (LPS) from gram-negative bacteria but also various other PAMPs (Fitzgerald *et al*., 2004). MD-2 was first described by Shimazu *et al*. in 1999 as a glycoprotein of 20-30kDa size that physically associated with TLR4 and conferred LPS responsiveness to the receptor (Shimazu *et al*., 1999). Activation of NF-κB and MAP kinases upon LPS stimulation of TLR-4 transfected HEK293 cells depended on the presence of MD-2 (Shimazu *et al*., 1999; Yang *et al*., 2000). Furthermore, MD-2 is

required for cell surface expression of TLR4 as in the absence of MD-2 the TLR4 receptor remains within the Golgi body (Nagai *et al*., 2002).

Stimulation of the TLR4-MD-2 complex results in induction of pro-inflammatory cytokines and chemokines. Signalling induced by TLR4-MD-2 involves pathways that are dependent and independent of the TLR adapter protein myeloid differentiation primary response protein MyD88 (MyD88). The MyD88 dependent pathways, induced by TLR4-MD-2, promote activation of NF-κB and cytokines such as IL-12, whereas the MyD88 independent pathways result in activation of the transcription factor IRF3 and lead to release of IFN-β and TNF as well as activation of NF-κB (Figure 1.3) (Fitzgerald *et al*., 2004). Primarily known to mediate responses to LPS, the TLR4-MD-2 complex has also been shown to be involved in immune responses to various other components of mammalian, bacterial and viral origin (Bulut *et al*., 2002; Flo *et al*., 2002; Ohashi *et al*., 2000; Rallabhandi *et al*., 2012). TLR4 is involved in detection of hsp such as *Chlamydia trachomatis* hsp 60 (Chsp60). Chsp60 has been shown to induce activation of NF-κB in RAW264.7 cells in a TLR4 and MD-2 dependent manner (Bulut *et al*., 2002). Furthermore, human hsp 60 has been shown to induce NO and TNF through TLR-4 (Ohashi *et al*., 2000). Other components detected by a TLR4-MD-2 complex include, the respiratory syncytial virus fusion protein and the mannuronic acid polymers that form the alginate capsule of *Pseudomonas aeruginosa* (Flo *et al*., 2002; Rallabhandi *et al*., 2012).

1.6.1.8. MD-2 during immune response to *M. tuberculosis*

M. tuberculosis has been shown to stimulate TLR4 via its antigens hsp 60, hsp 65 and hsp 70 (Bulut *et al*., 2005; Parveen *et al*., 2013). The presence of the TLR4 adapter protein MD-2 has been shown to be essential for at least hsp 65 and hsp 70 dependent TLR4 signalling (Bulut *et al*., 2005). Stimulation of murine macrophages with hsp 60, hsp 65 and hsp 70 results in secretion of TNF (Bulut *et al*., 2005; Parveen *et al*., 2013).

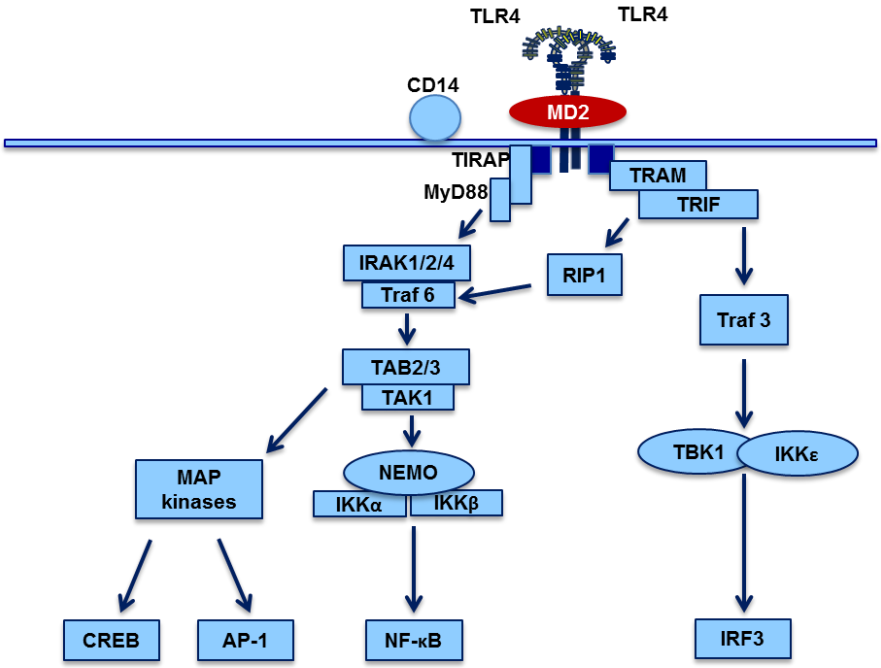

Figure 1.3 MD-2 and the TLR4 signalling pathway
Stimulation of the toll-like receptor (TLR) 4 receptor and its adapter protein MD-2 results in the receptor engaging with either the adapter proteins myeloid differentiation primary-response protein 88 (MyD88) and toll-interleukin 1 receptor (TIR) domain-containing adaptor protein (TIRAP) or the adapter proteins TIR domain-containing adapter protein inducing IFN-β (TRIF) and TRIF-related adapter molecule (TRAM). This leads to downstream signalling involving TNF receptor associated factors (TRAFs), IL-1R associated kinases (IRAKs), TAK1-binding protein (TAB), TGFβ-activated kinase (TAK) and TANK-binding kinase 1 (TBK1). This leads to activation of the transcription factors nuclear factor kappa-light-chain-enhancer of activated B cells (NF-κB), activator protein 1 (AP-1) and cyclic AMP-responsive element-binding protein (CREB) leading to induction of pro-inflammatory cytokine release as well as activation of the transcription factor interferon regulatory factor (IRF) leading to induction of type I interferons. NEMO, NF-kappa-B essential modulator; IKK, inhibitor of NF-κB kinase; MAP, mitogen activated protein; RIP1, receptor-interacting kinase.

In the case of hsp 60 the induction of TNF predominantly involved the activation of MAP kinase ERK1/2 (Parveen *et al*., 2013). In the absence of TLR4 the TNF response of murine macrophages to *M. tuberculosis* hsp65 was abolished and the response to hsp 70 was significantly reduced (Bulut *et al*., 2005). Even though *M. tuberculosis* hsp60 has previously been shown to also stimulate TLR2, in murine *Tlr4*$^{-/-}$ macrophages no TNF response was observed suggesting that *M. tuberculosis* hsp60 induced TNF solely through TLR4 (Parveen *et al*., 2013). A recent study by Lim *et al*. (2015) showed that TLR4 was also involved in the response to the mycobacterial 38kD antigen. Interaction of TLR4 with the 38kDa antigen was proposed to lead to endoplasmic reticulum stress responses and apoptotic cell death in murine macrophages (Lim *et al*., 2014).

However, *M. tuberculosis* infection studies in *Tlr4*$^{-/-}$ mice have produced conflicting results. Some studies found that TLR4 contributed to the immune response as TLR-4-deficient mice secreted significantly reduced levels of IL12p40, TNF and MCP-1, with the pulmonary recruitment of macrophages during infection being decreased. Additionally, increased mortality and bacterial load were observed during later stages of infection suggesting that TLR4 signalling contributed to the immune response in the late chronic phase of infection (Abel *et al*., 2002; Branger *et al*., 2004). In contrast other studies found that the absence of TLR4 had little effect on cytokine responses or survival of mice in high and low dose *M. tuberculosis* challenges (Kamath *et al*., 2003; Reiling *et al*., 2002)

1.6.2. Proteins involved in the regulation of NF-κB activation and the transcription factor NF-κB2

Three genes, *CHUK* (10q24.31), *BTRC* (10q24.32) and *NFKB2* (10q24.32) encoding proteins regulating activation of the transcription factor NF-κB or subunits of the transcription factor itself are present in the region on chromosome 10 that was linked to the magnitude of IFN-γ production in response to mycobacterial antigen (Newport *et al.* manuscript in preparation).

CHUK and *BTRC* encode IKK-α and β-TrCP, which are involved in activation of NF-κB transcription factors (Kanarek and Ben-Neriah, 2012; Liang *et al*., 2006; Liu *et al*., 2012). *NFKB2* encodes the p100 precursor protein of the NF-κB2/p52 transcription factor, which is processed into the mature form of the transcription factor upon activation of the NF-κB signalling pathway (Liang *et al*., 2006; Sun, 2012).

1.6.2.1. IKK-α, β-TrCP and NF-κB2 (p100/p52)

Stimulation of various receptors involved in innate and adaptive immune responses, including TLRs, NOD1 and NOD2, the IL-1 receptor, the TNF receptor (TNFR) and the TCR, results in activation of the transcription factor NF-κB (Hinz and Scheidereit, 2014). The family of NF-κB transcription factors consists of five structurally homologous proteins: NF-κB1/p50, NF-κB2/p52, RelA/p65, RelB and c-Rel (Hayden and Ghosh, 2014). All members of the transcription factor family share a common N-terminal domain (Rel homology domain), which facilitates the binding of the transcription factor to DNA (Hinz and Scheidereit, 2014). Under resting conditions the NF-κB proteins are maintained in the cytosol by NF-κB inhibitor proteins (IκB) in the form of homo- and heterodimers which translocate into the nucleus upon activation of an NF-κB signalling pathway (Kanarek and Ben-Neriah, 2012). The IKK complex, which consists of NEMO (also IKK-γ) and the serine threonine kinases IKK-α and IKK-β, is responsible for the regulation of the release of the NF-κB transcription factors sequestered in the cytosol (Liu *et al*., 2012). The IκB proteins are phosphorylated by either IKK-α or IKK-β targeting the IκB proteins for K48-polyubiquitination by the E3 ubiquitine ligase $SCF^{\beta\text{-}TrCP}$ complex and subsequent degradation by the proteasome (Kanarek and Ben-Neriah, 2012; Liu *et al*., 2012; Winston *et al*., 1999). The $SCF^{\beta\text{-}TrCP}$ complex consists of five proteins including the F-box protein β-TrCP, which is required for targeting the E3 ligase to the phosphorylated IκB (Winston *et al*., 1999). As a result, the transcription factor is released and translocated into the nucleus. The IκB family of NF-κB inhibitors consists of eight proteins IκBα/β/ε/ζ, IκBNS, Bcl-3 and the NF-κB transcription factor precursors p100 and p105 (Hayden and Ghosh, 2014). The NF-κB transcription factors p100

and p105 are translated as precursors that are structurally homologous to IκB and remain in the cytosol until they are processed by the proteasome into their mature forms p52 and p50 and subsequently translocate into the nucleus (Sun, 2012).

Stimulation of PRRs, cytokine receptors and antigen receptors results in the induction of the canonical NF-κB pathway (Figure 1.4) (Hinz and Scheidereit, 2014). The canonical NF-κB pathway commonly involves the IκB protein IκBα, the NF-κB heterodimers NF-κB1/RelA or NF-κB1/c-Rel and the E3 ubiquitine ligase complex $SCF^{\beta\text{-}TrCP}$ (Hinz and Scheidereit, 2014). This pathway has been shown to strictly depend on the presence of NEMO, whereas IKK-α is mostly dispensable (Silverman and Maniatis, 2001). Translocation of NF-κB1/RelA or NF-κB1/c-Rel induce transcription of genes involved in multiple cellular functions, however in terms of response to invading pathogens they are primarily involved in transcription of cytokines and chemokines (Wright and Silverstein, 1983).

The non-canonical NF-κB pathway is characterised by activation of primarily NF-κB2/RelB heterodimers in response to stimulation of a small number of specific receptors including CD40, B-lymphocyte activating factor (BAFF) receptor and lymphotoxin-α/β receptor (Figure 1.4) (Claudio *et al*., 2002; Dejardin *et al*., 2002). The non-canonical NF-κB pathway depends on IKK-α, but IKK-β and NEMO have been shown to be dispensable (Dejardin *et al*., 2002; Senftleben *et al*., 2001). Additionally, the NF-κB inducing kinase (NIK) as well as the E3 ubiquitine ligase complex $SCF^{\beta\text{-}TrCP}$ are required for induction of NF-κB2 precursor p100 processing (Ling *et al*., 1998; Malinin *et al*., 1997). The non-canonical NF-κB signalling pathway is involved in induction of genes that lead to the maturation of dendritic cells; differentiation of T-lymphocytes and thymic epithelial cells; B-lymphocyte maturation and survival; development of lymphoid organs and their architectural organization and bone metabolism (Karrer *et al*., 2000).

1.6.2.2. IKK-α, β-TrCP and NF-κB2 in the immune response to tuberculosis

Limited studies have focused on β-TrCP in the immune response against *M. tuberculosis*. However, it has been observed that in mice deficient for β-TrCP, the ubiquitination of IκBα, one of the main IκB proteins involved in signal transduction in the canonical NF-κB pathway, is impaired leading to inhibition of NF-κB activation (Nakayama *et al*., 2003). Various *M. tuberculosis* antigens induce the canonincal NF-κB pathway by stimulation of TLRs, NOD2, Dectin-1 and Mincle through a variety of signalling pathways that all converge on the IKK complex and consequently depend on the E3 ubiquitine ligase $SCF^{\beta\text{-}TrCP}$ complex (Bulut *et al*., 2005; Ferwerda *et al*., 2005; Ishikawa *et al*., 2009a; Prados-Rosales *et al*., 2011; van de Veerdonk *et al*., 2010). Induction of NOS and NO in response to mycobacterial ManLAM and IFN-γ has been shown to depend on an activated $SCF^{\beta\text{-}TrCP}$ complex in RAW264.7 cells (Morris *et al*., 2003). Furthermore, other receptors such as the TNF receptor, the IL-1 receptor and the TCR also induce the canonical NF-κB pathway, depend on the $SCF^{\beta\text{-}TrCP}$ complex and are involved in orchestrating the overall immune response to *M. tuberculosis* (Hinz and Scheidereit, 2014).

That this E3 ligase complex plays an important role in innate immune responses is further highlighted by the observation that several pathogens actively inhibit the $SCF^{\beta\text{-}TrCP}$ complex functions. Bacteria and viruses target β-TRCP and other proteins of the $SCF^{\beta\text{-}TrCP}$ complex to prevent ubiquitination of IκB proteins or other processes mediated by this complex (Diduk *et al*., 2008; Kim *et al*., 2005; van Buuren *et al*., 2014).

For example the bacterium *Shigella flexneri* injects effector proteins into the host cell using a type III secretion system including the protein OspG, which has been shown to interact with the E2 ligase UbcH5b that is part of the $SCF^{\beta TRCP}$ complex. Interaction of OspG with the $SCF^{\beta\text{-}TRCP}$ complex results in inhibition of TNF induced activation of NF-κB and *Shigella* strains lacking OspG induce stronger inflammatory responses compared to OspG-positive *Shigella* strains (Kim *et al*., 2005). Viruses have also targeted the same immune signalling pathway; the ectromelia virus, a murine poxvirus, prevents the activation of the NF-κB subunit RelA by directly targeting β-TrCP (van

Buuren *et al*., 2014). Furthermore, the Epstein-Barr virus protein LMP1, the HIV type 1 protein Vpu, and the vaccinia virus protein A49, have also been demonstrated to directly target β-TrCP, whereas rotaviruses induce degradation of β-TrCP (Coadou *et al*., 2003; Diduk *et al*., 2008; Evrard-Todeschi *et al*., 2006; Graff *et al*., 2009; Mansur *et al*., 2013) Additionally, β-TrCP has also been shown to contribute to processing of the p100 subunit of the noncanonical NF-κB activation pathway and may contribute to the immune response to tuberculosis in this way (Fong and Sun, 2002; Qu *et al*., 2004).

Both IKK-α and NF-κB2 are predominantly involved in the non-canonical NF-κB signalling pathway. Activation of NF-κB2, commonly as a heterodimer with RelB, is characteristic for the non-canonical NF-κB pathway. IKK-α is required for the translocation of NF-κB2/RelB heterodimer into the nucleus (Sun, 2012). The non-canonical NF-κB pathway has been shown to be essential for the development of γδ Th17 lymphocytes. Stimulation of the lymphotoxin β receptor induces the non-canonical NF-κB pathway resulting in activation of the transcription factors RORγt and RORα4, which in turn results in differentiation of thymic precursor lymphocytes into γδ Th17 lymphocytes. *Nfkb2*$^{-/-}$ mice have been shown to secrete reduced levels of IL-17 and mice deficient for RelB have been shown to have fewer IL17^{+} γδ T lymphocytes (Powolny-Budnicka *et al*., 2011).

IL-17 plays an important role in the induction of neutrophil-mediated immune responses and T-lymphocyte mediated IFN-γ responses in mycobacterial infection (Umemura *et al*., 2007). During infection with *M. bovis* BCG γδ T-lymphocytes have been shown to be the primary source of IL-17 in mice (Lockhart *et al*., 2006; Umemura *et al*., 2007). Mice deficient for IL-17 were shown to be impaired in their ability to form granulomas during mycobacterial infection even though little effect on other immune responses was observed (Okamoto Yoshida *et al*., 2010; Umemura *et al*., 2007).

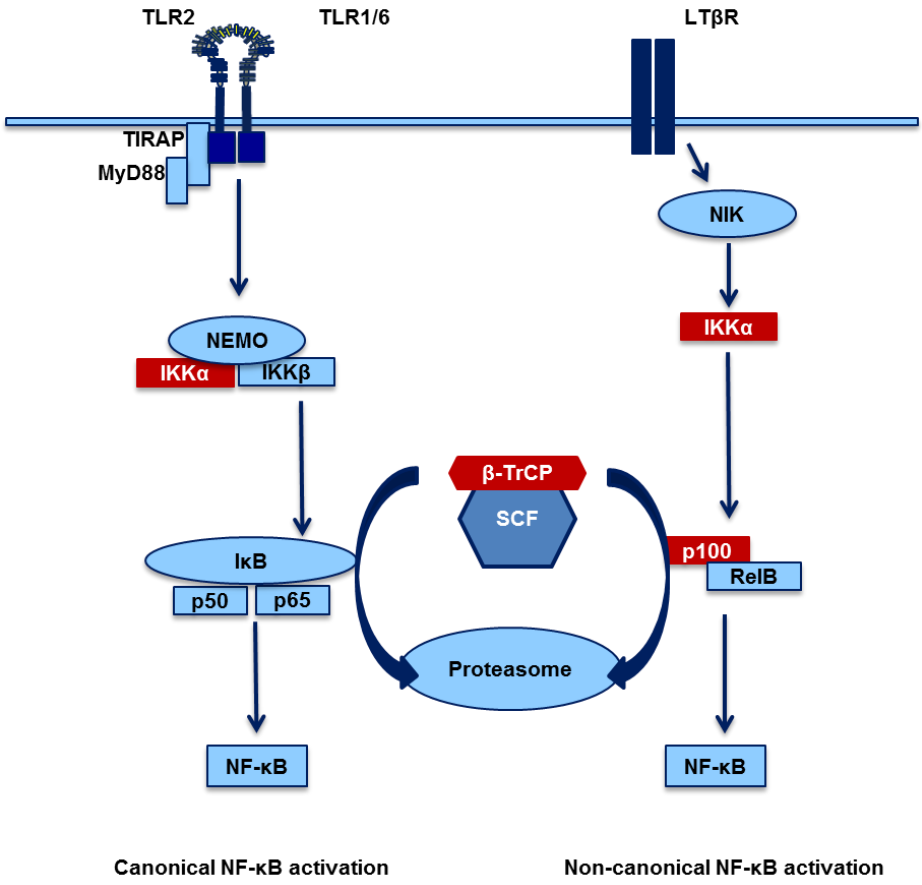

Figure 1.4 IKK-α, β-TrCP and NF-κB2 (p100/p52) as part of the canonical and non-canonical NF-κB signalling pathways
The Toll-like receptor (TLR) 2 and Lymphotoxin β receptor (LTβR) signalling pathways are shown as an example for the canonical and non-canonical NF-κB signalling pathway, respectively. Stimulation of TLR2 induces canonical NF-KB activation through the the inhibitor of NF-κB kinases (IKK) complex consisting of NF-κB essential modulator (NEMO) and the inhibitor of NF-κB kinases (IKK) α and IKKβ. IKKβ phosphorylates the inhibitor of κB (IκB) resulting in ubiquitination of IκB through the Skp, Cullin, F-box containing complex $(SCF)^{\beta\text{-}TrCP}$ and subsequent degradation of the IκB by the proteasome. This results in translocation of the NF-κB subunits p50 and p65 into the nucleus where they initiate transcription. Stimulation of the LTβR results in activation of the non-canonical NF-κB pathway, which depends on the NF-κB-inducing kinase (NIK) activating IKKα leading to phosphorylation of the p100 NF-κB subunit. Phosphorylated p100 is ubiquitinated by the $SCF^{\beta\text{-}TrCP}$ complex leading to processing of p100 into p52 and translocation of the transcription factor subunits p52 and RelB into the nucleus where they initiate transcription. MyD88, myeloid differentiation primary-response protein 88; TIRAP, toll-interleukin 1 receptor (TIR) domain-containing adaptor protein; β-TrCP, β-transducin repeat containing E3 ubiquitin protein ligase.

Additionally, IKK-α is part of the IKK complex, which is required for activation of the canonical NF-κB pathway (Liu *et al*., 2012). Only NEMO is completely essential for signal transduction in the canonical NF-κB pathway as IKK-β can compensate for the absence of IKK-α. However, IKK-α is not completely dispensable, as mouse embryonic fibroblasts from *Chuk*$^{-/-}$ mice have been shown to display reduced responses to stimulation with TNF and IL-1 even though the ability to activate NF-κB is not lost (Hu *et al*., 1999; Hu *et al*., 2001). This suggests that IKK-α contributes to an extent to the canonical NF-κB signalling pathway and may play a role in the immune response to *M. tuberculosis*.

1.6.3. Polymorphisms identified in candidate genes

To date no study has linked polymorphisms in *RIPK2* to susceptibility to infection with *M. tuberculosis*. However, two polymorphisms identified in *RIPK2* have been associated with susceptibility to infection with *M. leprae*. Additionally, the gene encoding NOD2, which directly associates with RIP2, has also been shown to carry polymorphisms that are associated with susceptibility to leprosy (Berrington *et al*., 2010; Grant *et al*., 2012; Sales-Marques *et al*., 2014; Zhang *et al*., 2011; Zhang *et al*., 2009).

Genome-wide association studies have linked the SNPs rs40457 and rs42490 in *RIPK2* to infection with *M. leprae* in a Chinese cohort and rs42490 to infection with *M. leprae* in a Vietnamese cohort (Grant *et al*., 2012; Zhang *et al*., 2011; Zhang *et al*., 2009). One of these SNPs (rs40457) was later found to interact with a SNP in *NOD2* (Zhang *et al*., 2011). Another study in an Indian cohort found no association between the polymorphisms rs40457 and rs42490 (Marcinek *et al*., 2013).

Additionally, a range of other polymorphisms identified in *NOD2* were associated with susceptibility to leprosy in various populations. These polymorphisms include rs8057341, which was associated with leprosy in a Brazilian cohort but not in a Vietnamese cohort (Grant *et al*., 2012; Sales-Marques *et al*., 2014). Further *NOD2* polymorphisms were associated with susceptibility to leprosy in a Nepalese cohort (Berrington *et al*., 2010). Several polymorphisms in *NOD2* have been associated with susceptibility to Crohn's

disease, however the *RIPK2* polymorphism rs2230801 was shown not be associated with increased susceptibility (Thiebaut *et al*., 2011).

Only one study to date has focused on the effect of MD-2 polymorphisms on susceptibility to tuberculosis. Xue *et al.* (2010) investigated -1625 G and 5 other commonly occurring SNPs in the promoter region of *LY96*, encoding MD-2, and demonstrated that there was no association between these polymorphisms and tuberculosis in the Chinese population (Xue *et al*., 2010). Additionally, one study found an association between two polymorphisms in *LY96* and gastric cancer induced by Helicobacter pylori-mediated inflammation (Castano-Rodriguez *et al*., 2014).

No polymorphisms identified in *NFKB2*, *CHUK* or *BTRC* have been associated with susceptibility to *M. tuberculosis* or any other bacterial infection.

1.7. Concluding remark

Tuberculosis is a major global health issue that affects almost one in three people globally claiming a life approximately every 20 seconds. MDR-TB and XDR-TB are on the rise globally and the only currently available vaccine, BCG, does not protect effectively against pulmonary tuberculosis in adults. Consequently new vaccines and treatments are urgently required to combat the global disease burden.

Host genetics have been shown to play a major role in susceptibility to tuberculosis and are a useful tool to identify immunological pathways which contribute to susceptibility/resistance to tuberculosis. Studies aiming to identify genes associated with susceptibility to tuberculosis have not been as informative as anticipated. Subsequently, a new model has been developed that uses BCG vaccination of newborns to identify genes associated with regulation of IFN-γ in response to mycobacterial antigen. These genes can then be studied to investigate functional effects of the genes on pathways involved in host-pathogen interaction.

1.8. Background and hypothesis

Only 10% of individuals that are infected with *M. tuberculosis* develop active disease suggesting that innate factors have a large influence on the outcome of infection (Kaufmann, 2001). A substantial amount of evidence points towards host genetics playing an important role in susceptibility to tuberculosis (Bellamy *et al*., 1998; Delgado *et al*., 2006; Khor *et al*., 2007; Li *et al*., 2011b; Stead *et al*., 1990; Stein *et al*., 2007). However, pinpointing genes that account for the difference in disease progression observed between infected individuals that do or do not get the disease has proven difficult (Newport, 2009). Studies aiming to associate host genes with susceptibility to tuberculosis have not been as informative as studies that aimed to identify the genetic basis of other diseases, such as Crohn's disease or cystic fibrosis (Hugot *et al*., 1996; Riordan *et al*., 1989). Subsequently, in recent years studies have started to focus on identifying genetic factors that determine the magnitude of immune effectors that play important roles during the immune response against *M. tuberculosis*, such as IFN-γ (Stein *et al*., 2003).

A genome-wide linkage analysis conducted by Newport *et al*. in the Gambia has linked the level of IFN-γ produced by BCG vaccinated newborns in response to stimulation with mycobacterial antigen to regions on chromosomes 8, 9 and 11. Within these three regions, five genes were identified that contribute to magnitude of IFN-γ response, namely *BTRC*, *CHUK*, *LY96*, *NFKB2* and *RIPK2* (Newport *et al*. manuscript in preparation).

1.9. Aims

1. To identify polymorphisms which potentially affect protein function, present in the candidate genes *RIPK2*, *LY96*, *NFKB2*, *CHUK* and *BTRC* in the Gambian population.

2. To determine the role of these candidate genes in the immune response to tuberculosis infection *in vitro* by infecting THP-1 derived macrophages depleted of the target gene with *M. tuberculosis*.

3. To characterise the effect of selected polymorphisms on protein function and immune responses.

2. Materials and Methods

2.1. Common buffers, media and gels

A number of buffers, media and gels were used repeatedly throughout the PhD and therefore have been tabulated with composition below for ease of presentation (Tables 2.1-2.3).

Buffer	Composition
ELISA wash buffer	Phosphate buffered saline, 0.1% (v/v) Tween 20[a]
Kinase reaction buffer	40mM Tris[b] (pH 7.5), 20mM $MgCl_2$[b]
NP40 cell lysis buffer	50mM Tris-HCl[a] (pH 7.4), 250mM NaCl[a], 5mM EDTA[a], 50mM NaF[b], 1mM Na_3VO_4[b], 1% (v/v) Nonidet P40[a], 0.02% (w/v) NaN_3[b]
Phosphate buffered saline (PBS)	137mM NaCl, 2.7mM KCl[a], 10mM Na_2HPO_4[a], 1.8mM KH_2PO_4[a] at pH 7.4
PBS-Tween (PBS-T)	137mM NaCl, 2.7mM KCl[a], 10mM Na_2HPO_4[a], 1.8mM KH_2PO_4[a] at pH 7.4, 0.05% (v/v) Tween 20
4x Running gel buffer	1.5M Tris-HCl (pH 8.8)
SDS-PAGE running buffer	192mM glycine[b], 25mM Tris, 0.1% (w/v) sodium dodecyl sulphate (SDS)[b]
4x SDS sample buffer	240mM Tris-HCl (pH 6.8), 8% (w/v) SDS, 40% (v/v) glycerol[b], 0.004% (v/v) bromophenol blue[b]
Sodium phosphate binding buffer	Sodium phosphate[a] 50mM (pH 8.0), 300mM NaCl, 0.01% (v/v) Tween 20
Sodium phosphate elution buffer	Sodium phosphate 50mM (pH 8.0), 300mM NaCl, 0.01% (v/v) Tween 20, 300mM imidazole[b]
Sodium phosphate lysis buffer	Sodium phosphate 50mM (pH 8.0), 300mM NaCl, 0.01% (v/v) Tween 20 , 1% (v/v) TritonX 100[a]
Sodium phosphate wash buffer	Sodium phosphate 50mM (pH 8.0), 300mM NaCl, 0.01% (v/v) Tween 20, 50mM imidazole
4x Stacking gel buffer	0.5M Tris-HCl (pH 6.8)
10x Tris borate EDTA (TBE) buffer	108g Tris, 55g boric acid[b], 20mM EDTA (pH 8.0) in 1l of H_2O
Tris buffered saline (TBS)	50mM Tris-HCl (pH 7.5), 150mM NaCl
TBS-Tween (TBS-T)	50mM Tris-HCl (pH 7.5), 150mM NaCl, 0.1% (v/v) Tween 20
Western blot transfer buffer	192mM glycine, 25mM Tris, 20% (v/v) methanol[a]

Table 2.1 Commonly used buffers

Reagents were purchased from: [a]Fisher Scientific, Loughborough, UK; [b]Sigma-Aldrich, Dorset, UK; [c]Oxoid, Basingstoke, UK; [d]Becton Dickinson, Oxford, UK; [e]Biorad, Hemel Hempstead, UK

Medium	Composition
Middlebrook 7H9 broth	1.88g Middlebrook 7H9[d], 40ml albumin dextrose complement (ADC)[d], 200µl Tween 80[b] and 360ml dH_2O
Middlebrook 7H10 agar	7.6g Middlebrook 7H10[d], 40ml oleic acid albumin dextrose complement (OADC)[d], 2ml glycerol and 360ml dH_2O
Luria-Bertani (LB) broth Lennox formulation	LB broth[a]: 10g tryptone, 5g yeast extract and 5g NaCl in 1L dH_2O
Nutrient agar plates	LB broth + 1.5% (w/v) Agar bacteriological[c]

Table 2.2 Commonly used media
Reagents were purchased from: [a]Fisher Scientific, Loughborough, UK; [b]Sigma-Aldrich, Dorset, UK; [c]Oxoid, Basingstoke, UK; [d]Becton Dickinson, Oxford, UK; [e]Biorad, Hemel Hempstead, UK

Gel	Composition
Polyacrylamide stacking gel	835µl 30% Acrylamide/Bis solution (29:1; Acrylamide:NN'-methylene bis acrylamide)[e], 1.25ml stacking gel buffer, 5µl Tetramethylethylenediamine, 0.1% (w/v) SDS, 0.15% (w/v) ammonium persulphate made up to 5 ml with dH_2O
10% polyacrylamide gel	3.3ml 30% Acrylamide/Bis solution (29:1; Acrylamide:NN'-methylene bis acrylamide)[e], 2.5ml running gel buffer, 10µl Tetramethylethylenediamine[a], 0.1% (w/v) SDS, 0.1% (w/v) ammonium persulphate[a] made up to 10 ml with dH2O

Table 2.3 Commonly used Acrylamide gels
Reagents were purchased from: [a] Fisher Scientific, Loughborough, UK;[b] Sigma-Aldrich, Dorset, UK; [c] Oxoid, Basingstoke, UK; [d] Becton Dickinson, Oxford, UK; [e] Biorad, Hemel Hempstead, UK

2.2. Polymerase chain reaction (PCR)

PCR amplification of Gambian DNA samples was carried out in a Mastercycler ep (Eppendorf AG, Hamburg, Germany) using 0.25µM forward and reverse primers, 0.8U iProof High-Fidelity DNA Polymerase (BioRad, Hemel Hempstead, UK), 200µM dNTPmix (Bioline Reagents Ltd, London, UK), 5x iProof High-Fidelity buffer (BioRad, Hemel Hempstead , UK) or 5x PCR optimiser kit buffer (Invitrogen, Paisley, UK) and 1mM or 2mM $MgCl_2$ (BioRad, Hemel Hempstead, UK), 10% DMSO (BioRad, Hemel Hempstead, UK) and at least 50ng genomic DNA in a 40µl reaction. PCR reactions were incubated for 30s at 98°C followed by 35 cycles of 98°C for 10s, 54°C – 65°C (depending on melting temperature of primer pairs) for 30s and 72°C for 45s with a final extension of 5min at 72°C. Primers were designed to amplify products 200bp up- and downstream of the targeted exons to include splice sites (Table 2.4-2.6).

PCR amplification of *RIPK2* was carried out in a Veriti 96-well Thermal cycler (Life Technologies, Paisley, UK). Full length *RIPK2* was PCR amplified from pDONR223-*RIPK2* (Addgene plasmid #23846) using the oligonucleotides listed in Table 2.7. PCR reactions contained 0.5μM forward and reverse primer, 0.5U iProof High-Fidelity DNA Polymerase, 200μM dNTPmix, 5x iProof High-Fidelity buffer and 1mM or 2mM $MgCl_2$ and at least 10ng of plasmid DNA in a 25μl reaction. PCR reactions were incubated for 30s at 98°C followed by 35 cycles of 98°C for 10s, 58°C – 60°C (depending on melting temperature of primer pairs) for 30s and 72°C for 30s with a final extension of 5min at 72°C. All oligonucleotides used as PCR primers (Table 2.4-2.7) were synthesised by Sigma-Aldrich (Sigma-Aldrich, Dorset, UK).

Target gene	Target exon		Primer	Sequence 5' – 3'
LY96	1	F	*LY96* E1F	TTCAGAGAAAGCCAAGCGTTA
		R	*LY96* E1R	ATGGCGTCAACATGAGTGTG
	2	F	*LY96* E2F	CCTTGCATGCAGGAGTCTTT
		R	*LY96* E2R	ATGGGAGACCTTGAAGCAGA
	3	F	*LY96* E3F	GAAGGCTCTTCTGTTTTTAGGC
		R	*LY96* E3R	TTCCAAGGAGGAACATAAAGG
	4	F	*LY96* E4F	TCCCCTAAGGGATAAGGTAGG
		R	*LY96* E4R	TCAGGAGGCTAAGGCAGGA
	5	F	*LY96* E5F	TTGTGATTCTAGATATTTGCGTGA
		R	*LY96* E5R	ACTCTTGCCCACATTCTTCC

Table 2.4 Oligonucleotides used for sequencing of *LY96* exons

Target gene	Target exon		Primer	Sequence 5' – 3'
NFKB2	1+2	F	*NFKB2* E2F	CAGACTGCCAGCCTCCTC
		R	*NFKB2* E2R	GACCCTGGTTTGGAGACAGA
	3	F	*NFKB2* E3F	CCTCGTGTCTGTCCACCTGT
		R	*NFKB2* E3R	AGCAGCAGTGACCATCCAAT
	4	F	*NFKB2* E4F	ACCCCCAGTCTGTCTCCAA
		R	*NFKB2* E4R	GGTCCAAGGGCATAGTAGCA
	5	F	*NFKB2* E5F	GCCTAAGCAGGTGAGTGAGC
		R	*NFKB2* E5R	CCTACTGGGCAGTCATGTCC
	6	F	*NFKB2* E6F	GGTGGTCTTCCCTGATCACA
		R	*NFKB2* E6R	GCCATGCAGTTCTTTCTTCC
	7	F	*NFKB2* E7F	CCAGTAGGTGCCCTCTACGC
		R	*NFKB2* E7R	AGGGAGAAGGAGCCATCACT
	8	F	*NFKB2* E8F	GGCCTCCGATTCTCTCTTCT
		R	*NFKB2* E8R	CAATAGCCAAGGCCACATTT
	9	F	*NFKB2* E9F	CCTCAAGCTGTGCAGTCAAA
		R	*NFKB2* E9R	CCCTAGCCCTGGGTACCTG
	10	F	*NFKB2* E10F	AAATGTGGCCTTGGCTATTG
		R	*NFKB2* E10R	CACCTTCCACCAGAGGGTAA
	11	F	*NFKB2* E11F	TAAATGGCCCCAGAGATTCC
		R	*NFKB2* E11R	TGCACCTCTTCCTTGTCTGG
	12	F	*NFKB2* E12F	TTACCCTCTGGTGGAAGGTG
		R	*NFKB2* E12R	ATACCTCGCTGCAGCATCTC
	13	F	*NFKB2* E13F	AACAGCGTGAAACCTCGTCT
		R	*NFKB2* E13R	GCCTACGTGTCTCCGTTCTC
	14	F	*NFKB2* E14F	CCTACAGCCCCTACCAGTCC
		R	*NFKB2* E14R	CTTAACGTTTCGCAGCACCT
	15	F	*NFKB2* E15F	GCTTGGTCTCTCCAAACTTCA
		R	*NFKB2* E15R	GGAGCTCCACTCTGAAGCAG
	16	F	*NFKB2* E16F	TTGAAAGCGAAGGATGCTCT
		R	*NFKB2* E16R	ACTGTCCACCAGCAGATCCA
	17	F	*NFKB2* E17F	TGGATCGGCATGGAGACT
		R	*NFKB2* E17R	TGAGACTGACCAGCCTTCAG
	18+19	F	*NFKB2* E18F	AGTGCCTGGATCTGCTGGT
		R	*NFKB2* E18R	CTGGGGATGCCTGATGCT
	19+20	F	*NFKB2* E19F	GCTGACATCCATGCTGAAAA
		R	*NFKB2* E19R	TCTGCAGAGCTGTATCACCAA
	21	F	*NFKB2* E20F	CAGCAGGTGAGAAGCATCAG
		R	*NFKB2* E20R	CTTGTCTCGGGTTTCTGGAC
	22	F	*NFKB2* E21F	TGCTAGACGGGCCAGAAG
		R	*NFKB2* E21R	GCAGGCAGCAGGTCAGTG
	23	F	*NFKB2* E22F	CTTTCCCGATCTGAGTCCAG
		R	*NFKB2* E22R	CCCCAAGGGCTTACTCTTTC

Table 2.5 Oligonucleotides used for sequencing of *NFKB2* exons

Target gene	Target exon		Primer	Sequence 5' – 3'
RIPK2	1	F	*RIPK2* F1	GGTGGTCGCTAACCAATCC
		R	*RIPK2* R1	GTGGAGGAATGCAACTGCT
	2	F	*RIPK2* F2	TTTAGCACTTTTACCTGTCAATG
		R	*RIPK2* R2	TCTCTTCCATTTCTACCCATGT
	3	F	*RIPK2* F3	TCAGCTGAAGAAAGACCCAAA
		R	*RIPK2* R3	GGTGATCTTGACAATTCAATTAAGA
	4	F	*RIPK2* F4	AGTCTCTCTTTTGAAATTTGTAATGTT
		R	*RIPK2* R4	TTCCAAGTCACATATGATAAAAATCC
	5	F	*RIPK2* F5	TCTTGCATGTAACGTTAAGCTTGT
		R	*RIPK2* R5	CAGGCGACAAAAATGAGGAC
	6	F	*RIPK2* F6	AAGCCCAAAATTAATGAGGTGA
		R	*RIPK2* R6	TTGTTACTCCTATCACACGATTTCTC
	7	F	*RIPK2* F7	TTTAGGTGTGTGGTTCATTTCA
		R	*RIPK2* R7	TGTCTGATATATAAGGGTTCTGGAAA
	8	F	*RIPK2* F8	CACTCCCAAAAATTCCCAAA
		R	*RIPK2* R8	GGCAGCAATGTTTTCCTCTC
	9	F	*RIPK2* F9	TTGATCGCAGGAGTTTGAGA
		R	*RIPK2* R9	CAGGTTCAAGCGATCTTTCC
	10	F	*RIPK2* F10	CACACAGGAAAAATATGGGACT
		R	*RIPK2* R10	GGTATAAATCACGGGGCAAA
	11	F	*RIPK2* F11.1	TGCCCCGTGATTTATACCAT
		R	*RIPK2* R11.1	ACTATCCTTTAAAAGTGGTTTCTGTT
		F	*RIPK2* F11.2	GCTTTATTGAAGGTTCTTTGGGTA
		R	*RIPK2* R11.2	AAAAAGTGCTCACACCGTACTTT

Table 2.6 Oligonucleotides used for sequencing of *RIPK2* exons

Target sequence		Sequence 5' – 3'
RIPK2	forward	GACAAGCTTATGAACGGGGAGGCCATCTGC
	reverse	GACTCTCGAGCGCATGCTTTTATTTTGAAGTA
HIS-*RIPK2*	forward	GACAAGCTTATGCATCATCACCATCACCATAACGGGGAGGCCATCTGCA
	reverse	GACTCTCGAGTTACATGCTTTTA

Table 2.7 Oligonucleotides used for cloning of *RIPK2* sequences
Restriction sites are underlined

2.3. Agarose gel electrophoresis

PCR products were resolved by agarose gel electrophoresis. Agarose gels contained 1% (w/v) agarose (Sigma- Aldrich, Dorset, UK), 1x TBE and either 0.01% (v/v) Ethidium bromide (Sigma-Aldrich, Dorset, UK) or 0.0015% (v/v) GelRed DNA stain (Biotium, CA, USA). Hyper ladder I (Bioline Reagents Ltd, London, UK) was used as a molecular weight marker and electrophoresis was carried out at 120V for 60–120 min. PCR products were visualised using a UV transilluminator (Gene Flash, Syngene BioImaging, UK).

2.4. SDS-Polyacrylamide gel electrophoresis (SDS-PAGE)

Cells were lysed in either NP-40 cell lysis or sodium phosphate lysis buffer for 30min on ice. Cell debris was pelleted by centrifugation or removed by filtration and supernatants were resolved on SDS-PAGE. Samples were mixed with 4x SDS sample buffer containing 5% (v/v) β-mercaptoethanol (Sigma- Aldrich, Dorset, UK) and boiled at 95°C for 10min prior to loading onto 10% (v/v) acrylamide gels. PageRuler Plus Prestained Protein Ladder (Fisher Scientific, Loughborough, UK) was used as a molecular weight marker. Gel electrophoresis was carried out at 200V for 75 min in SDS-PAGE running buffer.

2.5. Western blot analysis

Proteins were transferred from acrylamide gels to polyvenylidene difluoride (PVDF) membrane (Millipore, Watford, UK) at 400mA for 90min at 4°C in western blot transfer buffer. Membranes were blocked with either bovine serum albumin (BSA; Sigma-Aldrich, Dorset, UK) or milk (Marvel, Dublin, Ireland) depending on diluent of primary antibody (Table 2.8) overnight at 4°C. Purified RIP2 recombinant protein was detected with anti-V5 antibody (Life Technologies, Paisley, UK), anti-RIP2 antibody (RICK H-300; Santa Cruz

Biotechnology; Santa Cruz, CA) or anti-HIS (anti-HIS (C-term) HRP, Life Technologies, Paisley, UK). GAPDH was used as a loading control. Membranes were incubated with primary antibodies for 2h at room temperature (RT) at the dilutions listed in Table 2.8. Secondary HRP-conjugated antibodies were diluted in the same diluent as used for the primary antibody and were incubated for 1h at RT. Membranes were washed three times for 10min with either PBS-T or TBS-T after incubation with primary and secondary antibodies. Membranes were incubated with Amersham ECL Prime Western blotting Detection Reagent (GE Healthcare, Little Chalfont, UK) for 5min at RT before exposure to Amersham HyperfilmTM MP (GE Healthcare, Little Chalfont, UK). X-ray films were developed using x-ray processor SRX-101A (Konica Minolta, Basildon, UK).

2.6. Coomassie stain

For Coomassie staining of SDS-PAGE gels, acrylamide gels were washed with dH_20 for 15min before submerging in Gel Code Blue Stain Reagent (Fisher Scientific, Loughborough, UK) and incubated overnight at 4°C. Subsequently, gels were washed in dH_2O for 1h to yield a clear gel background.

2.7. Quantification of total protein

The total amount of protein present in cell lysates was quantified using Pierce™ BCA Protein Assay (Fisher Scientific, Loughborough, UK) according to the manufacturer's instructions.

2.8. Statistical analysis

Statistical analysis was performed using a two-tailed t-test in GraphPad Prism version 6.01 (GraphPad Software INC, SanDiego, CA). Results are expressed as mean ± SEM of at least three independent experiments or as mean ± SD when one representative experiment is shown. Significance was defined as * $p<0.05$ and ** $p< 0.01$.

Antigen	Antibody	Isotype	Diluent	Dilution used	Supplier
RIP2	Anti-RICK (H300)	Rabbit polyclonal IgG	3 % milk in TBS-T	1:200	Santa Cruz Biotechnology, San Diego, CA
V5-epitope	Anti-V5	Mouse monoclonal IgG_{2a}	5 % milk in PBS-T	1:5000	Life Technologies, Paisley, UK
C-terminal HIS	anti-HIS (C-term) HRP	Mouse monoclonal IgG_{2b}	5 % milk in PBS-T	1:5000	Life Technologies, Paisley, UK
GAPDH	GAPDH (14C10) Rabbit mAb	Rabbit monoclonal IgG	5 % BSA in TBS-T	1:5000	Cell Signalling Technology, Leiden, Netherlands
Mouse IgG	Anti-Mouse-IgG (Fab specific) Peroxidase antibody	HRP conjugated goat IgG	as primary antibody	1:20000	Sigma, Dorset, UK
Rabbit IgG	Anti- Rabbit- IgG (whole molecule) peroxidase antibody	HRP conjugated goat IgG	as primary antibody	1:25000	Sigma, Dorset, UK

Table 2.8 Antibodies used for western blot analysis

2.9. Study populations

A previous study investigating immune responses to BCG vaccination in the Gambia had enrolled a total of 236 singleton newborn babies and DNA was extracted from cord blood samples collected from all babies. Further details of this study and the immune responses measured have been published elsewhere (Finan *et al*., 2008). A total of 30 of these DNA samples were randomly selected for sequencing of candidate genes.

For SNP genotyping, 211 DNA samples from the above cohort and 309 DNA samples collected from a separate but similar study of immune responses to BCG in new-born twins were included (Finan *et al*., 2008; Newport *et al*., 2004). Genomic DNA had been extracted in the Gambia from cord-blood using a standard phenol-chloroform extraction method. In both studies, infants were vaccinated with BCG (BCG Denmark, Statens Serum Institute) within 24h of birth and IFN-γ responses to mycobacterial antigen was measured when infants were either 2 months (singleton cohort) or 5 months of age (twin cohort) (Finan *et al*., 2008; Newport *et al*., 2004).

2.10. DNA sequencing and sequence analysis

For DNA sequencing, PCR products were either PCR-purified or gel-extracted using QIAquick PCR purification kit or QIAquick gel extraction kit (QIAGEN, West Sussex, UK). Sequencing was carried out by Eurofins MWG Operon LLC (Eurofins Genomics, Ebersberg, Germany) using the same primer as for DNA PCR amplification (Tables 2.4-2.6). DNA sequences were aligned to reference sequences available in the ensemble database (Ensembl release 66-69) (Flicek *et al*., 2014) using Geneious version 5.5.6–6.1.5 (http://www.geneious.com).

2.11. Genotyping

Two SNPs (rs16900617 and rs40457) were previously genotyped for 518 newborns selected from both Gambian cohorts as part of a GWAS study led by Dr. Chris Finan. The SNPs were genotyped using Affymetrix's GeneChip® Mapping SNP 6.0 Array (Affymetrix, Santa Clara, CA) by Atlas Biolabs (Atlas Biolabs, Berlin, Germany).

A further four SNPs (rs2230801, rs35004667, rs10282832, rs42490) were genotyped during the course of this PhD in 269 infants from both Gambian cohorts. Genotyping of these SNPs was carried out by LGC Genomics (LGC Genomics, Herts, UK) by Kompetetive Allele Specific PCR (KASPTM) genotyping assay (He *et al*., 2014a).

2.12. IFN-γ response of BCG vaccinated newborns

Ex vivo IFN-γ response to mycobacterial antigen was measured in two cohorts of BCG vaccinated Gambian infants in the two previous studies described above (Finan *et al*., 2008; Newport *et al*., 2004). In the Finan *et al*. (2008) study, IFN-γ responses were measured 2 months post vaccination in a whole blood assay whereas Newport *et al*. (2004) measured IFN-γ response 5 months post vaccination in PBMCs (Finan *et al*., 2008; Newport *et al*., 2004). Further details of methodology used in each study can be found elsewhere, but briefly:

For the singleton study, 1-2ml of heparinized blood was diluted in RPMI 1640 medium (BioWittaker, Verviers, Belgium) and incubated in duplicate with mycobacterial or control antigen in 96-well plates (200µl/well) (Becton Dickinson, Rutherford, NJ) (Finan *et al*., 2008). Blood samples were stimulated with 10µg/ml PPD-RT49 (Statens Serum Institute, Denmark), 10µg/ml killed *M. tuberculosis* (Institute Pasteur du Brabant, Belgium), 10µg/ml *M. tuberculosis* short term culture filtrate (Statens Serum Institute, Denmark) or *M. bovis* BCG Ag85 complex (Institute Pasteur du Brabant, Belgium) for six days. Blood samples were stimulated with phytohaemaglutinin (Sigma Aldrich, Dorset, UK) for 2 days as positive control or incubated with medium alone as negative control. IFN-γ levels were measured using a commercially available enzyme-linked immunosorbent assay (ELISA) kit (BioSource, Europe, Fleurus, Belgium) with the lower limit for IFN-γ detection of 10pg/ml used as a cut-off for positive response.

For the twin study, PBMCs were isolated from blood samples by lymphoprep (Nycomed, Oslo, Norway) density gradient centrifugation and resuspended in RPMI 1640 supplemented with human AB serum (Sigma-Aldrich, ST Louis, MO). PBMCs were stimulated with 10µg/ml PPD-RT49

(Statens Serum Institute, Denmark), 10µg/ml killed *M. tuberculosis* (Institute Pasteur du Brabant, Belgium), 10µg/ml *M. tuberculosis* short term culture filtrate (Statens Serum Institute, Denmark) or *M. bovis* BCG Ag85 complex (Institute Pasteur du Brabant, Belgium) and 10µg/ml hsp 65 (GBF, Braunschweig, Germany). IFN-γ responses were measured in cell supernatants 6 days post stimulation using a commercially available ELISA kit (BioSource, Europe, Fleurus, Belgium). IFN-γ response was baselined by subtracting the IFN-γ production in unstimulated controls.

2.13. Cloning of wild type and variant *RIPK2*

2.13.1. Cloning strategy

Full length *RIPK2* was PCR amplified from pDONR223-*RIPK2* (Addgene plasmid #23846) using the oligonucleotides listed in table 2.7 (Sigma-Aldrich, Dorset, UK). The wild type (wt) *RIPK2* sequences were amplified as either full length *RIPK2* or as full length *RIKP2* with an N-terminal polyhistidine (HIS)-tag or N-terminal HIS-tag with a 15bp sequence separating the HIS-tag from the start of the *RIPK2* open reading frame. Sequences of HIS-tagged *RIPK2* encoded a stop codon at the C-terminus. *RIPK2* sequences were cloned into the expression vector pcDNA^{TM}6B (Invitrogen, Paisley, UK), using restriction sites *HindIII* and *XhoI* to create the plasmids pcDNA6_*RIPK2*wt_V5/HIS, pcDNA6_HIS*RIPK2*wt and pcDNA6_HIS_*RIPK2*wt (Table 2.9). Plasmid maps were drawn using Snap Gene® software (GSL Biotech LLC, Chicago, IL) (Appendix: Figures 9.1-9.6).

2.13.2. *E. coli* strain and culture conditions

NEB 5-alpha (genotype: *fhuA2* Δ(*argF-lacZ*)*U169 phoA glnV44*Φ*80*Δ (*lacZ*)M15 *gyrA96 recA1 relA1endA1 thi-1hsdR17*) competent *E. coli* (Subcloning Efficiency) (New England Biolabs, Hitchin, UK) were used for all

Plasmid	Recombinant Protein encoded	Restriction sites	Constitutively expressed	Expression enhanced by NF-κB activation	Experiments
pcDNA6B_*RIPK2*wt _V5/HIS	RIP2 wt V5/HIS	*HindIII*; *XhoI*	yes	yes	RIP2 affinity purification/ NF-κB/ AP-1 activation assay
pcDNA6B_*RIPK2*I259T _V5/HIS	RIP2 I259T V5/HIS	*HindIII*; *XhoI*	yes	yes	NF-κB/ AP-1 activation assay
pcDNA6B_*RIPK2*L268V _V5/HIS	RIP2 L268V V5/HIS	*HindIII*; *XhoI*	yes	yes	NF-κB/ AP-1 activation assay
pcDNA^{TM}6B	-	-	yes	yes	NF-κB/ AP-1 activation assay
pcDNA6_HIS*RIPK2*wt	HIS RIP2 wt	*HindIII*; *XhoI*	yes	yes	RIP2 affinity purification
pcDNA6_HIS*RIPK2*I259T	HIS RIP2 I259T	*HindIII*; *XhoI*	yes	yes	RIP2 affinity purification
pcDNA6_HIS*RIPK2*L268V	HIS RIP2 L268V	*HindIII*; *XhoI*	yes	yes	RIP2 affinity purification

Table 2.9 Plasmids used for *RIPK2* expression

transformations. *E. coli* were cultured in LB broth or were plated on nutrient agar plates. Cultures were incubated overnight at 37°C with shaking at 220rpm. Plates were incubated overnight at 37°C static. Growth media were supplemented with antibiotics where appropriate; 200µg/ml carbenicillin (Sigma Aldrich, Dorset, UK) or 10µg/ml spectinomycin (Sigma Aldrich, Dorset, UK). For frozen stocks 500µl of overnight liquid culture weas mixed with 500µl of 50% (v/v) glycerol and aliquots were stored at -80°C.

2.13.3. Transformation of *E. coli*

Plasmids were transformed into NEB 5-alpha Competent *E. coli* (Subcloning Efficiency) according to manufacturer's instructions with only minor amendments to the protocol. *E. coli* were thawed on ice and 50µl competent bacteria were mixed with 1–100ng plasmid DNA and left on ice for 30min. Cells were heat-shocked at 42°C for 30sec and placed on ice for a further 5min. 950µl of LB broth was added and the bacteria were grown at 37°C with shaking for 60min. Bacteria were plated on selective media and incubated overnight at 37°C.

2.13.4. Extraction of plasmid DNA

Overnight cultures of bacteria were pelleted by centrifugation at 3000 x g for 10min. Plasmid DNA from 5ml and 200ml cultures were purified using QIAprep® Spin Miniprep Kit and EndoFree® Plasmid Maxi Kit (QIAgen, Manchester, UK) respectively according to manufacturer's instructions.

2.13.5. DNA extraction

PCR amplified *RIPK2* DNA was resolved on 1% (w/v) agarose (Sigma-Aldrich, Dorset, UK) gels containing 0.001% (v/v) ethidium bromide (Sigma-Aldrich, Dorset, UK) and was extracted from the gel using a QIAquick® gel extraction kit (QIAgen, Manchester, UK) according to the manufacturer's instructions.

2.13.6. Restriction digestion and ligation

Digestion of *RIPK2* PCR products and pcDNA™6 was performed using restriction enzymes *HindIII*-HF and *XhoI* (New England Biolabs, Hitchin, UK).

10µg of DNA was digested in Cut Smart™ buffer (New England Biolabs, Hitchin, UK) overnight at 37°C. Subsequently, restriction enzymes were heat inactivated for 20min at 80°C. *RIPK2* PCR products and pcDNA™6 were ligated using T4 DNA ligase and T4 DNA ligase reaction buffer (New England Biolabs, Hitchin, UK) and incubated overnight at 4°C. Ligase was heat inactivated by incubation at 65°C for 10min before transformation of *E. coli*.

2.13.7. Site directed mutagenesis

Plasmids for expression of RIP2 variants RIP2 I259T (rs2230801) and RIP2 L268V (rs35004667) were created from pcDNA6B_HIS*RIPK2*wt (pcDNA6_HIS*RIPK2*I259T and pcDNA6_HIS*RIPK2*L268V) or pcDNA6B_*RIPK2*wt_V5/HIS (pcDNA6_*RIPK2*I259T_V5/HIS and pcDNA6_*RIPK2*L268V_V5/HIS) by site directed mutagenesis using the QuikChange Lightning Site-Directed Mutagenesis Kit (Agilent Technologies, Wokingham, UK) (Table 2.9). Oligonucleotides used for mutagenesis were synthesised and HPLC purified by Sigma-Aldrich (Sigma-Aldrich, Dorset, UK) (Table 2.10). Mutant strand synthesis from 50ng of DNA template and digestion of template DNA was carried out according to manufacturer's instructions. Subsequently, NEB 5-alpha Competent *E. coli* (Subcloning Efficiency) were transformed with the mutated plasmid as described in section 2.13.3.

Target sequence		Sequence 5' – 3'
rs2230801	F	AAGAAAGTTTGCCATATGATA**C**ACCTCACCGAGCACGTATG
	R	CATACGTGCTCGGTGAGGT**G**TATCATATGGCAAACTTTCTT
rs35004667	F	CGAGCACGTATGATCTCT**G**TAATAGAAAGTGGATGGG
	R	CCCATCCACTTTCTATTA**C**AGAGATCATACGTGCTCG

Table 2.10 Oligonucleotides used for site directed mutagenesis
The mutated base is shown in red.

2.13.8. Sequencing of DNA constructs

The sequences of all generated DNA constructs were confirmed by sequencing across the entire length of the insert. Sequencing primers were synthesised by Sigma-Aldrich (Sigma-Aldrich, Dorset, UK) and sequencing performed by Eurofins MWG Operon LLC (Eurofins Genomics, Ebersberg, Germany).

2.14. Cell lines and culture conditions

THP-1 Blue™ cells, a derivative of the human monocytic cell line THP-1 and HEK-Blue™ hNOD2 cells, a derivative of the human embryonic kidney cell line HEK293 were purchased from Invivogen (Invivogen, San Diego, CA).

THP-1 Blue™ cells stably express a secreted embryonic alkaline phosphatase (SEAP) reporter gene under the control of a promoter fused to five AP-1 and NF-κB binding sites. HEK-Blue™ hNOD2 express the same SEAP reporter gene and are also stably transfected with human *NOD2*.

THP-1 and THP-1 Blue™ cells were routinely cultured in RPMI 1640 medium containing L-glutamine (Invitrogen, Paisley, UK) whereas HEK293T and HEK-Blue™ hNOD2 cells were cultured in Dulbecco's Modified Eagle Medium (GE Healthcare, Little Chalfont, UK). Growth media were supplemented with 10% foetal bovine serum (FBS) (Invitrogen, Paisley, UK) and all cells were grown in the presence of 1% (v/v) HyClone™ Penicillin-Streptomycin solution (GE Healthcare, Little Chalfont, UK) and 100µg/ml Normocin™ (Invivogen, San Diego, CA) with exception of THP-1 cells used for *M. tuberculosis* infections, which were grown in antibiotic-free media. THP-1 blue™ cells were grown in the presence of 200µg/ml Zeocin™ (Invivogen, San Diego, CA). HEK-Blue™ hNOD2 cells were grown in the presence of 200µg/ml Zeocin™ and 100µg/ml Blasticidin (Invivogen, San Diego, CA). Cells were incubated at 37°C in a 5% CO_2 humidified incubator and passaged when 70% confluent.

2.15. Transient transfection of cell lines

THP-1, HEK293T and HEK-Blue™ hNOD2 were transiently transfected using chemical transfection reagents or electroporation with a plasmid containing the gene for green fluorescent protein (GFP) (pmaxGFP), a *Renilla* luciferase (pRL-CMV), a firefly luciferase (pGNL6) (Table 2.11) or the

Plasmid	Protein encoded	Constitutively expressed	Expression enhanced by NF-κB activation	Experiments	Reference
pGNL6	Firefly luciferase	no	yes	Optimisation of THP-1 transfection	(Khoury *et al*., 2007)
pRL-CMV	*Renilla* luciferase	yes	yes	Optimisation of THP-1 transfection	Promega (Promega, Southampton, UK)
pmaxGFP	Green fluorescent protein	yes	yes	Optimisation of THP-1 transfection	Lonza (Lonza, Cologne, Germany)

Table 2.11 Reporter plasmids used

Experiment	Plasmid	Culture vessel / amount of DNA (µg) used per well	Cell type/ no cells plated	Transfection reagent	Diluent	Volume transfection reagent (µl)	Total volume transfection complex (µl)	Incubation time (min)	Supplier
Optimisation of protocol for THP-1 transfection	pmaxGFP	12 well plate/ 2	THP-1 $4x10^5$ or HEK293T $2x10^5$	xtremeGene HP	opti-MEM	3	100	20-30	[a]
				FuGene6	opti-MEM	10	100	15	[b]
				JetPEI	NaCl	6	100	30	[c]
				PEI (1mg/ml)	opti-MEM	6	100	30	[d]
	pGR_CMV	96 well plate/ 0.2	THP-1 $1x10^5$ or HEK293T $0.5x10^5$	xtremeGene HP	opti-MEM	0.3	10	20-30	[a]
				FuGene6	opti-MEM	1	10	15	[b]
				JetPEI	NaCl	0.6	10	30	[c]
				PEI (1mg/ml)	opti-MEM	0.6	10	30	[d]
Purification of recombinant RIP2	pcDNA6_HIS*RIPK2*wt pcDNA6_HIS*RIPK2*I259T pcDNA6_HIS*RIPK2*L268V	$10cm^2$ plate/ 25	HEK293T $2x10^6$	PEI (1mg/ml)	opti-MEM	75	1000	30	[d]
NF-κB/AP-1 activation assay	pcDNA_*RIPK2*wt_V5/HIS pcDNA6_*RIPK2*I259T_V5/HIS pcDNA6_*RIPK2*L268V_V5/HIS	24 well plate/ 2	HEK-Blue™ hNOD2 $2x10^5$	xtremeGene HP	opti-MEM	3	100	20-30	[a]

Table 2.12 Transfections and transfection reagents used

[a] Roche, Burgess Hill, UK; [b] Promega, Southampton, UK; [c] Polyplus-transfection Inc, New York, NY; [d] Polysciences, Inc, Warrington, PA

recombinant RIP2-encoding plasmids described in sections 2.13.1 and 2.13.7.

2.15.1. Transfection using chemical reagents

For transfection using chemical transfection reagents, HEK293T/HEK-BlueTM hNOD2 cells were plated and allowed to adhere 24h prior to transfection, whereas THP-1 cells were plated and transfected simultaneously. Transfection complexes were formed at RT before being added drop-wise to wells of the tissue culture plate. Details of all transfections are listed in table 2.12.

2.15.2. Transfection by electroporation

THP-1 cells were transiently transfected with pGNL6 by nucleofection using a nucleofector 2B (Lonza, Cologne, Germany) according to the manufacturer's instructions. $1x10^6$ cells were resuspended in 100µl nucleofector solution V (Lonza, Cologne, Germany) containing 0.5µg of DNA. Cells were transfected using the THP-1 high viability programme U-001. Cells were plated immediately in 1.5ml RPMI complete medium in 12-well plates (Corning, Corning NY).

2.16. Fluorescence microscopy

pMAX-GFP transfected cells were grown in 6-well plates on 1.5cm glass cover slips coated with 30µg poly-L-ornithine (Sigma-Aldrich, Dorset, UK). Cover slips were fixed in 4% paraformaldehyde (Sigma-Aldrich, Dorset, UK) for 5min and washed with PBS before being incubated with DAPI (Sigma-Aldrich, Dorset, UK) dissolved in PBS containing 0.1% (v/v) Triton X100. Slides were mounted on microscope slides with anti-fade mounting medium (Citifuor LTD, London, UK). Fluorescence was visualised using a Leica DM 5000B microscope.

2.17. Luciferase assays

The enzyme activity of luciferase from two species (the firefly *Photinus pyralis* and the sea pansy *Renilla reniformis*) was measured. Firefly luciferase was expressed under the control of an experimentally inducible promoter

containing six NF-κB binding sites, whereas *Renilla* luciferase was under the control of a promoter that resulted in constitutive expression, which could be enhanced through NF-κB binding sites fused with the promoter.

Renilla luciferase activity of cells transfected with pRL-CMV was assayed using the *Renilla* Luciferase Assay System (Promega, Southampton, UK). Cells were washed with PBS before lysis in 50µl of 1x *Renilla* Luciferase Assay Lysis Buffer and incubation for 15min at RT.

Subsequently, 10µl of cell lysate was mixed with 20µl of luciferase assay buffer containing luciferase assay substrate. Luminescence was measured immediately in white opaque 96-well plates (Nunc, Roskilde, Denmark) on a Synergy HT plate reader (BioTEK, Potton, UK).

The luciferase activity present in THP-1 cells transfected with an NF-κB driven luciferase reporter plasmid (pGNL6) was measured using the Steady-Glo® luciferase assay (Promega, Southampton, UK). Cells were pelleted in V-bottom spin plates (Fisher Scientific, Loughborough, UK) by centrifugation at 270 x g for 10min before resuspension in 50µl Steady-Glo® luciferase reagent. Cells were incubated for 10min at RT and luminescence was read in 20µl of cell lysate in a white opaque 96-well plate on a Synergy HT plate reader.

2.18. Gene silencing in cell lines

RIPK2 expression was silenced in HEK-Blue™ hNOD2 and THP-1 cells by transfection with Silencer® Select *RIPK2* siRNA #s247 (Life Technologies, Paisley, UK). Silencer® Select Negative Control No.2 siRNA (Life Technologies, Paisley, UK) was used as a scrambled control for all siRNA transfections. Knock down of RIP2 was confirmed by western blot analysis.

2.18.1. Gene silencing in HEK-Blue™ hNOD2 cells

HEK-Blue™ hNOD2 cells were plated at a density of $1x10^5$ cells per well in 24-well plates in DMEM complete medium 48h prior to transfection. Immediately prior to transfection with *RIPK2* or scrambled control siRNAs, culture medium was replaced with DMEM without antibiotics (Penicillin, Streptomycin, Normocin, Blasticidin, Zeocin). To form transfection complexes, 1µl of lipofectamine RNAiMAX reagent (Life Technologies, Paisley, UK) and

50µM siRNA were diluted in 50µl of opti-MEM each, mixed together and incubated for 15min at RT. Transfection complexes were added drop-wise to wells of a tissue culture plate and incubated at 37°C for 48h.

2.18.2. Gene silencing in THP-1 cells

THP-1 cells were transfected with siRNAs by nucleofection using a nucleofector 2B according to the manufacturer's instructions. $1x10^6$ cells were resuspended in 100µl nucleofector solution V (Lonza, Cologne, Germany) containing 300nM siRNA. Cells were transfected using the THP-1 high efficiency programme V-001. After electroporation cells were plated immediately in 500µl RPMI complete medium containing 20nM Phorbol 12-myristate 13-acetate (PMA; Sigma-Aldrich, Dorset, UK,) in 48-well plates (Corning, Corning NY) to differentiate cells into macrophage-like cells. After stimulation with PMA for 24h the medium was replaced with PMA-free RPMI medium and cells were left to recover for a further 24h.

2.19. Cell viability assays

Cell viability of transfected and infected cells was assessed by either MTT assay or CellTiter-Glo® Luminescent Cell Viability Assay (Promega, Southampton, UK).

For MTT assays 100µl of thiazolyl blue tetrazolium bromide (Sigma-Aldrich, Dorset, UK) diluted to a concentration of 1mg/ml in culture medium was added to cells and incubated at 37°C overnight. Subsequently, 100µl MTT stop solution (0.04M HCl in isopropanol (Fisher Scientific, Loughborough, UK)) was added to cells and incubated for 37°C until all crystals were dissolved. Absorbance was measured at 580nm on a Synergy HT plate reader. For CellTiter-Glo® assays cells were lysed in 200µl or 400µl of CellTiter- Glo® reagent and incubated for 10min at RT. Luminescence was measured in 10µl of the cell lysate on a Synergy HT plate reader or in 50µl of cell lysate on a GloMax®-Multi Jr single tube reader (Promega, Southampton, UK).

2.20. Stimulation of NOD pathways

THP-1 Blue™ and HEK-Blue™ hNOD2 cells were stimulated with concentrations of MDP (Invivogen, San Diego, CA) ranging from 0.1-10µg/ml for 24h. In some experiments THP-1 Blue™ were co-stimulated with MDP and 10ng/ml LPS (ENZO Life Science, Lausen, Switzerland) for 24h.

Stimulation with 50ng/ml TNF (Preprotech, London, UK) was used as positive control for stimulation of HEK293T and HEK-Blue™ hNOD2 cells whereas 1-10µg/ml of the imidazoquinoline compound R-848 (Enzo Life Science, Lausen, Switzerland) and 10ng/ml of LPS were used as positive controls for stimulation of THP-1 cells. All ligands were diluted in culture medium.

2.21. Quanti Blue™ assay

Levels of SEAP in the cell supernatant induced by activation of NF-κB and AP-1 were measured by Quanti blue™ assay (Invivogen, San Diego, CA). For Quanti Blue™ assay, 20µl of cell-free supernatant were incubated with 200µl of Quanti Blue™ reagent (200mg/ml) at 37°C for 30min in a 96-well plate. Absorbance was measured on a Synergy HT plate reader at 630nm.

2.22. Protein purification

For affinity purification of wt and variant RIP2 protein, HEK293T cells were transfected with *RIPK2* wt plasmids pcDNA6_HIS*RIPK2*wt or pcDNA6_*RIPK2*wt_V5/HIS or plasmids encoding corresponding RIP2 variants (Section 2.13.1 and 2.13.7). Transfected HEK293T (30 x 10cm^2 plates) were harvested 72h post transfection. Cells were washed in PBS and lysed in 700µl of lysis buffer per 10cm^2 plate for 30min on ice. Either sodium phosphate or NP-40 cell lysis buffer were used to lyse cells depending on purification method. HEK293T lysates were clarified by centrifugation at 3000 x g for 30min and subsequently filtered through a 0.22µm filter (Millipore, Watford, UK). RIP2 was affinity purified by immobilised metal affinity chromatography, immunoprecipitation or affinity purification using an immobilised anti-V5 antibody.

2.22.1. Affinity purification of RIP2 by immobilised metal chelate chromatography

N- and C-terminally HIS-tagged RIP2 was purified by immobilised metal affinity chromatography using either HIS select® nickel magnetic agarose beads (Sigma-Aldrich, Dorset, UK) or a HIS GraviTrap™ TALON® column (GE Healthcare, Little Chalfont, UK). HEK293T cells were lysed in sodium phosphate lysis buffer and the lysate clarified by filtration.

For RIP2 purification using nickel magnetic agarose beads, 100µl of beads were washed twice with 500µl sodium phosphate binding buffer before 50µl of lysate and 200µl of sodium phosphate binding buffer were added to the beads and incubated for 1h at 4°C. The beads and the unbound protein fraction were separated by using a magnet. Beads were washed with 250µl sodium phosphate lysis buffer and 250µl sodium phosphate wash buffer before the bound fraction was eluted with 50µl sodium phosphate elution buffer.

For RIP2 purification using HIS GraviTrap™ TALON®, the column was equilibrated with 10ml of sodium phosphate binding buffer. Cell lysate was applied to the column and the unbound material collected and reapplied five times. The column was then washed twice with 10ml sodium phosphate binding buffer and twice with 10ml sodium phosphate wash buffer before the protein was eluted with 3ml sodium phosphate elution buffer. Eluted fractions were stored at -20°C.

2.22.2. Affinity purification by immunoprecipitation

To immunoprecipitate RIP2, it was expressed with a C-terminal V5-epitope. HEK293T cells were lysed in NP40 cell lysis buffer containing 1mM PMSF (Sigma-Aldrich, Dorset, UK) in DMSO (Sigma-Aldrich, Dorset, UK) and 10µl protease inhibitor cocktail (Sigma-Aldrich, Dorset, UK) per 1ml lysis buffer and clarified as described above. Cell lysates were incubated with anti-V5 antibody (Invitrogen, Paisley, UK) for 3h at 4°C. Subsequently lysates were added to polypropylene gravity flow columns (Fisher Scientific, Loughborough, UK) pre- packed with Pierce™ Protein G agarose (Fisher Scientific, Loughborough, UK) and incubated overnight at 4°C with rotation. The unbound protein fraction was eluted and the bound fraction washed with 3

column volumes of PBS. The bound fraction was eluted with three times 500µl 0.2M Glycine-HCl (pH 2.5) into 50µl 1M Tris-HCl (pH 9.0) and pH adjusted to pH 7.4. Eluted fractions were stored at -20°C

2.22.3. Affinity purification using immobilized anti-V5 antibody

Recombinant RIP2 was affinity purified by its V5-epitope using an immobilised anti-V5 antibody. Polypropylene gravity flow columns were packed with Anti-V5 Agarose Affinity Gel Antibody produced in mouse (Sigma-Aldrich, Dorset, UK) and agarose was washed with one column volume of PBS. Lysates were diluted 3-fold in NP40 cell lysis buffer before 3ml of cell lysate was applied to the column and incubated rotating overnight at 4°C. The column was eluted in three fractions of 500µl with 0.2M Glycine-HCl (pH 2.5) into 50µl 1M Tris-HCl (pH 9.0) and pH adjusted to pH 7.4. Alternatively the bound fraction was eluted using 3 x 500µl of 1.2M NaCl or out competed using 3 x 500µl of 100µg/ml V5-tag Peptide (Sigma-Aldrich, Dorset, UK). Eluted fractions were stored at -20°C.

2.22.4. Buffer exchange and concentration

Eluted fractions of purified RIP2 protein were buffer exchanged into kinase reaction buffer using Illustra NAP-5 columns (GE Healthcare, Little Chalfont, UK) and PD-10 Desalting Columns (GE Healthcare, Little Chalfont, UK) according to manufacturer's instructions. Fractions were concentrated to a final volume of 250-500µl after buffer exchange by centrifugation at 3000 x g using either Amicon Ultra-4 centrifugal filter units (Millipore, Watford, UK) or Vivaspin 20ml (Sartorius, Epsom, UK) dependent on initial volume.

2.22.5. Quantification of purified RIP2

Purified wt and mutant RIP2 was quantified by visualising serial dilutions of purified RIP2 alongside known concentrations of commercially available RIP2 (Promega, Southampton, UK) by western blot. Densitometry of protein bands was performed using ImageJ (Schneider *et al*., 2012).

2.23. Kinase assay

Kinase activity of purified wt and mutant RIP2 was measured using the RIPK2 Kinase Enzyme System (Promega, Southampton, UK). Kinase assays were performed in 96-well white opaque plates (Nunc, Roskilde, Denmark). Dilutions of purified kinase were incubated with 0.5µg substrate myelin basic protein (MBP; Promega, Southampton, UK) and 50µM ATP (Promega, Southampton, UK) in reaction buffer A (Promega, Southampton, UK)) for 1h at RT. Fifty µl of ADP-Glo^{TM} Reagent (Promega, Southampton, UK) was added to each well and incubated at RT for 40min in order to terminate the kinase reaction and diminish any remaining ATP. The ADP generated in the kinase reaction was then converted into ATP and subsequently into a luciferase signal by incubation with 100µl of kinase reaction reagent (Promega, Southampton, UK) for 30min at RT. Luminescence was measured using a Synergy HT plate reader.

2.24. *M. tuberculosis* strains and culture conditions

M. tuberculosis H37Rv was used for all experiments. Mycobacteria were grown in 10ml of 7H9 broth supplemented with ADC, at 37°C static and were passaged every 7 days. Mycobacteria were plated onto 7H10 solid medium supplemented with OADC. Plates were incubated static at 37°C for 4 weeks.

2.25. Infection of THP-1 cells with *M. tuberculosis*

THP-1 cells were transfected with *RIPK2* and control siRNAs and plated into 48-well plates in RPMI medium containing 20nm PMA (as described in section 2.18.2) prior to infection. After 24h of PMA stimulation, culture medium was replaced with PMA-free RPMI medium to remove dead cells. Cells were left to differentiate and recover for a further 24h before infecting with *M. tuberculosis*.

THP-1 cells were infected with late-log phase (7 day old culture) *M. tuberculosis* H37Rv (passages 5-8) at a multiplicity of infection (MOI) of 10:1 (bacteria: THP-1 cells). To prepare the inoculum, bacteria were collected by centrifugation at 3000 x g for 10min and resuspended in RPMI containing 10% FBS. Prior to infection of THP-1 cells, bacteria were syringed through a 25G x

0.5in needle (Becton Dickenson, Oxford, UK) to create a single cell suspension. THP-1 cells were incubated with bacteria for 2h at 37°C before unphagocytosed bacteria were removed. The culture medium was removed and the THP-1 cells were gently washed with RPMI medium before culture medium was replaced. Infected cells were incubated for up to 72h at 37°C in a humidified 5% CO_2 incubator.

2.26. Enzyme-linked immunosorbent assay (ELISA)

THP-1 supernatants were sterilised by filtration through 0.45µm and 0.22µm Corning® Costar® Spin-X® centrifuge tube filters (Sigma-Aldrich, Dorset, UK). Cytokine release was measured in cell-free cell supernatants in 384 well ELISA plates (Corning, Corning, NY). ELISA plates were coated with capturing antibody in PBS overnight at 4°C before plates were blocked with 2% (w/v) bovine serum albumin (Fisher Scientific, Loughborough, UK) in PBS for 1h at RT (Table 2.13). Samples and purified recombinant proteins used as standards were diluted in ELISA buffer and incubated for 2h at RT (Table 2.13). Plates were incubated with biotinylated detection antibody in ELISA buffer for 1h at RT followed by incubation with streptavidin horseradish peroxidase (HRP) conjugate (R&D systems, Minneapolis, MN) in ELISA buffer for 1h at RT (Table 2.13).

Plates were washed with ELISA wash buffer after each step and developed using TMB microwell peroxidase substrate solution (KPL, Gaithersburg, MD). The reaction was stopped by addition of ELISA stop solution (6% H_2SO_4; Fisher Scientific, Loughborough, UK) and the plates were read on a Synergy HT plate reader at 450nm.

Cytokine	Capture antibody Working concentration	Detection antibody Working concentration	Standard Top working concentration
TNF	4µg/ml[a]	0.5µg/ml[a]	10ng/ml[b]
IL-1β	2µg/ml[c]	0.4 µg/ml[c]	10ng/ml[b]
IP-10	2µg/ml[c]	0.1µg/ml[c]	5ng/ml[c]
IL-12p40	4µg/ml[c]	0.5µg/ml[c]	4ng/ml[c]

Table 2.13 Antibodies and standards used for ELISA
Tumor necrosis factor (TNF); Interleukin (IL); Interferon-γ inducing protein 10 (IP-10); [a]Becton Dickenson, Oxford, UK; [b]PreproTech, London, UK; [c]R&D Systems, Abingdon, UK

2.27. *M. tuberculosis* viable counting

The number of viable bacteria in the inoculums used for infection of THP-1-derived macrophage cells and intracellular survival of bacteria post infection were determined using a plate dilution method. To enumerate bacteria in the inoculum, 100µl of inoculum was serial diluted in 900µl PBS and 100µl plated in 10µl volumes onto 7H10 solid agar. Intracellular bacteria were enumerated by lysing THP-1-derived macrophage monolayers in 1ml of 0.25% (w/v) SDS. Cell lysates were syringed to remove cell debris and generate a single cell bacterial suspension before bacteria were serial-diluted in PBS and plated on 7H10 agar. Plates were incubated at 37°C static for 4 weeks.

3 Polymorphisms identified in the genes *RIPK2*, *LY96* and *NFKB2* by sequencing DNA samples of Gambian origin

3.1. Introduction

Only about 10% of individuals infected with *M. tuberculosis* develop active disease, suggesting that the majority of the population is intrinsically capable of mounting an effective immune response that at least contains the infection (Ottenhoff, 2012). This suggests that there is an innate, most likely genetic, component to host susceptibility to tuberculosis.

A number of association and linkage studies have attempted to link susceptibility to tuberculosis to human genes. However, despite the identification of a range of genes associated with susceptibility to tuberculosis, such as *SLC11A1* and *IFNGR1*, results have been inconclusive (Bellamy *et al*., 1998; Newport *et al*., 1996). This is most likely due to susceptibility to tuberculosis being a phenotype that is affected by a large number of genes that contribute to a small extent (Meyer and Thye, 2014; Newport, 2009).

Subsequently, in more recent years, studies aiming to identify genes that affect host susceptibility to tuberculosis have started to focus on surrogate markers for susceptibility tuberculosis that are affected by a smaller number of genes (Cobat *et al*., 2009; Stein *et al*., 2003). Surrogate markers that have been studied include the level of mycobacterial antigen-driven IFN-γ production, as IFN-γ is a crucial cytokine in the immune response to tuberculosis and also a quantitative trait that can easily be measured (Jepson et al., 2001; Newport, 2015; Stein et al., 2007). The magnitude of IFN-γ, in response to mycobacterial antigens in BCG vaccinated newborns from the Gambia was significantly linked to three regions on the genome (8q13-22, 10q23-25 and 11q23-25) (Newport *et al*. manuscript in preparation). Within these regions five genes were identified that are expressed in macrophages and dendritic cells and are involved in the immune response to tuberculosis. In the region 8q13-22 two genes were located that encoded proteins including the TLR4 adapter protein MD-2 and the serine/threonine kinase RIP2 that plays an essential role in NOD-dependent NF-κB activation; the region 10q23-25 encoded the kinase IKK-α and the F-box protein β-TrCP, which are both

involved in regulation of NF-κB activation. Additionally, this region encodes the transcription factor NF-κB2, which is part of the NF-κB transcription factor family (DiDonato *et al*., 1997; Inohara *et al*., 1998; Schmid *et al*., 1991; Shimazu *et al*., 1999; Yaron *et al*., 1998).

To explore whether any of these genes harbour polymorphisms that may influence the magnitude of mycobacterial antigen-induced IFN-γ production observed in the BCG-vaccinated Gambian neonates, selected candidate genes were sequenced in DNA samples from this study.

Both MD-2 and RIP2 directly associate with specific PRRs, namely TLR4 and NOD1/2, which are involved in the detection of *M. tuberculosis* antigens leading to induction of pro-inflammatory cytokines from macrophages and dendritic cells and IFN-γ from T-lymphocytes (Fitzgerald *et al*., 2004; Philpott *et al*., 2014). Consequently, polymorphisms present in these two genes might affect the magnitude of IFN-γ induced during infection with *M. tuberculosis*.

NF-κB2 is one of five homologous transcription factors of the NF-κB family (Hinz and Scheidereit, 2014). The transcription factor is involved in the non-canonically activated NF-κB pathway that regulates immunological processes such as maturation of dendritic cells and differentiation of lymphocytes (Sun, 2012). Polymorphisms harboured by this gene could have an effect on the magnitude of IFN-γ responses during infection with *M. tuberculosis* by affecting maturation and differentiation of cell populations involved in secretion of IFN-γ or induction of IFN-γ from T-lymphocytes

IKK-α and β-TrCP are also involved in activation of NF-κB and induction of pro-inflammatory cytokines (Hinz and Scheidereit, 2014). However, unlike MD-2 and RIP2, which are involved in specific signalling pathways, IKK-α and β-TrCP play crucial roles in transduction of signals from a range of receptors including among others TLRs, NLRs, IL-1R, TNFR, T-cell and B-cell receptors (Liu *et al*., 2012). Mice deficient of IKK-α have been shown to display developmental defects and die shortly after birth, whereas *Btrc*$^{-/-}$ mice have been shown to be viable, but males display reduced fertility (Guardavaccaro *et al*., 2003; Takeda *et al*., 1999). Consequently, these genes are less likely to harbour mutations that substantially affect protein function as acquired polymorphisms are less likely to be passed on to the next generation.

Subsequently, sequencing of the genes encoding RIP2, MD-2 and NF-κB2 was prioritised over sequencing of genes encoding IKK-α and β-TrCP.

3.2. Results

3.2.1. Polymorphisms identified among *RIPK2*, *LY96* and *NFKB2*

In order to identify variation among the genes of interest, each gene was sequenced in 30 DNA samples collected from a cohort of Gambian newborns (Finan *et al*., 2008). For each gene, primers were designed to amplify all exons including regions 200bp up- and downstream of the exon to include splice sites. To identify polymorphisms within the sequenced genes, sequence reads were aligned to reference sequences from exons and introns available in the ensemble database (Ensembl release 78) (Flicek *et al*., 2014). A total of 64 single SNPs were identified among the *RIPK2*, *LY96*, *NFKB2* (Table 3.1).

Identified SNPs	*RIPK2*	*LY96*	*NFKB2*
Total SNPs	**38**	**6**	**20**
CDS SNPs (total)	**6**	**0**	**2**
Non-synonymous SNPs	3	0	0
Synonymous SNPs	3	0	2
Intronic SNPs (total)	**25**	**5**	**14**
Potentially affecting splice sites	0	1	0
5'UTR SNPs	**3**	**0**	**0**
3'UTR SNPs	**2**	**1**	**0**
Up- downstream of gene	**2**	**0**	**4**

Table 3.1 Polymorphisms identified in *RIPK2*, *LY96* and *NFKB2*
Single nucleotide polymorphism (SNP); coding sequence (CDS); untranslated region (UTR)

3.2.2. Polymorphisms in *RIPK2*

A total of 38 polymorphisms (Figure 3.1 A) were identified within the eleven exons and the immediate surrounding intronic regions of *RIPK2* (Appendix; Table 9.1). Of the 38 identified polymorphisms, six SNPs were located within the coding sequence (CDS) of the gene. A further 25 polymorphisms were identified in intronic regions, five polymorphisms were present in either the 5' or 3' untranslated region (UTR) of the gene

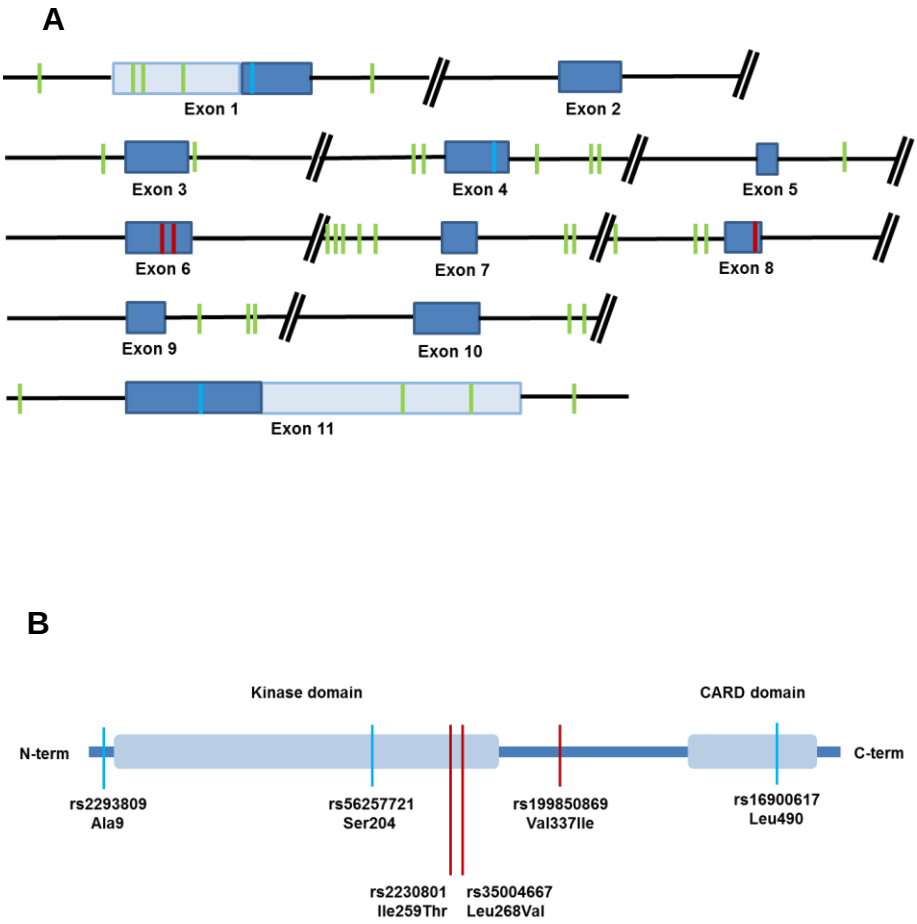

Figure 3.1 Schematic representation of polymorphisms identified in *RIPK2*/RIP2

(A) Schematic representation of *RIPK2*; exons are indicated in blue and regions of exons that are not translated in light blue. Polymorphisms outside the gene's CDS are indicated in green, non-synonymous polymorphisms in red and synonymous polymorphisms in blue. (B) Schematic representation of RIP2; non-synonymous mutations indicated in red, synonymous mutations in blue. The number underneath each polymorphism indicates how many of 30 DNA samples were homozogous/ heterozygous for each SNP.

and two polymorphisms were located immediately upstream and downstream of *RIPK2.* Out of the six polymorphisms identified in the CDS of *RIPK2*, three SNPs (rs2230801, rs35004667 and rs199850869) resulted in non-synonymous mutations within exons 6 and 8 of *RIPK2* (Figure 3.1 B).
The SNP rs2230801 was identified in 7 out of 30 sequenced Gambian DNA samples, rs35004667 was identified twice and rs199850869 only once. All of these variations were only observed as heterozygous polymorphisms.

The polymorphisms rs2230801 and rs35004667 were located in the kinase domain of *RIPK2*. Rs2230801 is a missense mutation resulting in an amino acid change from isoleucine to threonine (I259T). The software Polyphen2, which predicts the likelihood of missense mutations having a deleterious effect on the function of the protein, predicted that the mutation could possibly be damaging to the protein's function. SIFT, a similar prediction software suggested that the mutation would be tolerated in the protein. The SNP rs35004667 results in an amino acid change from leucine to valine (L268V), which was predicted to have deleterious effects on protein function by both prediction software SIFT and Polyphen2. The third identified non-synonymous polymorphism (rs199850869) is located in the intermediate domain of *RIPK2* and results in an amino acid change from valine to isoleucine (V337I). Both prediction software SIFT and Polyphen2 predictions agreed that this polymorphism is unlikely to affect protein function. The other three polymorphisms present in the CDS (rs16900617, rs2293809 and rs56257721) resulted in synonymous mutations. Additionally, the sequentially first seven polymorphisms identified in *RIPK2* (rs5893110, rs201500893, rs115517126, rs140020615, rs2293809, rs39499, rs431264) were all located within the predicted promoter sequence of the gene.

3.2.3. Polymorphisms in *LY96*

A total of six different SNPs were identified in the gene *LY96*, which encodes the TLR4 adapter protein MD-2 (Figure 3.2 A; Appendix; Table 9.2) (Shimazu *et al*., 1999). The six polymorphisms identified by sequencing Gambian DNA samples included five polymorphisms in intronic regions of the gene and one within the 3'UTR. The polymorphism identified within the 3'UTR (rs10282832) was located within close proximity of the sequence

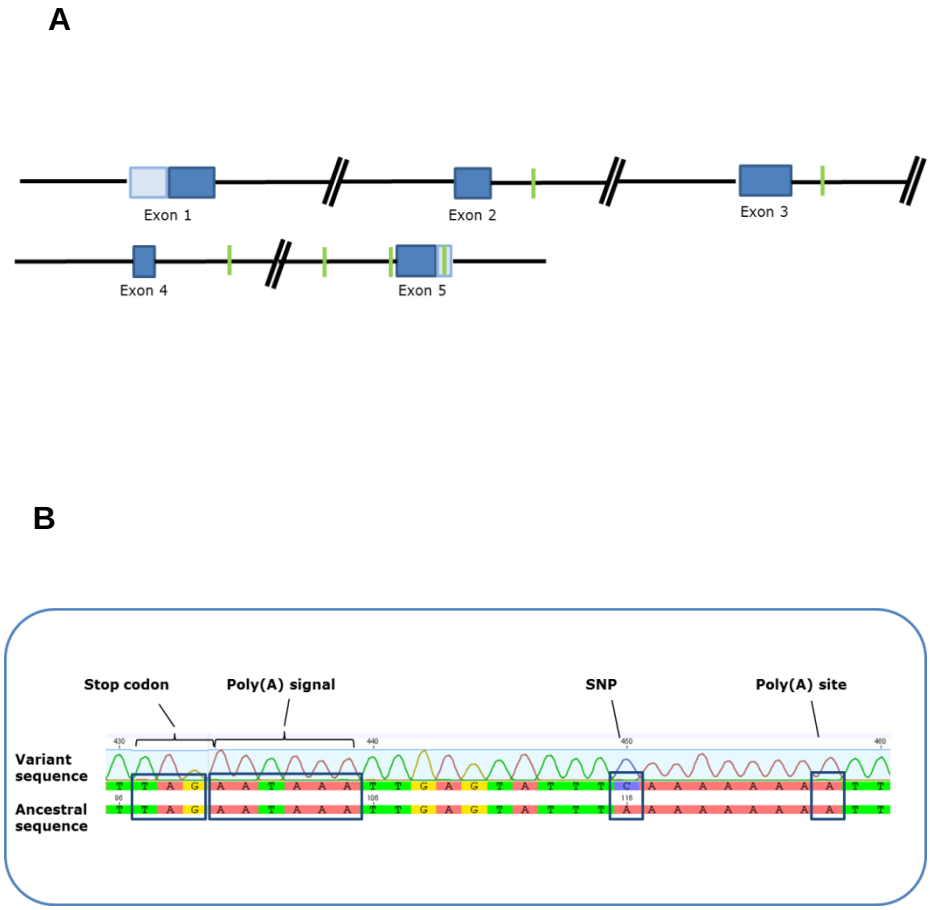

Figure 3.2 Schematic representation of polymorphisms identified in *LY96*

(A) Schematic representation of *LY96*; exons are indicated in blue and regions of exons that are not translated are in light blue. Polymorphisms outside the gene's CDS are indicated in green and synonymous polymorphisms in blue. (B) Sequence trace file showing the position of the SNP identified in the 3'UTR of *LY96* relative to the gene's stop codon, poly (A) signal and poly (A) site.

elements located downstream of the stop codon, which are involved in polyadenylation (Figure 3.2 B). This polymorphism was identified in 13 DNA samples (9 heterozygotes and 4 homozygotes). One additional polymorphism (rs11466003) was of interest. This intronic SNP was located within intron 4-5 7bp upstream of exon 5 in a potential splice site. 2 sequenced DNA samples were shown to be heterozygous for this mutation.

3.2.4. Polymorphisms in *NFKB2*

A total of 20 different SNPs were identified in the sequence of *NFKB2* (Figure 3.3; Appendix Table 9.3). Among the polymorphisms identified within the DNA sequences of *NFKB2*, three novel polymorphisms were identified. The novel polymorphisms included one upstream gene variant, one polymorphism located in intron 1-2 as well as one synonymous SNP located in exon 16. All novel SNPs identified were observed as heterozygous mutations in one or two of the 30 sequenced Gambian DNA samples. Of the polymorphisms that have previously been reported, two were located in up- and downstream regions of the gene, one SNP resulted in a synonymous mutation within exon 13, and 14 polymorphisms were located in intronic regions (Flicek *et al*., 2014). The sequentially first four identified polymorphisms (rs45502493, rs45526132 and two novel SNPs) overlap with the predicted promoter sequence of *NFKB2.* The polymorphism rs4919633, which resulted in a synonymous polymorphism within exon 13, occurred heterozygously in two of the sequenced DNA samples. The polymorphism is located within a predicted binding site for the transcriptional repressor CTCF (Ong and Corces, 2014). However, this binding site appears to be inactive in most cell types including monocytes (Flicek *et al*., 2014).

3.2.5. Distribution of alleles and genotypes in the Gambian population

To determine the distribution of some of the polymorphisms identified in the 30 Gambian DNA samples, three selected polymorphisms (rs19282832 (*LY96*), rs2230801 and rs35004667 (*RIPK2*)) were genotyped in a larger number of DNA samples. Furthermore, one polymorphism (rs42490) located in an intronic region of *RIPK2*, which has been associated with susceptibility to infection with *M. leprae* in a Chinese cohort, was also

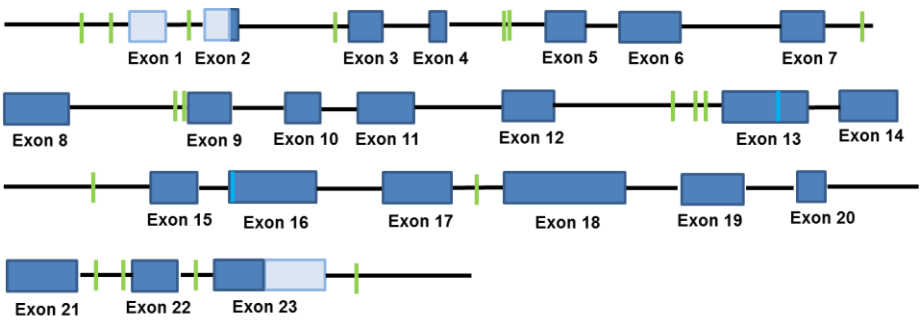

Figure 3.3 Schematic representation of polymorphisms identified in *NFKB2*

Schematic representation of *NFKB2*; exons are indicated in blue and regions of exons that are not translated are in light blue. Polymorphisms outside the gene's CDS are indicated in green and synonymous polymorphisms in blue.

chosen for genotyping (Zhang *et al*., 2011; Zhang *et al*., 2009). All SNPs were genotyped in 269 DNA samples collected from new-born twins and singleton new-born babies in the Gambia as only 269 of the original 518 DNA sample were still of adequate quality (Finan *et al*., 2008; Newport *et al*., 2004).

Additionally, genotyping data for two polymorphisms (rs16900617 and rs40457 (*RIPK2*)) was already available for 518 Gambian DNA samples collected from new born babies from the same cohort as used for genotyping the other polymorphisms (Finan *et al*., 2008; Newport *et al*., 2004). The polymorphism rs16900617 was of interest as it was identified in the CDS of *RIPK2* in the Gambian population, whereas rs40457 was associated with susceptibility to leprosy in a Chinese cohort (Zhang *et al*., 2011; Zhang *et al*., 2009).

SNP id	Gene	Location	Comment
rs10282832	*LY96*	3'UTR	Identified in the Gambian population
rs2230801	*RIPK2*	exon 6 – kinase domain	Identified in the Gambian population
rs35004667	*RIPK2*	exon 6 – kinase domain	Identified in the Gambian population
rs16900617	*RIPK2*	exon 11 – CARD domain	Identified in the Gambian population
rs42490	*RIPK2*	Intron 3-4	Associated with leprosy(Zhang *et al*., 2011; Zhang *et al*., 2009)
rs40457	*RIPK2*	Downstream gene variant	Associated with leprosy(Zhang *et al*., 2011; Zhang *et al*., 2009)

Table 3.2 Genotyped polymorphisms

The distribution of major and minor alleles observed in the genotyped samples from the Gambian population are shown in Figure 3.4. Minor alleles were observed at a range of different frequencies. The minor allele of rs35004667 was observed in 4%, the minor alleles of rs2230801 and rs40457 were observed in 10% whereas the minor alleles of rs16900617, rs10282832 and rs42490 were present in 30% of the population.

For all polymorphisms, except rs35004667, three different genotypes were identified (Figure 3.5). No homozygosity for the minor allele was observed for the polymorphism rs35004667. For three of the genotyped

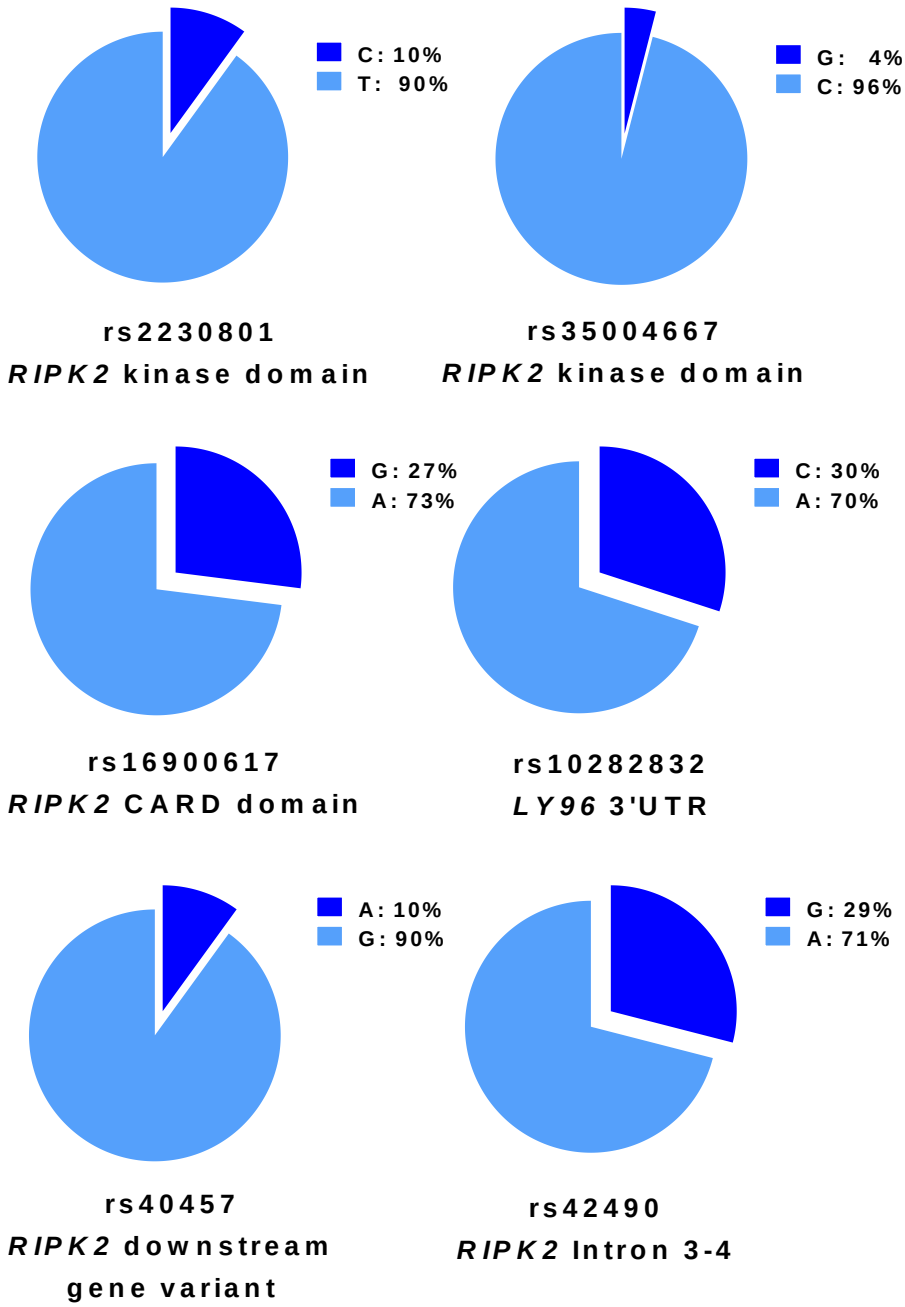

Figure 3.4 Distribution of alleles in the Gambian population
Each pie chart shows the distribution of alleles among the all the genotyped singleton new-borns and one individual per twin pair for each represented SNP. The major allele is shown in light blue and the minor allele is shown in dark blue

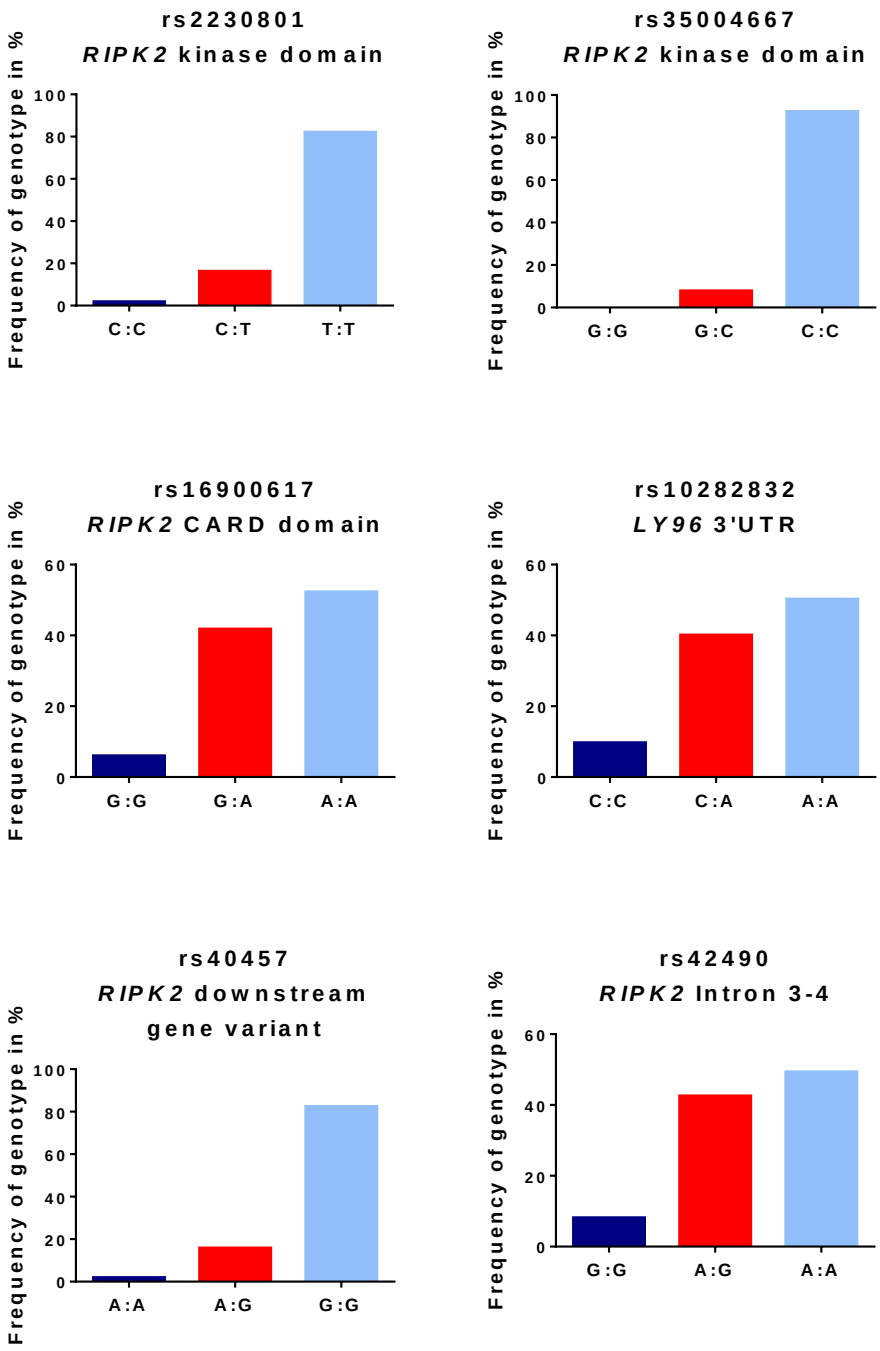

Figure 3.5 Distribution of genotypes in the Gambian population

Each graph shows the distribution of genotypes among all the genotyped singleton new-borns and one individual per twin pair for each represented SNP. Homozygous major alleles are indicated in light blue, heterozygous in red and homozygous minor alleles in dark blue.

polymorphisms (rs2230801, rs35004667, rs40457) over 80% of individuals were shown to be homozygous for the major allele. In contrast, the number of individuals heterozygous for the polymorphisms and the number of individuals homozygous for the major allele were similar for the polymorphisms rs16900617, rs10282832 and rs42490.

3.2.6. Comparison of IFN-γ responses by genotype

IFN-γ is a crucial cytokine in the immune response to *M. tuberculosis* infection, as it is required for activation of infected macrophages leading to induction of microbicidal pathways. To determine whether the genotype of four polymorphisms identified in the Gambian population had an impact on the magnitude of mycobacterial antigen-driven IFN-γ, the genotype of these SNPs were compared to IFN-γ responses measured by other studies. Additionally, genotypes of two polymorphisms associated with susceptibility to leprosy were compared to magnitude of IFN-γ response.

The genotype of the infants was compared to the magnitude of IFN-γ levels previously measured and reported by Newport *et al.* (2004) and Finan *et al.* (2008) (Finan *et al*., 2008; Newport *et al*., 2004). Briefly, in these studies infants were vaccinated with BCG within 24 hours of birth and *ex vivo* IFN-γ levels from PBMCs or whole blood were measured in response to PPD or killed *M. tuberculosis*, either two months (Finan *et al*., 2008) or five months (Newport *et al*., 2004) post vaccination. These specific mycobacterial antigens were chosen as IFN-γ responses to both PPD and killed *M. tuberculosis* have been shown to be heritable in the Gambian population (Newport *et al*., 2004). The magnitude of mycobacterial antigen-driven IFN-γ response was compared between the different genotypes for each polymorphism in each of the two infant cohorts. Comparing IFN-γ responses induced by PPD stimulation demonstrated that a significant difference was only observed for the polymorphism rs16900617 in the twin-cohort in which IFN-γ responses were measured five months post vaccination (Figure 3.6). The difference was only observed between individuals that were homozygous for the major allele and heterozygous individuals, but not between individuals homozygous for the minor and major allele. In the cohort

in which IFN-γ responses were measured in whole blood two months post

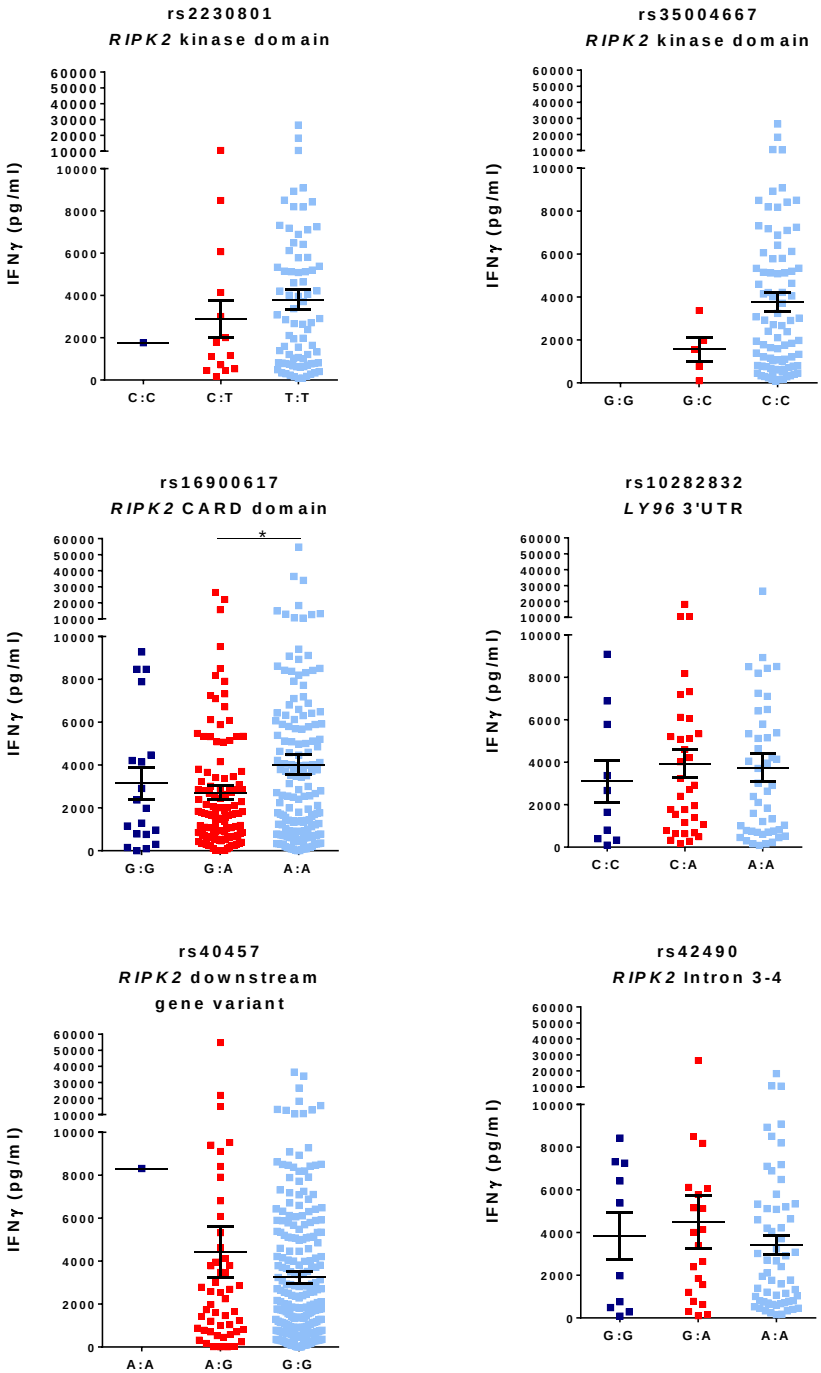

Figure 3.6 IFN-γ responses of PPD stimulated PBMCs from BCG-vaccinated newborns genotyped for six polymorphisms
PBMCs were stimulated *ex vivo* with PPD 5 months post BCG vaccination (cohort of newborn twin pairs). Data presented as mean ± SEM. ***P*<0.05

vaccination, no significant differences were observed after stimulation with PPD for any of the polymorphisms (Figure 3.7). Similarly, stimulation with killed *M. tuberculosis* only induced significantly different levels of IFN-γ in the presence of different genotypes of rs16900617 when IFN-γ responses were measured five months but not two months post vaccination (Figure 3.8 and 3.9).

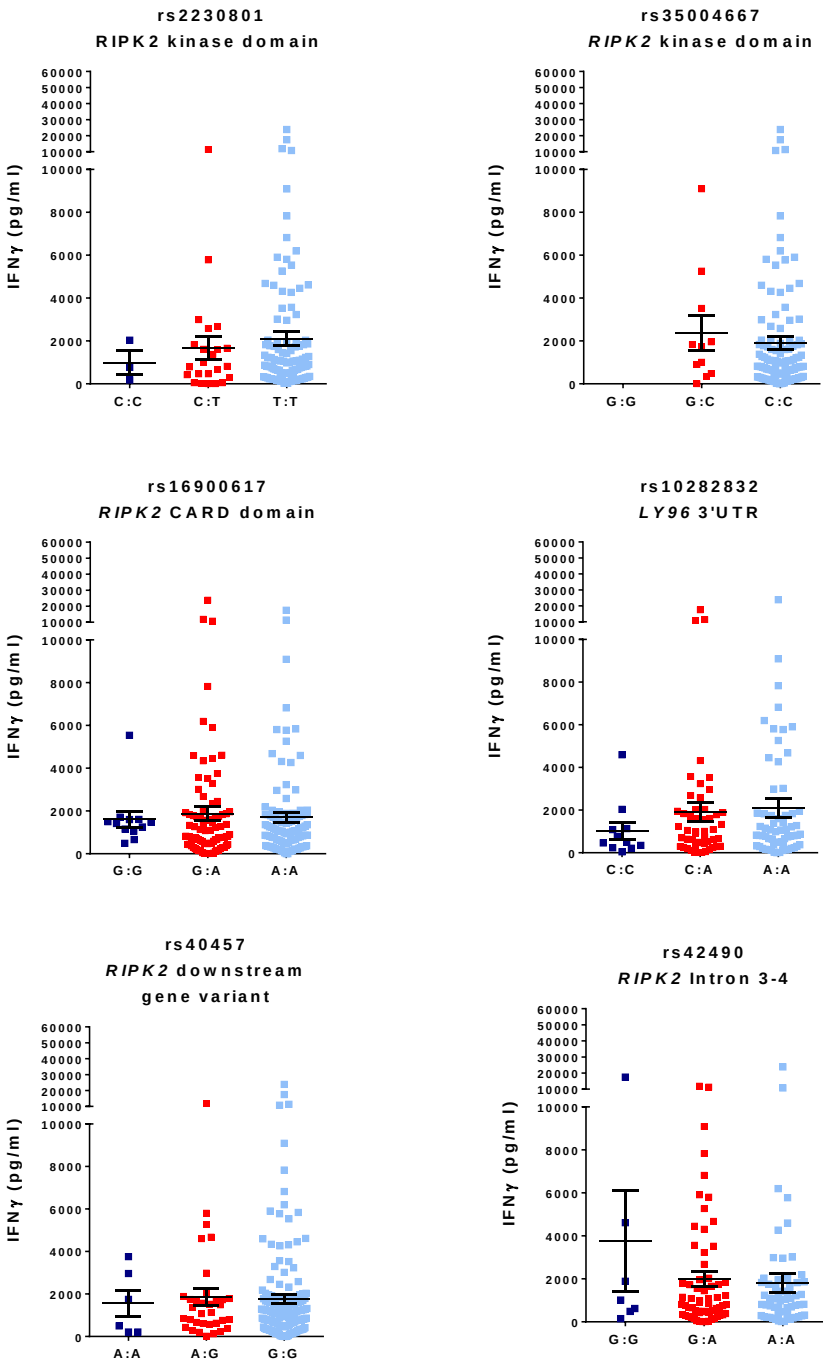

Figure 3.7 IFN-γ responses of PPD stimulated whole blood from BCG-vaccinated newborns genotyped for six polymorphisms

Whole blood was stimulated *ex vivo* with PPD 2 months post BCG vaccination (cohort of single newborns). Data presented as mean ± SEM.

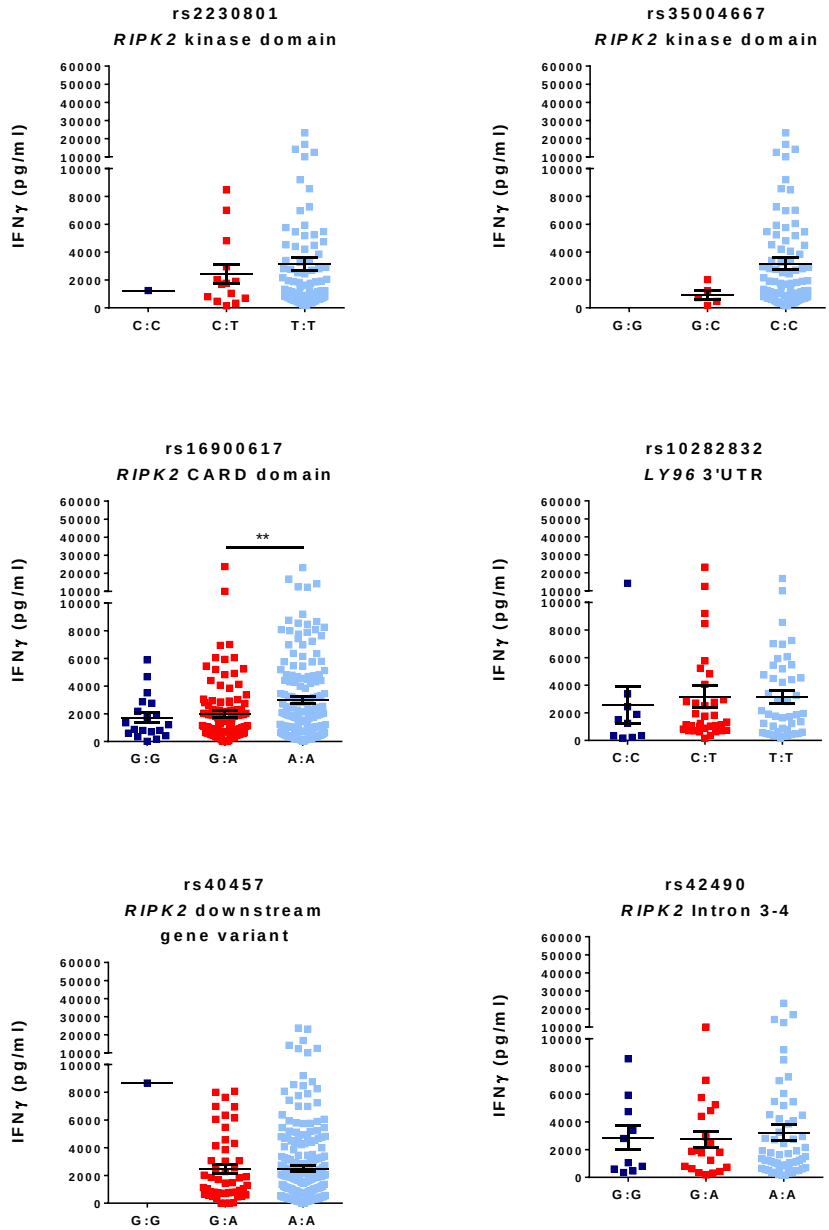

Figure 3.8 IFN-γ responses of killed *M. tuberculosis* stimulated PBMCs from BCG-vaccinated newborns genotyped for six polymorphisms

PBMCs were stimulated *ex vivo* with killed *M. tuberculosis* 5 months post BCG vaccination (cohort of newborn twin pairs). Data presented as mean ± SEM. ****** *P*<0.01

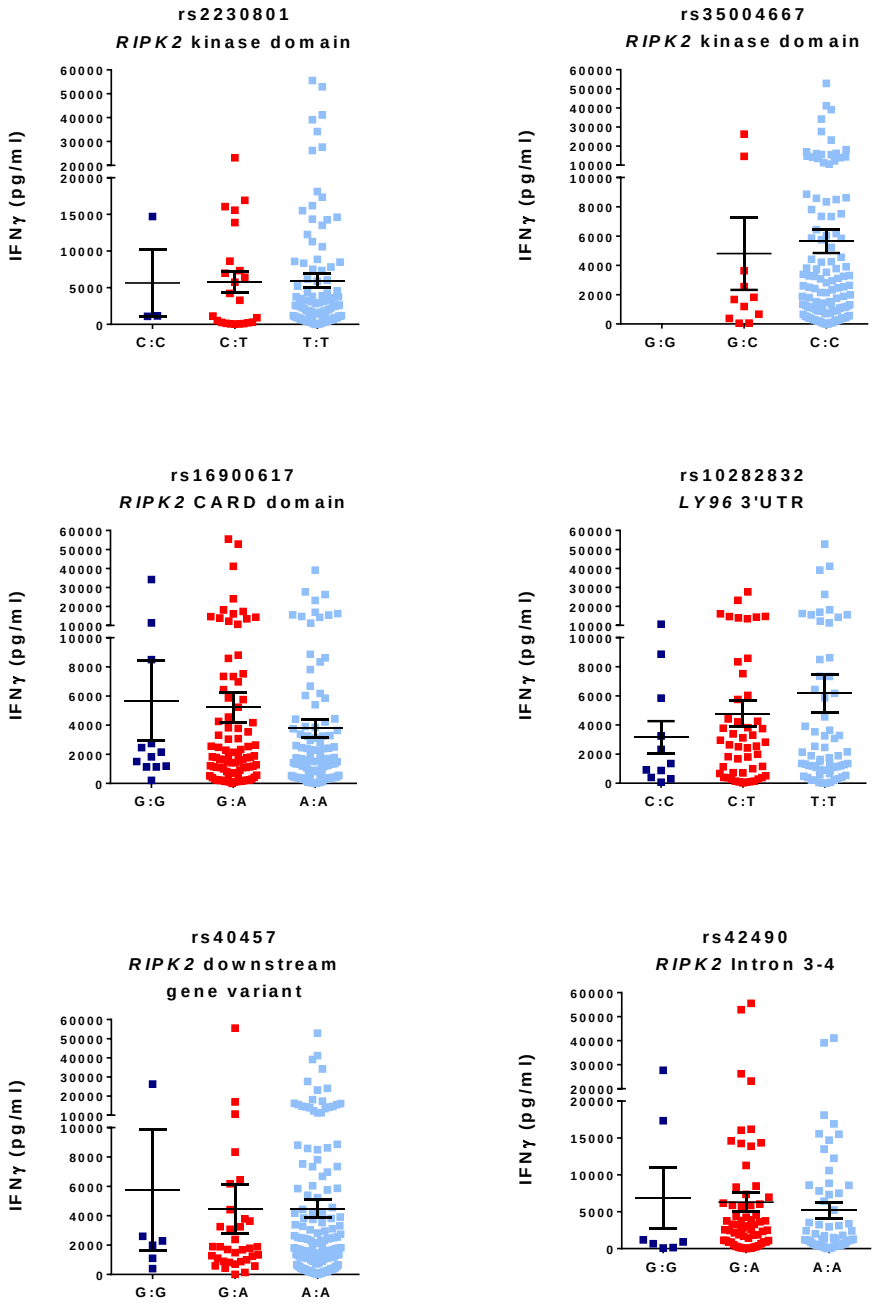

Figure 3.9 IFN-γ responses of killed *M. tuberculosis* stimulated whole blood from BCG-vaccinated newborns genotyped for six polymorphisms

Whole blood was stimulated *ex vivo* with killed *M. tuberculosis* 2 months post BCG vaccination (cohort of single newborns). Data presented as mean ± SEM.

3.3. Discussion

3.3.1. Polymorphisms identified among *RIPK2*, *LY96* and *NFKB2*

The genes *RIPK2, LY96 and NFKB2* were linked to magnitude of mycobacterial antigen-driven IFN-γ in BCG vaccinated newborns in the Gambia. To identify variants of these genes which might in part account for differences in the IFN-γ response observed, all exons of these genes were sequenced in 30 DNA samples of Gambian origin.

RIPK2 encodes RIP2 kinase, which consists of an N-terminal kinase domain and a C-terminal CARD domain, which is required for interaction of RIP2 with the NOD receptors and an intermediate domain that connects these two functional domains (Hasegawa *et al*., 2008; Inohara *et al*., 2000; McCarthy *et al*., 1998). RIP2 has been shown to be essential for downstream signalling upon activation of the NOD receptors, NOD1 and NOD2 (Park *et al*., 2007b). Upon activation of the NOD receptors, NOD and RIP2 associate inducing signalling cascades that result in activation of NF-κB and induction of pro-inflammatory cytokines (Ogura *et al*., 2001; Park *et al*., 2007b). Interaction of NOD with RIP2 has been shown to induce RIP2 to auto-phosphorylate (Tigno-Aranjuez *et al*., 2010).

Among the 38 polymorphisms identified in *RIPK2*, three (rs2230801/I259T, rs35004667/L268V and rs199850869/V337I) resulted in changes of amino acids and two of these were shown to affect the kinase domain of the protein. Both polymorphisms located in the kinase domain were suggested to have an effect on protein function by prediction software and therefore might affect the kinase activity of the protein. To date no published studies have investigated the effect of polymorphisms that occur naturally in the *RIPK2* kinase domain. Three experimentally introduced polymorphisms have been shown to abolish kinase activity of RIP2. These mutations include one mutation of an ATP binding site (K47) and mutation of two conserved aspartic acid residues in the kinase domain (D146 and D164) (McCarthy *et al*., 1998; Thome *et al*., 1998; Windheim *et al*., 2007). Studies involving these mutations have shown that in the absence of RIP2 kinase activity, expression levels of the protein are reduced (Hasegawa *et al*., 2008; Lu *et al*., 2005; Nembrini *et al*., 2009; Windheim *et al*., 2007). Conflicting results have been

published with regard to the importance of the kinase activity of RIP2 in NOD induced NF-κB activation. Whereas initial studies reported that the kinase activity was redundant, more recent evidence points towards a requirement for RIP2 kinase activity for optimal induction of NF-κB (Hasegawa *et al*., 2008; McCarthy *et al*., 1998; Navas *et al*., 1999; Thome *et al*., 1998; Tigno-Aranjuez *et al*., 2010). Additionally, NOD2 is involved in induction of autophagy in response to *S. flexneri* and *L. monocytogenes* and RIP2 kinase activity has been suggested to play a role in this process (Anand *et al*., 2011; Homer *et al*., 2012; Travassos *et al*., 2010). Another experimentally introduced mutation in the RIP2 kinase domain, which affects downstream signalling events, is the ubiquitination site K209. RIP2 signalling has been shown to be ubiquitin-regulated and K63-ubiquitination on K209 is essential for signal transduction after NOD activation (Hasegawa *et al*., 2008).

Neither of the polymorphisms identified in the kinase domain (rs2230801/I259T and rs35004667/L268V) of RIP2 has previously been identified in association studies investigating mycobacterial infection or any other disease phenotype. The polymorphism rs2230801 was studied in the context of Crohn's disease, but no association was found (Thiebaut *et al*., 2011).

Another non-synonymous mutation (rs199850869/V337I) which was identified in by sequencing Gambian DNA samples was located in the intermediate domain of *RIPK2.* Prediction software suggested that this polymorphism was unlikely to have an effect on protein function. Additionally, the intermediate domain of RIP2 has been shown to be required for interaction of RIP2 with NEMO, which is required for transduction of signals upon activation of the NOD receptors (Inohara *et al*., 2000). However, the identified polymorphism does not lie within the region of amino acids 293-319 that is essential for RIP2/NEMO interaction (Hasegawa *et al*., 2008). Additionally, a further 6 polymorphisms were located in the predicted promoter region of *RIPK2, w*here they could potentially have adverse effects on transcription factor binding.

LY96 encodes the adapter protein MD-2 which confers LPS responsiveness and responsiveness to some other PAMPs, to the TLR4 receptor. No polymorphisms affecting the CDS of *LY96* were identified among

the 30 Gambian DNA samples sequenced. However, one identified polymorphism (rs10282832) was located in the 3'UTR of the gene between the poly (A) signal, a sequence element that regulates polyadenylation of the mRNA of MD-2 and the poly (A) site, the actual polyadenylation site, 19nt further downstream. The canonical poly (A) signal consists of the nucleotide hexamer AAUAAA and in the *LY96* gene this signal is located immediately downstream of the stop codon (Yang and Doublie, 2011). The poly (A) signal sequence is highly conserved and functions as a recognition site for the proteins that form the machinery required for polyadenylation (Yang and Doublie, 2011). Polymorphisms affecting the poly (A) signal have been identified in various genes leading to altered levels of gene expression and have also been associated with disease phenotypes (Higgs *et al*., 1983; Kozyrev *et al*., 2007; Orkin *et al*., 1985). As the polymorphism rs10282832 is located 11bp downstream of the poly (A) signal of *LY96* it is possible that the polymorphism affects the interaction of mRNA with proteins required for 3'UTR processing and subsequently mRNA stability. However, unlike the actual poly (A) signal, the regions surrounding this signal sequence including the poly (A) site are poorly conserved and therefore the polymorphism identified in *LY96* might not have any functional effect (Hoarau *et al*., 2004). Furthermore, one study by Vervoort *et al*. (1997) identified a mutation in the β-glucuronidase gene that was located between two poly (A) signals. This polymorphism had no effect on levels of stable mRNA (Vervoort *et al*., 1997).

None of the *LY96* polymorphisms identified in the Gambian population have previously been studied with regard to susceptibility to mycobacterial or other bacterial infection. A range of other *LY96* polymorphisms, located in the promoter region of the gene, have been investigated in a Chinese population. However, none of the studied polymorphisms were associated with increased susceptibility to tuberculosis (Xue *et al*., 2010). Additionally, two polymorphisms (rs11465996 and rs16938755) an upstream gene and an intron variant of *LY96* were shown to be significantly associated with *Helicobacter pylori* induced gastric cancer in a Chinese population (Castano-Rodriguez *et al*., 2014).

NFKB2 encodes one of the five structurally homologous NF-κB transcription factors present in most cells, that are involved in induction of gene

expression upon various stimuli, including pathogenic assault (Hinz and Scheidereit, 2014). No non-synonymous mutations were identified from sequencing 30 DNA samples of Gambian origin. Apart from four polymorphisms identified in the predicted promoter region of the gene, none were likely to have functional effects. The absence of functional polymorphisms in this gene might be a consequence of the gene being less likely to accumulate functional polymorphisms, due to the important role it plays in many biological processes. Mutations in *NFKB2* have been shown to lead to immune-deficiencies and anterior pituitary hormone deficiency in humans (Brue *et al*., 2014).

3.3.2. Distribution of alleles and genotypes in the Gambian population

To estimate the distribution of alleles and genotypes of 4 selected polymorphisms that were identified in the Gambian population, the SNPs were genotyped in a large number of DNA samples of Gambian origin. Additionally, 2 polymorphisms were selected for genotyping because they were previously linked to susceptibility to infection with *M. leprae* in a Chinese cohort (Zhang *et al*., 2011; Zhang *et al*., 2009). These SNPs occur in the Gambian population, however were not identified in the 30 sequenced Gambian DNA samples, because both SNPs were located in regions of the gene that were not sequenced (only exons, and 200 base pairs upstream and downstream of each exon were sequenced). These two polymorphisms were located within a long intron between exon 3 and 4 and 20 kb downstream of *RIPK2*.

The 1000 Genome project consortium has sequenced and characterised genomes from 1092 individuals from 14 different populations. Comparing the allele and genotype frequencies observed in the Gambian population to frequencies of these SNPs reported by the 1000 genome project has highlighted some of the differences between the distribution of these SNPs in the Gambian and other populations (Abecasis *et al*., 2012).

Comparison of the allele frequencies of the polymorphisms rs2230801, rs35004667, rs16900617 and rs10282832 demonstrated that the minor alleles for these SNPs occurred more frequently in the Gambian population compared to the minor alleles in the Asian, American and European populations. The minor alleles of the polymorphisms rs16900617 and rs10282832 occurred at

frequencies of 27% and 30% respectively, in the Gambian population (Abecasis *et al*., 2012). In contrast, the minor allele of 16900617 occurred at frequencies of only 4% and 7% in American and Asian populations respectively and the minor allele of rs10282832 occurred at a frequency of 3% in American populations. This might suggest that there are selective advantages for carriage of these less common alleles in African populations. Additionally, the polymorphism rs10282832, rs35004667 and rs16900617 have not been reported for European and/or Asian populations at all, which reflects that the African population is an older, more genetically diverse population compared to other populations (Abecasis *et al*., 2012; Tishkoff and Williams, 2002).

Comparison of the genotypes observed in the Gambian population to genotype frequencies in other populations demonstrated that individuals heterozygous or homozygous for the minor allele were more frequent in the Gambian population. In particular, the distributions of the polymorphisms rs16900617 and rs10282832 showed differences. About 90% of American and/or Asian populations have been reported to be homozygous for the major allele of these polymorphisms, whereas in the Gambian population, the number of individuals homozygous for the major allele and the number of individuals heterozygous for the polymorphism occurred almost equally (Abecasis *et al*., 2012).

The distribution of alleles of the polymorphisms rs40457 and rs42490 varies between different populations. For the SNP rs40457 the A allele constituted the minor allele in African and European populations (29-41%), whereas in Asian and American populations the G allele constituted the minor allele (30-46%). In the Gambian population the A allele was found to be the minor allele for rs40457, which occurred less frequently relative to other African populations (10%). For rs42490 the G allele constituted the minor allele in African and European populations (29-39%) whereas the A allele constituted the minor allele in Asian and American populations (45-46%). In the Gambian population, the G allele represented 29% of the alleles which is identical to the estimated average reported for African populations (Abecasis *et al*., 2012).

Genotypes observed for the polymorphism rs40457 vary greatly between different populations (homozygosity A allele: 2-48%; heterozygosity: 16-54%; homozygosity: 1-82%). The Gambian population demonstrated one of the lowest prevalence of homozygosity of the A allele and the highest prevalence of homozygosity of the G allele. The distribution of genotypes observed for rs42490 also varied between European/African and American/Asian populations and the distribution in the Gambian population resembled the distribution in African and European populations (Abecasis *et al*., 2012).

In a Chinese cohort, susceptibility to infection with *M. leprae* was linked to the A allele of rs42490 and the G allele of rs40457, which are the minor alleles for these polymorphisms in this population (Zhang *et al*., 2011; Zhang *et al*., 2009). However, these alleles constitute the major alleles in the Gambian population. It is likely that different selection pressures act on these alleles in the different populations. As the prevalence of leprosy is similar in the Gambia and in China, the exposure to *M. leprae* is unlikely to be a contributing selection pressure (2014; WHO, 2011). This is unsurprising as the prevalence of leprosy is very low (2014).

3.3.3. Comparison of IFN-γ responses of different genotypes

To determine whether the presence of certain polymorphisms identified in the Gambian population affected the level of IFN-γ induced in response to mycobacterial antigen, genotypes and IFN-γ levels were compared in two Gambian infant cohorts.

A significant difference was only observed between individuals homozygous for the major allele of the polymorphism rs16900617 and heterozygous individuals. The polymorphism rs16900617 is a synonymous mutation within the CARD domain of *RIPK2*, which is required for interaction of RIP2 and the NOD2 receptor. It is possible that the protein levels of RIP2 are affected by this polymorphism as changing the codon might affect the abundance of the corresponding tRNA species. Alternatively, changes in the DNA sequence could potentially affect the folding of the mRNA. More likely is the explanation that the polymorphism is in linkage disequilibrium with another polymorphism that affects IFN-γ levels.

Overall, numbers of genotyped individuals are too low to show any significant differences for any of the other polymorphisms. It is also of note that the IFN-γ levels measured in the cohort of Gambian singleton newborns, two months post vaccination, are significantly lower than the IFN-γ response measured in the twin cohort five months post vaccination. This suggests that either measuring IFN-γ in a whole blood assay is less effective or that measuring immunogenicity at two months post vaccination is too early with regard to the age of the children or the time it takes for an immune response to develop. Hence the IFN-γ responses measured in the Gambian twin cohort might be more representative.

3.3.4. Selection of polymorphisms for further study

The genes *RIPK2*, *LY96* and *NFKB2* selected for sequencing were linked to the magnitude of IFN-γ induced in response to mycobacterial antigen from BCG vaccinated newborns from a Gambian cohort. Among the 64 polymorphisms identified in these genes, in DNA samples from the Gambian population, were three that were of particular interest as they potentially impacted on protein function or expression level and subsequently might affect induction of IFN-γ. These included two non-synonymous polymorphisms in the kinase domain of *RIPK2* (rs2230801 and rs35004667) and a polymorphism located in the 3'UTR of *LY96* (rs10282832). As polymorphisms that occur frequently are more likely to be responsible for the differences in magnitude of IFN-γ observed in the Gambian population, selected polymorphisms were genotyped to determine their prevalence in the overall population. This highlighted that the minor alleles of the polymorphisms rs10282832, rs16900617 and rs42490 were present in 30% of the population. However, significant differences in the magnitude of mycobacterial antigen-driven interferon-γ was only observed in the presence of different genotypes of rs16900617.

The non-synonymous polymorphisms in the kinase domain of *RIPK2* (rs2230801 and rs35004667), the polymorphism rs102082832, identified in the 3'UTR of *LY96*, and a synonymous mutation in *RIPK2* (rs16900617) were considered the ones most likely to effect protein function or expression among the 64 identified polymorphisms. However, as the polymorphism rs10282832

is located in the 3'UTR and rs16900617 is a synonymous mutation, the impact of these polymorphisms in immune response would be a result of effects on the mRNA instead of effects on the protein *per se*. Consequently, RNA samples would be required to study the effects of these polymorphisms on, for example, RNA stability. Unfortunately, DNA samples, but no blood samples to extract RNA were available for study of these polymorphisms, which are not present in the European population. Consequently, only the non-synonymous polymorphisms identified in the kinase domain of *RIPK2* were selected for further investigation.

4 Significance of RIP2 during *M. tuberculosis* infection

4.1 Introduction

RIP2 is a kinase that interacts directly with the NOD receptors, NOD1 and NOD2 and is essential for downstream signalling and NF-κB activation upon stimulation of the receptors (Magalhaes *et al*., 2011; Park *et al*., 2007b). The NOD receptors are cytosolic PRRs that detect peptidoglycan fragments resulting in the induction of pro-inflammatory cytokines through activation of NF-κB and AP-1. The NOD signalling pathway has been shown to be activated within one hour of *M. tuberculosis* internalisation by macrophages causing the phosphorylation and ubiquitination of RIP2 (Pandey *et al*., 2009; Yang *et al*., 2007).

The extent to which NOD2 contributes to immune responses during *M. tuberculosis* infection has been explored primarily in murine infection models. Induction of TNF, IL-1β, IL-12p40, type 1 IFN and nitric oxide production by macrophages in response to mycobacterial antigen have partly been attributed to the activation of NOD2 (Brooks *et al*., 2011; Divangahi *et al*., 2008; Gandotra *et al*., 2007; Leber *et al*., 2008; Pandey *et al*., 2009). Other contradictory studies have found that the absence of NOD2 does not affect TNF and type 1 IFN secretion in murine macrophages (Manzanillo *et al*., 2012; Pandey *et al*., 2009). In addition, one study observed that bacterial survival in human monocyte-derived macrophages depleted of NOD2 was increased compared to wild type macrophages (Brooks *et al*., 2011). In contrast, studies using *Nod2*$^{-/-}$ mice revealed that *M. tuberculosis* infection was controlled as well as in wild type mice, suggesting that there may be differences in the requirement for NOD2 in the control of *M. tuberculosis* in human and murine macrophages (Divangahi *et al*., 2008; Gandotra *et al*., 2007).

Murine *Nod1*$^{-/-}$ macrophages have been shown to secrete reduced levels of TNF compared to wild type macrophages during infection with *M. tuberculosis* (Ferwerda *et al*., 2005). However, in HEK293 cells transfected with Nod1 only low levels of NF-κB activation were observed after stimulation with mycobacterial antigen, suggesting that the NOD1-RIP2-NF-κB signalling

cascade might play a lesser role in immune response to *M. tuberculosis* infection.

Both NOD1 and NOD2 signalling pathways converge at RIP2; consequently absence of RIP2 is hypothesised to be equivalent to the loss of both NOD receptors. Only one study has investigated the contribution of RIP2 to immune responses to *M. tuberculosis* infection. RIP2-deficient murine macrophages were shown to produce reduced levels of IFN-α and IFN-β compared to wild type macrophages, with similar levels of TNF release (Pandey *et al*., 2009). To date no study has investigated the role of RIP2 during infection with *M. tuberculosis* in human macrophages.

To study the functional significance of RIP2 in human macrophage responses to *M. tuberculosis*, human THP-1-derived macrophage-like cells were depleted of RIP2 prior to infection. The effect of RIP2 deficiency on bacterial survival, macrophage cytokine responses and macrophage cell viability was measured over a 72h time course.

4.2 Results

4.2.1 Infection of THP-1 cells with *M. tuberculosis* H37Rv

The monocytic cell line THP-1 was used to study immune responses to *M. tuberculosis* in human macrophages. THP-1 cells were stimulated with PMA 48h prior to infection to induce the monocytes to adhere to the culture vessel and differentiate into macrophage-like cells. Subsequently, 24h later the PMA was removed and cells were left to recover for a further 24h. THP-1-derived macrophages were infected with *M. tuberculosis* H37Rv at an MOI of 10:1 (bacilli:macrophages) for 2h before extracellular bacilli were removed and the cell monolayer washed with warm RPMI medium.

THP-1 cells were lysed at 24h intervals over a 72h time course to assess survival of intracellular *M. tuberculosis* and macrophages (Figure 4.1). Counting viable *M. tuberculosis* bacilli (colony forming units per ml) over time showed that bacilli were multiplying intracellularly between 24h and 48h of infection. After this time point the levels of intracellular bacteria started to fall (Figure 4.1 A).

The viability of THP-1-derived macrophages was estimated using the CellTiter-Glo® assay. This assay measures the luminescence signal generated by ATP from viable cells as a surrogate for metabolic activity and cell viability. The lysis buffer used to permeabilise eukaryotic cells in order to release ATP and estimate cell viability does not lyse *M. tuberculosis* bacilli. Consequently, a very low luminescence signal was generated from axenic bacterial cultures (Figure 4.1 B). Therefore, this assay was suitable to measure macrophage viability in the presence of infecting *M. tuberculosis* bacilli. Using this assay, THP-1 cell viability gradually decreased over the course of the infection. After 24h and 48h of infection 40% and 80% less viable cells, respectively, were observed. Less than 5% of the original macrophage monolayer was present at 72h post infection, where the loss of THP-1 cells likely confounded the bacterial viable counts (Figure 4.1 B).

Levels of pro-inflammatory cytokines IL-1β, TNF, IP-10 and IL-12p40 secreted into the cell supernatant by THP-1 cells were measured by ELISA (Figure 4.2). IL-1β, TNF and IP-10 were induced by infection with *M. tuberculosis*. Levels

of TNF peaked at 24h post infection and then decreased over the following 48h. In contrast, IL-1β release peaked at 48h post infection. Levels of IP-10 in cell supernatants were maintained at all three time points after infection. The release of IL-12p40 was too low to be detected by ELISA at any time point. None of these cytokines were detected in cell supernatants of uninfected cells.

4.2.2 Knock down of RIP2

To investigate the contribution of RIP2 to macrophage responses to *M. tuberculosis* infection, THP-1 cells were depleted of RIP2 by transfection with siRNA. To optimise the knock-down of RIP2 in THP-1 cells, macrophages were transfected with *RIPK2* siRNA, scrambled control RNA or left untreated. The knock-down was assessed by immune blot using an anti-RIP2 antibody over a 120h time course (Figure 4.3). RIP2 was almost undetectable at 48h, 72h and 96h after transfection with *RIPK2* siRNA. Reduced RIP2 levels were observed at 120h after transfection with siRNA compared to cells transfected with scrambled control siRNA. As RIP2 protein levels remained knocked-down for almost 120h after transfection with *RIPK2* siRNA in THP-1 cells these cells could be used to study host-pathogen interaction between macrophages and *M. tuberculosis* in the absence of RIP2.

4.2.3 Survival of electroporated THP-1 cells

Transfection by electroporation typically results in the death of 50-60% of transfected cells. To assess the impact of transfection by electroporation on long-term cell viability of THP-1–derived macrophages after transfection, macrophages were transfected with siRNA and cell viability of transfected cells was assessed using CellTiter-Glo® assay over 120h (Figure 4.4). The viability of THP-1-derived macrophages dropped by only about 10% between 48h and 120h after transfection.

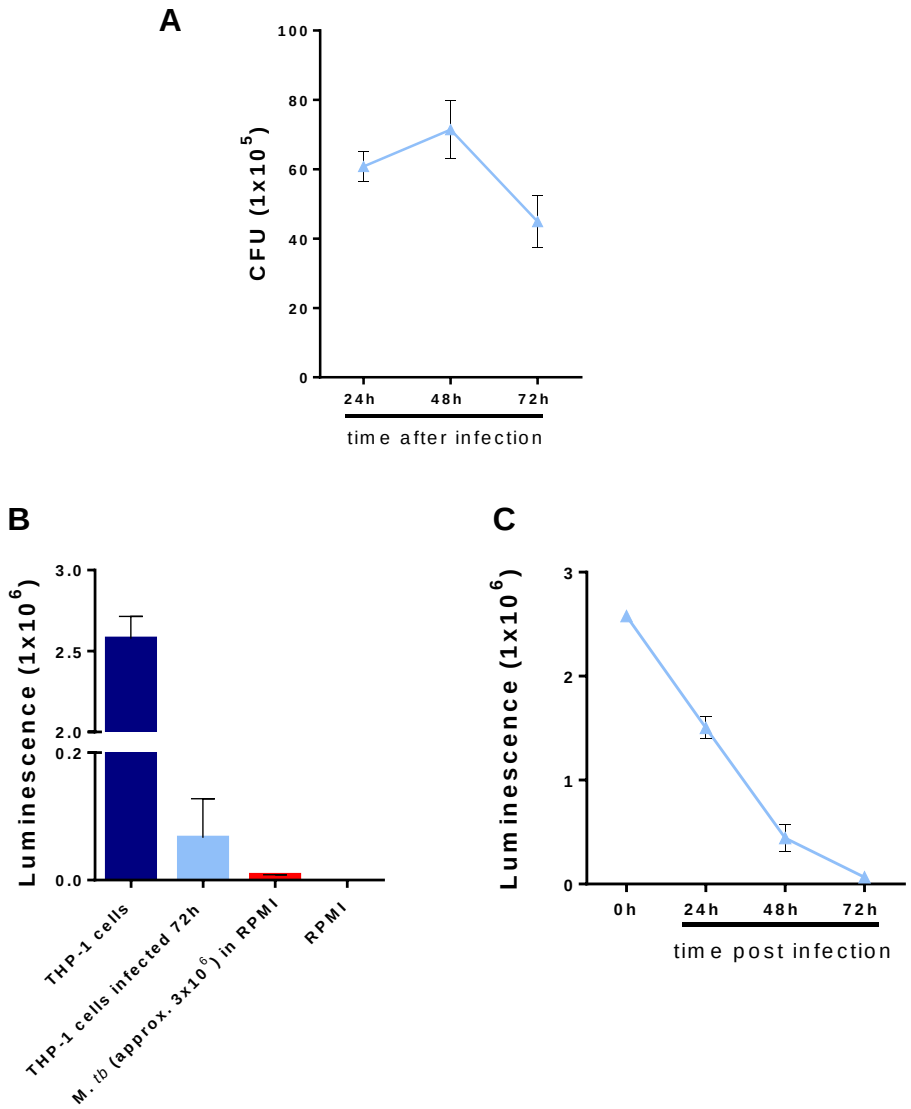

Figure 4.1 Infection of THP-1 cells with *M. tuberculosis* decreases macrophage viability

THP-1-derived macrophages were incubated with *M. tuberculosis* H37Rv for various lengths of time prior to lysis and measurement of bacterial and host survival. (A) *M. tuberculosis* survival was assessed by cfu counts/ml using a serial dilution method. (B) and (C) Viability of THP-1 cells was measured using a CellTiter-Glo® assay in uninfected THP-1 cells and through a 72h time course after infection. Pooled data are shown from three independent experiments. Results are expressed as mean ± SEM.

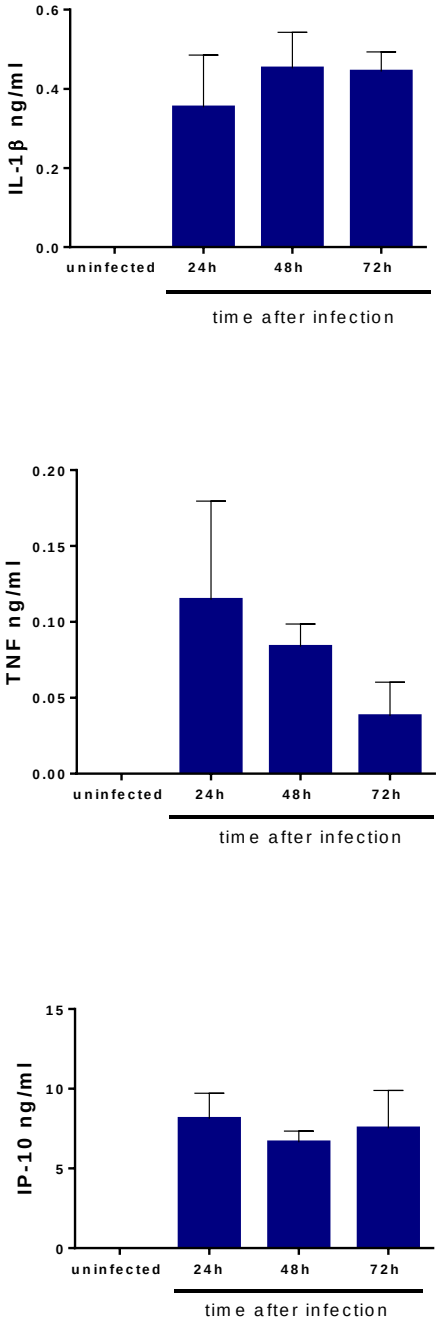

Figure 4.2 *M. tuberculosis* infected THP-1 cells secrete IL-1β, TNF and IP-10

Levels of cytokine secreted by THP-1-derived macrophages infected with *M. tuberculosis* H37Rv were measured by ELISA in cell supernatants 24h, 48h and 72h post infection. Data are shown from one representative experiment of three independent experiments. Results are expressed as mean ± SD.

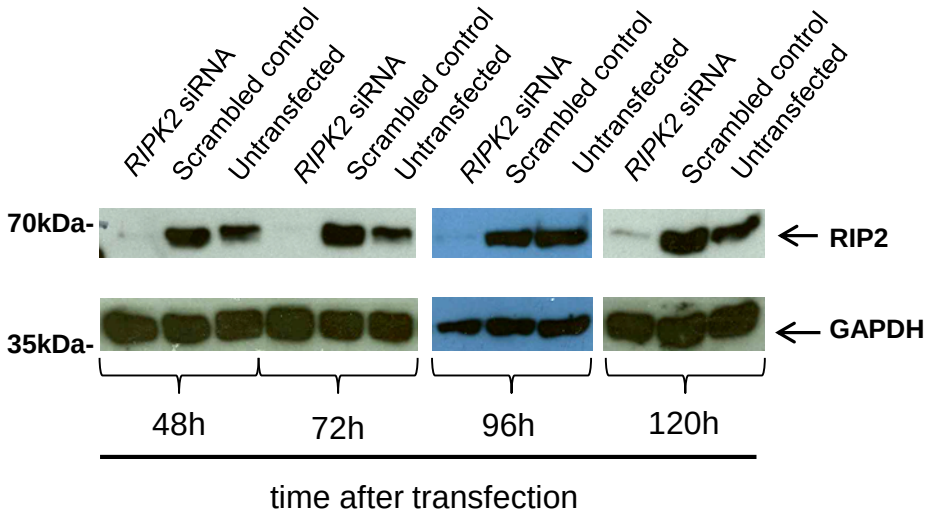

Figure 4.3 Gene knock-down of *RIPK2* in THP-1 cells
THP-1 cells were transfected with *RIPK2* siRNA or scrambled control siRNAs by electroporation. Presence of RIP2 in cell lysates was determined by immuno-blotting of 20µl of cell lysate at various time points after transfection using anti-RIP2 antibody (1:200 dilution in 3% milk in TBS-T).

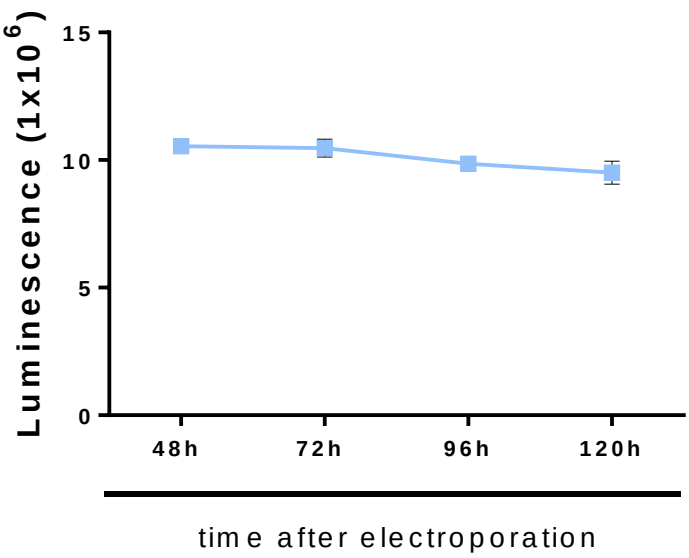

Figure 4.4 Gene knock-down of RIPK2 does not result in significant cell death
Viability of *RIPK2* siRNA transfected THP-1-derived macrophages was assessed 48h, 72h, 96h and 120h post transfection using CellTiter-Glo® assay. Results are expressed as mean ± SD.

4.2.4 Absence of RIP2 does not affect *M. tuberculosis* or macrophage survival during infection

To determine whether the absence of RIP2 affected the level of bacterial or macrophage survival during infection with *M. tuberculosis*, bacterial survival was assessed by counting CFU, and macrophage viability was measured using CellTiter-Glo® assay. No significant differences were observed in the number of intracellular bacteria in RIP2-deficient macrophages compared to macrophages transfected with scrambled control siRNA. Fewer intracellular bacteria were observed at 24h after infection of siRNA-transfected macrophages compared to untransfected cells (Figure 4.5 A). Measuring metabolic activity of macrophages showed that viability of infected macrophages decreased at a similar rate over time in RIP2-deficient and scrambled siRNA transfected cells (Figure 4.5 B). Overall, the depletion of RIP2 did not affect the viability of infecting *M. tuberculosis* or host macrophages after infection.

4.2.5 RIP2 regulates induction of IL-1β during infection with *M. tuberculosis*

To investigate whether the absence of RIP2 affected the induction of cytokines during mycobacterial infection, the level of IL-1β, TNF and IP-10 were measured in cell supernatants of infected macrophages after transfection with *RIPK2* siRNA or scrambled control siRNA. RIP2-deficiency led to a significant reduction in IL-1β secretion at 24h, 48h and 72h post infection compared scrambled control siRNA-transfected macrophages (Figure 4.6). The levels of TNF and IP-10 secretion were unaffected by depletion of RIP2 (Figure 4.6). Of note, IL-1β and TNF levels (but not IP-10) appeared to be higher in infected macrophages that were transfected with siRNAs compared to untransfected wild type macrophages (Figure 4.2 and 4.6).

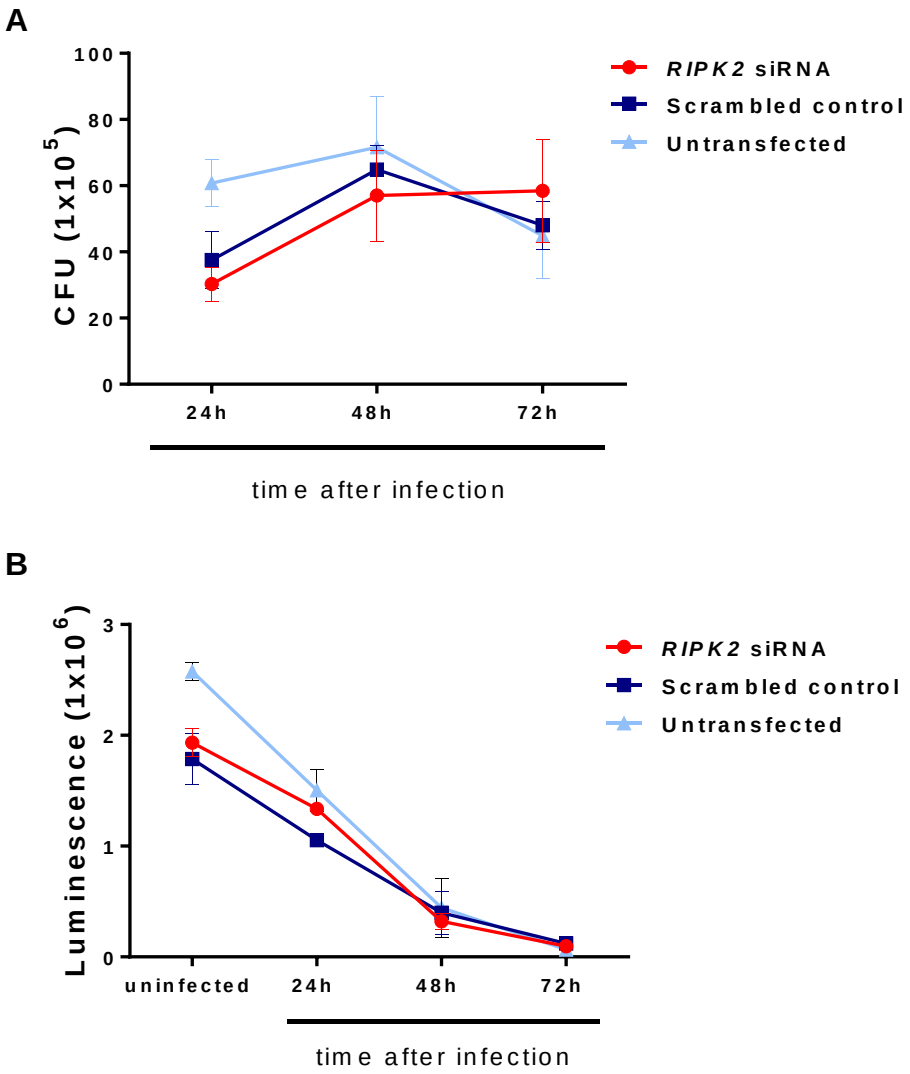

Figure 4.5 RIP2-deficiency has no effect on the viability of *M. tuberculosis* or macrophages

(A) The numbers of intracellular bacteria were estimated by viable counting at various time points after infection of transfected THP-1-derived macrophages (*RIPK2* siRNA or scrambled control). (B) Viability of THP-1-derived macrophages was determined using CellTiter-Glo® assay in transfected cells before and after infection. Results shown are pooled data from three independent experiments expressed as mean ± SEM.

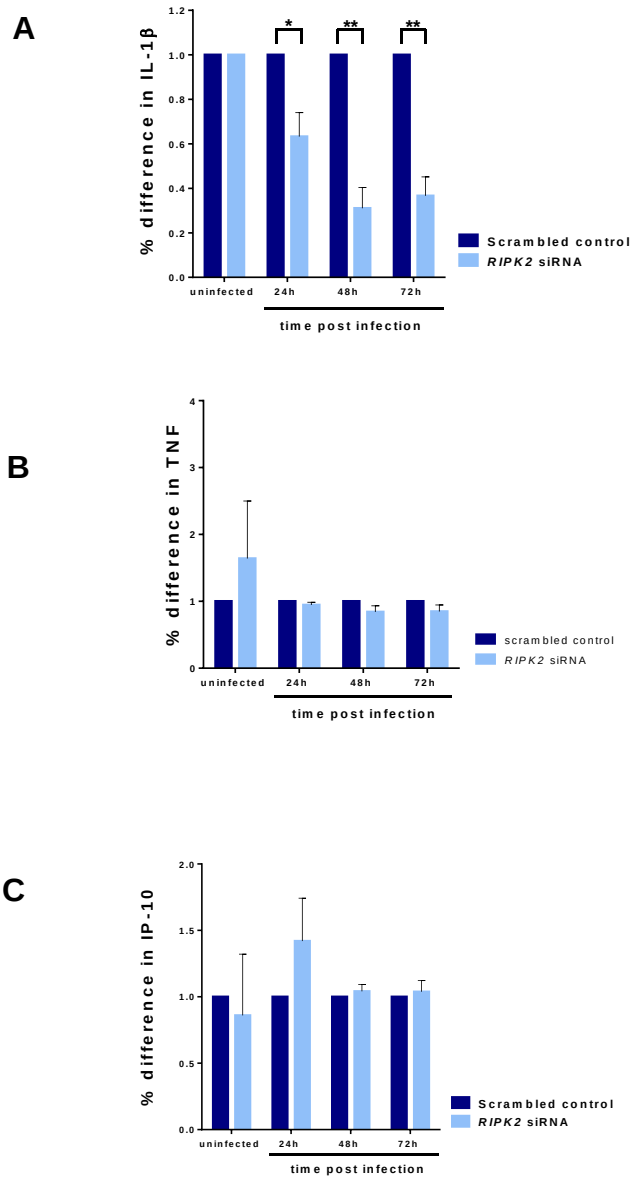

Figure 4.6 *RIPK2* gene knock-down results in decreased secretion of IL-1β but not TNF and IP-10 from *M. tuberculosis* infected THP-1-derived macrophages

THP-1-derived macrophages were infected with *M. tuberculosis* H37Rv (MOI 10:1) 48h after transfection and (A) IL-1β, (B) TNF and (C) IP-10 were measured in cell free supernatants by ELISA. Pooled data are shown from three independent experiments. Results are expressed as mean ± SEM with ***** defined as $p<0.05$ and ****** defined as $p<0.01$.

4.3 Discussion

RIPK2 encoding the RIP2 kinase was associated with magnitude of IFN-γ response to mycobacterial antigen in a genome-wide linkage analysis in the Gambian population. Two non-synonymous polymorphisms were identified in the kinase domain of *RIPK2* in DNA samples of Gambian origin. Both polymorphisms were predicted to have detrimental effects on the function of RIP2.

RIP2 plays an essential role in transduction of downstream signals upon activation of the NLRs, NOD1 and NOD2, leading to induction of pro-inflammatory cytokines. Several studies have investigated the contribution of NOD signalling to immune responses to *M. tuberculosis*. However, most studies to date have focused on the role of NOD2 only, rather than the combined effect of both receptors by targeting RIP2 that acts downstream of both NOD1 and NOD2 receptors. Furthermore, the majority of studies have used murine rather than human models of infection. To our knowledge no studies have focused on the role of RIP2 in human macrophages after *M. tuberculosis* infection.

The human monocytic cell line THP-1 was chosen to investigate the contribution of RIP2 to the response of macrophages to *M. tuberculosis*. THP-1 cells can be differentiated into macrophage-like cells by stimulation with phorbol diesters such as PMA (Tsuchiya *et al*., 1982; Tsuchiya *et al*., 1980). PMA-differentiated THP-1 cells readily phagocytose *M. tuberculosis* and are frequently used to study host-pathogen interactions.

THP-1-derived macrophages were infected with the virulent *M. tuberculosis* laboratory strain H37Rv at an MOI of 10:1. This relatively high MOI ensured that a high number of bacilli were likely to be phagocytosed, allowing host-pathogen interactions to be monitored across a short time frame (24h-48h post infection). This was important as depletion of RIP2 by transfection with siRNA only achieved effective knock down for 48h-96h. Additionally, a higher inoculum increased the chance of activation of cytosolic receptors such as the NOD receptors.

CFU counting of intracellular bacteria at 24h demonstrated that bacilli were successfully phagocytosed by THP-1-derived macrophages. *M. tuberculosis*

numbers increased for a further 24h before decreasing, which corresponds to the drop in viable macrophages available to infect at 72h post infection. The number of viable macrophages was shown to gradually decrease over the course of infection with approximately 20% of the macrophage monolayer intact after 48h and only 5% at 72h post infection. Consequently, the decrease in bacterial numbers 72h after infection suggested the presence of large numbers of extracellular bacteria rather than control of intracellular mycobacterial replication by the macrophage population.

4.3.1 Absence of RIP2 does not affect *M. tuberculosis* or macrophage survival during infection

In the current study neither macrophage survival nor bacterial survival was altered over 72h infection in the absence of RIP2 relative to THP-1-derived macrophages transfected with scrambled control siRNAs. A study by Brooks *et al*. (2011) showed that in the absence of NOD2, *M. tuberculosis* H37Rv (and *M. bovis* BCG) growth in human monocyte-derived macrophages was significantly increased at 24h post infection (Brooks *et al*., 2011). This difference might be due to the different cell types used in the two studies, monocyte-derived macrophages versus THP-1-derived macrophages. Brooks *et al.* (2011) also investigated the effect of NOD2-deficiency in murine BMDMs after infection with *M. tuberculosis* or *M. bovis* BCG. Growth of *M. tuberculosis* was unaffected in *Nod2*$^{-/-}$ murine macrophages, whereas growth of *M. bovis* BCG was enhanced, but only at 72h and 168h post infection. Consequently the authors concluded that there are differences in the requirement for NOD2 in the control of intracellular growth of *M. tuberculosis* in human and murine macrophages (Brooks *et al*., 2011). It has previously been shown by other studies that NOD2 is not required for controlling growth of *M. tuberculosis* in mice (Divangahi *et al*., 2008; Gandotra *et al*., 2007).

4.3.2 RIP2 regulates induction of IL-1β but not TNF or type I interferons during infection with *M. tuberculosis*

THP-1-derived macrophages were shown to induce TNF, IL-1β and IP-10 upon infection with *M. tuberculosis*. The relative levels of TNF, IL-1β and IP-10 secreted from *M. tuberculosis* infected THP-1 cells in the current study correspond with those previously reported (Cheruvu *et al*., 2007; Faksri *et al*., 2014; Friedland *et al*., 1993; Rajavelu and Das, 2010; Sharma *et al*., 2003; Tanveer *et al*., 2009).

TLR2 detects various mycobacterial antigens such as LMs and PIMs and several lipoproteins and is thought to be one of the main receptors responsible for induction of TNF during infection with *M. tuberculosis* (Drage *et al*., 2009; Prados-Rosales *et al*., 2011; Underhill *et al*., 1999). Co-stimulation of TLR2 and NOD2 results in synergistic responses leading to secretion of substantially higher levels of TNF (Ferwerda *et al*., 2005). Furthermore, studies using murine as well as human macrophages have shown that, in the absence of NOD2, TNF secretion during *M. tuberculosis* infection is significantly reduced suggesting a role for NOD2 signalling in the induction of TNF upon stimulation with mycobacterial antigen (Brooks *et al*., 2011; Divangahi *et al*., 2008; Ferwerda *et al*., 2005; Gandotra *et al*., 2007). Subsequently, in the current study the level of TNF secreted by RIP2 depleted THP-1-derived macrophages was measured during infection with *M. tuberculosis*. However, no differences between RIP2 positive and negative macrophages were observed. This difference might be due to the cell types utilised as all previous studies used primary cells (human and murine) whereas the current study used a monocytic leukemia cell line. Nevertheless, a study by Pandey *et al.* (2009) verifies the current study reporting no effect on TNF mRNA induction in NOD2 and RIP2-deficient murine macrophages (Pandey *et al*., 2009).

In the current study, RIP2 depleted THP-1-derived macrophages were shown to secrete significantly reduced levels of IL-1β compared to macrophages transfected with scrambled control siRNAs. This is in accordance with a study by Brooks *et al.* (2011) which demonstrated that in the absence of NOD2, human macrophages produced significantly reduced levels of IL-1β (Brooks *et al*., 2011). Additionally, PBMCs from individuals with

mutations in *NOD2* were also found to release significantly lower levels of IL-1β in response to *M. tuberculosis* infection compared to PBMCs from healthy volunteers (Kleinnijenhuis *et al*., 2009). NOD2, TLR2 and TLR6 have been shown to contribute to induction of IL-1β during *M. tuberculosis* infection, and co-stimulation of TLR2 and NOD2 results in synergistically enhanced IL-1β production (Brooks *et al*., 2011; Ferwerda *et al*., 2005; Kleinnijenhuis *et al*., 2009). Interestingly, IL-1β may be induced independently of TLRs *in vivo*, as mice lacking the TLR adapter proteins TRIF and MyD88 secrete increased levels of IL-1β compared to wild type mice (Mayer-Barber *et al*., 2010). This further suggests an important role for NOD2/RIP2 dependent induction of IL-1β secretion during *M. tuberculosis* infection.

A study by Pandey *et al.* (2009) demonstrated that NOD2 and RIP2 substantially contributed to the induction of type I IFNs in murine BMDMs after *M. tuberculosis* infection (Pandey et al., 2009). Subsequently, to investigate whether the absence of RIP2 affected induction of type I IFNs during infection with *M. tuberculosis*, IP-10 levels were measured in infected THP-1-derived macrophages as a surrogate for induction of type I IFNs (Petry *et al*., 2006). No change was observed in secretion of IP-10 between RIP2-deficient and wild type macrophages. This again could be attributed to the difference between cell types used in each study, or the difference between murine and human macrophages. However, Manzanillo *et al*. (2012) found that levels of type I IFNs were unchanged in the absence of NOD2 in murine BMDMs infected with *M. tuberculosis* (Manzanillo *et al*., 2012). That the absence of RIP2 did not affect levels of IP-10 is probably unsurprising. Several PRRs contribute to the induction of type I IFNs during infection with *M. tuberculosis*, including the intracellular DNA sensors IFI16, DDX41 and STING, making the role of NOD2 in this process probably redundant (Ishikawa *et al*., 2009b; Manzanillo *et al*., 2012; Parvatiyar *et al*., 2012; Unterholzner *et al*., 2010).

IL-12 secreted from macrophages plays an important role in the induction of IFN-γ from T-lymphocytes in the cell-mediated control of *M. tuberculosis*. Furthermore, two studies demonstrated that in the absence of NOD2 the secretion of IL-12p40 was significantly reduced (Divangahi *et al*., 2008; Gandotra *et al*., 2007). Therefore, the current study aimed to determine the level of IL-12p40 secreted from infected THP-1-derived macrophages

depleted of RIP2. However, IL-12 levels induced by both RIP2-deficient and wild type macrophages cells were not sufficient to be detected by ELISA.

Both studies conducted in *Nod2*$^{-/-}$ deficient mice found that despite reduced levels of TNF, IL-12p40 and IFN-γ in these animals, the mice were capable of controlling *M. tuberculosis* growth as well as wild type mice (Divangahi *et al*., 2008; Gandotra *et al*., 2007). However, Brooks *et al*. (2011) highlighted that there might be differences in the requirement for NOD signalling in the control of *M. tuberculosis* growth during infection of murine and human macrophages (Brooks *et al*., 2011). Evidence increasingly highlights fundamental differences in the innate immune response of macrophages of human and murine origin. For example, mice are able to control *M. tuberculosis* infection in the absence of *Nramp1* whereas mutations in the human equivalent *SLC11A1* render individuals susceptible to infection (Bellamy *et al*., 1998; Li *et al*., 2011b; North *et al*., 1999).

4.3.3 Significance of IL-1β during *M. tuberculosis* infection

Both this study and Brooks *et al*. (2011) observed that in human macrophages IL-1β secretion was significantly reduced in the absence of NOD2 or RIP2 after *M. tuberculosis* infection (Brooks *et al*., 2011). IL-1β has been shown to play an important role in immune responses to *M. tuberculosis*; in the absence of IL-1β mice display an increased bacterial burden and quickly succumb to infection (Mayer-Barber *et al*., 2010). Furthermore, IL-1β is induced during the early stages of infection resulting in recruitment of neutrophils to the site of infection (Kang *et al*., 2011).

IL-1β and type I IFN are two major cytokines that affect the outcome of *M. tuberculosis* infection (Mayer-Barber *et al*., 2014). Both cytokines have been proposed to regulate each other and subsequently IL-1β is crucial to balance levels of type I IFN as excess of type I IFNs is associated with increased bacterial loads and uncontrolled infection (Mayer-Barber *et al*., 2011; Mayer-Barber *et al*., 2014). IL-1β has been suggested to dampen down type I IFN responses through the induction of prostaglandins through COX-2 (Mayer-Barber *et al*., 2014). In turn type I IFN induces IL-10 and IL-1 receptor antagonist and inhibits caspase 1 contributing to down regulation of IL-1β,

thereby preventing inflammatory tissue damage induced by excess IL-1β (Mayer-Barber *et al*., 2014; Nathan and Ding, 2010).

4.3.4 Effect of electroporation on cytokine responses

Comparing cytokine responses of *M. tuberculosis* infected macrophages transfected by electroporation with siRNA compared to macrophages that were not transfected prior to infection showed that some cytokine responses were increased. In uninfected cells (transfected or untranfected) levels of cytokine were negligible. However, in *M. tuberculosis*-infected cells, cytokine levels of IL-1β and TNF but not IP-10 were increased by 10-fold in transfected cells compared to untransfected cells. Stimulation of THP-1 cells and other monocytic cells with PMA has been shown to induce secretion of TNF and IL-1β. However both transfected and untransfected cells in this study were stimulated with PMA to induce differentiation. Therefore, PMA stimulation cannot account for the observed differences (Park *et al*., 2007a; Wang and Alpert, 1995). This suggests that transfection is likely to be responsible for the differences observed. It is possible that electroporation or the introduction of double-stranded RNA affects the immune activation state of the THP-1-derived macrophages subsequently affecting TNF and IL-1β responses during later infection or stimulation. As the TNF responses of infected cells transfected with *RIPK2* siRNA and scrambled siRNA were similar the differences are unlikely to be siRNA sequence-specific.

Two non-synonymous polymorphisms have been identified in RIP2 in DNA samples of Gambian origin. Both these polymorphisms are located in the kinase domain of the protein and have been predicted to affect the function of RIP2.

Additionally, we demonstrate here that depletion of RIP2 in *M. tuberculosis* infected THP-1-derived macrophages leads to significant reduction in levels of IL-1β, a critical cytokine in the immune response to tuberculosis. This corresponds to other studies investigating the importance of the NOD signalling pathway during *M. tuberculosis* infection of human macrophages suggesting that RIP2 might play a significant role in the immune response of human macrophages to *M. tuberculosis* infection (Brooks *et al*., 2011; Kleinnijenhuis *et al*., 2009). Consequently, the functional significance of the

RIP2 polymorphisms identified in the Gambian cohort, on RIP2 function and NOD-dependent immune responses should be further investigated.

5. Kinase activity of RIP2 variants

5.1. Introduction

RIP2 is a kinase that is essential for the induction of NF-κB and MAP kinase, JNK, extracellular-signal-regulated kinases (ERK) 1/2 and p38 MAP kinase upon stimulation of the NOD-receptors (Kobayashi *et al*., 2002; Park *et al*., 2007b). RIP2 was initially identified as a serine threonine kinase based on sequence homology, and Dorsch *et al*. (2006) mapped an auto-phosphorylation site to serine 176 (Dorsch *et al*., 2006; McCarthy *et al*., 1998; Thome *et al*., 1998). Later it was demonstrated that RIP2 was also able to auto-phosphorylated on tyrosine 474 (Tigno-Aranjuez *et al*., 2010).

Mutation of the RIP2 lysine residue K47, which acts as an essential ATP binding site, as well as mutation of the conserved aspartic acid residues D146 and D164 have been shown to render RIP2 kinase inactive (McCarthy *et al*., 1998; Thome *et al*., 1998; Windheim *et al*., 2007). In the absence of kinase activity, protein expression of RIP2 was significantly reduced in murine bone marrow derived macrophages and HEK293 cells (Nembrini *et al*., 2009; Windheim *et al*., 2007). This decrease in RIP2 protein abundance was observed despite the presence of normal mRNA levels (Lu *et al*., 2005; Nembrini *et al*., 2009). Furthermore, inhibition of RIP2 kinase activity using the kinase inhibitor SB203508 also affected expression levels of RIP2 protein, suggesting that the kinase activity of RIP2 is required for maintenance of RIP2 protein stability (Windheim *et al*., 2007). However, the significance of RIP2 kinase activity in downstream signalling is less clear. Early studies found that kinase dead mutants induced activation of NF-κB and JNK equally well or more efficiently than wild type RIP2 kinase (Eickhoff *et al*., 2004; McCarthy *et al*., 1998; Thome *et al*., 1998; Windheim *et al*., 2007). Whereas, other studies have demonstrated that kinase dead RIP2 resulted in significantly reduced levels of NF-κB and AP-1 activation suggesting that kinase activity was required for optimal induction of cytokine responses upon stimulation of the NOD receptors (Hasegawa *et al*., 2008; Inohara *et al*., 2000; Navas *et al*., 1999; Nembrini *et al*., 2009; Tigno-Aranjuez *et al*., 2010). Furthermore, some of these studies attributed the loss in NF-κB activity to reduction of RIP2

protein levels due to the absence of kinase activity rather than the requirement for kinase activity for downstream signalling (Hasegawa *et al*., 2008; Nembrini *et al*., 2009).

The RIP2 variants I259T and L268V identified in the Gambian population both harbour non-synonymous polymorphisms within the kinase domain of the protein. Both polymorphisms were predicted *in silico* to affect protein function by the prediction software Polyphen2 and therefore were likely to affect kinase activity (Adzhubei *et al*., 2010). As the kinase activity of RIP2 has been suggested to play an important role in function of the protein, the aim of this chapter was to determine whether the RIP2 variants I259T and L268V displayed altered levels of kinase activity compared to wild type RIP2.

5.2. Results

5.2.1. Expression of recombinant RIP2

To show that recombinant RIP2 was expressed, a time course of expression was performed on HEK293T cells. Transfected cells were lysed at various time points post transfection and the levels of recombinant protein expressed were determined by western blot analysis by detecting the V5-epitope of the protein. Recombinant RIP2 could be detected 24h after transfection and expression levels increased over the next 72h (Figure 5.1).

5.2.2. Affinity purification of RIP2 with C-terminal HIS-tag

To establish a method for purification of active RIP2 kinase, the complete DNA sequence of wild type RIPK2 was cloned into pcDNA6B (Plasmid map: Appendix; Figure 9.2). The cloning strategy was designed to express recombinant RIP2 with both a V5-epitope and a HIS-tag at the C-terminus. Recombinant protein was expressed in HEK293T cells. Purification of the expressed RIP2 from cell lysates was first attempted by means of nickel magnetic agarose beads via the HIS-tag. Bound protein was eluted from the nickel beads using 300mM imidazole in sodium phosphate buffer. Western blot analysis of the initial cell lysate and eluted fractions, using an antibody targeting the V5-epitope, detected a single protein band at approximately 65kDa (Figure 5.2). This corresponds to the size of V5- and HIS-tagged RIP2. However, no RIP2 could be detected in elution fractions from the purification suggesting that the HIS-tag on the recombinant protein either failed to bind the nickel beads or was not eluted. Furthermore, the recombinant RIP2 could not be detected by an anti-HIS antibody in the cell lysates demonstrating that the HIS-tag on RIP2 was not accessible for binding (data not shown).

5.2.3. Affinity purification of C-terminally V5-tagged RIP2 by immunoprecipitation

Despite the C-terminal HIS-tag not being accessible for binding, the recombinant RIP2 could be detected by an anti-V5 antibody (Figure 5.1).

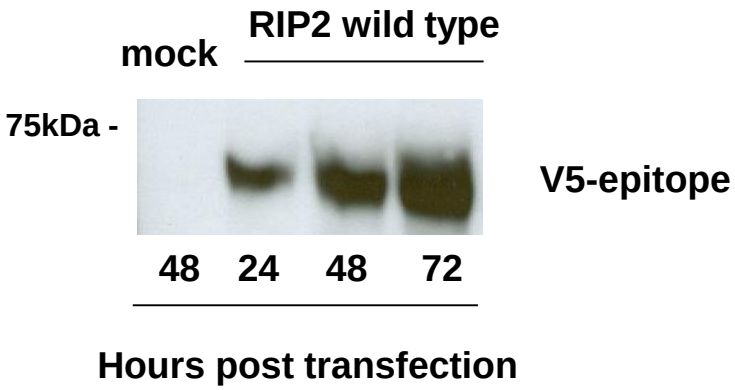

Figure 5.1 Expression of recombinant RIP2 in HEK293T
Cell lysates (25µl) from HEK293T cells transfected with pcDNA6_RIP2wt_V5/HIS were analysed by immuno blotting. Recombinant protein was detected with an anti-V5 antibody (1:5000 dilution in 5% milk in PBS-T).

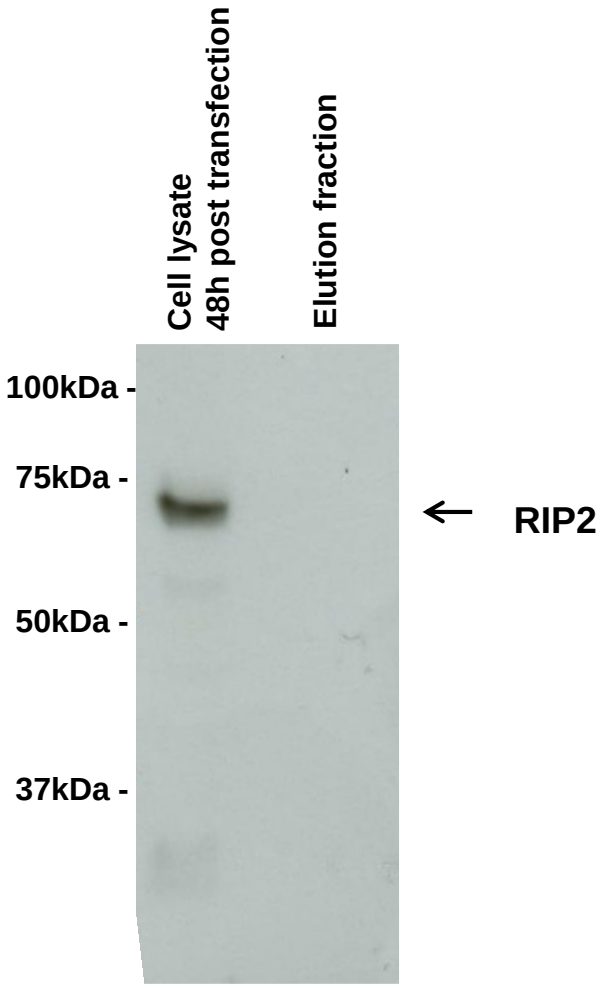

Figure 5.2 Recombinant RIP2 cannot be purified via a C-terminal HIS-tag

Recombinant RIP2 from 500µl of HEK293T cell lysates was affinity-purified using 50µl HIS select® nickel magnetic agarose beads. Expression of recombinant protein was analysed by immuno blotting of 25µl of lysate and elution fraction using an anti-V5 antibody (1:5000 dilution in 5% milk in PBS-T).

Therefore, purification of RIP2 was attempted by immunoprecipitation using the V5-epitope. Lysates of HEK293T cells expressing RIP2 recombinant protein were incubated with anti-V5 antibody for 3h before being applied to a gravity flow column packed with protein G agarose. The bound protein was eluted from the column with 0.2M glycine (pH 2.5) in three elution fractions of 500µl.

Western blot analysis of the cell lysate demonstrated the presence of a 65kDa protein corresponding to recombinant RIP2. It also highlighted the presence of four other proteins: 60kDa, 37kDa and 20kDa proteins were present in slightly smaller amounts than RIP2 and a faint band indicated the presence of a 32kDa protein (Figure 5.3; lanes 1). Western blot analysis of the immunoprecipitation elution fractions showed that predominantly the 20kDa protein was present predominantly in the first fraction and very small amounts of all other proteins (lane 3). In the second fraction only the 20kDa protein was present (lane 4). No proteins were detected in the third elution fraction (lane 5). It appeared that most of the RIP2 had not bound to the column.

5.2.4. Affinity purification using anti-V5 agarose and 0.2M glycine

As immunoprecipitation of RIP2 recombinant protein preferentially purified a protein of 20kDa, that was also present in the cell lysate, purification of RIP2 was attempted using anti-V5 antibody immobilised on agarose beads. Cell lysates were incubated with anti-V5 antibody coated agarose beads overnight. Subsequently lysates and resin were packed into a gravity flow column and unbound protein eluted with 0.2M glycine.

Western blot analysis of the cell lysate using anti-V5 antibody demonstrated the presence of a protein of approximately 65kDa corresponding to RIP2 recombinant protein (Figure 5.4; lane 1). A strong band indicated the presence of large amounts of an approximately 32kDa protein and lower amounts of a 55kDa, which might be RIP2 degradation products. The bound protein was eluted from the column in three elution fractions of 500µl of 0.2M glycine into a neutralising solution of 1M Tris-HCl (pH 9.0). Western blot analysis of the elution fractions demonstrated that the first and third elution fraction (Figure 5.4; lanes 4 and 6) contained mainly

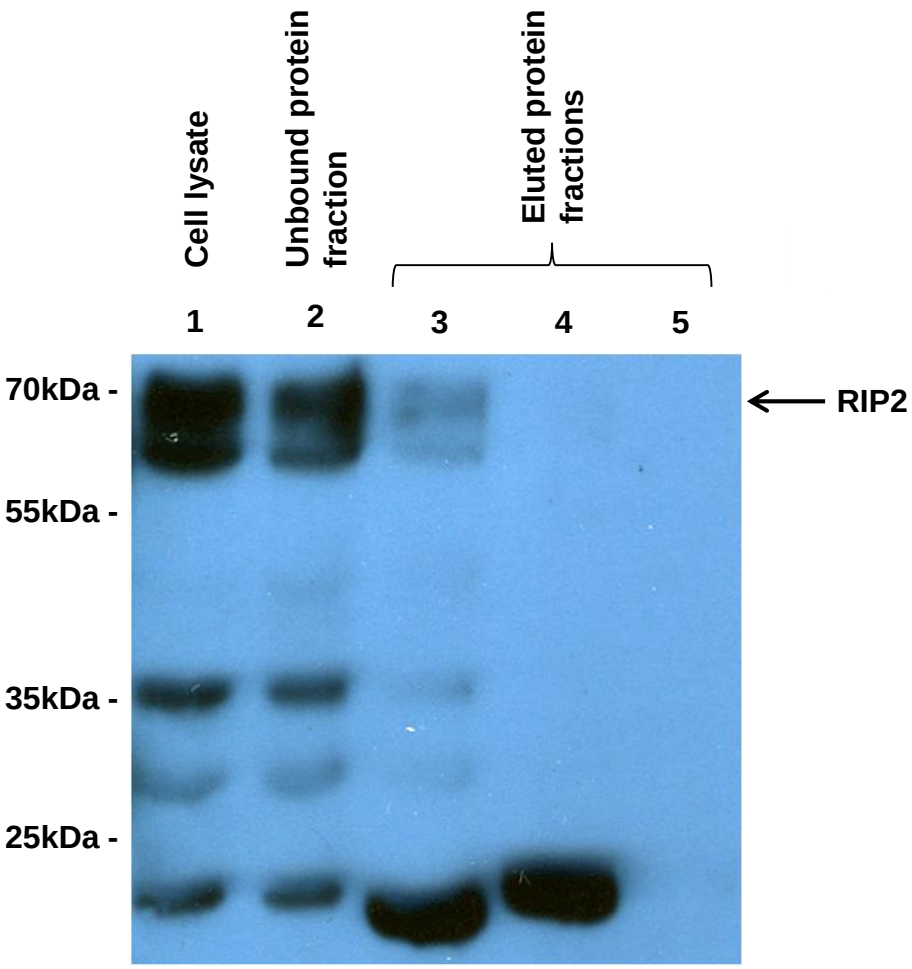

Figure 5.3 Recombinant RIP2 cannot be purified by immunoprecipitation
RIP2 was immunoprecipitated from 3ml of HEK293T cell lysate via a C-terminal V5-epitope. Cell lysate was incubated with an anti-V5 antibody for 3h prior to affinity purification using 0.5ml protein G agarose. Western blot analysis was performed on 25µl of the purification fractions using an anti-V5 antibody (1:5000 dilution in 5% milk in PBS-T).

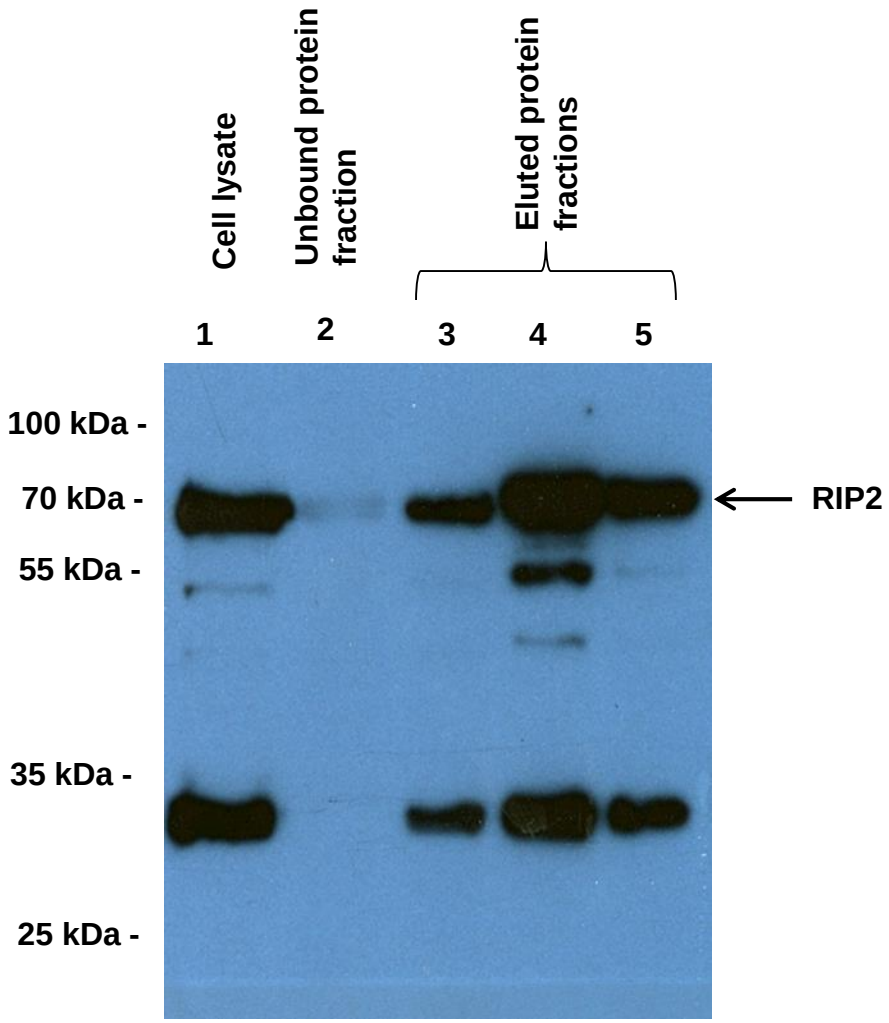

Figure 5.4 Recombinant RIP2 cannot be affinity purified using anti-v5 agarose
RIP2 was affinity purified from 3ml of HEK293T cell lysate via a C-terminal V5-tag using 0.5ml anti-V5 agarose. Western blot analysis was performed on 25µl of purification fractions using an anti-V5 antibody (1:5000 dilution in 5% milk in PBS-T).

full length RIP2 recombinant protein and the 32kDa protein. Both proteins were present in equal amounts. The second elution fraction (lane 5) also contained both these proteins but also other proteins in lesser amounts. Western blot analysis of the unbound fraction indicated that the 32kDa protein was completely cleared from the unbound fraction, whereas some RIP2 recombinant protein remained in the unbound fraction suggesting that the 32kDa protein bound preferentially to the beads.

As the 32kDa protein appeared to bind preferentially to the anti-V5 agarose, it had to be removed from the lysate prior to RIP2 purification. In order to remove the smaller competing protein the cell lysates were pre-cleared with anti-V5 agarose prior to purification of RIP2. Then the pre-cleared protein fraction was incubated overnight with anti-V5 agarose. Bound protein was eluted in three fractions with a 0.2M glycine solution as before (Figure 5.5).

Western blot analysis of the elution fractions revealed that RIP2 was eluted in the second and third fraction. Only one protein of size corresponding to recombinant RIP2 was identified (Figure 5.5 A). Coomassie staining of SDS-PAGE gels demonstrated that the second and third elution fractions contained only minor amounts of other contaminating proteins (Figure 5.5 B)

5.2.5. Kinase activity of purified RIP2

The kinase activity of the purified RIP2 was assayed by measuring the amount of ADP generated as a result of myelin basic protein (MBP) protein phosphorylation by RIP2.

RIP2 kinases were incubated with MBP protein and 50μM ATP. Subsequently the kinase reaction was terminated and the remaining ATP was degraded. The RIP2 generated ADP was first converted into ATP and then into a luminescent signal.

To ensure that the amount of purified RIP2 added to the assay was sufficient to generate a luminescent signal, the purified wild type RIP2 was quantified by applying serial dilutions of the purified RIP2 on SDS-PAGE gel alongside a known concentration of commercial RIP2 kinase (Figure 5.6). Two concentrations of commercially available active RIP2 kinase (50ng and

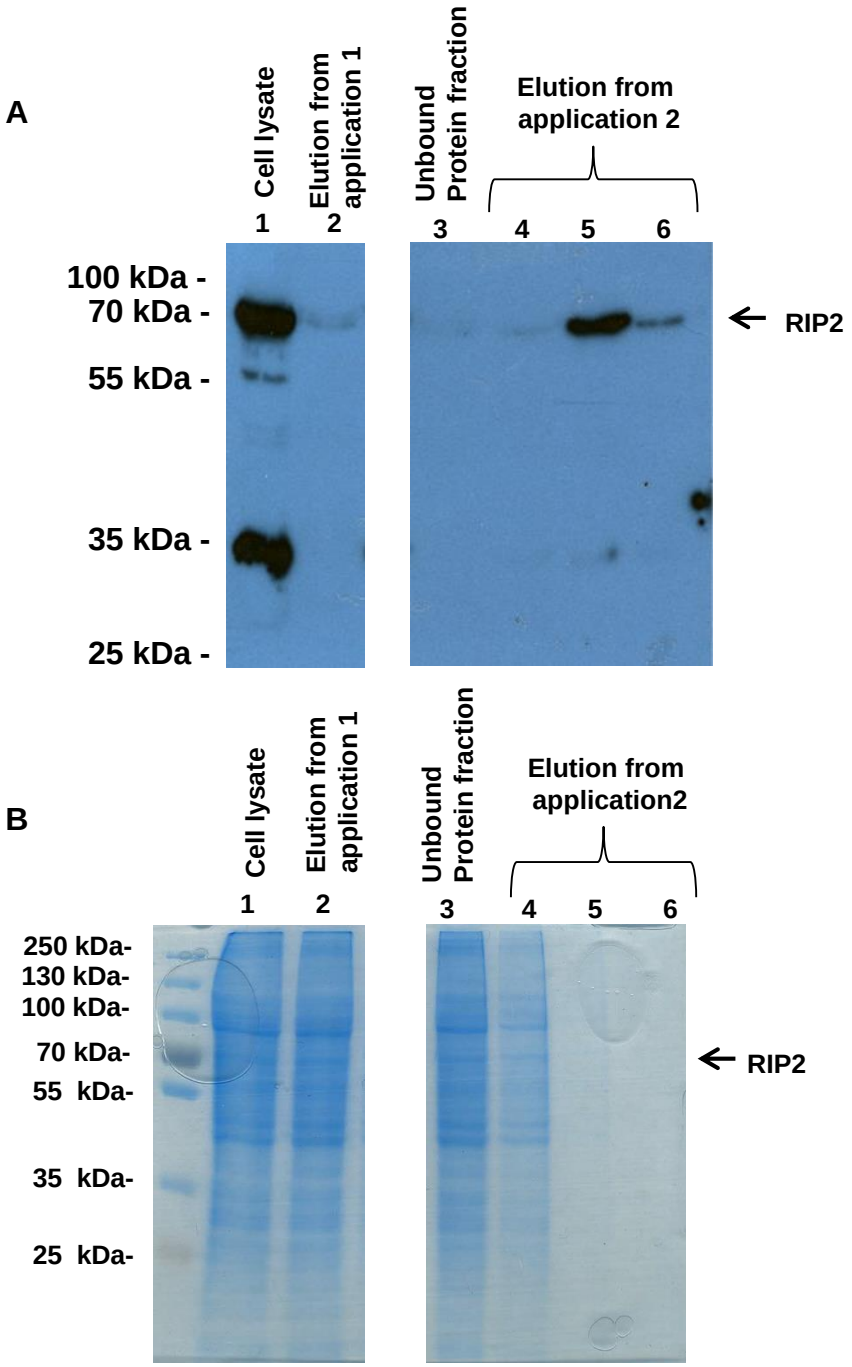

Figure 5.5 Recombinant RIP2 can be purified by affinity chromatography using anti-V5 agarose in a two-step process
RIP2 was purified from 3ml of HEK293T cell lysates subjected to two separate incubations with 0.5ml of anti-V5 agarose. The eluted fraction from the first incubation was applied to fresh anti-V5 agarose for second incubation step (A) Western blot analysis was performed on 25µl of purification fractions using an anti-V5 antibody (1:5000 dilution in 5% milk in PBS-T). (B) Purity of elution fractions were tested by Coomassie staining of the SDS-PAGE gel.

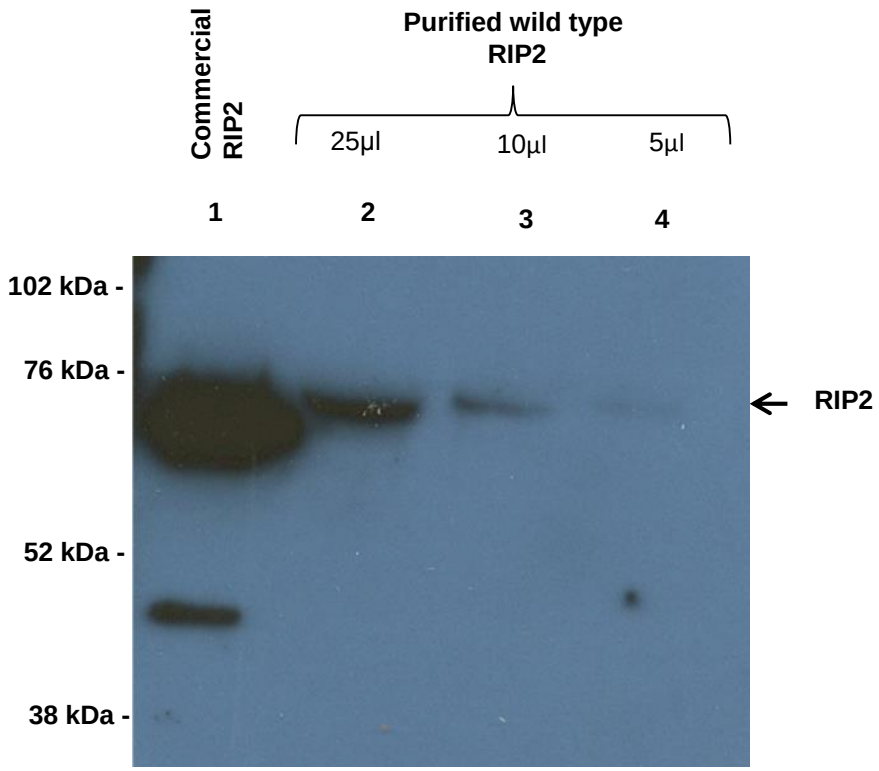

Figure 5.6 Quantification of recombinant RIP2 purified using anti-V5 agarose

Concentration of purified RIP2 was quantified by applying serial dilutions of purified recombinant RIP2 on SDS-PAGE alongside 1µg of commercial RIP2. Western blot analysis was performed using anti-RIP2 antibody (1:200 dilution in 3% milk in TBS-T).

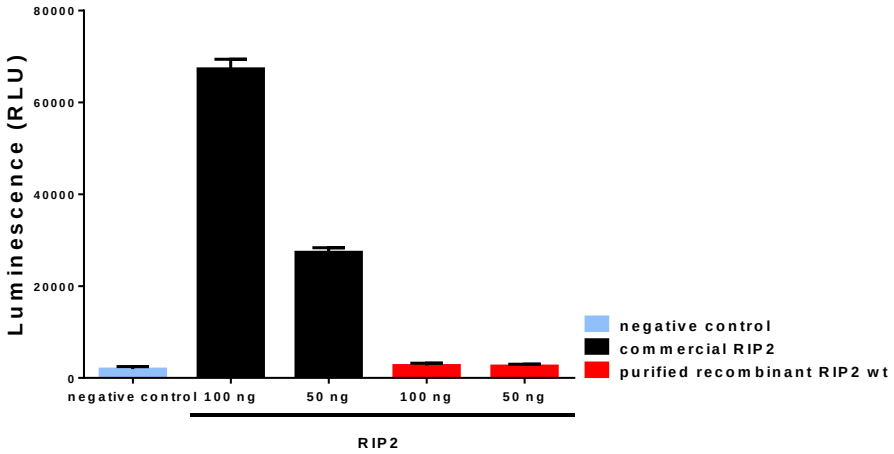

Figure 5.7 Recombinant RIP2 purified using anti-V5 agarose is not kinase active

Kinase activity of purified and commercial RIP2 was assayed in an *in vitro* kinase assay. Results are expressed as mean ± SD.

100ng) were tested in the kinase assay; both concentrations generated a strong dose dependent luminescence signal (Figure 5.7). In the absence of RIP2 kinase, almost no luminescence was detected. When the purified recombinant wild type RIP2 (50ng and 100ng) was tested in the kinase assay, the luminescence signal generated was similar to that of the negative control (Figure 5.7). Furthermore, the luminescence signal generated by the purified recombinant wild type RIP2 kinase was not dose dependent suggesting that the purified wild type RIP2 was not kinase active.

5.2.6. Affinity purification using anti-V5 agarose and V5-peptide

As the elution of RIP2 from the anti-V5 agarose beads using 0.2M glycine (pH 2.5) resulted in the loss of RIP2 kinase activity, RIP2 had to be eluted from the column by other means. As in previous experiments, anti-V5 agarose beads were incubated overnight with lysates from HEK293T cells expressing recombinant RIP2. To ensure that the kinase activity of RIP2 was maintained during elution, a V5-peptide was added to outcompete the bound protein.

Western blot analysis of the HEK293T cell lysates using an anti-V5 antibody demonstrated the presence of a protein corresponding to the size of RIP2 in lane 1 (Figure 5.8). Immuno blot analysis of the unbound fraction (lane 2) and three elution fractions (lanes 3-5) demonstrated that even though RIP2 bound to the V5-agarose, the peptide was unable to displace the bound protein. Three final elution fractions (lanes 6-8) using three times 500µl of 0.2M glycine confirmed that protein was bound to the agarose but that the peptide had failed to displace it. A high concentration (1.2 M) of NaCl was also tested as an eluent, but failed to elute bound RIP2 from the column.

5.2.7. Affinity purification of N-terminally HIS-tagged RIP2

Purification using affinity chromatography with anti-V5 antibody required a 0.2M glycine solution (pH 2.5) to elute the bound protein, which we hypothesise diferentially affects RIP2 kinase activity. Moreover, the anti-V5 antibody preferentially purified a protein of 32kDa. The amount of this contaminating protein in the purified protein fraction could be minimised but not abolished. Therefore, a different strategy was required for purifying

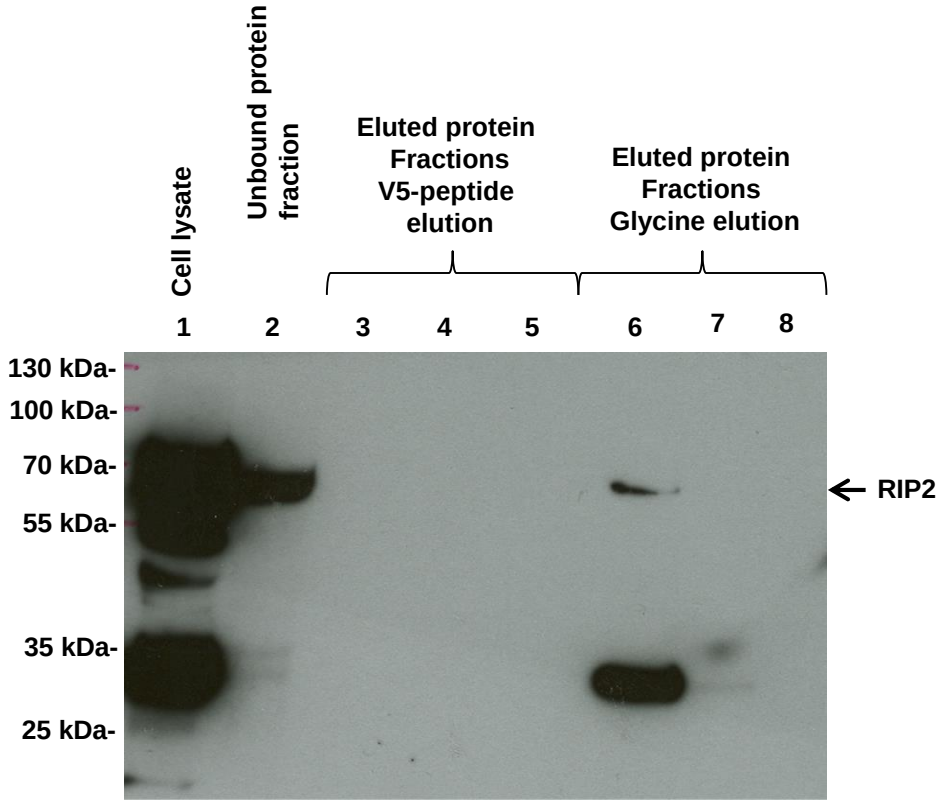

Figure 5.8 Recombinant RIP2 cannot be released from anti-V5 agarose competition with a V5-peptide

RIP2 was affinity purified from 3ml of HEK293T cell lysate via a C-terminal V5-epitope using 0.5ml anti-V5 agarose and western blot analysis was performed on 25µl of purification fractions using an anti-V5 antibody (1:5000 dilution in 5% milk in PBS-T). Elution of bound protein from the column was tested with 3x 0.5ml V5-peptide (100µg/ml) (lanes 3-5) and 3x 0.5ml 0.2M glycine (lanes 6-8).

kinase active RIP2. DNA coding for full-length wild type RIP2 with a HIS-tag at the N-terminus was cloned into pcDNA6 and the construct was expressed in HEK293T cells. Cell lysates were applied to a cobalt charged affinity resin packed into a gravity flow column. The bound protein was eluted with 300mM imidazole in sodium phosphate buffer. Purified protein was buffer-exchanged into kinase reaction buffer and concentrated to a final volume of 250µl.

Western blot analysis of all fractions of the purification, using an anti-RIP2 antibody, indicated relatively pure RIP2 in elution and concentrated fractions (Figure 5.9 A). Coomassie staining of SDS-PAGE gels demonstrated that the eluted and the concentrated fraction contained only minor amounts of contaminants (Figure 5.9 B).

5.2.8. Generation and purification of RIP2 kinase variants

The polymorphisms rs2230801 and rs35004667 were introduced into the HIS-tagged wild type *RIPK2* construct by site directed mutagenesis. These two variants of RIP2 (RIP2 I259T and RIP2 L268V) were expressed and purified as described for wild type RIP2 (Figure 5.10 A and 5.11 A). Only minor amounts of contaminating proteins were detected by Coomassie staining of all protein fractions (Figure 5.10 B and 5.11 B).

5.2.9. Effect of variants RIP2 I259T and RIP2 L268V on kinase activity of RIP2 compared to wild type

The kinase activity of the wild type and variant RIP2 proteins were compared using the *in vitro* kinase assay described above. To ensure equal loading of recombinant RIP2 into the assay, the concentration of each recombinant RIP2 was quantified by comparing dilutions of the purified recombinant proteins to each other and to a commercially-available RIP2 standard by western blot analysis (Figure 5.12).

Kinase activity of 40ng, 25ng and 12.5ng of purified wild type RIP2 kinase was measured as described previously (Figure 5.13). The wild type RIP2 purified via metal chelate chromatography resulted in the generation of a strong luminescent signal in the kinase assay, indicating that this purification method maintained RIP2 kinase activity. A dose-dependent luminescent signal was observed, with 40ng of wild type kinase generating a

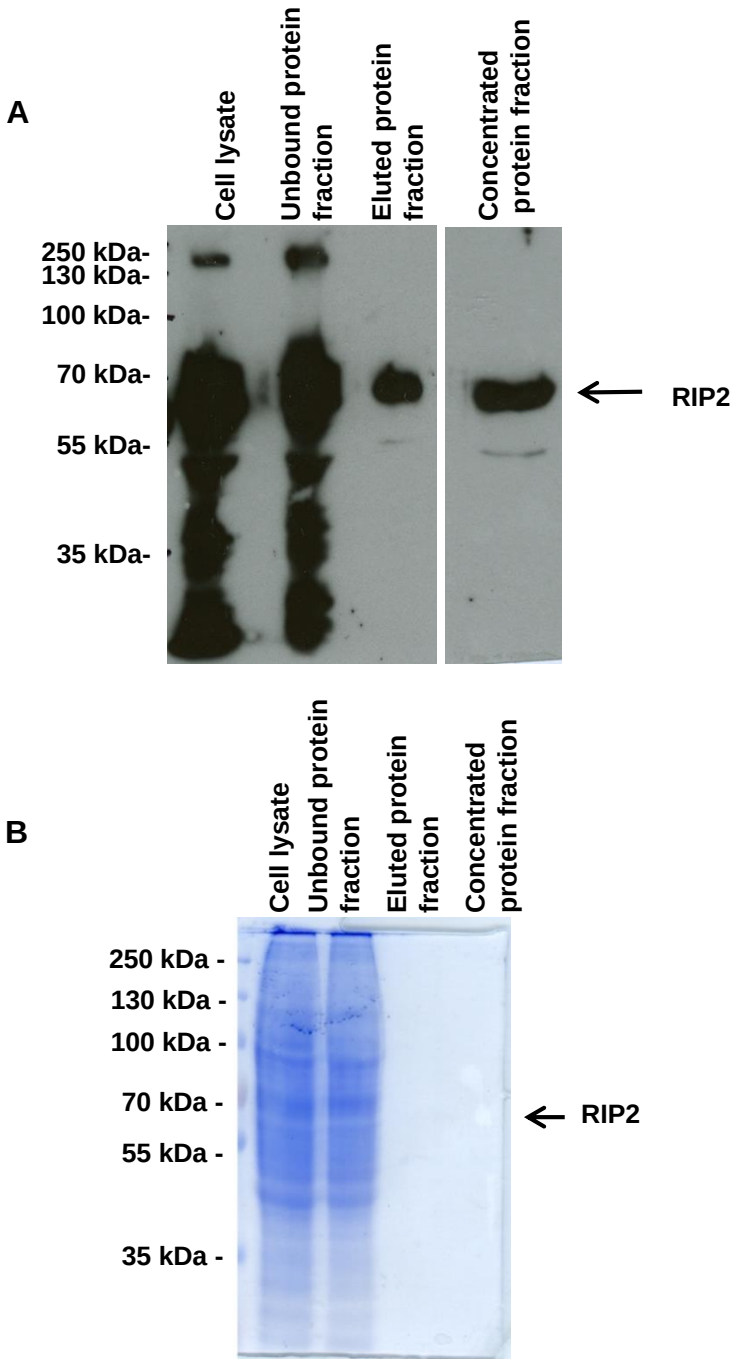

Figure 5.9 Recombinant RIP2 can be purified using metal chelate chromatography via an N-terminal HIS-tag
Recombinant RIP2 from 3ml HEK293T lysates was purified via an N-terminal HIS-tag using a HIS GraviTrap™ TALON®. (A) Western blot analysis of 25µl of purification fractions was performed using an anti-RIP2 antibody (1:200 dilution in 3% milk in TBS-T). (B) Coomassie stain of SDS-PAGE was performed on all purification fractions.

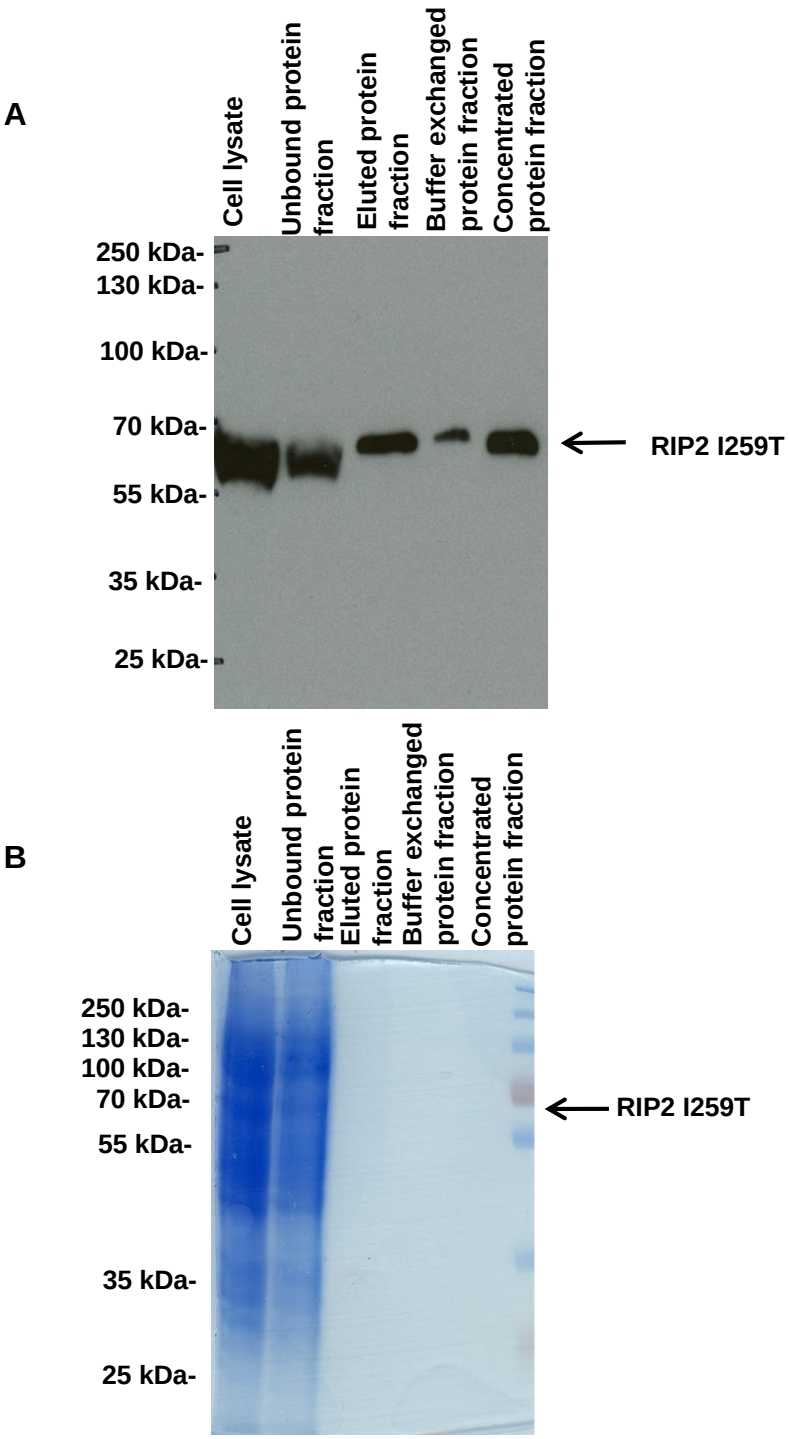

Figure 5.10 Recombinant RIP2 I259T can be purified using metal chelate chromatography via an N-terminal HIS-tag
Recombinant RIP2 I259T from HEK293T lysates was purified via an N-terminal HIS-tag using a HIS GraviTrap™ TALON®. (A) Western blot analysis of 25µl of purification fraction was performed using an anti-RIP2 antibody (1:200 dilution in 3% milk in TBS-T) and (B) Coomassie stain of SDS-PAGE were performed on all purification fractions.

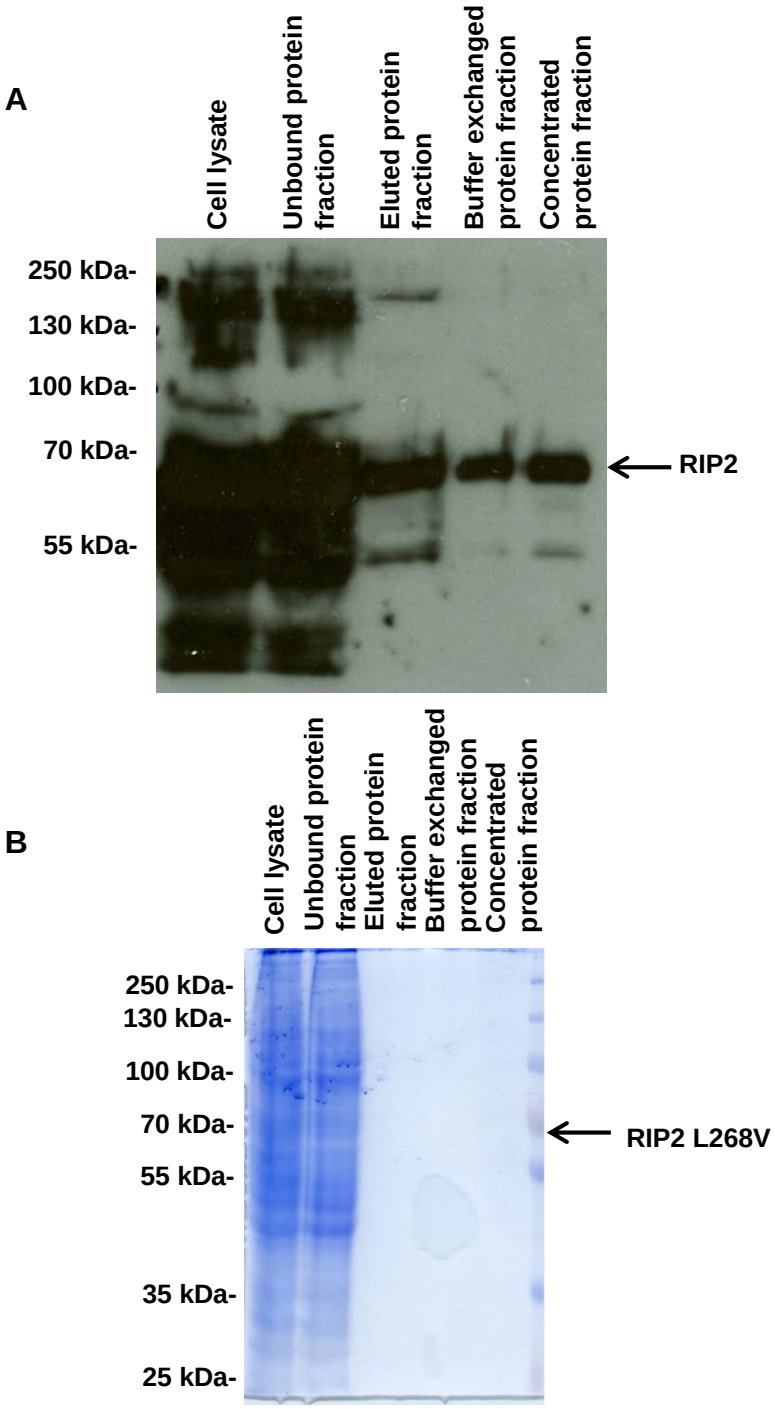

Figure 5.11 Recombinant RIP2 L268V can be purified using metal chelate chromatography via an N-terminal HIS-tag
Recombinant RIP2 L268V from HEK293T lysates was purified via an N-terminal HIS-tag using a HIS GraviTrap™ TALON®. (A) Western blot analysis of 25µl of purification fractions was performed using an anti-RIP2 antibody (1:200 dilution in 3% milk in TBS-T). (B) Coomassie stain of SDS-PAGE was performed on all purification fractions.

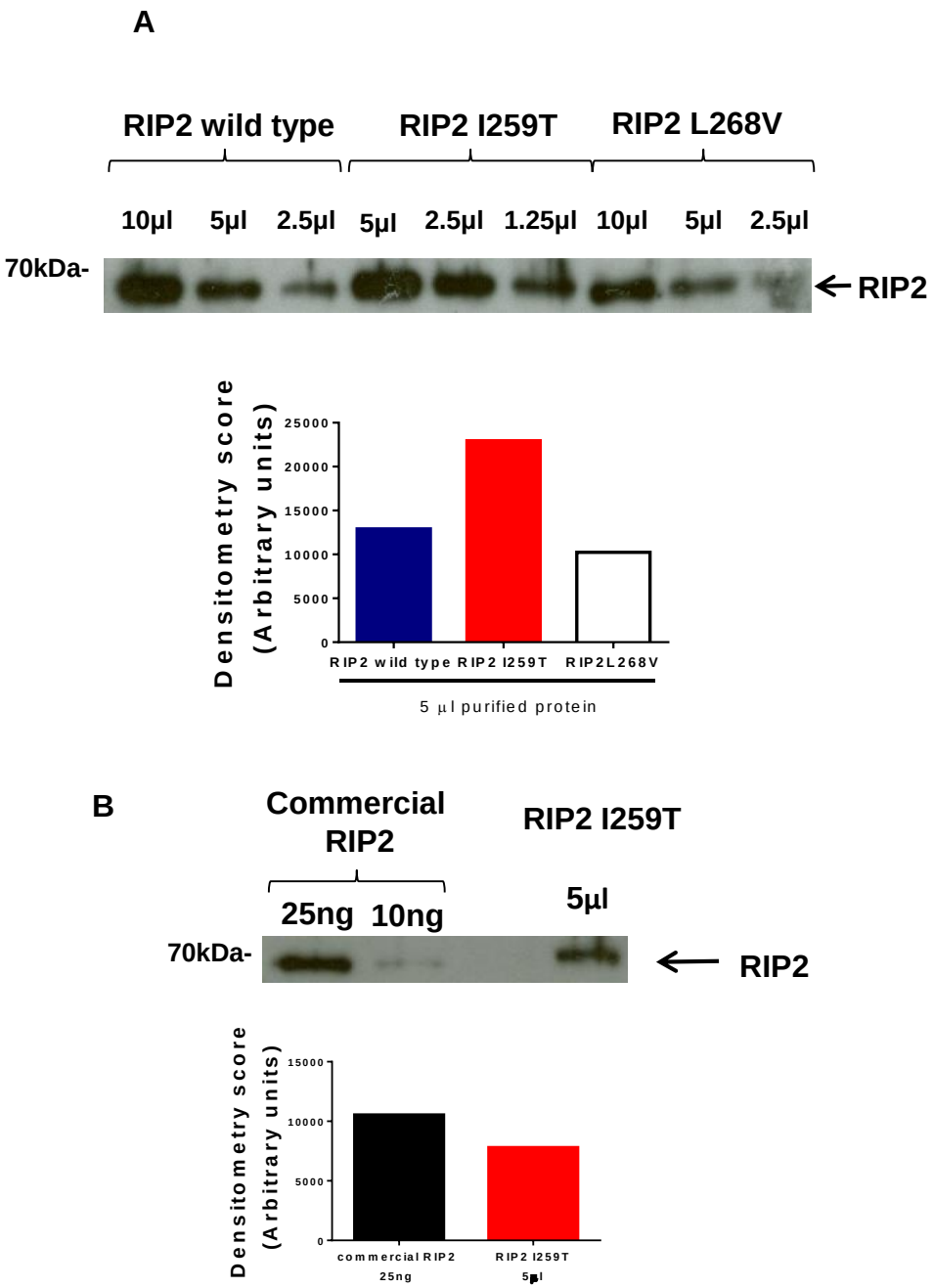

Figure 5.12 Relative quantification of wild type and variant RIP2 recombinant protein

(A) The relative concentration of wild type and variant RIP2 recombinant proteins were compared by western blot analysis using anti-RIP2 antibody (1:200 dilution in 3% milk in TBS-T) and subsequent densitometric analysis. (B) The concentration of the purified RIP2 proteins was standardised by comparison of purified with commercially available RIP2.

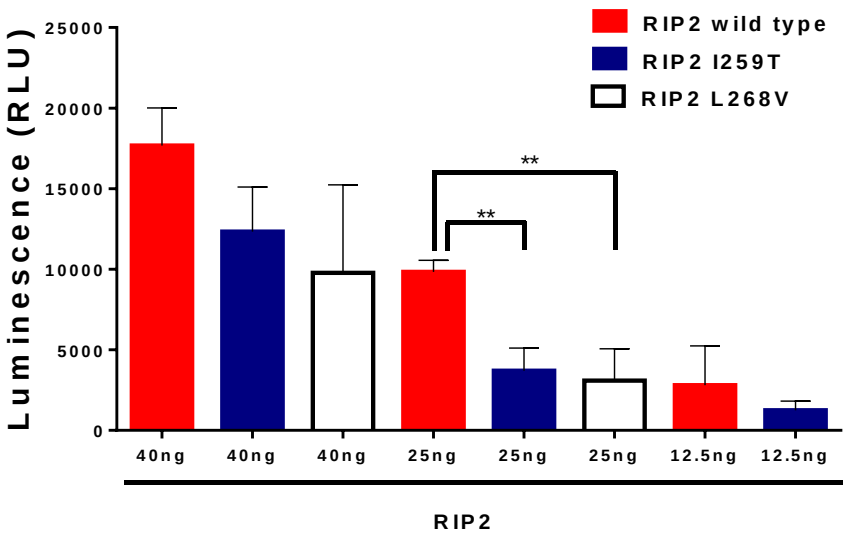

Figure 5.13 RIP2 variants have reduced kinase activity
Kinase activity of purified wild type RIP2 and RIP2 variants I259T and L268V was assayed in an *in vitro* kinase assay. Results were normalised to the negative control and expressed as mean ± SD with ****** defined as $p<0.01$.

signal approximately 3-fold greater than the negative control and 25ng of wild type kinase producing a signal ~2-fold greater than the negative control.

The kinase activity of RIP2 I259T was measured using 40ng, 25ng and 12.5ng of purified variant RIP2 whereas the kinase activity of RIP2 L268V was only measured at 40ng and 25ng of purified variant RIP2 as a lower protein yield of this RIP2 variant was purified. The kinase activity of both variants was significantly reduced compared to wild type RIP2, with a reduction of about 60% for RIP2 I259T and 70% for RIP2 L268V respectively, at a concentration of 25ng. The kinase activity of 40ng of variant RIP2 indicated a similar trend, 30% and 45% reduction in activity for RIP2 I259T and RIP2 L268V respectively.

5.3. Discussion

5.3.1. Expression and purification of RIP2

The RIP2 variants RIP2 I259T and RIP2 L268V identified in the Gambian population both carry a non-synonymous polymorphism in the kinase domain of the protein. To explore whether these RIP2 variants displayed altered kinase activity, recombinant wild type RIP2 and RIP2 bearing one or the other of these variations were expressed in a mammalian system. RIP2 was affinity purified and the kinase activity of the proteins measured in an *in vitro* kinase assay.

The recombinant RIP2 was expressed in a mammalian expression system to ensure that the protein was correctly folded and post- translationally modified as these modifications may be required to maintain protein functionality. HEK293T cells were chosen to express recombinant RIP2 as this human cell line can easily be transfected and produces high yields of the expressed protein as cells express the SV40 large T antigen. The SV40 large T antigen allows episomal replication of plasmids that encode the SV40 promoter and origin, increasing the yield of expressed protein.

There are no publications to date that report glycosylation or disulfide bond formation in RIP2. However, *in silico* analysis suggests that RIP2 is likely to be N-glycosylated at three sites and also heavily O-glycosylated (Gupta *et al*., 2004; Steentoft *et al*., 2013). Using two different prediction algorithms for disulfide bond formation, RIP2 was predicted to form three disulfide bonds by one analysis whereas an alternative analysis predicted no disulfide bond formation (Ceroni *et al*., 2006; Ferre and Clote, 2006).

Initially a C-terminal HIS-tag was chosen for purification of RIP2 as Cai *et al.* (2013) had previously purified RIP2 using this tag (Cai *et al*., 2013). A polyhistidine tag was considered most suitable as it allows rapid and economical small scale manual purification by means of immobilised metal affinity chromatography. Moreover, this purification strategy allowed elution with imidazole, ensuring that structure and function of the protein are preserved. However, the RIP2 recombinant protein expressed with a C-terminal HIS-tag failed to bind to nickel-charged magnetic agarose beads and

was not detected by an anti-HIS antibody, suggesting that a C-terminal HIS-tag is not accessible for binding in this system. RIP2 has been predicted to form disulfide bonds which would not be formed when the protein is expressed in a prokaryotic expression system (Ferre and Clote, 2006). Therefore the protein expressed by Cai *et al*, (2013) in an *E. coli* expression system, may have folded differently resulting in a more accessible tag (Cai *et al*., 2013). Furthermore, the RIP2 recombinant protein used in the current study bears a seven amino acid linker, a V5-epitope and a three amino acid linker between the RIP2 open reading frame and the HIS tag. This may also have influenced accessibility of the HIS-tag.

The RIP2 recombinant protein additionally contained a C-terminal V5-epitope that could be detected by an anti V5-epitope antibody. Therefore, purification of RIP2 was attempted by immunoprecipitation and affinity purification using this alternative tag. Western blot analysis of the cell lysates subjected to immunoprecipitation indicated the presence of V5-tagged proteins of different sizes. All identified proteins were smaller than the expected size of recombinant RIP2, suggesting that some of the expressed RIP2 protein was degraded. Similarly, cell lysates subjected to affinity purification showed the presence of a V5-epitope tagged protein of about 32kDa that was present in equal amounts to RIP2 recombinant protein. As protease inhibitors were added to the cell lysis buffers it is likely that degradation of the protein may have occurred as the expressed protein accumulated in the cells. This is feasible since the expression of immune signalling proteins, such as RIP2, are tightly regulated in cells. In either case, the smallest V5-tagged degradation product bound most readily to the anti-V5 agarose, preventing purification of high yields of pure RIP2 recombinant protein. Lu *et al.* (2005) have reported successful purification of recombinant RIP2 using a construct containing a C-terminal V5-epitope and HIS-tag identical to that used in this study. However, a crucial difference was that the recombinant RIP2 used in the study by Lu *et al*. (2005) lacked the CARD domain of RIP2 (Lu *et al*., 2005). Other studies have also reported that truncation of the CARD domain is important for expression of recombinant RIP2 (Tao *et al*., 2009), possibly because it leads to aggregation of the expressed protein inside the cell.

Pre-clearing by incubation of the lysate with a V5-antibody prior to purification allowed the removal of the RIP2 degradation products and purification of pure RIP2 recombinant protein, because the smaller protein bound more readily to the anti-V5 agarose beads.

Another issue that was encountered was that recombinant RIP2 kinase purified by this method had a greatly reduced kinase activity in comparison to commercially-available RIP2. This absence of kinase activity could be due to the elution conditions used in the purification. Low pH glycine buffers effectively dissociate antibody-antigen binding, but the low pH can result in denaturation of some proteins. Even though the elution was immediately neutralised, these conditions may still have resulted in the loss of RIP2 kinase activity. Elution buffers using V5 peptide or 1.2M NaCl failed to elute the bound protein fraction effectively; whether milder elution conditions might maintain kinase activity remains unknown at this time.

As an alternative, RIP2 was expressed with either an N-terminal HIS-tag or an N-terminal HIS-tag connected by a five amino acid linker. Both versions of RIP2 were shown to bind and purify equally well by metal chelate chromatography, regardless of the presence of the linker. Furthermore, kinase activity of the wild type recombinant protein was maintained after purification. The kinase activity of wild type RIP2 was assayed using three concentrations of the recombinant protein. Kinase activity was dose- dependent suggesting that all three concentrations were within the range of the kinase assay. However, the lowest RIP2 kinase concentration tested (12.5ng) resulted in a luminescence signal only marginally exceeding back ground luminescence, suggesting that 12.5ng of kinase was close to the lower detection limit of this assay.

5.3.2. RIP2 variants display reduced kinase activity

Comparison of the kinase activity of wild type RIP2 I259T and RIP2 L268V highlighted that the kinase of both RIP2 variants displayed reduced activity. RIP2 I259T displayed a 60% reduction in kinase activity compared to wild type RIP2. The prediction software SIFT, which predicts the effects of amino acid substitution on protein function, determined that this polymorphism was likely to be tolerated in the full length isoform of RIP2, but was predicted

to have deleterious effects on protein function in the truncated isoform of RIP2 (Ng and Henikoff, 2001). However, the purified protein contained only the full length isoform of RIP2. This is in accordance with the prediction algorithm Polyphen2, which suggested that the polymorphism would affect both isoforms (Adzhubei *et al*., 2010).

RIP2L268V displayed reduced kinase activity by 70% compared to wild type RIP2. This is consistent with the SIFT prediction that this polymorphism would have deleterious effects on protein function (Ng and Henikoff, 2001).

A number of mutations have been shown to result in loss of RIP2 kinase activity (McCarthy *et al*., 1998; Thome *et al*., 1998; Windheim *et al*., 2007). These include a conserved lysine residue K47 in the ATP binding site of RIP2 and mutations of two conserved aspartic acid residues in the kinase domain D146 and D164 (McCarthy *et al*., 1998; Thome *et al*., 1998; Windheim *et al*., 2007). Protein expression of these RIP2 variants has been demonstrated to result in significantly reduced RIP2 expression levels (Hasegawa *et al*., 2008; Lu *et al*., 2005; Nembrini *et al*., 2009; Windheim *et al*., 2007). The altered protein stability of RIP2 protein has been directly attributed to loss of kinase activity as inhibition of RIP2 with the kinase inhibitor SB203508 also affected expression levels (Windheim *et al*., 2007). Furthermore, expression of kinase dead RIP2 was reduced despite the expression of normal mRNA levels (Lu *et al*., 2005; Nembrini *et al*., 2009). This suggests that expression levels of the RIP2 variants I259T and L268V might be affected by the reduced kinase activity observed in the affected donors from the Gambian cohort.

Evidence regarding the importance of RIP2 kinase activity for downstream signalling is conflicting. Various studies have demonstrated that NOD-dependant activation of NF-κB and JNK remained unaffected in the absence of kinase activity (Eickhoff *et al*., 2004; McCarthy *et al*., 1998; Thome *et al*., 1998) Other groups found that kinase activity was required for optimal induction of NF-κB, and that NF-κB and cytokine responses were significantly reduced if RIP2 was kinase inactive (Hasegawa *et al*., 2008; Nembrini *et al*., 2009; Tigno-Aranjuez *et al*., 2010). Two studies hypothesised that a lack of kinase activity affected downstream signalling because in the absence of an active kinase, expression levels of RIP2 drop below the levels required for optimal NOD-dependent signalling (Hasegawa *et al*., 2008; Nembrini *et al*.,

2009). Other studies demonstrated that RIP2 kinase inactive variants were expressed at significantly lower levels, but the lower expression levels did not affect downstream signalling. Both of the RIP2 variants in these previous studies actually induced NF-κB and JNK more effectively than wild type RIP2 (Eickhoff *et al*., 2004; Windheim *et al*., 2007). As both RIP2 variants here demonstrated significantly reduced kinase activity it is possible that they could alter downstream signalling upon activation of the NOD receptors either by influencing expression levels of the RIP2 protein or by directly affecting activation of NF-κB or the MAP kinases, JNK, p38 kinase and ERK1/2.

RIP2 with an N-terminal HIS-tag expressed in HEK293T cells was affinity purified by metal chelate chromatography and the kinase activity of the protein was maintained. Both RIP2 variants RIP2 I259T and RIP2 L268V identified in the Gambian population have been shown to display significantly reduced kinase activity *in vitro*. Loss of RIP2 kinase activity has been previously linked to RIP2 protein stability and reduced NF-KB and JNK activation. Therefore, further exploration of the functional significance of reduced kinase activity on protein expression levels and NOD-dependent activation of NF-κB and MAP kinases is needed.

6. Effects of RIP2 variants on downstream signalling of NOD2

6.1. Introduction

RIP2 plays an essential role in the downstream signalling of the two nucleotide-binding oligomerisation domain (NOD) receptors NOD1 and NOD2 (Kobayashi *et al*., 2002). NOD1 and NOD2 are intracellular pattern recognition receptors that have been demonstrated to detect peptidoglycan fragments iE-DAP and MDP respectively in the cytosol (Girardin *et al*., 2003a; Inohara *et al*., 2003). These NOD receptors have been shown to play an important role in the immune response to intracellular bacterial pathogens such as *M. tuberculosis*, *Listeria monocytogenes* and *Chlamydophila pneumonia* (Chin *et al*., 2002; Pandey *et al*., 2009; Shimada *et al*., 2009).

Stimulation of the NOD-receptors induces the activation of NF-κB and the MAP kinases JNK, p38 MAP kinase, ERK1 and ERK2 (Chin *et al*., 2002; Kobayashi *et al*., 2002; Yang *et al*., 2007). RIP2 has been shown to be essential for NOD-mediated cell activation, as downstream signalling was abrogated in the absence of RIP2 (Kobayashi *et al*., 2002; Magalhaes *et al*., 2011; Park *et al*., 2007b).

Upon stimulation, NOD1 or NOD2 auto-oligomerise inducing interaction with RIP2 kinase through the CARD domain of these proteins (Inohara *et al*., 2000; Ogura *et al*., 2001). Activation of NOD receptors causes RIP2 to auto-phosphorylate which leads to the recruitment of ubiquitin ligases, which conjugate RIP2 with ubiquitin chains (Bertrand *et al*., 2009; Damgaard *et al*., 2012; Tigno-Aranjuez *et al*., 2010; Yang *et al*., 2013). These ubiquitin chains facilitate the interaction of RIP2 with the TAB2/TAB3/TAK1complex which drives activation of MAP kinases and NF-κB (Bertrand *et al*., 2009; Damgaard *et al*., 2012; Hasegawa *et al*., 2008).

Several studies have shown that NOD2 signalling contributes to the immune response induced by *M. tuberculosis* infection. Infection of macrophages with *M. tuberculosis* has been shown to result in phosphorylation of RIP2 within 30min and ubiquitination of RIP2 within 1h of infection (Abecasis *et al*., 2012; Pandey *et al*., 2009). Moreover, NOD2 signalling has been demonstrated to significantly contribute to release of IL-

12p40 from murine macrophages and dendritic cells during *M. tuberculosis* infection (Gandotra *et al*., 2007). It has long been understood that IL-12p40 plays a crucial role in the immune response to tuberculosis, inducing migration of dendritic cells to the draining lymph node during infection as well as being required for antigen-specific production of IFN-γ by $CD4^+$ T-cells (Cooper *et al*., 2002; Khader *et al*., 2006).

In addition, NOD2 signalling also contributes to secretion of pro-inflammatory cytokines IL-1β, TNF and IFN-β from human and murine macrophages during infection with *M. tuberculosis* (Brooks *et al*., 2011; Ferwerda *et al*., 2005; Pandey *et al*., 2009). Additionally, *M. tuberculosis* expresses a glycolylated form of MDP, which is a more potent inducer of NOD2-dependent NF-κB and JNK activation than the acetylated MDP present in other bacteria such as *Listeria monocytogenes or Salmonella typhimurium* (Coulombe *et al*., 2009).

However, NOD1 is hypothesised to play only a minor role in the immune response to *M. tuberculosis* as murine *Nod1*$^{-/-}$ macrophages produce TNF and IFN-β at levels that are comparable to wild type macrophages (Ferwerda *et al*., 2005; Pandey *et al*., 2009). *M. tuberculosis* antigen also results in only modest activation of NF-κB in NOD1 transfected HEK293T cells (Ferwerda *et al*., 2005).

The aim of this chapter was to characterise the effects of the RIP2 variants RIP2 I259T and RIP2 L268V identified in the Gambian population (Chapter 3). Both RIP2 variants were shown to affect the kinase activity of the protein (Chapter 5). The role of the RIP2 kinase activity in NOD2-dependend activation of NF-κB is controversial with some studies having demonstrated that the kinase activity is required for optimal induction of NF-κB activation and cytokine release (Eickhoff et al., 2004; McCarthy et al., 1998; Nembrini et al., 2009; Thome et al., 1998; Tigno-Aranjuez et al., 2010). Subsequently, the functional significance of the RIP2 variants on NOD-dependent activation of NF-κB and AP-1 was studied in an *in vitro* system.

6.2. Results

6.2.1. Stimulation of NOD2 signalling pathways in THP-1 Blue™ cells

Stimulation of the NOD2 receptor induces activation of NF-κB as well as activation of AP-1 (Kobayashi *et al*., 2002; Yang *et al*., 2007). Therefore a THP-1 cell line (THP-1 Blue™) stably transfected with a SEAP reporter gene under the control of a promoter fused to five NF-κB and AP-1 binding sites was used in this study to measure activation of the NOD2 signalling pathway.

The ligand detected by the NOD2 receptor is the dipeptide MDP, which is ubiquitously present in bacterial peptidoglycan (Inohara *et al*., 2003). In order to demonstrate that MDP stimulated the NOD2 signalling pathways and induced activation of NF-κB and AP-1 in THP-1 Blue™ cells, cells were stimulated with MDP (0.1-10µg/ml) for 24h. Measuring levels of SEAP in cell supernatants demonstrated that stimulation with MDP induced a small dose dependent response in these cells (Figure 6.1).

Substantial activation of an NF-κB/AP-1 SEAP reporter was observed after co- stimulation with MDP and 1ng/ml of LPS. Co-stimulation resulted in a dose-dependent synergistic response inducing activation of an NF-κB/AP-1-driven SEAP reporter that was approximately 3-fold greater than the response in cells stimulated with LPS alone (Figure 6.1).

6.2.2. Transient transfection of THP-1 cells

THP-1 cells expressing wild type and variant RIP2 were necessary to measure the influence of the RIP2 variants on NOD-dependent NF-κB and AP-1 activation. In order to develop a method for transient transfection of THP-1 cells, cells were chemically transfected with plasmids encoding GFP or *Renilla* luciferase using a variety of transfection reagents. Transfection with DNA coding for GFP clearly demonstrated that transfection efficiencies achieved in THP-1 cells were extremely low compared to transfection efficiencies observed in other cell types such as HEK293T cells (Figure 6.2 A and B). Measurement of cell viability of THP-1 cells by CellTiter-Glo® assay after transfection demonstrated that none of the transfection reagents had a substantial effect on cell viability (Figure 6.2 C). Hence, the poor transfection

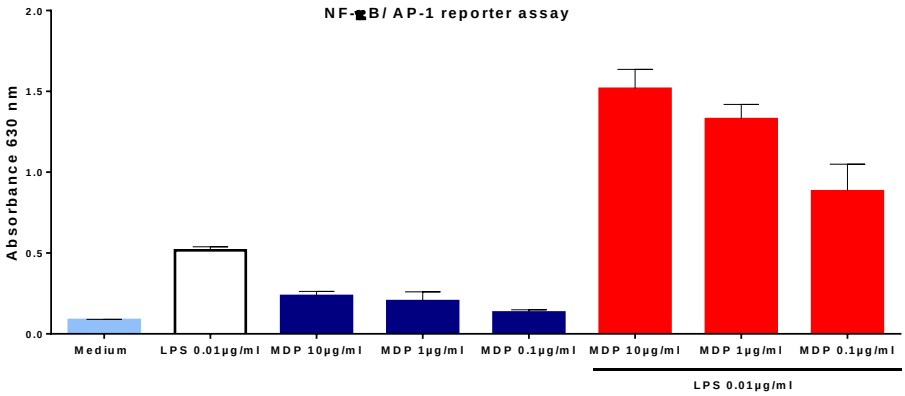

Figure 6.1 THP-1 cells respond synergistically to co-stimulation with MDP and LPS

Activation of NF-κB and AP-1 was measured in response to treatment with MDP +/- LPS in cell free supernatants using a NF-κB/AP-1 reporter assay. Results are expressed as mean ± SD. Data is representative of two independent experiments.

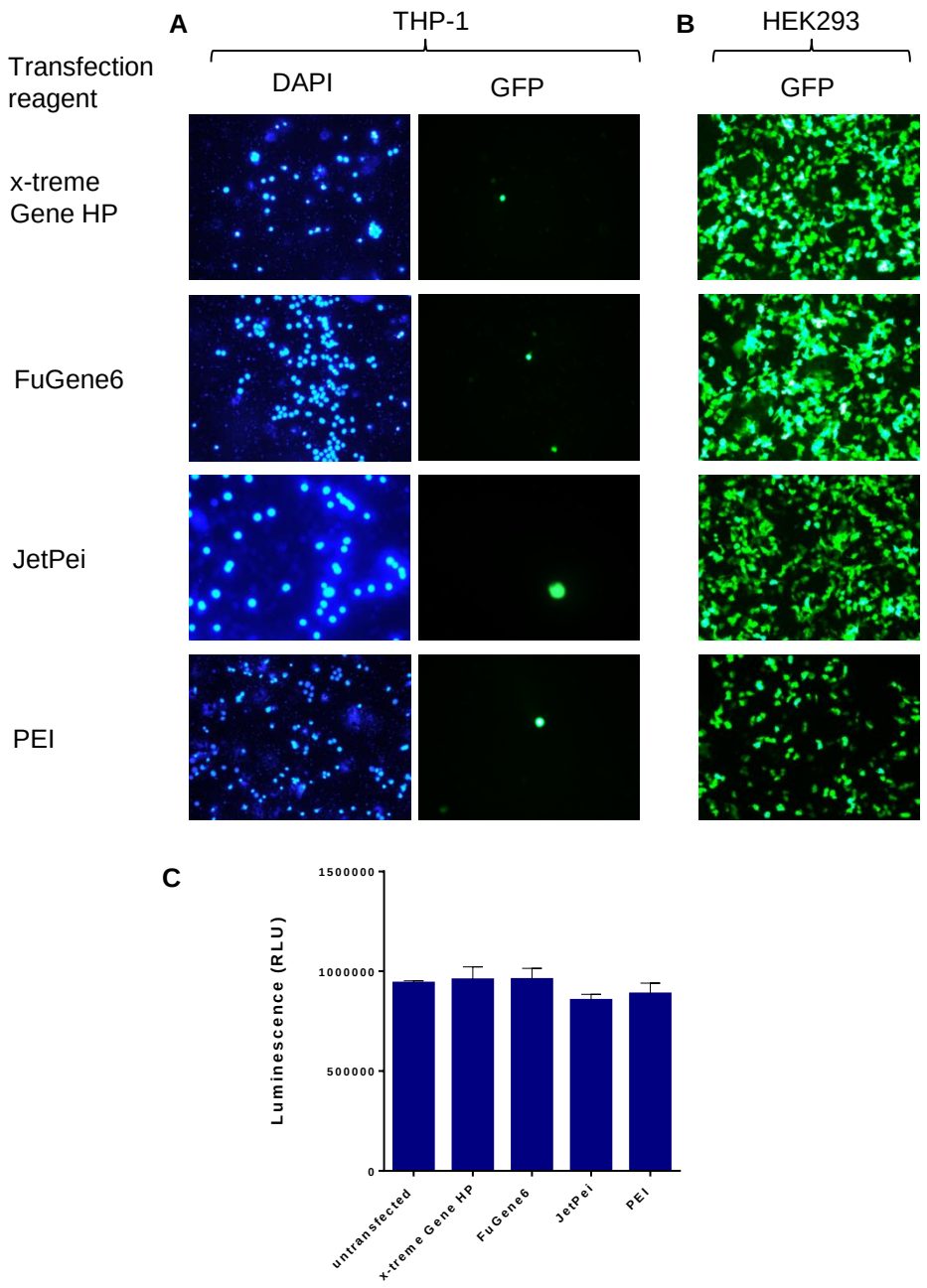

Figure 6.2 THP-1 cells cannot be effectively transfected with plasmid DNA by chemical transfection

THP-1 and HEK293T cells were transiently transfected with pmaxGFP. Fluorescence of THP-1 cells (A) and HEK293T (B) transiently transfected with GFP; Green: GFP, Blue: DAPI stained nuclei (C) Cell viability of transfected THP-1 cells was assayed using CellTiter-Glo® 24 h post transfection. Results are expressed as mean ± SD. Data shown is representative of two independent experiments.

efficiencies could not be attributed to toxic effects of the transfection reagents.

THP-1 cells were also transfected with constitutively expressed *Renilla* luciferase, which is under the control of a promoter that can be further induced by NF-κB activation. Hence, in cells transfected with this luciferase a strong luminescent signal should be present, that is significantly increased upon activation of NF-κB. When THP-1 cells were transfected with this luciferase only a low luminescent signal was observed, which was not reliably increased by stimulation with the imidazoquinoline TLR7/8 ligand R-848 (Figure 6.3 B).

6.2.3. Nucleofection of THP-1 cells

As transfection of THP-1 cells with chemical reagents resulted in very low transfection efficiencies, electroporation was chosen as an alternative method. THP-1 cells were transiently transfected with an NF-κB-driven luciferase reporter plasmid (pGNL6) using nucleofection. Cells were incubated at 37°C for 24h after transfection to allow recovery and were then stimulated for a further 24h with 1µg/ml of R-848, a potent NF-κB inducer in THP-1 cells.

To check the function of the inducible luciferase, HEK293T cells were transfected with pGNL6 and stimulated with TNF. Transfection with the luciferase reporter plasmid resulted in substantial increase in luciferase back ground signal. Additionally, stimulation of transfected cells resulted in an increase in the luciferase signal compared to unstimulated transfected cells (Figure 6.4 A). In a series of pilot experiments THP-1 cells were transfected with the same plasmid vector and stimulated with R-848. Transfection with the luciferase reporter plasmid did not result in an increase of background luciferase signals compared to untransfected cells. Furthermore, stimulation with R-848 did not result in an increase in the luciferase signal in any of the experiments (Figure 6.4 B). This could be due to a number of reasons including failure of plasmid up take by the cells, little or no expression of the transfected DNA or cell death. Comparison of the cell viability of untransfected cells, mock-transfected (electroporated without

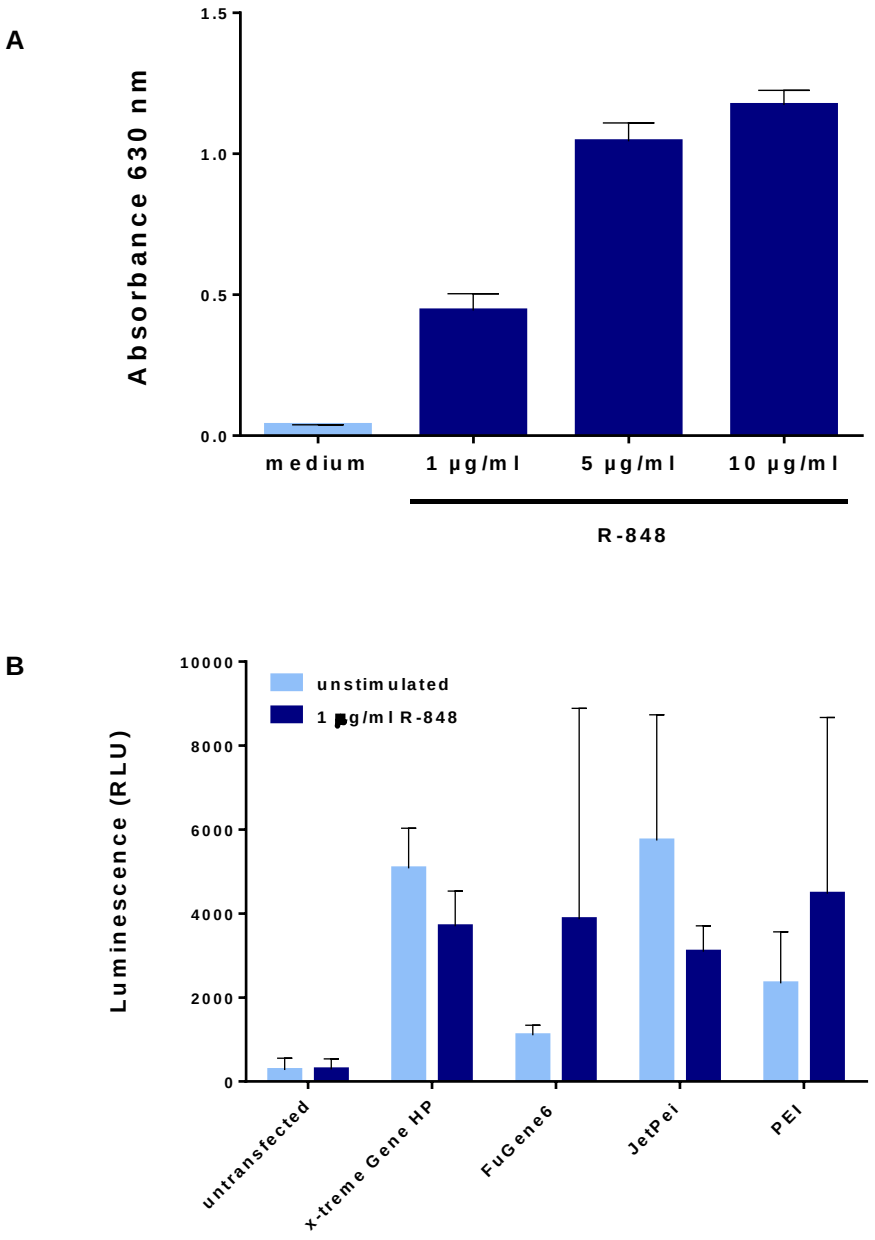

Figure 6.3 THP-1 cells cannot efficiently be transfected with plasmid DNA by chemical transfection and do not respond to R-848 stimulation after transfection

(A) Stimulation of THP-1 Blue™ cells with R-848 to confirm NF-κB/AP-1 SEAP reporter activation by this ligand. (B) Transfection of THP-1 cells with pRL-CMV encoding *Renillla* luciferase. Cells were stimulated with R-848 and luciferase activity was measured 24h later. Results are expressed as mean ± SD.

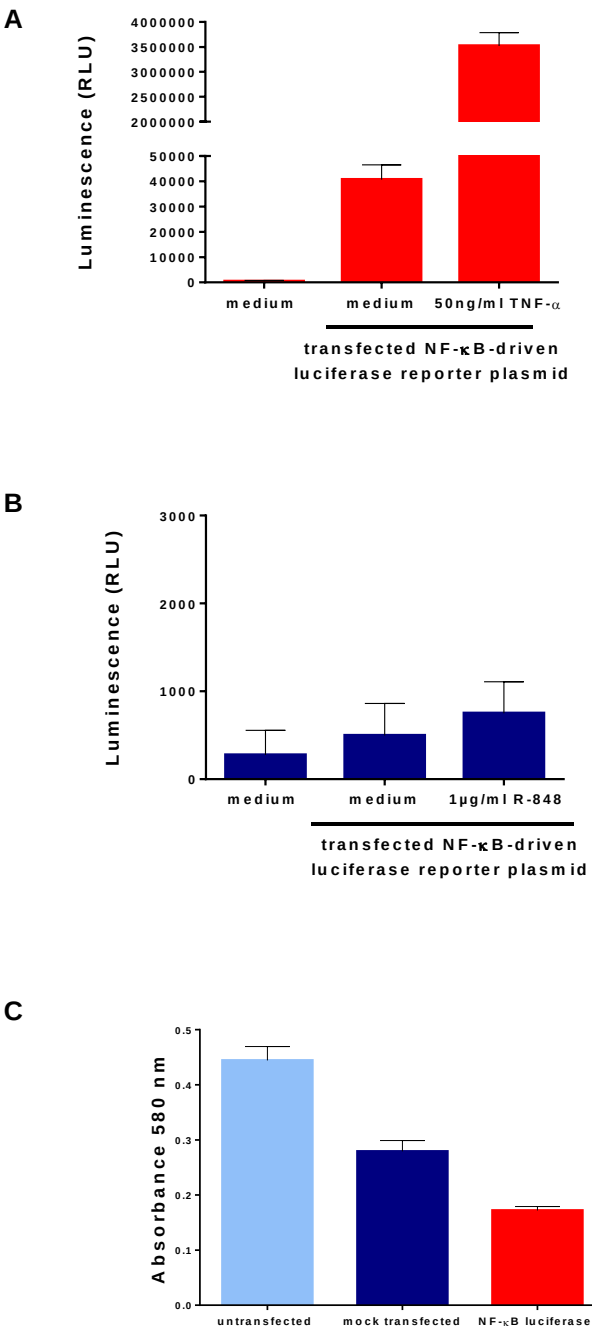

Figure 6.4 THP-1 cells cannot be transfected with plasmid DNA by electroporation

HEK293 cells (A) and THP-1 cells (B) were transfected with an NF-κB luciferase reporter plasmid and stimulated for 24h with R-848 or TNF before measurement of luciferase activity. (C) Viability of THP-1 cells 48h after transfection measured using MTT assay. Results were expressed as mean ± SD.

DNA) cells and cells transfected with NF-κB luciferase reporter showed that nucleofection reduced cell viability substantially. Cell viability was measured 48h after transfection and was decreased by approximately 40% in the mock transfected cells and approximately 65% in the NF-κB luciferase reporter plasmid transfected cells compared to untransfected cells (Figure 6.4 C).

6.2.4. Stimulation of HEK-Blue™ hNOD2 cells with MDP

THP-1 cells did not express transfected plasmids at levels high enough to allow study of the effects of the RIP2 variants on NOD-dependent NF-κB and AP-1 SEAP reporter activation, therefore HEK cells were chosen as an alternative *in vitro* expression system. HEK cells do not express NOD2 (Barnich *et al*., 2005), however, expression of recombinant NOD2 in HEK293 cells enables these cells to robustly respond to stimulation of NOD2 (Ferwerda *et al*., 2005). Hence, in this study, HEK-Blue™ hNOD2 cells that are stably transfected with a NOD2 receptor plasmid were used in this study. HEK-Blue™ hNOD2 cells also stably express a SEAP reporter gene under the control of a promoter that is fused to NF-κB and AP-1 binding sites allowing quantification of levels of NF-κB and AP-1 activation.

Stimulation of HEK-Blue™ hNOD2 cells with MDP at concentrations ranging from 0.001-10µg/ml resulted in a dose-dependent activation of the SEAP reporter. The greatest response was achieved by stimulation with 0.1µg/ml MDP. A similar level of activation was observed after treatment of HEK-Blue™ hNOD2 cells with 50ng/ml TNF which was used as a positive control (Figure 6.5).

6.2.5. Expression of RIP2 in HEK-Blue™ hNOD2 cells

To study the effects of the RIP2 variants it was important that the recombinant protein was over-expressed compared to the endogenous RIP2 background. To identify whether recombinant RIP2 was expressed at greater levels than endogenous RIP2, HEK-Blue™ hNOD2 cells were transfected with wild type RIP2 or the RIP2 variants I259T or L268V. Western blot

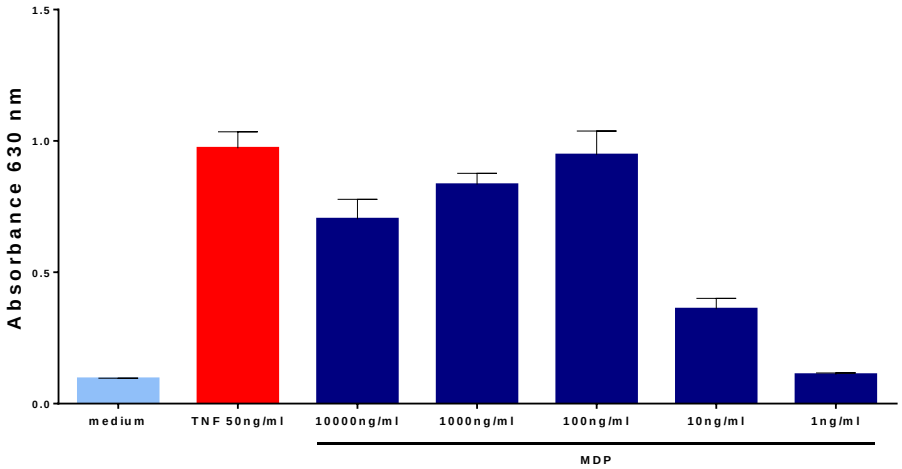

Figure 6.5 HEK-Blue™ hNOD2 cells respond in a dose-dependent manner to stimulation with MDP
Activation of NF-κB/AP-1 in response to treatment with MDP was measured in cell free supernatants of HEK-Blue™ hNOD2 cells using a SEAP reporter assay 24h post stimulation. Results were expressed as mean ± SD.

analysis of mock-transfected cells 48h post transfection using anti-RIP2 antibody revealed the presence of a 61kDa protein, which corresponded to the endogenous form of RIP2. In cells that were transfected with recombinant RIP2 wild type or RIP2 variants two bands corresponding to the 61kDa endogenous RIP2 and the 65kDa recombinant RIP2 were present highlighting that both endogenous and recombinant RIP2 were expressed at similar levels (Figure 6.6).

6.2.6. Stability of RIP2 variants

As the expression of a kinase dead RIP2 variant was previously reported to be much lower than that of wild type RIP2 in HEK293 cells, the expression of the RIP2 variants I259T and L268V were tested by immune blot analysis in HEK-Blue™ hNOD2 cells (Lu *et al*., 2005; Windheim *et al*., 2007). Both variants were expressed at levels similar to those observed for wild type recombinant RIP2 (Figure 6.7).

6.2.7. Depletion of endogenous RIP2 in HEK-Blue™ hNOD2 cells

Both endogenous and recombinant RIP2 were expressed at similar levels, so endogenous RIP2 was depleted by siRNA in order to prevent the effects of the RIP2 variants on the NF-κB/AP-1 SEAP reporter activity being masked by the presence of endogenous RIP2.

HEK-Blue™ hNOD2 cells were transfected with either *RIPK2* siRNA or a scrambled control and incubated for up to 72h. Western blot analysis of RIP2 using anti-RIP2 antibody demonstrated that levels of RIP2 were slightly decreased 24h post transfection compared to the scrambled control. A significant loss of RIP2 was observed in *RIPK2* siRNA transfected cells 48h after transfection, and RIP2 was almost undetectable 72h after knockdown (Figure 6.8).

To show the effect of RIP2 depletion on NOD-dependent NF-κB/AP-1 SEAP reporter activity, HEK-Blue™ hNOD2 were stimulated with MDP after knock down of RIP2. Cells lacking RIP2 induced significantly less activation of the NF-κB/AP-1 SEAP reporter showing compared to cells transfected with scrambled controls (Figure 6.9).

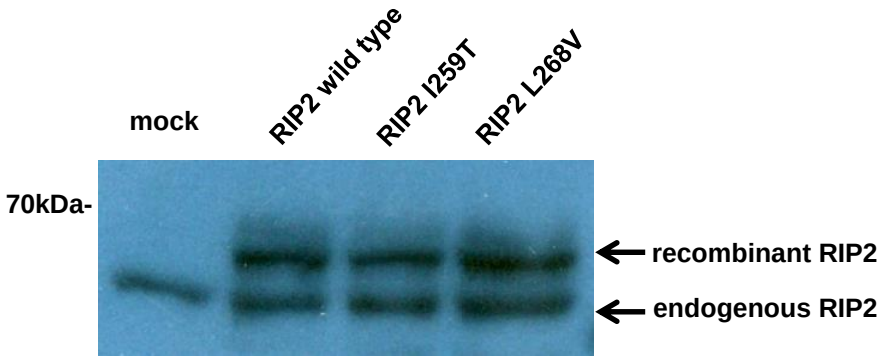

Figure 6.6 Recombinant RIP2 and endogenous RIP2 are expressed equally in HEK cells
Cell lysates from HEK-Blue™ hNOD2 cells transfected with DNA coding for recombinant wild type or variant RIP2 48h post transfection. Recombinant and endogenous RIP2 was detected in 20µl cell lysate using anti-RIP2 antibody (1:200 dilution in 3% milk in TBS-T).

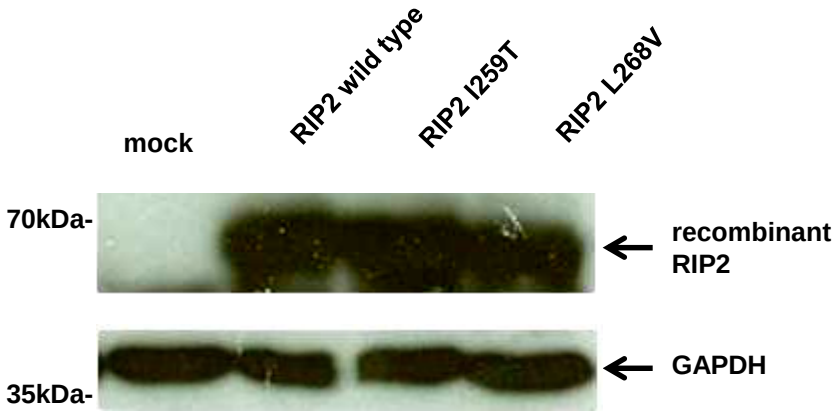

Figure 6.7 Recombinant wild type and variant RIP2 are expressed at equal levels in HEK cells
Cell lysates from HEK-Blue™ hNOD2 cells transfected with recombinant wild type and variant RIP2 72h post transfection. Protein was detected in 20µl cell lysate using anti-RIP2 antibody (1:200 dilution in 3% milk in TBS-T).

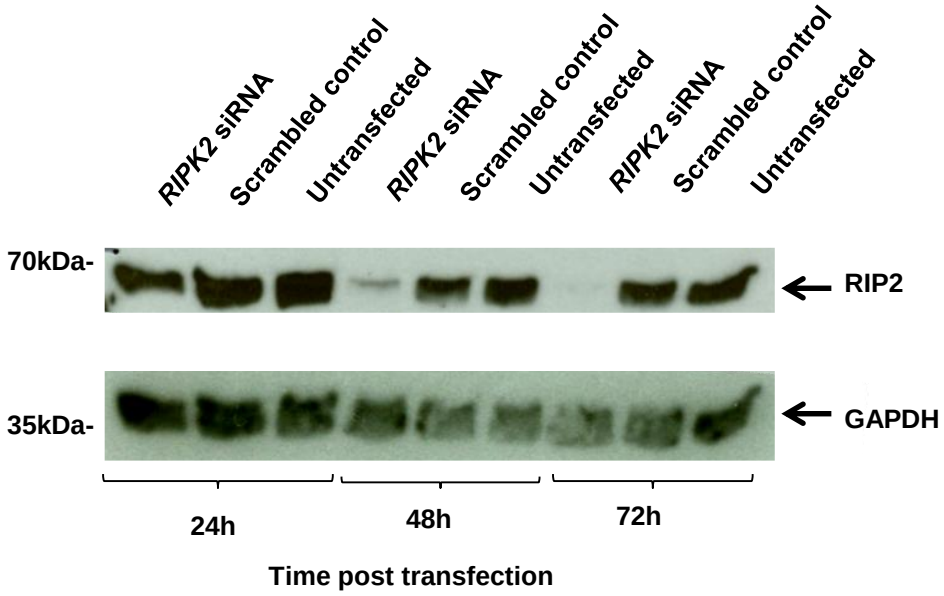

Figure 6.8 Endogenously expressed RIP2 is significantly knocked down 48h/72h after transfection of HEK-Blue™ hNOD2 cells with *RIPK2* siRNA

Knock down of RIP2 was confirmed by immuno blotting of 20µl cell lysates using an anti-RIP2 antibody (1:200 dilution in 3% milk in TBS-T).

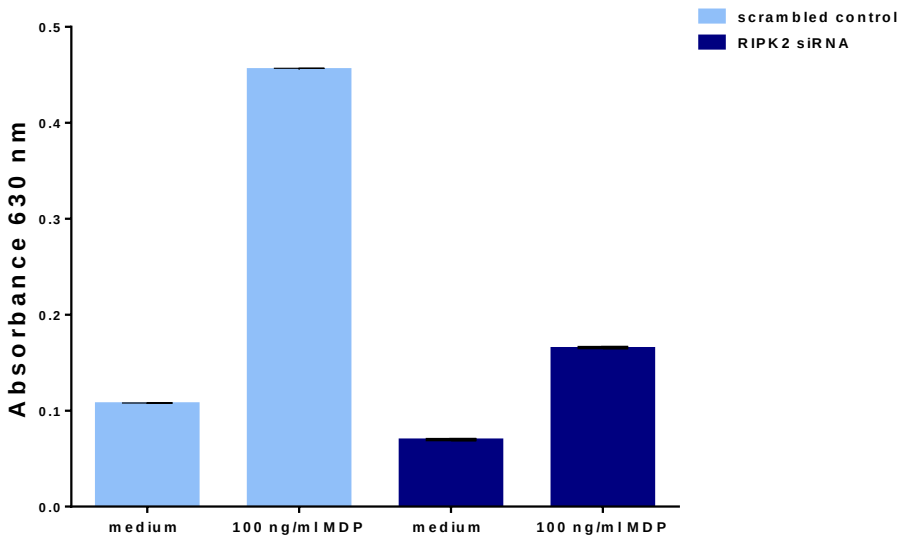

Figure 6.9 Depletion of RIP2 in HEK-Blue™ hNOD2 cells results in reduced response to MDP

Cells were transfected with *RIPK2* siRNA or scrambled control siRNA for 48h after which cells were stimulated with MDP for 24h and NF-κB and AP-1 activation was measured using an SEAP reporter assay. Data are representative of three independent experiments. Results are expressed as mean ± SD.

6.2.8. Transfection with wild type and variant recombinant RIP2 restores NOD2-mediated NF-κB/AP-1 SEAP reporter activation in RIP2-depleted cells

In order to show whether the ability of the RIP2 variants to mediate NOD2-dependent NF-κB/AP-1 SEAP reporter activation differed from wild type RIP2, RIP2-depleted cells were transfected with wild type or variant recombinant RIP2 and stimulated with MDP.

HEK-Blue™ hNOD2 were transfected with either *RIPK2* siRNA or a scrambled control siRNA and were incubated for 48h. Subsequently, cells were replated and left to adhere for 24h before transfection with pcDNA6_RIP2_V5/HIS or empty control vector (pcDNA6). Cells were incubated for 48h after transfection before stimulation with MDP. Activation of NF-κB/AP-1 was measured after 24h of stimulation using a SEAP reporter assay in cell-free supernatants (Figure 6.10).

Western blot analysis of cell lysates from transfected cells with anti-RIP2 antibody demonstrated that reconstitution of RIP2 expressed from a vector in RIP2 depleted cells was successful, with recombinant protein being substantially over-expressed compared to the endogenous RIP2 levels (Figure 6.11 A).

Expression of recombinant RIP2 only induced minimal activation of NF-κB/AP-1 SEAP reporter in the absence of MDP stimulation. NF-κB/AP-1 SEAP reporter activation induced by MDP stimulation in cells depleted of endogenous RIP2 and transfected with wild type or variant recombinant RIP2 was higher than in cells transfected only with an empty control vector. However, a slight drop in levels of NF-κB/AP-1 SEAP reporter activation was observed in cells transfected with a control vector opposed to untransfected cells, suggesting that transfection of a plasmid after RIP2 depletion by siRNA affected the viability of cells (Figure 6.11 B). When cell viability of HEK-Blue™ hNOD2 cells was assessed using CellTiter-Glo®, it became apparent that the cell viability of cells transfected with siRNA, followed by transfection with pcDNA6 was approximately 45% lower than that of cells only transfected with siRNAs (Figure 6.11 C).

Correcting the values for NF-κB/AP-1 activation to account for differences in cell viability demonstrated that transfection of RIP2-depleted

cells with a plasmid encoding recombinant wild type RIP2 restored the activation of NF-κB/AP-1 after NOD2-pathway stimulation to levels similar to those observed in the cells transfected with scrambled control siRNA (Figure 6.11 D). Transfection with an empty pcDNA6 plasmid did not restore the activation of NF-κB/AP-1 after MDP stimulation, suggesting that the transfected recombinant RIP2 was able to restore NOD2/RIP2 signalling cascades resulting in NF-κB/AP-1 SEAP reporter activation. Transfection of RIP2-depleted cells with the RIP2 variants I259T and L268V resulted in levels of NOD2-induced NF-κB/AP-1 SEAP reporter activation that were similar to that observed in cells transfected with wild type RIP2. This suggested that, even though these RIP2 variants displayed reduced kinase activity compared to wild type RIP2, their ability to facilitate downstream signalling resulting in NF-κB/AP-1 SEAP activation upon NOD2 stimulation was unaffected (Figure 6.11 D).

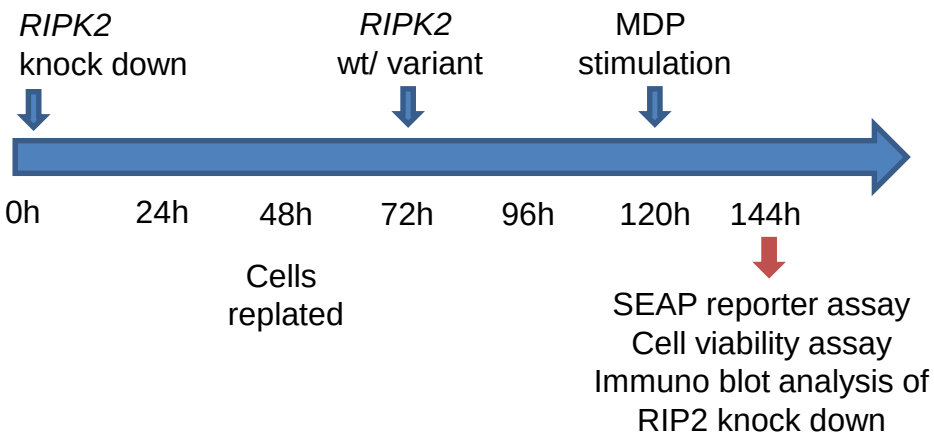

Figure 6.10 Overview of experimental protocol for determination of effect of RIP2 variants in HEK-Blue™ hNOD2 cells

RIP2 knock-down was first performed in these cells to remove the endogenous RIP2 protein so that biological effect of variant RIP2 could be determined.

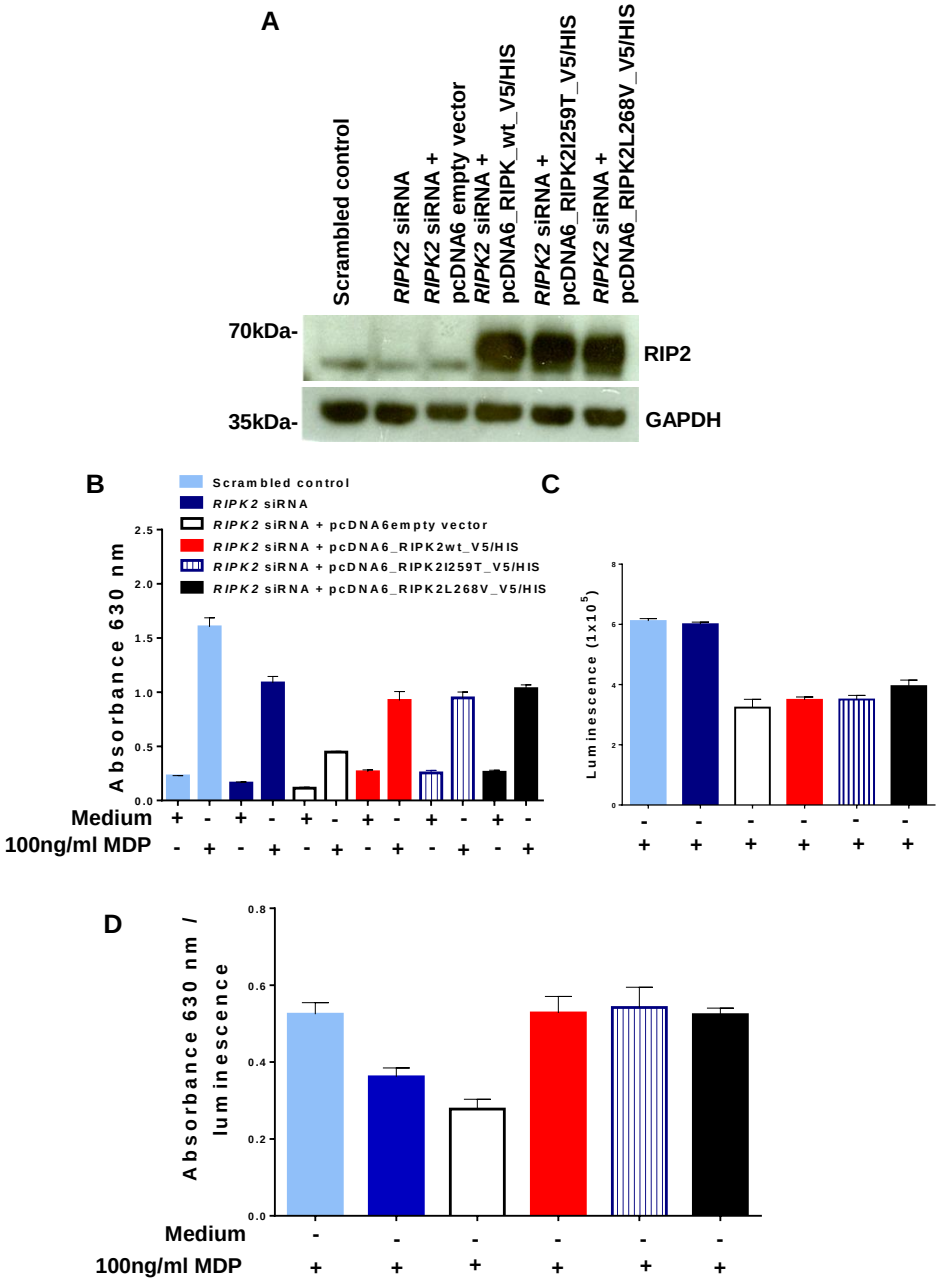

Figure 6.11 Recombinant wild type and variant RIP2 restores NOD2-dependent NF-κB/AP-1 SEAP reporter activation in RIP2 depleted HEK-Blue™ hNOD2 cells

HEK-Blue™ hNOD2 cells were transfected with *RIPK2* siRNA. Cells depleted of RIP2 were transfected with DNA coding for wild type or variant RIP2 and stimulated for 24h with 100ng/ml MDP. (A) Expression of RIP2 in cell lysates (20µl) was analysed by immuno blot using anti-RIP2 antibody (1:200 dilution in 3% milk in TBS-T). (B) Activation of NF-κB and AP-1 after 24h of MDP stimulation was measured a SEAP reporter assay. (C) Cell viability was measured by CellTiter-Glo® (D) Level of SEAP after 24 MDP stimulation represented as SEAP corrected for cell viability. Data are representative of three independent experiments. Results are expressed as mean ± SD.

6.3. Discussion

6.3.1. Stimulation of NOD2 signalling pathways in THP-1 Blue™ cells

In order to study the effects of the RIP2 variants identified in the Gambian population on the NOD signalling pathway, the RIP2 variants were expressed in an *in vitro* system.

Initially the acute leukemia cell line THP-1 was selected as these cells are a relevant model for assaying macrophage-*M. tuberculosis* interaction (Stokes and Doxsee, 1999). THP-1 cells are monocytic cells that can be differentiated into macrophage-like cells by stimulation with phorbol diesters such as PMA (Tsuchiya *et al*., 1982; Tsuchiya *et al*., 1980). PMA-differentiated THP-1 cells readily phagocytose *M. tuberculosis* and are frequently used to study host pathogen interaction during infection *in vitro* (Greco *et al*., 2012; Sanjurjo *et al*., 2013).

THP-1 cells express the NOD receptors, NOD1 and NOD2 (Ogura *et al*., 2001; Uehara *et al*., 2005). Various studies suggest that NOD2 signalling contributes to the immune response to *M. tuberculosis* infection, whereas NOD1 signalling is thought to play only a minor role (Ferwerda *et al*., 2005; Pandey *et al*., 2009). NOD2 contributes to the secretion of cytokines such as IL-1β, IL-12p40, TNF and IFN-β from human and murine macrophages during infection with *M. tuberculosis*; in the absence of NOD2, the levels of these cytokines are reduced (Ferwerda *et al*., 2005; Gandotra *et al*., 2007; Pandey *et al*., 2009). However, NOD1-deficient macrophages were able to secrete cytokines at levels comparable to wild type macrophages during *M. tuberculosis* infection (Ferwerda *et al*., 2005; Pandey *et al*., 2009). Given the more significant role of NOD2 in an immune response to *M. tuberculosis*, the RIP2 variants were studied in the context of NOD2 rather than NOD1 signalling.

To confirm that NOD2 dependent activation of NF-κB/AP-1 SEAP reporter could be induced in THP-1 cells, these cells were stimulated with the NOD2 ligand MDP. The stimulation of THP-1 cells with MDP resulted in very low levels of NF-κB/AP-1 SEAP reporter activation. This limited response to MDP corresponds to previous reports that stimulation of THP-1 cells with MDP

induced only low levels of IL-8 and no TNF (Nahid *et al*., 2011; Yang *et al*., 2001). However, when these cells are co-stimulated with MDP and LPS, IL-8 production is significantly greater than that induced by either ligand alone (Yang *et al*., 2001). This observation corresponds with the findings of the current study, where THP-1 cells stimulated with LPS and MDP resulted in significantly increased activation of NF-κB/AP-1 SEAP reporter compared to stimulation with either ligand on its own.

It has been well documented that stimulation of the NOD2 receptor induces synergistic responses upon co-stimulation of TLR receptors in various cell types including human monocytic cells and murine peritoneal macrophages (Coulombe *et al*., 2009; Ferwerda *et al*., 2005; Yang *et al*., 2001). Ferwerda *et al*. (2005) demonstrated that co-stimulation of human monocytic cells with MDP and the mycobacterial 19-kDa lipoprotein, a specific TLR2 ligand, had synergistic effects on the secretion of TNF, IL-1β and IL-6 (Ferwerda *et al*., 2005). Furthermore, co-stimulation of murine peritoneal macrophages with MDP and LPS resulted in secretion of substantial levels of TNF whereas in the absence of LPS no secretion of TNF is observed (Coulombe *et al*., 2009). Overall, THP-1 cells are not an ideal model system to study activation of the NOD2 signalling pathway as stimulation of the NOD2 receptor alone does not strongly induce activation of NF-κB/AP-1 SEAP reporter. However, as co-stimulation of the cells with MDP and LPS results in a synergistic response, these cells may be used to study the effects of RIP2 variants on activation of NF-κB/AP-1 SEAP reporter upon stimulation of NOD2.

6.3.2. Transient transfection of THP-1 cells

To study the effect of the RIP2 variants on NOD signalling, THP-1 cells were required to be transiently transfected with the RIP2 variants. To optimise transfection of THP-1 cells, cells were transfected with a plasmid encoding GFP, an NF-κB luciferase reporter or a constitutively expressed *Renilla* luciferase using various transfection reagents or electroporation.

The main issue encountered in the experiments using chemical transfection agents was that transfection efficiencies were extremely low. Alternatively, transfection by electroporation resulted in high levels of cell death, with approximately 65% of cells dying as a result of the transfection.

When HEK293T cells are transfected with the NF-κB driven luciferase reporter this results in a substantial increase in luciferase back ground levels and a significant induction of luciferase signal above back ground level when NF-κB is activated through stimulation. However, THP-1 cells transfected with the same plasmid by electroporation produced neither an increase in back ground luciferase levels was observed nor was an increase in luciferase signal after stimulation of the cells with R-848. This suggests that either plasmids were not taken up, not expressed very well or possibly degraded upon uptake. Furthermore, stimulation of transfected THP-1 cells with R-848 induced only a very small increase in the luminescent signal which also could be due to the cell having lost its capacity to induce a robust NF-κB response.

A few studies have reported successful transfection of THP-1 cells with the lipid based transfection reagent lipofectamine, the non-liposomal reagent x-tremeGene HP and also electroporation. An optimised protocol for transfection of THP-1 cells using nucleofection has been published (Maess *et al*., 2011; Schnoor *et al*., 2009). However, transfection of THP-1 cells is notoriously difficult and the number of reports in the literature that demonstrate successfully transfected THP-1 cells is relatively small. Bibliographic database searches revealed that there are <50 publications describing data from transiently transfected THP-1 cells compared to over 40,000 publications reporting the use of transiently transfected HEK293 cells.

Even though all transfection methods used in the current study achieved some degree of transfection, the efficiencies were low as the plasmids were not taken up, not expressed or degraded upon uptake. Monocytic cells like THP-1 cells express high levels of RIP2; the transfection efficiencies achieved here were unlikely to be high enough to result in the over-expression of the RIP2 variants relative to the endogenous RIP2 background present in a population of THP-1 cells where only a small proportion are successfully transfected (McCarthy *et al*., 1998).

In order to prevent the effect of the RIP2 variants being masked by endogenous RIP2, the cells would need to be depleted of the endogenous RIP2 prior to transfection. Knock-down of genes in THP-1 cells can be achieved by electroporation with siRNAs. Even though substantial cell death is observed during transfection, knock down of the target gene is successfully

achieved in surviving cells. That transfection with siRNAs is more feasible than transfection with a plasmid vector might be due to the significant size difference between the siRNA (20-24bp) and the plasmid vector (about 5kb). However, it is unlikely that THP-1 cells that have been electroporated twice to transfect them with siRNA and a plasmid vector can be used to study the effect of the RIP2 variants.

6.3.3. Study of RIP2 variants in HEK-Blue™ hNOD2 cells

THP-1 cells are a human monocytic cell line that can be differentiated into macrophage-like cells for studying immune signalling pathways that are involved in immune responses to tuberculosis. However, THP-1 cells are not genetically tractable and did not efficiently express transfected plasmid vectors to allow the exploration of the functional significance of RIP2 variants on NOD signalling. Consequently, a genetically tractable HEK cell line was chosen to study the effects of the RIP2 variants instead. A disadvantage of this cell line is that HEK cells are not naturally infected with *M. tuberculosis* as active phagocytosis is required for infection. In addition, HEK cells do not express NOD2 (Barnich *et al*., 2005). However, transfection of HEK cells with NOD2 enables the cells to respond to stimulation with MDP, leading to activation of NF-κB and MAP kinases (Ferwerda *et al*., 2005). Therefore, HEK-Blue™ hNOD2 cells were utilised in this study as this cell line is stably transfected with a NOD2 receptor, avoiding the need for transient transfections and ensuring that equal levels of NOD2 are expressed in all experiments. HEK-Blue™ hNOD2 cells were shown to respond to stimulation with MDP in a dose-dependent manner. Moreover, HEK cells responded to MDP stimulation activating the NF-κB/AP-1 SEAP reporter without the requirement for LPS co-stimulation. This was a major advantage as it allowed direct measurement of the NOD2 signalling pathway without cross-activation of NF-κB/AP-1 through TLR4 that does not signal through RIP2.

HEK cells can be easily transfected with plasmid vectors using transfection reagents without the need for electroporation, thus maintaining cell viability. In addition, high levels of RIP2 recombinant protein are expressed in these cells. HEK-Blue™ hNOD2 cells expressed equal levels of both endogenous and recombinant proteins. Therefore, endogenous RIP2 was

depleted prior to transfection of the RIP2 variants allowing the effect of the recombinant RIP2 kinases on NOD-dependent NF-κB/AP-1 SEAP reporter activation to be studied.

6.3.4. Kinase deficient RIP2 variants do not affect NOD-dependent activation of SEAP reporter

Expression of the RIP2 variants in HEK-Blue™ hNOD2 depleted of endogenous RIP2 restored NOD2 signalling to the same extent as expression of recombinant wild type RIP2, demonstrating that the reduced kinase activity observed in these RIP2 polymorphisms had no effect on NF-κB/AP-1 SEAP reporter activation.

It has been observed that the kinase dead RIP2 variant K47A resulted in reduced protein expression levels in HEK293 and murine BMMs despite levels of RIP2 K47A mRNA being similar to wild type RIP2 mRNA (Lu *et al*., 2005; Nembrini *et al*., 2009; Windheim *et al*., 2007). Treatment with the RIP2 kinase inhibitor SB203580 also affected expression levels of RIP2 suggesting that RIP2 kinase activity might be required for stability of the protein (Nembrini *et al*., 2009; Windheim *et al*., 2007). In the current study both RIP2 variants I259T and L268V were expressed at levels similar to wild type RIP2 when transfected into HEK-Blue™ hNOD2 cells. This suggests that these specific polymorphisms do not affect protein stability, even though the polymorphisms do influence kinase activity. Another possibility is that the reduced level of kinase activity displayed by both RIP2 variants was sufficient to maintain protein stability.

Reports in the literature regarding the significance of the kinase activity of RIP2 for NOD-dependent signalling are conflicting. In agreement with the findings of this work, previous studies have demonstrated that RIP2 devoid of kinase activity mediated activation of NF-κB to the same extent as wild type RIP2 (Eickhoff *et al*., 2004; McCarthy *et al*., 1998; Thome *et al*., 1998). However, these studies induced activation of the NOD signalling pathway by over-expression of RIP2 rather than stimulation with a NOD ligand. In the current study, recombinant RIP2 was expressed at a level that resulted in little activation of NF-κB/AP-1 SEAP reporter in the absence of MDP stimulation. Other studies that used MDP rather than over-expression of RIP2 to activate

the NOD pathway have shown that the absence of kinase activity resulted in reduced activation of the NF-κB/AP-1 SEAP reporter (Hasegawa *et al*., 2008; Navas *et al*., 1999; Nembrini *et al*., 2009; Tigno-Aranjuez *et al*., 2010). However, two of these studies attributed the reduction in NF-κB activation and cytokine release observed to reduced RIP2 protein levels in the absence of kinase activity as opposed to kinase activity *per se* (Hasegawa *et al*., 2008; Nembrini *et al*., 2009). Other studies demonstrated that the expression of kinase inactive variants of RIP2 in HEK293 cells resulted in more efficient activation of NF-κB and JNK compared to wild type RIP2 (Eickhoff *et al*., 2004; Windheim *et al*., 2007).

The main difference between the RIP2 variants identified in the Gambian population and the RIP2 variants described in the literature, is that the polymorphisms in the current study resulted in reduced kinase activity only, whereas the mutations studied in the other studies completely abolish the kinase activity (Hasegawa *et al*., 2008; Navas *et al*., 1999; Nembrini *et al*., 2009; Tigno-Aranjuez *et al*., 2010). Consequently, this indicates that either RIP2 kinase activity is redundant for downstream signalling or needs to be completely abrogated to affect downstream signalling.

It is possible that, like other kinases such as the serine-threonine kinase RIP1, RIP2 does not require kinase activity for signal transduction. RIP1 kinase mediates downstream signalling upon stimulation of the TNF receptor and has been shown to induce activation of NF-κB and p38 MAP kinase independently of its kinase activity (Lee *et al*., 2004). Ubiquitination has been identified as a mechanism that regulates RIP2 downstream signalling. RIP2 is ubiquitinated upon activation of the NOD receptors and this process leads to the recruitment of TAK1 to the IKK complex and MAP kinases, resulting in the activation of NF-κB and AP-1 (Hasegawa *et al*., 2008; Yang *et al*., 2007). Moreover, the ubiquitination of RIP2 is essential for NOD-dependent activation of NF-κB, JNK, p38 MAP kinase and Erk1/2 (Damgaard *et al*., 2012; Hasegawa *et al*., 2008; Yang *et al*., 2013; Yang *et al*., 2007). Lysine 209 has been identified as an essential ubiquitination site in RIP2. Ubiquitination at this site occurs independently of RIP2 kinase activity, further supporting the hypothesis that RIP2 kinase activity is not required for downstream signalling (Hasegawa *et al*., 2008). However, it is unlikely that the kinase activity of RIP2

is completely redundant, as the kinase domain comprises over 50% of the protein. RIP2 kinase activity has been shown to be required for NOD2-dependent autophagy, a cellular process which is involved in the control of some intracellular pathogens such as *L. monocytogenes* and *Salmonella flexneri*, but so far has not been implicated in the response to *M. tuberculosis* (Anand *et al*., 2011).

The RIP2 kinase variants I259T and V268L display significantly reduced kinase activity compared to wild type but were expressed at levels similar to recombinant wild type RIP2 The level of NOD2-dependent NF-κB/AP-1 SEAP reporter activation observed in the presence of the RIP2 variants was comparable to wild type RIP2 suggesting that the kinase activity of RIP2 is not required for NF-κB/AP-1 SEAP reporter activation. However, NOD2- dependent autophagy and possibly other unidentified downstream signalling pathways are dependent on the kinase activity, which may be affected by the reduced kinase activity observed in these RIP2 variants.

7. Summary and future work

With 9 million new cases and 1.5 million deaths every year, tuberculosis is a major cause of morbidity and mortality worldwide (WHO, 2014). The outcome of infection is influenced by multiple factors including the environment, pathogen genetic determinants as well as innate host factors. This gives rise to only 10% of infected individuals estimated to progress to active disease (Ottenhoff, 2012). A substantial amount of evidence points towards host genetics playing an important role in susceptibility to tuberculosis. However, pinpointing the genes that account for differences in disease progression has proven difficult, as tuberculosis is such a complex disease affected by so many factors (Bellamy *et al*., 1998; Delgado *et al*., 2006; Khor *et al*., 2007; Li *et al*., 2011b; Newport, 2009; Stead *et al*., 1990; Stein *et al*., 2007). To gain a better understanding of the genetic determinants that influence the outcome of infection, studies in recent years have focused on identifying genes that are involved in regulation of immune responses crucial for the control of tuberculosis, such as induction of TNF or IFN-γ (Bowdish *et al*., 2013; Jepson *et al*., 2001; Stein *et al*., 2003; Stein *et al*., 2007).

One recent study conducted by Newport *et al.* investigated IFN-γ responses to mycobacterial antigen in BCG vaccinated neonates in the Gambia. The magnitude of IFN-γ responses was linked to three regions on chromosomes 8, 9 and 11 which encode five genes involved in immune response during infection with *M. tuberculosis* (Newport *et al*. manuscript in preparation). Of these genes, two encoded the proteins MD-2 and RIP2. These genes interact directly with the PRRs TLR4 and NOD1 and NOD2 respectively mediating NF-κB activation and the release of pro-inflammatory cytokines, which are of particular importance in immune response to tuberculosis.

A total of 44 polymorphisms were identified among the genes encoding RIP2 and MD-2 in the Gambian population. However, only one identified polymorphism was significantly linked to magnitude of IFN-γ (Chapter 3).

However, two non-synonymous polymorphisms (rs2230801/I259T and rs35004667/268V) were identified in the kinase domain of RIP2. Both polymorphisms were predicted to have adverse effects on protein function.

RIP2 is an essential kinase in the NOD signalling pathways which plays an important role in the immune response to intracellular pathogens including *M. tuberculosis*. RIP2 has previously been shown to be involved in the induction of IL-1β, TNF, IL-12p40 and type I interferons during infection with *M. tuberculosis* of human and murine macrophages (Brooks *et al*., 2011; Gandotra *et al*., 2007; Pandey *et al*., 2009). Furthermore, despite *Nod2-/-* mice controlling *M. tuberculosis* infection equally well as wt mice, a more recent study has shown that in human macrophages the NOD2 signalling pathway plays a role in controlling *M. tuberculosis* infection (Brooks et al., 2011; Divangahi et al., 2008; Gandotra et al., 2007). In accordance with this the current study showed that in human macrophages RIP2 significantly contributed to the induction of IL-1β during *M. tuberculosis* infection (Chapter 4).

The polymorphisms identified in RIP2 caused a significant reduction in kinase activity which had no effect on protein stability or downstream NF-κB activity (Chapter 5 and 6). Several studies demonstrated that in the absence of RIP2 kinase activity expression levels of RIP2 are reduced (Lu et al., 2005; Nembrini et al., 2009; Windheim et al., 2007). As expression levels of the RIP2 variants in the current study were not affected it is possible that kinase activity of RIP2 needs to be completely abolished to affect protein stability.

Reports regarding the significance of RIP2 kinase activity in NOD-dependent NF-κB activation have been controversial. Several previous studies have demonstrated that RIP2 kinase activity is required for optimal induction of NF-κB and cytokine responses upon stimulation of the NOD receptors (Nembrini *et al*., 2009; Tigno-Aranjuez *et al*., 2010). However, in contrast to this, various studies have reported that the kinase activity of RIP2 is not required for NF-κB activation (Eickhoff et al., 2004; McCarthy et al., 1998; Thome et al., 1998). The results of the current study are in agreement with the latter studies, suggesting that that either kinase activity of RIP2 is not required for activation of NF-κB or it has to be completely abolished to affect activation of NF-κB. This seems plausible as the RIP2 homolog RIP1 kinase has been shown to mediate TNFR-dependent activation of NF-κB in the absence of kinase activity (Lee et al., 2004).

In addition to contributing to pro-inflammatory cytokine induction, stimulation of NOD1 and NOD2 results in the induction of autophagy. Auto-phagosome formation during NOD-dependent autophagy has been shown to require the kinase activity of RIP2 (Cooney *et al*., 2010; Homer *et al*., 2012). Even though this cellular process has not yet been reported to be involved in the immune response to *M. tuberculosis*, it contributes to the immune response to several intracellular pathogens such as *L. monocytogenes* and *S. flexneri* and other forms of autophagy have been shown to play important roles in control of *M. tuberculosis* infection (Anand et al., 2011; Deretic et al., 2015; Travassos et al., 2010). As RIP2 kinase activity is required for induction of auto-phagosome formation during autophagy, it would be interesting to investigate the effects of the identified RIP2 variants on induction of NOD-dependent autophagy.

In summary, to our knowledge, this is the first report of naturally occurring RIP2 variants that display significantly reduced kinase activity. This reduction in kinase activity did not affect NOD2-dependent activation of NF-κB/AP-1 suggesting that RIP2 kinase activity is not essential for this process. However, it is possible that the identified variants impact on other cellular processed such as NOD-dependent autophagy and affect immune response to intracellular pathogens such as *M. tuberculosis*.

8. References

1929. THE CALMETTE-GUERIN VACCINE. Am J Public Health Nations Health 19, 82-83.

2000. Diagnostic Standards and Classification of Tuberculosis in Adults and Children. This official statement of the American Thoracic Society and the Centers for Disease Control and Prevention was adopted by the ATS Board of Directors, July 1999. This statement was endorsed by the Council of the Infectious Disease Society of America, September 1999. Am J Respir Crit Care Med 161, 1376-1395.

2014. Global leprosy update, 2013; reducing disease burden. Wkly Epidemiol Rec 89, 389-400.

Abdalla, H., Srinivasan, L., Shah, S., Mayer-Barber, K.D., Sher, A., Sutterwala, F.S., Briken, V., 2012. Mycobacterium tuberculosis infection of dendritic cells leads to partially caspase-1/11-independent IL-1beta and IL-18 secretion but not to pyroptosis. PLoS One 7, e40722.

Abecasis, G.R., Auton, A., Brooks, L.D., DePristo, M.A., Durbin, R.M., Handsaker, R.E., Kang, H.M., Marth, G.T., McVean, G.A., 2012. An integrated map of genetic variation from 1,092 human genomes. Nature 491, 56-65.

Abel, B., Thieblemont, N., Quesniaux, V.J., Brown, N., Mpagi, J., Miyake, K., Bihl, F., Ryffel, B., 2002. Toll-like receptor 4 expression is required to control chronic Mycobacterium tuberculosis infection in mice. J Immunol 169, 3155-3162.

Ablasser, A., Bauernfeind, F., Hartmann, G., Latz, E., Fitzgerald, K.A., Hornung, V., 2009. RIG-I-dependent sensing of poly(dA:dT) through the induction of an RNA polymerase III-transcribed RNA intermediate. Nat Immunol 10, 1065-1072.

Abubakar, I., Pimpin, L., Ariti, C., Beynon, R., Mangtani, P., Sterne, J.A., Fine, P.E., Smith, P.G., Lipman, M., Elliman, D., Watson, J.M., Drumright, L.N., Whiting, P.F., Vynnycky, E., Rodrigues, L.C., 2013. Systematic review and meta-analysis of the current evidence on the duration of protection by bacillus Calmette-Guerin vaccination against tuberculosis. Health Technol Assess 17, 1-372, v-vi.

Adzhubei, I.A., Schmidt, S., Peshkin, L., Ramensky, V.E., Gerasimova, A., Bork, P., Kondrashov, A.S., Sunyaev, S.R., 2010. A method and server for predicting damaging missense mutations. Nat Methods 7, 248-249.

Altare, F., Lammas, D., Revy, P., Jouanguy, E., Doffinger, R., Lamhamedi, S., Drysdale, P., Scheel-Toellner, D., Girdlestone, J., Darbyshire, P., Wadhwa, M., Dockrell, H., Salmon, M., Fischer, A., Durandy, A., Casanova, J.L., Kumararatne, D.S., 1998. Inherited interleukin 12 deficiency in a child with bacille Calmette-Guerin and Salmonella enteritidis disseminated infection. J Clin Invest 102, 2035-2040.

Anand, P.K., Tait, S.W., Lamkanfi, M., Amer, A.O., Nunez, G., Pages, G., Pouyssegur, J., McGargill, M.A., Green, D.R., Kanneganti, T.D., 2011. TLR2 and RIP2 pathways mediate autophagy of Listeria monocytogenes via extracellular signal-regulated kinase (ERK) activation. J Biol Chem 286, 42981-42991.

Armstrong, J.A., Hart, P.D., 1971. Response of cultured macrophages to Mycobacterium tuberculosis, with observations on fusion of lysosomes with phagosomes. J Exp Med 134, 713-740.

Armstrong, J.A., Hart, P.D., 1975. Phagosome-lysosome interactions in cultured macrophages infected with virulent tubercle bacilli. Reversal of the usual nonfusion pattern and observations on bacterial survival. J Exp Med 142, 1-16.

Babb, C., van der Merwe, L., Beyers, N., Pheiffer, C., Walzl, G., Duncan, K., van Helden, P., Hoal, E.G., 2007. Vitamin D receptor gene polymorphisms and sputum conversion time in pulmonary tuberculosis patients. Tuberculosis (Edinb) 87, 295-302.

Bafica, A., Scanga, C.A., Feng, C.G., Leifer, C., Cheever, A., Sher, A., 2005. TLR9 regulates Th1 responses and cooperates with TLR2 in mediating optimal resistance to Mycobacterium tuberculosis. J Exp Med 202, 1715-1724.

Baghdadi, J.E., Orlova, M., Alter, A., Ranque, B., Chentoufi, M., Lazrak, F., Archane, M.I., Casanova, J.L., Benslimane, A., Schurr, E., Abel, L., 2006. An autosomal dominant major gene confers predisposition to pulmonary tuberculosis in adults. J Exp Med 203, 1679-1684.

Barnes, P.F., Fong, S.J., Brennan, P.J., Twomey, P.E., Mazumder, A., Modlin, R.L., 1990. Local production of tumor necrosis factor and IFN-gamma in tuberculous pleuritis. J Immunol 145, 149-154.

Barnich, N., Aguirre, J.E., Reinecker, H.C., Xavier, R., Podolsky, D.K., 2005. Membrane recruitment of NOD2 in intestinal epithelial cells is essential for nuclear factor-{kappa}B activation in muramyl dipeptide recognition. J Cell Biol 170, 21-26.

Behr, M.A., Wilson, M.A., Gill, W.P., Salamon, H., Schoolnik, G.K., Rane, S., Small, P.M., 1999. Comparative genomics of BCG vaccines by whole-genome DNA microarray. Science 284, 1520-1523.

Bellamy, R., Beyers, N., McAdam, K.P., Ruwende, C., Gie, R., Samaai, P., Bester, D., Meyer, M., Corrah, T., Collin, M., Camidge, D.R., Wilkinson, D., Hoal-Van Helden, E., Whittle, H.C., Amos, W., van Helden, P., Hill, A.V., 2000. Genetic susceptibility to tuberculosis in Africans: a genome-wide scan. Proc Natl Acad Sci U S A 97, 8005-8009.

Bellamy, R., Ruwende, C., Corrah, T., McAdam, K.P., Whittle, H.C., Hill, A.V., 1998. Variations in the NRAMP1 gene and susceptibility to tuberculosis in West Africans. N Engl J Med 338, 640-644.

Berrington, W.R., Macdonald, M., Khadge, S., Sapkota, B.R., Janer, M., Hagge, D.A., Kaplan, G., Hawn, T.R., 2010. Common polymorphisms in the NOD2 gene region are associated with leprosy and its reactive states. J Infect Dis 201, 1422-1435.

Bertrand, M.J., Doiron, K., Labbe, K., Korneluk, R.G., Barker, P.A., Saleh, M., 2009. Cellular inhibitors of apoptosis cIAP1 and cIAP2 are required for innate immunity signaling by the pattern recognition receptors NOD1 and NOD2. Immunity 30, 789-801.

Bhatt, K., Hickman, S.P., Salgame, P., 2004. Cutting edge: a new approach to modeling early lung immunity in murine tuberculosis. J Immunol 172, 2748-2751.

Bosio, C.M., Gardner, D., Elkins, K.L., 2000. Infection of B cell-deficient mice with CDC 1551, a clinical isolate of Mycobacterium tuberculosis: delay in dissemination and development of lung pathology. J Immunol 164, 6417-6425.

Bowdish, D.M., Sakamoto, K., Lack, N.A., Hill, P.C., Sirugo, G., Newport, M.J., Gordon, S., Hill, A.V., Vannberg, F.O., 2013. Genetic variants of MARCO are associated with susceptibility to pulmonary tuberculosis in a Gambian population. BMC Med Genet 14, 47.

Branger, J., Leemans, J.C., Florquin, S., Weijer, S., Speelman, P., Van Der Poll, T., 2004. Toll-like receptor 4 plays a protective role in pulmonary tuberculosis in mice. Int Immunol 16, 509-516.

Brightbill, H.D., Libraty, D.H., Krutzik, S.R., Yang, R.B., Belisle, J.T., Bleharski, J.R., Maitland, M., Norgard, M.V., Plevy, S.E., Smale, S.T., Brennan, P.J., Bloom, B.R., Godowski, P.J., Modlin, R.L., 1999. Host defense mechanisms triggered by microbial lipoproteins through toll-like receptors. Science 285, 732-736.

Brooks, M.N., Rajaram, M.V., Azad, A.K., Amer, A.O., Valdivia-Arenas, M.A., Park, J.H., Nunez, G., Schlesinger, L.S., 2011. NOD2 controls the nature of the inflammatory response and subsequent fate of Mycobacterium tuberculosis and M. bovis BCG in human macrophages. Cell Microbiol 13, 402-418.

Brue, T., Quentien, M., Khetchoumian, K., Bensa, M., Capo-Chichi, J., Delemer, B., Balsalobre, A., Nassif, C., Papadimitriou, D.T., Pagnier, A., Hasselmann, C., Patry, L., Schwartzentruber, J., Souchon, P., Takayasu, S., Enjalbert, A., Van Vliet, G., Majewski, J., Drouin, J., Samuels, M.E., 2014. Mutations in NFKB2 and potential genetic heterogeneity in patients with DAVID syndrome, having variable endocrine and immune deficiencies. BMC Med Genet 15, 139.

Bulut, Y., Faure, E., Thomas, L., Karahashi, H., Michelsen, K.S., Equils, O., Morrison, S.G., Morrison, R.P., Arditi, M., 2002. Chlamydial heat shock protein 60 activates macrophages and endothelial cells through Toll-like receptor 4 and MD2 in a MyD88-dependent pathway. J Immunol 168, 1435-1440.

Bulut, Y., Michelsen, K.S., Hayrapetian, L., Naiki, Y., Spallek, R., Singh, M., Arditi, M., 2005. Mycobacterium tuberculosis heat shock proteins use diverse Toll-like receptor pathways to activate pro-inflammatory signals. J Biol Chem 280, 20961-20967.

Burgner, D., Usen, S., Rockett, K., Jallow, M., Ackerman, H., Cervino, A., Pinder, M., Kwiatkowski, D.P., 2003. Nucleotide and haplotypic diversity of the NOS2A promoter region and its relationship to cerebral malaria. Hum Genet 112, 379-386.

Bustamante, J., Arias, A.A., Vogt, G., Picard, C., Galicia, L.B., Prando, C., Grant, A.V., Marchal, C.C., Hubeau, M., Chapgier, A., de Beaucoudrey, L., Puel, A., Feinberg, J., Valinetz, E., Janniere, L., Besse, C., Boland, A., Brisseau, J.M., Blanche, S., Lortholary, O., Fieschi, C., Emile, J.F., Boisson-Dupuis, S., Al-Muhsen, S., Woda, B., Newburger, P.E., Condino-Neto, A., Dinauer, M.C., Abel, L., Casanova, J.L., 2011. Germline CYBB mutations that selectively affect macrophages in kindreds with X-linked predisposition to tuberculous mycobacterial disease. Nat Immunol 12, 213-221.

Bustamante, J., Boisson-Dupuis, S., Abel, L., Casanova, J.L., 2014. Mendelian susceptibility to mycobacterial disease: Genetic, immunological, and clinical features of inborn errors of IFN-gamma immunity. Semin Immunol 26, 454-470.

Byun, E.H., Kim, W.S., Kim, J.S., Jung, I.D., Park, Y.M., Kim, H.J., Cho, S.N., Shin, S.J., 2012. Mycobacterium tuberculosis Rv0577, a novel TLR2 agonist, induces maturation of dendritic cells and drives Th1 immune response. FASEB J 26, 2695-2711.

Caccamo, N., Meraviglia, S., La Mendola, C., Guggino, G., Dieli, F., Salerno, A., 2006. Phenotypical and functional analysis of memory and effector human CD8 T cells specific for mycobacterial antigens. J Immunol 177, 1780-1785.

Cai, X., Wang, M., Kong, H., Liu, J., Liu, Y., Xia, W., Zou, M., Wang, J., Su, H., Xu, D., 2013. Prokaryotic expression, purification and functional characterization of recombinant human RIP2. Mol Biol Rep 40, 59-65.

Cambier, C.J., Takaki, K.K., Larson, R.P., Hernandez, R.E., Tobin, D.M., Urdahl, K.B., Cosma, C.L., Ramakrishnan, L., 2014. Mycobacteria manipulate macrophage recruitment through coordinated use of membrane lipids. Nature 505, 218-222.

Caron, E., Hall, A., 1998. Identification of two distinct mechanisms of phagocytosis controlled by different Rho GTPases. Science 282, 1717-1721.

Caruso, A.M., Serbina, N., Klein, E., Triebold, K., Bloom, B.R., Flynn, J.L., 1999. Mice deficient in CD4 T cells have only transiently diminished levels of IFN-gamma, yet succumb to tuberculosis. J Immunol 162, 5407-5416.

Castano-Rodriguez, N., Kaakoush, N.O., Pardo, A.L., Goh, K.L., Fock, K.M., Mitchell, H.M., 2014. Genetic polymorphisms in the Toll-like receptor signalling pathway in Helicobacter pylori infection and related gastric cancer. Hum Immunol 75, 808-815.

Ceroni, A., Passerini, A., Vullo, A., Frasconi, P., 2006. DISULFIND: a disulfide bonding state and cysteine connectivity prediction server. Nucleic Acids Res 34, W177-181.

Chackerian, A.A., Alt, J.M., Perera, T.V., Dascher, C.C., Behar, S.M., 2002. Dissemination of Mycobacterium tuberculosis is influenced by host factors and precedes the initiation of T-cell immunity. Infect Immun 70, 4501-4509.

Chang, J.T., Wherry, E.J., Goldrath, A.W., 2014. Molecular regulation of effector and memory T cell differentiation. Nat Immunol 15, 1104-1115.

Chapgier, A., Boisson-Dupuis, S., Jouanguy, E., Vogt, G., Feinberg, J., Prochnicka-Chalufour, A., Casrouge, A., Yang, K., Soudais, C., Fieschi, C., Santos, O.F., Bustamante, J., Picard, C., de Beaucoudrey, L., Emile, J.F., Arkwright, P.D., Schreiber, R.D., Rolinck-Werninghaus, C., Rosen-Wolff, A., Magdorf, K., Roesler, J., Casanova, J.L., 2006. Novel STAT1 alleles in otherwise healthy patients with mycobacterial disease. PLoS Genet 2, e131.

Cheruvu, M., Plikaytis, B.B., Shinnick, T.M., 2007. The acid-induced operon Rv3083-Rv3089 is required for growth of Mycobacterium tuberculosis in macrophages. Tuberculosis (Edinb) 87, 12-20.

Chieppa, M., Bianchi, G., Doni, A., Del Prete, A., Sironi, M., Laskarin, G., Monti, P., Piemonti, L., Biondi, A., Mantovani, A., Introna, M., Allavena, P., 2003. Cross-linking of the mannose receptor on monocyte-derived dendritic cells activates an anti-inflammatory immunosuppressive program. J Immunol 171, 4552-4560.

Chimusa, E.R., Zaitlen, N., Daya, M., Moller, M., van Helden, P.D., Mulder, N.J., Price, A.L., Hoal, E.G., 2014. Genome-wide association study of ancestry-specific TB risk in the South African Coloured population. Hum Mol Genet 23, 796-809.

Chin, A.I., Dempsey, P.W., Bruhn, K., Miller, J.F., Xu, Y., Cheng, G., 2002. Involvement of receptor-interacting protein 2 in innate and adaptive immune responses. Nature 416, 190-194.

Clark, R., Kupper, T., 2005. Old meets new: the interaction between innate and adaptive immunity. J Invest Dermatol 125, 629-637.

Claudio, E., Brown, K., Park, S., Wang, H., Siebenlist, U., 2002. BAFF-induced NEMO-independent processing of NF-kappa B2 in maturing B cells. Nat Immunol 3, 958-965.

Coadou, G., Gharbi-Benarous, J., Megy, S., Bertho, G., Evrard-Todeschi, N., Segeral, E., Benarous, R., Girault, J.P., 2003. NMR studies of the phosphorylation motif of the HIV-1 protein Vpu bound to the F-box protein beta-TrCP. Biochemistry 42, 14741-14751.

Cobat, A., Gallant, C.J., Simkin, L., Black, G.F., Stanley, K., Hughes, J., Doherty, T.M., Hanekom, W.A., Eley, B., Beyers, N., Jais, J.P., van Helden, P., Abel, L., Hoal, E.G., Alcais, A., Schurr, E., 2010. High heritability of antimycobacterial immunity in an area of hyperendemicity for tuberculosis disease. J Infect Dis 201, 15-19.

Cobat, A., Gallant, C.J., Simkin, L., Black, G.F., Stanley, K., Hughes, J., Doherty, T.M., Hanekom, W.A., Eley, B., Jais, J.P., Boland-Auge, A., van Helden, P., Casanova, J.L., Abel, L., Hoal, E.G., Schurr, E., Alcais, A., 2009. Two loci control tuberculin skin test reactivity in an area hyperendemic for tuberculosis. J Exp Med 206, 2583-2591.

Cobat, A., Hoal, E.G., Gallant, C.J., Simkin, L., Black, G.F., Stanley, K., Jais, J.P., Yu, T.H., Boland-Auge, A., Grange, G., Delacourt, C., van Helden, P., Casanova, J.L., Abel, L., Alcais, A., Schurr, E., 2013. Identification of a major locus, TNF1, that controls BCG-triggered tumor necrosis factor production by leukocytes in an area hyperendemic for tuberculosis. Clin Infect Dis 57, 963-970.

Cobat, A., Poirier, C., Hoal, E., Boland-Auge, A., de La Rocque, F., Corrard, F., Grange, G., Migaud, M., Bustamante, J., Boisson-Dupuis, S., Casanova, J.L., Schurr, E., Alcais, A., Delacourt, C., Abel, L., 2015. Tuberculin skin test negativity is under tight genetic control of chromosomal region 11p14-15 in settings with different tuberculosis endemicities. J Infect Dis 211, 317-321.

Cooke, G.S., Campbell, S.J., Bennett, S., Lienhardt, C., McAdam, K.P., Sirugo, G., Sow, O., Gustafson, P., Mwangulu, F., van Helden, P., Fine, P., Hoal, E.G., Hill, A.V., 2008. Mapping of a novel susceptibility locus suggests a role for MC3R and CTSZ in human tuberculosis. Am J Respir Crit Care Med 178, 203-207.

Cooney, R., Baker, J., Brain, O., Danis, B., Pichulik, T., Allan, P., Ferguson, D.J., Campbell, B.J., Jewell, D., Simmons, A., 2010. NOD2 stimulation induces autophagy in dendritic cells influencing bacterial handling and antigen presentation. Nat Med 16, 90-97.

Cooper, A.M., Kipnis, A., Turner, J., Magram, J., Ferrante, J., Orme, I.M., 2002. Mice lacking bioactive IL-12 can generate protective, antigen-specific cellular responses to mycobacterial infection only if the IL-12 p40 subunit is present. J Immunol 168, 1322-1327.

Coulombe, F., Divangahi, M., Veyrier, F., de Leseleuc, L., Gleason, J.L., Yang, Y., Kelliher, M.A., Pandey, A.K., Sassetti, C.M., Reed, M.B., Behr, M.A., 2009. Increased NOD2-mediated recognition of N-glycolyl muramyl dipeptide. J Exp Med 206, 1709-1716.

Court, N., Vasseur, V., Vacher, R., Fremond, C., Shebzukhov, Y., Yeremeev, V.V., Maillet, I., Nedospasov, S.A., Gordon, S., Fallon, P.G., Suzuki, H., Ryffel, B., Quesniaux, V.F., 2010. Partial redundancy of the pattern recognition receptors, scavenger receptors, and C-type lectins for the long-term control of Mycobacterium tuberculosis infection. J Immunol 184, 7057-7070.

Dalton, D.K., Pitts-Meek, S., Keshav, S., Figari, I.S., Bradley, A., Stewart, T.A., 1993. Multiple defects of immune cell function in mice with disrupted interferon-gamma genes. Science 259, 1739-1742.

Damgaard, R.B., Nachbur, U., Yabal, M., Wong, W.W., Fiil, B.K., Kastirr, M., Rieser, E., Rickard, J.A., Bankovacki, A., Peschel, C., Ruland, J., Bekker-Jensen, S., Mailand, N., Kaufmann, T., Strasser, A., Walczak, H., Silke, J., Jost, P.J., Gyrd-Hansen, M., 2012. The ubiquitin ligase XIAP recruits LUBAC for NOD2 signaling in inflammation and innate immunity. Mol Cell 46, 746-758.

Davila, S., Hibberd, M.L., Hari Dass, R., Wong, H.E., Sahiratmadja, E., Bonnard, C., Alisjahbana, B., Szeszko, J.S., Balabanova, Y., Drobniewski, F., van Crevel, R., van de Vosse, E., Nejentsev, S., Ottenhoff, T.H., Seielstad, M., 2008. Genetic association and expression studies indicate a role of toll-like receptor 8 in pulmonary tuberculosis. PLoS Genet 4, e1000218.

de Beaucoudrey, L., Samarina, A., Bustamante, J., Cobat, A., Boisson-Dupuis, S., Feinberg, J., Al-Muhsen, S., Janniere, L., Rose, Y., de Suremain, M., Kong, X.F., Filipe-Santos, O., Chapgier, A., Picard, C., Fischer, A., Dogu, F., Ikinciogullari, A., Tanir, G., Al-Hajjar, S., Al-Jumaah, S., Frayha, H.H., AlSum, Z., Al-Ajaji, S., Alangari, A., Al-Ghonaium, A., Adimi, P., Mansouri, D., Ben-Mustapha, I., Yancoski, J., Garty, B.Z., Rodriguez-Gallego, C., Caragol, I., Kutukculer, N., Kumararatne, D.S., Patel, S., Doffinger, R., Exley, A., Jeppsson, O., Reichenbach, J., Nadal, D., Boyko, Y., Pietrucha, B., Anderson, S., Levin, M., Schandene, L., Schepers, K., Efira, A., Mascart, F., Matsuoka, M., Sakai, T., Siegrist, C.A., Frecerova, K., Bluetters-Sawatzki, R., Bernhoft, J., Freihorst, J., Baumann, U., Richter, D., Haerynck, F., De Baets, F., Novelli, V., Lammas, D., Vermylen, C., Tuerlinckx, D., Nieuwhof, C., Pac, M., Haas, W.H., Muller-Fleckenstein, I., Fleckenstein, B., Levy, J., Raj, R., Cohen, A.C., Lewis, D.B., Holland, S.M., Yang, K.D., Wang, X., Jiang, L., Yang, X., Zhu, C., Xie, Y., Lee, P.P., Chan, K.W., Chen, T.X., Castro, G., Natera, I., Codoceo, A., King, A., Bezrodnik, L., Di Giovani, D., Gaillard, M.I., de Moraes-Vasconcelos, D., Grumach, A.S., da Silva Duarte, A.J., Aldana, R., Espinosa-Rosales, F.J., Bejaoui, M., Bousfiha, A.A., Baghdadi, J.E., Ozbek, N., Aksu, G., Keser, M., Somer, A., Hatipoglu, N., Aydogmus, C., Asilsoy, S., Camcioglu, Y., Gulle, S., Ozgur, T.T., Ozen, M., Oleastro, M., Bernasconi, A., Mamishi, S., Parvaneh, N., Rosenzweig, S., Barbouche, R., Pedraza, S., Lau, Y.L., Ehlayel, M.S., Fieschi, C., Abel, L., Sanal, O., Casanova, J.L., 2010. Revisiting human IL-12Rbeta1 deficiency: a survey of 141 patients from 30 countries. Medicine (Baltimore) 89, 381-402.

de Jonge, M.I., Pehau-Arnaudet, G., Fretz, M.M., Romain, F., Bottai, D., Brodin, P., Honore, N., Marchal, G., Jiskoot, W., England, P., Cole, S.T., Brosch, R., 2007. ESAT-6 from Mycobacterium tuberculosis dissociates from its putative chaperone CFP-10 under acidic conditions and exhibits membrane-lysing activity. J Bacteriol 189, 6028-6034.

de la Salle, H., Mariotti, S., Angenieux, C., Gilleron, M., Garcia-Alles, L.F., Malm, D., Berg, T., Paoletti, S., Maitre, B., Mourey, L., Salamero, J., Cazenave, J.P., Hanau, D., Mori, L., Puzo, G., De Libero, G., 2005. Assistance of microbial glycolipid antigen processing by CD1e. Science 310, 1321-1324.

Deffur, A., Mulder, N.J., Wilkinson, R.J., 2013. Co-infection with Mycobacterium tuberculosis and human immunodeficiency virus: an overview and motivation for systems approaches. Pathog Dis 69, 101-113.

Dejardin, E., Droin, N.M., Delhase, M., Haas, E., Cao, Y., Makris, C., Li, Z.W., Karin, M., Ware, C.F., Green, D.R., 2002. The lymphotoxin-beta receptor induces different patterns of gene expression via two NF-kappaB pathways. Immunity 17, 525-535.

Delgado, J.C., Baena, A., Thim, S., Goldfeld, A.E., 2006. Aspartic acid homozygosity at codon 57 of HLA-DQ beta is associated with susceptibility to pulmonary tuberculosis in Cambodia. J Immunol 176, 1090-1097.

Deretic, V., Kimura, T., Timmins, G., Moseley, P., Chauhan, S., Mandell, M., 2015. Immunologic manifestations of autophagy. J Clin Invest 125, 75-84.

Dey, B., Bishai, W.R., 2014. Crosstalk between Mycobacterium tuberculosis and the host cell. Semin Immunol 26, 486-496.

DiDonato, J.A., Hayakawa, M., Rothwarf, D.M., Zandi, E., Karin, M., 1997. A cytokine-responsive IkappaB kinase that activates the transcription factor NF-kappaB. Nature 388, 548-554.

Diduk, S.V., Smirnova, K.V., Pavlish, O.A., Gurtsevitch, V.E., 2008. Functionally significant mutations in the Epstein-Barr virus LMP1 gene and their role in activation of cell signaling pathways. Biochemistry (Mosc) 73, 1134-1139.

Dieli, F., Ivanyi, J., Marsh, P., Williams, A., Naylor, I., Sireci, G., Caccamo, N., Di Sano, C., Salerno, A., 2003. Characterization of lung gamma delta T cells following intranasal infection with Mycobacterium bovis bacillus Calmette-Guerin. J Immunol 170, 463-469.

Divangahi, M., Mostowy, S., Coulombe, F., Kozak, R., Guillot, L., Veyrier, F., Kobayashi, K.S., Flavell, R.A., Gros, P., Behr, M.A., 2008. NOD2-deficient mice have impaired resistance to Mycobacterium tuberculosis infection through defective innate and adaptive immunity. J Immunol 181, 7157-7165.

Dorhoi, A., Nouailles, G., Jorg, S., Hagens, K., Heinemann, E., Pradl, L., Oberbeck-Muller, D., Duque-Correa, M.A., Reece, S.T., Ruland, J., Brosch, R., Tschopp, J., Gross, O., Kaufmann, S.H., 2012. Activation of the NLRP3 inflammasome by Mycobacterium tuberculosis is uncoupled from susceptibility to active tuberculosis. Eur J Immunol 42, 374-384.

Dorman, S.E., Picard, C., Lammas, D., Heyne, K., van Dissel, J.T., Baretto, R., Rosenzweig, S.D., Newport, M., Levin, M., Roesler, J., Kumararatne, D., Casanova, J.L., Holland, S.M., 2004. Clinical features of dominant and recessive interferon gamma receptor 1 deficiencies. Lancet 364, 2113-2121.

Dorsch, M., Wang, A., Cheng, H., Lu, C., Bielecki, A., Charron, K., Clauser, K., Ren, H., Polakiewicz, R.D., Parsons, T., Li, P., Ocain, T., Xu, Y., 2006. Identification of a regulatory autophosphorylation site in the serine-threonine kinase RIP2. Cell Signal 18, 2223-2229.

Drage, M.G., Pecora, N.D., Hise, A.G., Febbraio, M., Silverstein, R.L., Golenbock, D.T., Boom, W.H., Harding, C.V., 2009. TLR2 and its co-receptors determine responses of macrophages and dendritic cells to lipoproteins of Mycobacterium tuberculosis. Cell Immunol 258, 29-37.

Eickhoff, J., Hanke, M., Stein-Gerlach, M., Kiang, T.P., Herzberger, K., Habenberger, P., Muller, S., Klebl, B., Marschall, M., Stamminger, T., Cotten, M., 2004. RICK activates a NF-kappaB-dependent anti-human cytomegalovirus response. J Biol Chem 279, 9642-9652.

Etna, M.P., Giacomini, E., Severa, M., Coccia, E.M., 2014. Pro- and anti-inflammatory cytokines in tuberculosis: a two-edged sword in TB pathogenesis. Semin Immunol 26, 543-551.

Evrard-Todeschi, N., Gharbi-Benarous, J., Bertho, G., Coadou, G., Megy, S., Benarous, R., Girault, J.P., 2006. NMR studies for identifying phosphopeptide ligands of the HIV-1 protein Vpu binding to the F-box protein beta-TrCP. Peptides 27, 194-210.

Faksri, K., Chaiprasert, A., Pardieu, C., Casali, N., Palaga, T., Prammananan, T., Palittapongarnpim, P., Prayoonwiwat, N., Drobniewski, F., 2014. Heterogeneity of phenotypic characteristics of the modern and ancestral Beijing strains of Mycobacterium tuberculosis. Asian Pac J Allergy Immunol 32, 124-132.

Ferre, F., Clote, P., 2006. DiANNA 1.1: an extension of the DiANNA web server for ternary cysteine classification. Nucleic Acids Res 34, W182-185.

Ferwerda, G., Girardin, S.E., Kullberg, B.J., Le Bourhis, L., de Jong, D.J., Langenberg, D.M., van Crevel, R., Adema, G.J., Ottenhoff, T.H., Van der Meer, J.W., Netea, M.G., 2005. NOD2 and toll-like receptors are nonredundant recognition systems of Mycobacterium tuberculosis. PLoS Pathog 1, 279-285.

Fieschi, C., Dupuis, S., Catherinot, E., Feinberg, J., Bustamante, J., Breiman, A., Altare, F., Baretto, R., Le Deist, F., Kayal, S., Koch, H., Richter, D., Brezina, M., Aksu, G., Wood, P., Al-Jumaah, S., Raspall, M., Da Silva Duarte, A.J., Tuerlinckx, D., Virelizier, J.L., Fischer, A., Enright, A., Bernhoft, J., Cleary, A.M., Vermylen, C., Rodriguez-Gallego, C., Davies, G., Blutters-Sawatzki, R., Siegrist, C.A., Ehlayel, M.S., Novelli, V., Haas, W.H., Levy, J., Freihorst, J., Al-Hajjar, S., Nadal, D., De Moraes Vasconcelos, D., Jeppsson, O., Kutukculer, N., Frecerova, K., Caragol, I., Lammas, D., Kumararatne, D.S., Abel, L., Casanova, J.L., 2003. Low penetrance, broad resistance, and favorable outcome of interleukin 12 receptor beta1 deficiency: medical and immunological implications. J Exp Med 197, 527-535.

Fieschi, C., Dupuis, S., Picard, C., Smith, C.I., Holland, S.M., Casanova, J.L., 2001. High levels of interferon gamma in the plasma of children with complete interferon gamma receptor deficiency. Pediatrics 107, E48.

Filipe-Santos, O., Bustamante, J., Haverkamp, M.H., Vinolo, E., Ku, C.L., Puel, A., Frucht, D.M., Christel, K., von Bernuth, H., Jouanguy, E., Feinberg, J., Durandy, A., Senechal, B., Chapgier, A., Vogt, G., de Beaucoudrey, L., Fieschi, C., Picard, C., Garfa, M., Chemli, J., Bejaoui, M., Tsolia, M.N., Kutukculer, N., Plebani, A., Notarangelo, L., Bodemer, C., Geissmann, F., Israel, A., Veron, M., Knackstedt, M., Barbouche, R., Abel, L., Magdorf, K., Gendrel, D., Agou, F., Holland, S.M., Casanova, J.L., 2006. X-linked susceptibility to mycobacteria is caused by mutations in NEMO impairing CD40-dependent IL-12 production. J Exp Med 203, 1745-1759.

Finan, C., Ota, M.O., Marchant, A., Newport, M.J., 2008. Natural variation in immune responses to neonatal Mycobacterium bovis Bacillus Calmette-Guerin (BCG) Vaccination in a Cohort of Gambian infants. PLoS One 3, e3485.

Fine, P.E., 1995. Variation in protection by BCG: implications of and for heterologous immunity. Lancet 346, 1339-1345.

Fitzgerald, K.A., Rowe, D.C., Golenbock, D.T., 2004. Endotoxin recognition and signal transduction by the TLR4/MD2-complex. Microbes Infect 6, 1361-1367.

Flicek, P., Amode, M.R., Barrell, D., Beal, K., Billis, K., Brent, S., Carvalho-Silva, D., Clapham, P., Coates, G., Fitzgerald, S., Gil, L., Giron, C.G., Gordon, L., Hourlier, T., Hunt, S., Johnson, N., Juettemann, T., Kahari, A.K., Keenan, S., Kulesha, E., Martin, F.J., Maurel, T., McLaren, W.M., Murphy, D.N., Nag, R., Overduin, B., Pignatelli, M., Pritchard, B., Pritchard, E., Riat, H.S., Ruffier, M., Sheppard, D., Taylor, K., Thormann, A., Trevanion, S.J., Vullo, A., Wilder, S.P., Wilson, M., Zadissa, A., Aken, B.L., Birney, E., Cunningham, F., Harrow, J., Herrero, J., Hubbard, T.J., Kinsella, R., Muffato, M., Parker, A., Spudich, G., Yates, A., Zerbino, D.R., Searle, S.M., 2014. Ensembl 2014. Nucleic Acids Res 42, D749-755.

Flo, T.H., Ryan, L., Latz, E., Takeuchi, O., Monks, B.G., Lien, E., Halaas, O., Akira, S., Skjak-Braek, G., Golenbock, D.T., Espevik, T., 2002. Involvement of toll-like receptor (TLR) 2 and TLR4 in cell activation by mannuronic acid polymers. J Biol Chem 277, 35489-35495.

Flores-Villanueva, P.O., Ruiz-Morales, J.A., Song, C.H., Flores, L.M., Jo, E.K., Montano, M., Barnes, P.F., Selman, M., Granados, J., 2005. A functional promoter polymorphism in monocyte chemoattractant protein-1 is associated with increased susceptibility to pulmonary tuberculosis. J Exp Med 202, 1649-1658.

Fong, A., Sun, S.C., 2002. Genetic evidence for the essential role of beta-transducin repeat-containing protein in the inducible processing of NF-kappa B2/p100. J Biol Chem 277, 22111-22114.

Fratti, R.A., Chua, J., Vergne, I., Deretic, V., 2003. Mycobacterium tuberculosis glycosylated phosphatidylinositol causes phagosome maturation arrest. Proc Natl Acad Sci U S A 100, 5437-5442.

Freches, D., Korf, H., Denis, O., Havaux, X., Huygen, K., Romano, M., 2013. Mice genetically inactivated in interleukin-17A receptor are defective in long-term control of Mycobacterium tuberculosis infection. Immunology 140, 220-231.

Friedland, J.S., Shattock, R.J., Johnson, J.D., Remick, D.G., Holliman, R.E., Griffin, G.E., 1993. Differential cytokine gene expression and secretion after phagocytosis by a human monocytic cell line of Toxoplasma gondii compared with Mycobacterium tuberculosis. Clin Exp Immunol 91, 282-286.

Fritz, J.H., Girardin, S.E., Fitting, C., Werts, C., Mengin-Lecreulx, D., Caroff, M., Cavaillon, J.M., Philpott, D.J., Adib-Conquy, M., 2005. Synergistic stimulation of human monocytes and dendritic cells by Toll-like receptor 4 and NOD1- and NOD2-activating agonists. Eur J Immunol 35, 2459-2470.

Gagneux, S., Small, P.M., 2007. Global phylogeography of Mycobacterium tuberculosis and implications for tuberculosis product development. Lancet Infect Dis 7, 328-337.

Gandotra, S., Jang, S., Murray, P.J., Salgame, P., Ehrt, S., 2007. Nucleotide-binding oligomerization domain protein 2-deficient mice control infection with Mycobacterium tuberculosis. Infect Immun 75, 5127-5134.

Girardin, S.E., Boneca, I.G., Carneiro, L.A., Antignac, A., Jehanno, M., Viala, J., Tedin, K., Taha, M.K., Labigne, A., Zahringer, U., Coyle, A.J., DiStefano, P.S., Bertin, J., Sansonetti, P.J., Philpott, D.J., 2003a. Nod1 detects a unique muropeptide from gram-negative bacterial peptidoglycan. Science 300, 1584-1587.

Girardin, S.E., Boneca, I.G., Viala, J., Chamaillard, M., Labigne, A., Thomas, G., Philpott, D.J., Sansonetti, P.J., 2003b. Nod2 is a general sensor of peptidoglycan through muramyl dipeptide (MDP) detection. J Biol Chem 278, 8869-8872.

Gomez, L.M., Anaya, J.M., Vilchez, J.R., Cadena, J., Hinojosa, R., Velez, L., Lopez-Nevot, M.A., Martin, J., 2007. A polymorphism in the inducible nitric oxide synthase gene is associated with tuberculosis. Tuberculosis (Edinb) 87, 288-294.

Gong, T., Yang, M., Qi, L., Shen, M., Du, Y., 2013. Association of MCP-1 -2518A/G and -362G/C variants and tuberculosis susceptibility: a meta-analysis. Infect Genet Evol 20, 1-7.

Gopal, R., Lin, Y., Obermajer, N., Slight, S., Nuthalapati, N., Ahmed, M., Kalinski, P., Khader, S.A., 2012. IL-23-dependent IL-17 drives Th1-cell responses following Mycobacterium bovis BCG vaccination. Eur J Immunol 42, 364-373.

Gordon, S., 2003. Alternative activation of macrophages. Nat Rev Immunol 3, 23-35.

Graff, J.W., Ettayebi, K., Hardy, M.E., 2009. Rotavirus NSP1 inhibits NFkappaB activation by inducing proteasome-dependent degradation of beta-TrCP: a novel mechanism of IFN antagonism. PLoS Pathog 5, e1000280.

Grant, A.V., Alter, A., Huong, N.T., Orlova, M., Van Thuc, N., Ba, N.N., Thai, V.H., Abel, L., Schurr, E., Alcais, A., 2012. Crohn's disease susceptibility genes are associated with leprosy in the Vietnamese population. J Infect Dis 206, 1763-1767.

Greco, E., Quintiliani, G., Santucci, M.B., Serafino, A., Ciccaglione, A.R., Marcantonio, C., Papi, M., Maulucci, G., Delogu, G., Martino, A., Goletti, D., Sarmati, L., Andreoni, M., Altieri, A., Alma, M., Caccamo, N., Di Liberto, D., De Spirito, M., Savage, N.D., Nisini, R., Dieli, F., Ottenhoff, T.H., Fraziano, M., 2012. Janus-faced liposomes enhance antimicrobial innate immune response in Mycobacterium tuberculosis infection. Proc Natl Acad Sci U S A 109, E1360-1368.

Greenwood, C.M., Fujiwara, T.M., Boothroyd, L.J., Miller, M.A., Frappier, D., Fanning, E.A., Schurr, E., Morgan, K., 2000. Linkage of tuberculosis to chromosome 2q35 loci, including NRAMP1, in a large aboriginal Canadian family. Am J Hum Genet 67, 405-416.

Griffiths, G., Nystrom, B., Sable, S.B., Khuller, G.K., 2010. Nanobead-based interventions for the treatment and prevention of tuberculosis. Nat Rev Microbiol 8, 827-834.

Gringhuis, S.I., Kaptein, T.M., Wevers, B.A., Theelen, B., van der Vlist, M., Boekhout, T., Geijtenbeek, T.B., 2012. Dectin-1 is an extracellular pathogen sensor for the induction and processing of IL-1beta via a noncanonical caspase-8 inflammasome. Nat Immunol 13, 246-254.

Gruenheid, S., Pinner, E., Desjardins, M., Gros, P., 1997. Natural resistance to infection with intracellular pathogens: the Nramp1 protein is recruited to the membrane of the phagosome. J Exp Med 185, 717-730.

Guardavaccaro, D., Kudo, Y., Boulaire, J., Barchi, M., Busino, L., Donzelli, M., Margottin-Goguet, F., Jackson, P.K., Yamasaki, L., Pagano, M., 2003. Control of meiotic and mitotic progression by the F box protein beta-Trcp1 in vivo. Dev Cell 4, 799-812.

Gupta, R., Jung, E., Brunak, S., 2004. Prediction of N-glycosylation sites in human proteins. in preparation.

Guwatudde, D., Nakakeeto, M., Jones-Lopez, E.C., Maganda, A., Chiunda, A., Mugerwa, R.D., Ellner, J.J., Bukenya, G., Whalen, C.C., 2003. Tuberculosis in household contacts of infectious cases in Kampala, Uganda. Am J Epidemiol 158, 887-898.

Hambleton, S., Salem, S., Bustamante, J., Bigley, V., Boisson-Dupuis, S., Azevedo, J., Fortin, A., Haniffa, M., Ceron-Gutierrez, L., Bacon, C.M., Menon, G., Trouillet, C., McDonald, D., Carey, P., Ginhoux, F., Alsina, L., Zumwalt, T.J., Kong, X.F., Kumararatne, D., Butler, K., Hubeau, M., Feinberg, J., Al-Muhsen, S., Cant, A., Abel, L., Chaussabel, D., Doffinger, R., Talesnik, E., Grumach, A., Duarte, A., Abarca, K., Moraes-Vasconcelos, D., Burk, D., Berghuis, A., Geissmann, F., Collin, M., Casanova, J.L., Gros, P., 2011. IRF8 mutations and human dendritic-cell immunodeficiency. N Engl J Med 365, 127-138.

Hansen, J.M., Golchin, S.A., Veyrier, F.J., Domenech, P., Boneca, I.G., Azad, A.K., Rajaram, M.V., Schlesinger, L.S., Divangahi, M., Reed, M.B., Behr, M.A., 2014. N-glycolylated peptidoglycan contributes to the immunogenicity but not pathogenicity of Mycobacterium tuberculosis. J Infect Dis 209, 1045-1054.

Harris, D.P., Haynes, L., Sayles, P.C., Duso, D.K., Eaton, S.M., Lepak, N.M., Johnson, L.L., Swain, S.L., Lund, F.E., 2000. Reciprocal regulation of polarized cytokine production by effector B and T cells. Nat Immunol 1, 475-482.

Hasegawa, M., Fujimoto, Y., Lucas, P.C., Nakano, H., Fukase, K., Nunez, G., Inohara, N., 2008. A critical role of RICK/RIP2 polyubiquitination in Nod-induced NF-kappaB activation. EMBO J 27, 373-383.

Hattori, Y., Morita, D., Fujiwara, N., Mori, D., Nakamura, T., Harashima, H., Yamasaki, S., Sugita, M., 2014. Glycerol monomycolate is a novel ligand for the human, but not mouse macrophage inducible C-type lectin, Mincle. J Biol Chem 289, 15405-15412.

Hawkes, M., Li, X., Crockett, M., Diassiti, A., Finney, C., Min-Oo, G., Liles, W.C., Liu, J., Kain, K.C., 2010. CD36 deficiency attenuates experimental mycobacterial infection. BMC Infect Dis 10, 299.

Hawn, T.R., Dunstan, S.J., Thwaites, G.E., Simmons, C.P., Thuong, N.T., Lan, N.T., Quy, H.T., Chau, T.T., Hieu, N.T., Rodrigues, S., Janer, M., Zhao, L.P., Hien, T.T., Farrar, J.J., Aderem, A., 2006. A polymorphism in Toll-interleukin 1 receptor domain containing adaptor protein is associated with susceptibility to meningeal tuberculosis. J Infect Dis 194, 1127-1134.

Hayden, M.S., Ghosh, S., 2014. Regulation of NF-kappaB by TNF family cytokines. Semin Immunol 26, 253-266.

He, C., Holme, J., Anthony, J., 2014a. SNP genotyping: the KASP assay. Methods Mol Biol 1145, 75-86.

He, Y., Wu, K., Hu, Y., Sheng, L., Tie, R., Wang, B., Huang, H., 2014b. gammadelta T cell and other immune cells crosstalk in cellular immunity. J Immunol Res 2014, 960252.

Heyckendorf, J., Olaru, I.D., Ruhwald, M., Lange, C., 2014. Getting personal perspectives on individualized treatment duration in multidrug-resistant and extensively drug-resistant tuberculosis. Am J Respir Crit Care Med 190, 374-383.

Higgs, D.R., Goodbourn, S.E., Lamb, J., Clegg, J.B., Weatherall, D.J., Proudfoot, N.J., 1983. Alpha-thalassaemia caused by a polyadenylation signal mutation. Nature 306, 398-400.

Hinz, M., Scheidereit, C., 2014. The IkappaB kinase complex in NF-kappaB regulation and beyond. EMBO Rep 15, 46-61.

Hoarau, J.J., Cesari, M., Caillens, H., Cadet, F., Pabion, M., 2004. HLA DQA1 genes generate multiple transcripts by alternative splicing and polyadenylation of the 3' untranslated region. Tissue Antigens 63, 58-71.

Homer, C.R., Kabi, A., Marina-Garcia, N., Sreekumar, A., Nesvizhskii, A.I., Nickerson, K.P., Chinnaiyan, A.M., Nunez, G., McDonald, C., 2012. A dual role for receptor-interacting protein kinase 2 (RIP2) kinase activity in nucleotide-binding oligomerization domain 2 (NOD2)-dependent autophagy. J Biol Chem 287, 25565-25576.

Homer, C.R., Richmond, A.L., Rebert, N.A., Achkar, J.P., McDonald, C., 2010. ATG16L1 and NOD2 interact in an autophagy-dependent antibacterial pathway implicated in Crohn's disease pathogenesis. Gastroenterology 139, 1630-1641, 1641 e1631-1632.

Houben, D., Demangel, C., van Ingen, J., Perez, J., Baldeon, L., Abdallah, A.M., Caleechurn, L., Bottai, D., van Zon, M., de Punder, K., van der Laan, T., Kant, A., Bossers-de Vries, R., Willemsen, P., Bitter, W., van Soolingen, D., Brosch, R., van der Wel, N., Peters, P.J., 2012. ESX-1-mediated translocation to the cytosol controls virulence of mycobacteria. Cell Microbiol 14, 1287-1298.

Hsu, T., Hingley-Wilson, S.M., Chen, B., Chen, M., Dai, A.Z., Morin, P.M., Marks, C.B., Padiyar, J., Goulding, C., Gingery, M., Eisenberg, D., Russell, R.G., Derrick, S.C., Collins, F.M., Morris, S.L., King, C.H., Jacobs, W.R., Jr., 2003. The primary mechanism of attenuation of bacillus Calmette-Guerin is a loss of secreted lytic function required for invasion of lung interstitial tissue. Proc Natl Acad Sci U S A 100, 12420-12425.

Hu, Y., Baud, V., Delhase, M., Zhang, P., Deerinck, T., Ellisman, M., Johnson, R., Karin, M., 1999. Abnormal morphogenesis but intact IKK activation in mice lacking the IKKalpha subunit of IkappaB kinase. Science 284, 316-320.

Hu, Y., Baud, V., Oga, T., Kim, K.I., Yoshida, K., Karin, M., 2001. IKKalpha controls formation of the epidermis independently of NF-kappaB. Nature 410, 710-714.

Hugot, J.P., Laurent-Puig, P., Gower-Rousseau, C., Olson, J.M., Lee, J.C., Beaugerie, L., Naom, I., Dupas, J.L., Van Gossum, A., Orholm, M., Bonaiti-Pellie, C., Weissenbach, J., Mathew, C.G., Lennard-Jones, J.E., Cortot, A., Colombel, J.F., Thomas, G., 1996. Mapping of a susceptibility locus for Crohn's disease on chromosome 16. Nature 379, 821-823.

Hunter, S.W., Brennan, P.J., 1990. Evidence for the presence of a phosphatidylinositol anchor on the lipoarabinomannan and lipomannan of Mycobacterium tuberculosis. J Biol Chem 265, 9272-9279.

Inohara, N., del Peso, L., Koseki, T., Chen, S., Nunez, G., 1998. RICK, a novel protein kinase containing a caspase recruitment domain, interacts with CLARP and regulates CD95-mediated apoptosis. J Biol Chem 273, 12296-12300.

Inohara, N., Koseki, T., Lin, J., del Peso, L., Lucas, P.C., Chen, F.F., Ogura, Y., Nunez, G., 2000. An induced proximity model for NF-kappa B activation in the Nod1/RICK and RIP signaling pathways. J Biol Chem 275, 27823-27831.

Inohara, N., Ogura, Y., Fontalba, A., Gutierrez, O., Pons, F., Crespo, J., Fukase, K., Inamura, S., Kusumoto, S., Hashimoto, M., Foster, S.J., Moran, A.P., Fernandez-Luna, J.L., Nunez, G., 2003. Host recognition of bacterial muramyl dipeptide mediated through NOD2. Implications for Crohn's disease. J Biol Chem 278, 5509-5512.

Ishikawa, E., Ishikawa, T., Morita, Y.S., Toyonaga, K., Yamada, H., Takeuchi, O., Kinoshita, T., Akira, S., Yoshikai, Y., Yamasaki, S., 2009a. Direct recognition of the mycobacterial glycolipid, trehalose dimycolate, by C-type lectin Mincle. J Exp Med 206, 2879-2888.

Ishikawa, H., Ma, Z., Barber, G.N., 2009b. STING regulates intracellular DNA-mediated, type I interferon-dependent innate immunity. Nature 461, 788-792.

Ito, T., Schaller, M., Hogaboam, C.M., Standiford, T.J., Chensue, S.W., Kunkel, S.L., 2007. TLR9 activation is a key event for the maintenance of a mycobacterial antigen-elicited pulmonary granulomatous response. Eur J Immunol 37, 2847-2855.

Jamieson, S.E., Miller, E.N., Black, G.F., Peacock, C.S., Cordell, H.J., Howson, J.M., Shaw, M.A., Burgner, D., Xu, W., Lins-Lainson, Z., Shaw, J.J., Ramos, F., Silveira, F., Blackwell, J.M., 2004. Evidence for a cluster of genes on chromosome 17q11-q21 controlling susceptibility to tuberculosis and leprosy in Brazilians. Genes Immun 5, 46-57.

Jena, M., Srivastava, A.K., Singh, R.K., Sharma, P.R., Das, P.K., Bamezai, R.N., 2014. NOS2A promoter (CCTTT)n association with TB lacks independent functional correlation amongst Indians. Tuberculosis (Edinb) 94, 81-86.

Jepson, A., Fowler, A., Banya, W., Singh, M., Bennett, S., Whittle, H., Hill, A.V., 2001. Genetic regulation of acquired immune responses to antigens of Mycobacterium tuberculosis: a study of twins in West Africa. Infect Immun 69, 3989-3994.

Jouanguy, E., Altare, F., Lamhamedi, S., Revy, P., Emile, J.F., Newport, M., Levin, M., Blanche, S., Seboun, E., Fischer, A., Casanova, J.L., 1996. Interferon-gamma-receptor deficiency in an infant with fatal bacille Calmette-Guerin infection. N Engl J Med 335, 1956-1961.

Juarez, E., Carranza, C., Hernandez-Sanchez, F., Leon-Contreras, J.C., Hernandez-Pando, R., Escobedo, D., Torres, M., Sada, E., 2012. NOD2 enhances the innate response of alveolar macrophages to Mycobacterium tuberculosis in humans. Eur J Immunol 42, 880-889.

Kamath, A.B., Alt, J., Debbabi, H., Behar, S.M., 2003. Toll-like receptor 4-defective C3H/HeJ mice are not more susceptible than other C3H substrains to infection with Mycobacterium tuberculosis. Infect Immun 71, 4112-4118.

Kanarek, N., Ben-Neriah, Y., 2012. Regulation of NF-kappaB by ubiquitination and degradation of the IkappaBs. Immunol Rev 246, 77-94.

Kang, D.D., Lin, Y., Moreno, J.R., Randall, T.D., Khader, S.A., 2011. Profiling early lung immune responses in the mouse model of tuberculosis. PLoS One 6, e16161.

Kang, P.B., Azad, A.K., Torrelles, J.B., Kaufman, T.M., Beharka, A., Tibesar, E., DesJardin, L.E., Schlesinger, L.S., 2005. The human macrophage mannose receptor directs Mycobacterium tuberculosis lipoarabinomannan-mediated phagosome biogenesis. J Exp Med 202, 987-999.

Karrer, U., Althage, A., Odermatt, B., Hengartner, H., Zinkernagel, R.M., 2000. Immunodeficiency of alymphoplasia mice (aly/aly) in vivo: structural defect of secondary lymphoid organs and functional B cell defect. Eur J Immunol 30, 2799-2807.

Kaufmann, S.H., 2001. How can immunology contribute to the control of tuberculosis? Nat Rev Immunol 1, 20-30.

Keane, J., Gershon, S., Wise, R.P., Mirabile-Levens, E., Kasznica, J., Schwieterman, W.D., Siegel, J.N., Braun, M.M., 2001. Tuberculosis associated with infliximab, a tumor necrosis factor alpha-neutralizing agent. N Engl J Med 345, 1098-1104.

Khader, S.A., Partida-Sanchez, S., Bell, G., Jelley-Gibbs, D.M., Swain, S., Pearl, J.E., Ghilardi, N., Desauvage, F.J., Lund, F.E., Cooper, A.M., 2006. Interleukin 12p40 is required for dendritic cell migration and T cell priming after Mycobacterium tuberculosis infection. J Exp Med 203, 1805-1815.

Khader, S.A., Pearl, J.E., Sakamoto, K., Gilmartin, L., Bell, G.K., Jelley-Gibbs, D.M., Ghilardi, N., deSauvage, F., Cooper, A.M., 2005. IL-23 compensates for the absence of IL-12p70 and is essential for the IL-17 response during tuberculosis but is dispensable for protection and antigen-specific IFN-gamma responses if IL-12p70 is available. J Immunol 175, 788-795.

Khor, C.C., Chapman, S.J., Vannberg, F.O., Dunne, A., Murphy, C., Ling, E.Y., Frodsham, A.J., Walley, A.J., Kyrieleis, O., Khan, A., Aucan, C., Segal, S., Moore, C.E., Knox, K., Campbell, S.J., Lienhardt, C., Scott, A., Aaby, P., Sow, O.Y., Grignani, R.T., Sillah, J., Sirugo, G., Peshu, N., Williams, T.N., Maitland, K., Davies, R.J., Kwiatkowski, D.P., Day, N.P., Yala, D., Crook, D.W., Marsh, K., Berkley, J.A., O'Neill, L.A., Hill, A.V., 2007. A Mal functional variant is associated with protection against invasive pneumococcal disease, bacteremia, malaria and tuberculosis. Nat Genet 39, 523-528.

Khoury, M., Adriaansen, J., Vervoordeldonk, M.J., Gould, D., Chernajovsky, Y., Bigey, P., Bloquel, C., Scherman, D., Tak, P.P., Jorgensen, C., Apparailly, F., 2007. Inflammation-inducible anti-TNF gene expression mediated by intra-articular injection of serotype 5 adeno-associated virus reduces arthritis. J Gene Med 9, 596-604.

Kim, D.W., Lenzen, G., Page, A.L., Legrain, P., Sansonetti, P.J., Parsot, C., 2005. The Shigella flexneri effector OspG interferes with innate immune responses by targeting ubiquitin-conjugating enzymes. Proc Natl Acad Sci U S A 102, 14046-14051.

Kleinnijenhuis, J., Joosten, L.A., van de Veerdonk, F.L., Savage, N., van Crevel, R., Kullberg, B.J., van der Ven, A., Ottenhoff, T.H., Dinarello, C.A., van der Meer, J.W., Netea, M.G., 2009. Transcriptional and inflammasome-mediated pathways for the induction of IL-1beta production by Mycobacterium tuberculosis. Eur J Immunol 39, 1914-1922.

Kleinnijenhuis, J., Oosting, M., Joosten, L.A., Netea, M.G., Van Crevel, R., 2011. Innate immune recognition of Mycobacterium tuberculosis. Clin Dev Immunol 2011, 405310.

Kobayashi, K., Inohara, N., Hernandez, L.D., Galan, J.E., Nunez, G., Janeway, C.A., Medzhitov, R., Flavell, R.A., 2002. RICK/Rip2/CARDIAK mediates signalling for receptors of the innate and adaptive immune systems. Nature 416, 194-199.

Koch, R., 1882. Die Aetiologie der Tuberculosis. Berliner Klinische Wocheschrift, 221-238.

Kozyrev, S.V., Lewen, S., Reddy, P.M., Pons-Estel, B., Witte, T., Junker, P., Laustrup, H., Gutierrez, C., Suarez, A., Francisca Gonzalez-Escribano, M., Martin, J., Alarcon-Riquelme, M.E., 2007. Structural insertion/deletion variation in IRF5 is associated with a risk haplotype and defines the precise IRF5 isoforms expressed in systemic lupus erythematosus. Arthritis Rheum 56, 1234-1241.

Ladel, C.H., Daugelat, S., Kaufmann, S.H., 1995. Immune response to Mycobacterium bovis bacille Calmette Guerin infection in major histocompatibility complex class I- and II-deficient knock-out mice: contribution of CD4 and CD8 T cells to acquired resistance. Eur J Immunol 25, 377-384.

Leber, J.H., Crimmins, G.T., Raghavan, S., Meyer-Morse, N.P., Cox, J.S., Portnoy, D.A., 2008. Distinct TLR- and NLR-mediated transcriptional responses to an intracellular pathogen. PLoS Pathog 4, e6.

Lecine, P., Esmiol, S., Metais, J.Y., Nicoletti, C., Nourry, C., McDonald, C., Nunez, G., Hugot, J.P., Borg, J.P., Ollendorff, V., 2007. The NOD2-RICK complex signals from the plasma membrane. J Biol Chem 282, 15197-15207.

Lee, T.H., Shank, J., Cusson, N., Kelliher, M.A., 2004. The kinase activity of Rip1 is not required for tumor necrosis factor-alpha-induced IkappaB kinase or p38 MAP kinase activation or for the ubiquitination of Rip1 by Traf2. J Biol Chem 279, 33185-33191.

Lee, W.B., Kang, J.S., Yan, J.J., Lee, M.S., Jeon, B.Y., Cho, S.N., Kim, Y.J., 2012. Neutrophils Promote Mycobacterial Trehalose Dimycolate-Induced Lung Inflammation via the Mincle Pathway. PLoS Pathog 8, e1002614.

Li, L., Qiao, D., Fu, X., Lao, S., Zhang, X., Wu, C., 2011a. Identification of M. tuberculosis-specific Th1 cells expressing CD69 generated in vivo in pleural fluid cells from patients with tuberculous pleurisy. PLoS One 6, e23700.

Li, X., Yang, Y., Zhou, F., Zhang, Y., Lu, H., Jin, Q., Gao, L., 2011b. SLC11A1 (NRAMP1) polymorphisms and tuberculosis susceptibility: updated systematic review and meta-analysis. PLoS One 6, e15831.

Liang, C., Zhang, M., Sun, S.C., 2006. beta-TrCP binding and processing of NF-kappaB2/p100 involve its phosphorylation at serines 866 and 870. Cell Signal 18, 1309-1317.

Lim, Y., Choi, J., Lee, J., Choi, C.H., Kim, H., Song, C., 2014. Mycobacterium tuberculosis 38-kDa antigen induces endoplasmic reticulum stress-mediated apoptosis via toll-like receptor 2/4. Apoptosis.

Ling, L., Cao, Z., Goeddel, D.V., 1998. NF-kappaB-inducing kinase activates IKK-alpha by phosphorylation of Ser-176. Proc Natl Acad Sci U S A 95, 3792-3797.

Liu, F., Xia, Y., Parker, A.S., Verma, I.M., 2012. IKK biology. Immunol Rev 246, 239-253.

Lockhart, E., Green, A.M., Flynn, J.L., 2006. IL-17 production is dominated by gammadelta T cells rather than CD4 T cells during Mycobacterium tuberculosis infection. J Immunol 177, 4662-4669.

Lu, C., Wang, A., Dorsch, M., Tian, J., Nagashima, K., Coyle, A.J., Jaffee, B., Ocain, T.D., Xu, Y., 2005. Participation of Rip2 in lipopolysaccharide signaling is independent of its kinase activity. J Biol Chem 280, 16278-16283.

Maess, M.B., Buers, I., Robenek, H., Lorkowski, S., 2011. Improved protocol for efficient nonviral transfection of premature THP-1 macrophages. Cold Spring Harb Protoc 2011, pdb prot5612.

Magalhaes, J.G., Lee, J., Geddes, K., Rubino, S., Philpott, D.J., Girardin, S.E., 2011. Essential role of Rip2 in the modulation of innate and adaptive immunity triggered by Nod1 and Nod2 ligands. Eur J Immunol 41, 1445-1455.

Maglione, P.J., Xu, J., Casadevall, A., Chan, J., 2008. Fc gamma receptors regulate immune activation and susceptibility during Mycobacterium tuberculosis infection. J Immunol 180, 3329-3338.

Maglione, P.J., Xu, J., Chan, J., 2007. B cells moderate inflammatory progression and enhance bacterial containment upon pulmonary challenge with Mycobacterium tuberculosis. J Immunol 178, 7222-7234.

Mahasirimongkol, S., Yanai, H., Mushiroda, T., Promphittayarat, W., Wattanapokayakit, S., Phromjai, J., Yuliwulandari, R., Wichukchinda, N., Yowang, A., Yamada, N., Kantipong, P., Takahashi, A., Kubo, M., Sawanpanyalert, P., Kamatani, N., Nakamura, Y., Tokunaga, K., 2012. Genome-wide association studies of tuberculosis in Asians identify distinct at-risk locus for young tuberculosis. J Hum Genet 57, 363-367.

Mahasirimongkol, S., Yanai, H., Nishida, N., Ridruechai, C., Matsushita, I., Ohashi, J., Summanapan, S., Yamada, N., Moolphate, S., Chuchotaworn, C., Chaiprasert, A., Manosuthi, W., Kantipong, P., Kanitwittaya, S., Sura, T., Khusmith, S., Tokunaga, K., Sawanpanyalert, P., Keicho, N., 2009. Genome-wide SNP-based linkage analysis of tuberculosis in Thais. Genes Immun 10, 77-83.

Malinin, N.L., Boldin, M.P., Kovalenko, A.V., Wallach, D., 1997. MAP3K-related kinase involved in NF-kappaB induction by TNF, CD95 and IL-1. Nature 385, 540-544.

Mansur, D.S., Maluquer de Motes, C., Unterholzner, L., Sumner, R.P., Ferguson, B.J., Ren, H., Strnadova, P., Bowie, A.G., Smith, G.L., 2013. Poxvirus targeting of E3 ligase beta-TrCP by molecular mimicry: a mechanism to inhibit NF-kappaB activation and promote immune evasion and virulence. PLoS Pathog 9, e1003183.

Manzanillo, P.S., Shiloh, M.U., Portnoy, D.A., Cox, J.S., 2012. Mycobacterium tuberculosis activates the DNA-dependent cytosolic surveillance pathway within macrophages. Cell Host Microbe 11, 469-480.

Marcinek, P., Jha, A.N., Shinde, V., Sundaramoorthy, A., Rajkumar, R., Suryadevara, N.C., Neela, S.K., van Tong, H., Balachander, V., Valluri, V.L., Thangaraj, K., Velavan, T.P., 2013. LRRK2 and RIPK2 variants in the NOD 2-mediated signaling pathway are associated with susceptibility to Mycobacterium leprae in Indian populations. PLoS One 8, e73103.

Mayer-Barber, K.D., Andrade, B.B., Barber, D.L., Hieny, S., Feng, C.G., Caspar, P., Oland, S., Gordon, S., Sher, A., 2011. Innate and adaptive interferons suppress IL-1alpha and IL-1beta production by distinct pulmonary myeloid subsets during Mycobacterium tuberculosis infection. Immunity 35, 1023-1034.

Mayer-Barber, K.D., Andrade, B.B., Oland, S.D., Amaral, E.P., Barber, D.L., Gonzales, J., Derrick, S.C., Shi, R., Kumar, N.P., Wei, W., Yuan, X., Zhang, G., Cai, Y., Babu, S., Catalfamo, M., Salazar, A.M., Via, L.E., Barry, C.E., 3rd, Sher, A., 2014. Host-directed therapy of tuberculosis based on interleukin-1 and type I interferon crosstalk. Nature 511, 99-103.

Mayer-Barber, K.D., Barber, D.L., Shenderov, K., White, S.D., Wilson, M.S., Cheever, A., Kugler, D., Hieny, S., Caspar, P., Nunez, G., Schlueter, D., Flavell, R.A., Sutterwala, F.S., Sher, A., 2010. Caspase-1 independent IL-1beta production is critical for host resistance to mycobacterium tuberculosis and does not require TLR signaling in vivo. J Immunol 184, 3326-3330.

McCarthy, J.V., Ni, J., Dixit, V.M., 1998. RIP2 is a novel NF-kappaB-activating and cell death-inducing kinase. J Biol Chem 273, 16968-16975.

McElvania Tekippe, E., Allen, I.C., Hulseberg, P.D., Sullivan, J.T., McCann, J.R., Sandor, M., Braunstein, M., Ting, J.P., 2010. Granuloma formation and host defense in chronic Mycobacterium tuberculosis infection requires PYCARD/ASC but not NLRP3 or caspase-1. PLoS One 5, e12320.

Melo, M.D., Catchpole, I.R., Haggar, G., Stokes, R.W., 2000. Utilization of CD11b knockout mice to characterize the role of complement receptor 3 (CR3, CD11b/CD18) in the growth of Mycobacterium tuberculosis in macrophages. Cell Immunol 205, 13-23.

Meyer, C.G., Thye, T., 2014. Host genetic studies in adult pulmonary tuberculosis. Semin Immunol 26, 445-453.

Miller, E.N., Jamieson, S.E., Joberty, C., Fakiola, M., Hudson, D., Peacock, C.S., Cordell, H.J., Shaw, M.A., Lins-Lainson, Z., Shaw, J.J., Ramos, F., Silveira, F., Blackwell, J.M., 2004. Genome-wide scans for leprosy and tuberculosis susceptibility genes in Brazilians. Genes Immun 5, 63-67.

Mishra, B.B., Moura-Alves, P., Sonawane, A., Hacohen, N., Griffiths, G., Moita, L.F., Anes, E., 2010. Mycobacterium tuberculosis protein ESAT-6 is a potent activator of the NLRP3/ASC inflammasome. Cell Microbiol 12, 1046-1063.

Miyake, Y., Toyonaga, K., Mori, D., Kakuta, S., Hoshino, Y., Oyamada, A., Yamada, H., Ono, K., Suyama, M., Iwakura, Y., Yoshikai, Y., Yamasaki, S., 2013. C-type lectin MCL is an FcRgamma-coupled receptor that mediates the adjuvanticity of mycobacterial cord factor. Immunity 38, 1050-1062.

Mogensen, T.H., 2009. Pathogen recognition and inflammatory signaling in innate immune defenses. Clin Microbiol Rev 22, 240-273, Table of Contents.

Moller, M., Hoal, E.G., 2010. Current findings, challenges and novel approaches in human genetic susceptibility to tuberculosis. Tuberculosis (Edinb) 90, 71-83.

Moller, M., Nebel, A., Valentonyte, R., van Helden, P.D., Schreiber, S., Hoal, E.G., 2009. Investigation of chromosome 17 candidate genes in susceptibility to TB in a South African population. Tuberculosis (Edinb) 89, 189-194.

Morris, K.R., Lutz, R.D., Choi, H.S., Kamitani, T., Chmura, K., Chan, E.D., 2003. Role of the NF-kappaB signaling pathway and kappaB cis-regulatory elements on the IRF-1 and iNOS promoter regions in mycobacterial lipoarabinomannan induction of nitric oxide. Infect Immun 71, 1442-1452.

Motulsky, A.G., 1960. Metabolic polymorphisms and the role of infectious diseases in human evolution. Hum Biol 32, 28-62.

Nagai, Y., Akashi, S., Nagafuku, M., Ogata, M., Iwakura, Y., Akira, S., Kitamura, T., Kosugi, A., Kimoto, M., Miyake, K., 2002. Essential role of MD-2 in LPS responsiveness and TLR4 distribution. Nat Immunol 3, 667-672.

Nahid, M.A., Satoh, M., Chan, E.K., 2011. Mechanistic role of microRNA-146a in endotoxin-induced differential cross-regulation of TLR signaling. J Immunol 186, 1723-1734.

Nakayama, K., Hatakeyama, S., Maruyama, S., Kikuchi, A., Onoe, K., Good, R.A., Nakayama, K.I., 2003. Impaired degradation of inhibitory subunit of NF-kappa B (I kappa B) and beta-catenin as a result of targeted disruption of the beta-TrCP1 gene. Proc Natl Acad Sci U S A 100, 8752-8757.

Nathan, C., Ding, A., 2010. Nonresolving inflammation. Cell 140, 871-882.

Navas, T.A., Baldwin, D.T., Stewart, T.A., 1999. RIP2 is a Raf1-activated mitogen-activated protein kinase kinase. J Biol Chem 274, 33684-33690.

Nembrini, C., Kisielow, J., Shamshiev, A.T., Tortola, L., Coyle, A.J., Kopf, M., Marsland, B.J., 2009. The kinase activity of Rip2 determines its stability and consequently Nod1- and Nod2-mediated immune responses. J Biol Chem 284, 19183-19188.

Netea, M.G., van Crevel, R., 2014. BCG-induced protection: effects on innate immune memory. Semin Immunol 26, 512-517.

Newport, M.J., 2009. Why hasn't human genetics told us more about tuberculosis? Int J Tuberc Lung Dis 13, 1049-1050.

Newport, M.J., 2015. The genetic regulation of infant immune responses to vaccination. Front Immunol 6, 18.

Newport, M.J., Goetghebuer, T., Weiss, H.A., Whittle, H., Siegrist, C.A., Marchant, A., 2004. Genetic regulation of immune responses to vaccines in early life. Genes Immun 5, 122-129.

Newport, M.J., Huxley, C.M., Huston, S., Hawrylowicz, C.M., Oostra, B.A., Williamson, R., Levin, M., 1996. A mutation in the interferon-gamma-receptor gene and susceptibility to mycobacterial infection. N Engl J Med 335, 1941-1949.

Ng, P.C., Henikoff, S., 2001. Predicting deleterious amino acid substitutions. Genome Res 11, 863-874.

Nigou, J., Zelle-Rieser, C., Gilleron, M., Thurnher, M., Puzo, G., 2001. Mannosylated lipoarabinomannans inhibit IL-12 production by human dendritic cells: evidence for a negative signal delivered through the mannose receptor. J Immunol 166, 7477-7485.

North, R.J., LaCourse, R., Ryan, L., Gros, P., 1999. Consequence of Nramp1 deletion to Mycobacterium tuberculosis infection in mice. Infect Immun 67, 5811-5814.

Noss, E.H., Pai, R.K., Sellati, T.J., Radolf, J.D., Belisle, J., Golenbock, D.T., Boom, W.H., Harding, C.V., 2001. Toll-like receptor 2-dependent inhibition of macrophage class II MHC expression and antigen processing by 19-kDa lipoprotein of Mycobacterium tuberculosis. J Immunol 167, 910-918.

Ogura, Y., Inohara, N., Benito, A., Chen, F.F., Yamaoka, S., Nunez, G., 2001. Nod2, a Nod1/Apaf-1 family member that is restricted to monocytes and activates NF-kappaB. J Biol Chem 276, 4812-4818.

Ohashi, K., Burkart, V., Flohe, S., Kolb, H., 2000. Cutting edge: heat shock protein 60 is a putative endogenous ligand of the toll-like receptor-4 complex. J Immunol 164, 558-561.

Okamoto Yoshida, Y., Umemura, M., Yahagi, A., O'Brien, R.L., Ikuta, K., Kishihara, K., Hara, H., Nakae, S., Iwakura, Y., Matsuzaki, G., 2010. Essential role of IL-17A in the formation of a mycobacterial infection-induced granuloma in the lung. J Immunol 184, 4414-4422.

Ong, C.T., Corces, V.G., 2014. CTCF: an architectural protein bridging genome topology and function. Nat Rev Genet 15, 234-246.

Orkin, S.H., Cheng, T.C., Antonarakis, S.E., Kazazian, H.H., Jr., 1985. Thalassemia due to a mutation in the cleavage-polyadenylation signal of the human beta-globin gene. EMBO J 4, 453-456.

Ottenhoff, T.H., 2012. New pathways of protective and pathological host defense to mycobacteria. Trends Microbiol 20, 419-428.

Pandey, A.K., Yang, Y., Jiang, Z., Fortune, S.M., Coulombe, F., Behr, M.A., Fitzgerald, K.A., Sassetti, C.M., Kelliher, M.A., 2009. NOD2, RIP2 and IRF5 play a critical role in the type I interferon response to Mycobacterium tuberculosis. PLoS Pathog 5, e1000500.

Park, E.K., Jung, H.S., Yang, H.I., Yoo, M.C., Kim, C., Kim, K.S., 2007a. Optimized THP-1 differentiation is required for the detection of responses to weak stimuli. Inflamm Res 56, 45-50.

Park, J.H., Kim, Y.G., McDonald, C., Kanneganti, T.D., Hasegawa, M., Body-Malapel, M., Inohara, N., Nunez, G., 2007b. RICK/RIP2 mediates innate immune responses induced through Nod1 and Nod2 but not TLRs. J Immunol 178, 2380-2386.

Parvatiyar, K., Zhang, Z., Teles, R.M., Ouyang, S., Jiang, Y., Iyer, S.S., Zaver, S.A., Schenk, M., Zeng, S., Zhong, W., Liu, Z.J., Modlin, R.L., Liu, Y.J., Cheng, G., 2012. The helicase DDX41 recognizes the bacterial secondary messengers cyclic di-GMP and cyclic di-AMP to activate a type I interferon immune response. Nat Immunol 13, 1155-1161.

Parveen, N., Varman, R., Nair, S., Das, G., Ghosh, S., Mukhopadhyay, S., 2013. Endocytosis of Mycobacterium tuberculosis heat shock protein 60 is required to induce interleukin-10 production in macrophages. J Biol Chem.

Pathak, S.K., Basu, S., Bhattacharyya, A., Pathak, S., Kundu, M., Basu, J., 2005. Mycobacterium tuberculosis lipoarabinomannan-mediated IRAK-M induction negatively regulates Toll-like receptor-dependent interleukin-12 p40 production in macrophages. J Biol Chem 280, 42794-42800.

Peng, M.Y., Wang, Z.H., Yao, C.Y., Jiang, L.N., Jin, Q.L., Wang, J., Li, B.Q., 2008. Interleukin 17-producing gamma delta T cells increased in patients with active pulmonary tuberculosis. Cell Mol Immunol 5, 203-208.

Petry, H., Cashion, L., Szymanski, P., Ast, O., Orme, A., Gross, C., Bauzon, M., Brooks, A., Schaefer, C., Gibson, H., Qian, H., Rubanyi, G.M., Harkins, R.N., 2006. Mx1 and IP-10: biomarkers to measure IFN-beta activity in mice following gene-based delivery. J Interferon Cytokine Res 26, 699-705.

Philpott, D.J., Sorbara, M.T., Robertson, S.J., Croitoru, K., Girardin, S.E., 2014. NOD proteins: regulators of inflammation in health and disease. Nat Rev Immunol 14, 9-23.

Png, E., Alisjahbana, B., Sahiratmadja, E., Marzuki, S., Nelwan, R., Balabanova, Y., Nikolayevskyy, V., Drobniewski, F., Nejentsev, S., Adnan, I., van de Vosse, E., Hibberd, M.L., van Crevel, R., Ottenhoff, T.H., Seielstad, M., 2012. A genome wide association study of pulmonary tuberculosis susceptibility in Indonesians. BMC Med Genet 13, 5.

Powolny-Budnicka, I., Riemann, M., Tanzer, S., Schmid, R.M., Hehlgans, T., Weih, F., 2011. RelA and RelB transcription factors in distinct thymocyte populations control lymphotoxin-dependent interleukin-17 production in gammadelta T cells. Immunity 34, 364-374.

Prados-Rosales, R., Baena, A., Martinez, L.R., Luque-Garcia, J., Kalscheuer, R., Veeraraghavan, U., Camara, C., Nosanchuk, J.D., Besra, G.S., Chen, B., Jimenez, J., Glatman-Freedman, A., Jacobs, W.R., Jr., Porcelli, S.A., Casadevall, A., 2011. Mycobacteria release active membrane vesicles that modulate immune responses in a TLR2-dependent manner in mice. J Clin Invest 121, 1471-1483.

Prezzemolo, T., Guggino, G., La Manna, M.P., Di Liberto, D., Dieli, F., Caccamo, N., 2014. Functional Signatures of Human CD4 and CD8 T Cell Responses to Mycobacterium tuberculosis. Front Immunol 5, 180.

Prigozy, T.I., Sieling, P.A., Clemens, D., Stewart, P.L., Behar, S.M., Porcelli, S.A., Brenner, M.B., Modlin, R.L., Kronenberg, M., 1997. The mannose receptor delivers lipoglycan antigens to endosomes for presentation to T cells by CD1b molecules. Immunity 6, 187-197.

Qu, Z., Qing, G., Rabson, A., Xiao, G., 2004. Tax deregulation of NF-kappaB2 p100 processing involves both beta-TrCP-dependent and -independent mechanisms. J Biol Chem 279, 44563-44572.

Rajavelu, P., Das, S.D., 2010. Kinetics of chemokine secretion in human macrophages infected with various strains of Mycobacterium tuberculosis. Indian J Med Microbiol 28, 201-206.

Rallabhandi, P., Phillips, R.L., Boukhvalova, M.S., Pletneva, L.M., Shirey, K.A., Gioannini, T.L., Weiss, J.P., Chow, J.C., Hawkins, L.D., Vogel, S.N., Blanco, J.C., 2012. Respiratory syncytial virus fusion protein-induced toll-like receptor 4 (TLR4) signaling is inhibited by the TLR4 antagonists Rhodobacter sphaeroides lipopolysaccharide and eritoran (E5564) and requires direct interaction with MD-2. MBio 3.

Reiley, W.W., Calayag, M.D., Wittmer, S.T., Huntington, J.L., Pearl, J.E., Fountain, J.J., Martino, C.A., Roberts, A.D., Cooper, A.M., Winslow, G.M., Woodland, D.L., 2008. ESAT-6-specific CD4 T cell responses to aerosol Mycobacterium tuberculosis infection are initiated in the mediastinal lymph nodes. Proc Natl Acad Sci U S A 105, 10961-10966.

Reiling, N., Holscher, C., Fehrenbach, A., Kroger, S., Kirschning, C.J., Goyert, S., Ehlers, S., 2002. Cutting edge: Toll-like receptor (TLR)2- and TLR4-mediated pathogen recognition in resistance to airborne infection with Mycobacterium tuberculosis. J Immunol 169, 3480-3484.

Reynolds, H.Y., 1987. Bronchoalveolar lavage. Am Rev Respir Dis 135, 250-263.

Rieder, H.L., 2003. [Clarification of the Luebeck infant tuberculosis]. Pneumologie 57, 402-405.

Riordan, J.R., Rommens, J.M., Kerem, B., Alon, N., Rozmahel, R., Grzelczak, Z., Zielenski, J., Lok, S., Plavsic, N., Chou, J.L., et al., 1989. Identification of the cystic fibrosis gene: cloning and characterization of complementary DNA. Science 245, 1066-1073.

Rodrigues, L.C., Diwan, V.K., Wheeler, J.G., 1993. Protective effect of BCG against tuberculous meningitis and miliary tuberculosis: a meta-analysis. Int J Epidemiol 22, 1154-1158.

Rolph, M.S., Raupach, B., Kobernick, H.H., Collins, H.L., Perarnau, B., Lemonnier, F.A., Kaufmann, S.H., 2001. MHC class Ia-restricted T cells partially account for beta2-microglobulin-dependent resistance to Mycobacterium tuberculosis. Eur J Immunol 31, 1944-1949.

Rook, G.A., 2007. Th2 cytokines in susceptibility to tuberculosis. Curr Mol Med 7, 327-337.

Rovin, B.H., Lu, L., Saxena, R., 1999. A novel polymorphism in the MCP-1 gene regulatory region that influences MCP-1 expression. Biochem Biophys Res Commun 259, 344-348.

Roy, A., Eisenhut, M., Harris, R.J., Rodrigues, L.C., Sridhar, S., Habermann, S., Snell, L., Mangtani, P., Adetifa, I., Lalvani, A., Abubakar, I., 2014. Effect of BCG vaccination against Mycobacterium tuberculosis infection in children: systematic review and meta-analysis. BMJ 349, g4643.

Ruefli-Brasse, A.A., Lee, W.P., Hurst, S., Dixit, V.M., 2004. Rip2 participates in Bcl10 signaling and T-cell receptor-mediated NF-kappaB activation. J Biol Chem 279, 1570-1574.

Sales-Marques, C., Salomao, H., Fava, V.M., Alvarado-Arnez, L.E., Amaral, E.P., Cardoso, C.C., Dias-Batista, I.M., da Silva, W.L., Medeiros, P., da Cunha Lopes Virmond, M., Lana, F.C., Pacheco, A.G., Moraes, M.O., Mira, M.T., Pereira Latini, A.C., 2014. NOD2 and CCDC122-LACC1 genes are associated with leprosy susceptibility in Brazilians. Hum Genet 133, 1525-1532.

Samstein, M., Schreiber, H.A., Leiner, I.M., Susac, B., Glickman, M.S., Pamer, E.G., 2013. Essential yet limited role for CCR2(+) inflammatory monocytes during Mycobacterium tuberculosis-specific T cell priming. Elife 2, e01086.

Sanjurjo, L., Amezaga, N., Vilaplana, C., Caceres, N., Marzo, E., Valeri, M., Cardona, P.J., Sarrias, M.R., 2013. The scavenger protein apoptosis inhibitor of macrophages (AIM) potentiates the antimicrobial response against Mycobacterium tuberculosis by enhancing autophagy. PLoS One 8, e79670.

Saunders, B.M., Frank, A.A., Orme, I.M., Cooper, A.M., 2002. CD4 is required for the development of a protective granulomatous response to pulmonary tuberculosis. Cell Immunol 216, 65-72.

Schaible, U.E., Winau, F., Sieling, P.A., Fischer, K., Collins, H.L., Hagens, K., Modlin, R.L., Brinkmann, V., Kaufmann, S.H., 2003. Apoptosis facilitates antigen presentation to T lymphocytes through MHC-I and CD1 in tuberculosis. Nat Med 9, 1039-1046.

Scheidereit, C., 2006. IkappaB kinase complexes: gateways to NF-kappaB activation and transcription. Oncogene 25, 6685-6705.

Schlesinger, L.S., Bellinger-Kawahara, C.G., Payne, N.R., Horwitz, M.A., 1990. Phagocytosis of Mycobacterium tuberculosis is mediated by human monocyte complement receptors and complement component C3. J Immunol 144, 2771-2780.

Schmid, R.M., Perkins, N.D., Duckett, C.S., Andrews, P.C., Nabel, G.J., 1991. Cloning of an NF-kappa B subunit which stimulates HIV transcription in synergy with p65. Nature 352, 733-736.

Schneider, C.A., Rasband, W.S., Eliceiri, K.W., 2012. NIH Image to ImageJ: 25 years of image analysis. Nat Methods 9, 671-675.

Schnoor, M., Buers, I., Sietmann, A., Brodde, M.F., Hofnagel, O., Robenek, H., Lorkowski, S., 2009. Efficient non-viral transfection of THP-1 cells. J Immunol Methods 344, 109-115.

Schoenen, H., Huber, A., Sonda, N., Zimmermann, S., Jantsch, J., Lepenies, B., Bronte, V., Lang, R., 2014. Differential control of Mincle-dependent cord factor recognition and macrophage responses by the transcription factors C/EBPbeta and HIF1alpha. J Immunol 193, 3664-3675.

Senftleben, U., Cao, Y., Xiao, G., Greten, F.R., Krahn, G., Bonizzi, G., Chen, Y., Hu, Y., Fong, A., Sun, S.C., Karin, M., 2001. Activation by IKKalpha of a second, evolutionary conserved, NF-kappa B signaling pathway. Science 293, 1495-1499.

Sepulveda, R.L., Heiba, I.M., King, A., Gonzalez, B., Elston, R.C., Sorensen, R.U., 1994. Evaluation of tuberculin reactivity in BCG-immunized siblings. Am J Respir Crit Care Med 149, 620-624.

Serbina, N.V., Jia, T., Hohl, T.M., Pamer, E.G., 2008. Monocyte-mediated defense against microbial pathogens. Annu Rev Immunol 26, 421-452.

Sharma, M.K., Al-Azem, A., Wolfe, J., Hershfield, E., Kabani, A., 2003. Identification of a predominant isolate of Mycobacterium tuberculosis using molecular and clinical epidemiology tools and in vitro cytokine responses. BMC Infect Dis 3, 3.

Sharma, S.K., Mohan, A., Sharma, A., 2012. Challenges in the diagnosis & treatment of miliary tuberculosis. Indian J Med Res 135, 703-730.

Shen, Y., Zhou, D., Qiu, L., Lai, X., Simon, M., Shen, L., Kou, Z., Wang, Q., Jiang, L., Estep, J., Hunt, R., Clagett, M., Sehgal, P.K., Li, Y., Zeng, X., Morita, C.T., Brenner, M.B., Letvin, N.L., Chen, Z.W., 2002. Adaptive immune response of Vgamma2Vdelta2+ T cells during mycobacterial infections. Science 295, 2255-2258.

Shimada, K., Chen, S., Dempsey, P.W., Sorrentino, R., Alsabeh, R., Slepenkin, A.V., Peterson, E., Doherty, T.M., Underhill, D., Crother, T.R., Arditi, M., 2009. The NOD/RIP2 pathway is essential for host defenses against Chlamydophila pneumoniae lung infection. PLoS Pathog 5, e1000379.

Shimazu, R., Akashi, S., Ogata, H., Nagai, Y., Fukudome, K., Miyake, K., Kimoto, M., 1999. MD-2, a molecule that confers lipopolysaccharide responsiveness on Toll-like receptor 4. J Exp Med 189, 1777-1782.

Silverman, N., Maniatis, T., 2001. NF-kappaB signaling pathways in mammalian and insect innate immunity. Genes Dev 15, 2321-2342.

Simeone, R., Bobard, A., Lippmann, J., Bitter, W., Majlessi, L., Brosch, R., Enninga, J., 2012. Phagosomal rupture by Mycobacterium tuberculosis results in toxicity and host cell death. PLoS Pathog 8, e1002507.

Simeone, R., Bottai, D., Brosch, R., 2009. ESX/type VII secretion systems and their role in host-pathogen interaction. Curr Opin Microbiol 12, 4-10.

Simmons, D.P., Canaday, D.H., Liu, Y., Li, Q., Huang, A., Boom, W.H., Harding, C.V., 2010. Mycobacterium tuberculosis and TLR2 agonists inhibit induction of type I IFN and class I MHC antigen cross processing by TLR9. J Immunol 185, 2405-2415.

Stanley, S.A., Johndrow, J.E., Manzanillo, P., Cox, J.S., 2007. The Type I IFN response to infection with Mycobacterium tuberculosis requires ESX-1-mediated secretion and contributes to pathogenesis. J Immunol 178, 3143-3152.

Stead, W.W., Senner, J.W., Reddick, W.T., Lofgren, J.P., 1990. Racial differences in susceptibility to infection by Mycobacterium tuberculosis. N Engl J Med 322, 422-427.

Steentoft, C., Vakhrushev, S.Y., Joshi, H.J., Kong, Y., Vester-Christensen, M.B., Schjoldager, K.T., Lavrsen, K., Dabelsteen, S., Pedersen, N.B., Marcos-Silva, L., Gupta, R., Bennett, E.P., Mandel, U., Brunak, S., Wandall, H.H., Levery, S.B., Clausen, H., 2013. Precision mapping of the human O-GalNAc glycoproteome through SimpleCell technology. EMBO J 32, 1478-1488.

Stein, C.M., Guwatudde, D., Nakakeeto, M., Peters, P., Elston, R.C., Tiwari, H.K., Mugerwa, R., Whalen, C.C., 2003. Heritability analysis of cytokines as intermediate phenotypes of tuberculosis. J Infect Dis 187, 1679-1685.

Stein, C.M., Zalwango, S., Chiunda, A.B., Millard, C., Leontiev, D.V., Horvath, A.L., Cartier, K.C., Chervenak, K., Boom, W.H., Elston, R.C., Mugerwa, R.D., Whalen, C.C., Iyengar, S.K., 2007. Linkage and association analysis of candidate genes for TB and TNFalpha cytokine expression: evidence for association with IFNGR1, IL-10, and TNF receptor 1 genes. Hum Genet 121, 663-673.

Stein, C.M., Zalwango, S., Malone, L.L., Won, S., Mayanja-Kizza, H., Mugerwa, R.D., Leontiev, D.V., Thompson, C.L., Cartier, K.C., Elston, R.C., Iyengar, S.K., Boom, W.H., Whalen, C.C., 2008. Genome scan of M. tuberculosis infection and disease in Ugandans. PLoS One 3, e4094.

Stenger, S., Hanson, D.A., Teitelbaum, R., Dewan, P., Niazi, K.R., Froelich, C.J., Ganz, T., Thoma-Uszynski, S., Melian, A., Bogdan, C., Porcelli, S.A., Bloom, B.R., Krensky, A.M., Modlin, R.L., 1998. An antimicrobial activity of cytolytic T cells mediated by granulysin. Science 282, 121-125.

Stokes, R.W., Doxsee, D., 1999. The receptor-mediated uptake, survival, replication, and drug sensitivity of Mycobacterium tuberculosis within the macrophage-like cell line THP-1: a comparison with human monocyte-derived macrophages. Cell Immunol 197, 1-9.

Sturgill-Koszycki, S., Schlesinger, P.H., Chakraborty, P., Haddix, P.L., Collins, H.L., Fok, A.K., Allen, R.D., Gluck, S.L., Heuser, J., Russell, D.G., 1994. Lack of acidification in Mycobacterium phagosomes produced by exclusion of the vesicular proton-ATPase. Science 263, 678-681.

Sulis, G., Roggi, A., Matteelli, A., Raviglione, M.C., 2014. Tuberculosis: epidemiology and control. Mediterr J Hematol Infect Dis 6, e2014070.

Sun, S.C., 2012. The noncanonical NF-kappaB pathway. Immunol Rev 246, 125-140.

Takeda, K., Takeuchi, O., Tsujimura, T., Itami, S., Adachi, O., Kawai, T., Sanjo, H., Yoshikawa, K., Terada, N., Akira, S., 1999. Limb and skin abnormalities in mice lacking IKKalpha. Science 284, 313-316.

Tanveer, M., Hasan, Z., Kanji, A., Hussain, R., Hasan, R., 2009. Reduced TNF-alpha and IFN-gamma responses to Central Asian strain 1 and Beijing isolates of Mycobacterium tuberculosis in comparison with H37Rv strain. Trans R Soc Trop Med Hyg 103, 581-587.

Tao, L., Zalwango, S., Chervenak, K., Thiel, B., Malone, L.L., Qiu, F., Mayanja-Kizza, H., Boom, W.H., Stein, C.M., 2013. Genetic and shared environmental influences on interferon-gamma production in response to Mycobacterium tuberculosis antigens in a Ugandan population. Am J Trop Med Hyg 89, 169-173.

Tao, M., Scacheri, P.C., Marinis, J.M., Harhaj, E.W., Matesic, L.E., Abbott, D.W., 2009. ITCH K63-ubiquitinates the NOD2 binding protein, RIP2, to influence inflammatory signaling pathways. Curr Biol 19, 1255-1263.

Thiebaut, R., Douchin, V., Jung, C., Merlin, F., Colombel, J.F., Lemann, M., Almer, S., Tysk, C., O'Morain, C., Gassull, M., Finkel, Y., Zouali, H., Pascoe, L., Hugot, J.P., 2011. RIP2 polymorphisms in inflammatory bowel diseases. Inflamm Bowel Dis 17, 1055.

Thome, M., Hofmann, K., Burns, K., Martinon, F., Bodmer, J.L., Mattmann, C., Tschopp, J., 1998. Identification of CARDIAK, a RIP-like kinase that associates with caspase-1. Curr Biol 8, 885-888.

Thuong, N.T., Hawn, T.R., Thwaites, G.E., Chau, T.T., Lan, N.T., Quy, H.T., Hieu, N.T., Aderem, A., Hien, T.T., Farrar, J.J., Dunstan, S.J., 2007. A polymorphism in human TLR2 is associated with increased susceptibility to tuberculous meningitis. Genes Immun 8, 422-428.

Thwaites, G.E., van Toorn, R., Schoeman, J., 2013. Tuberculous meningitis: more questions, still too few answers. Lancet Neurol 12, 999-1010.

Thye, T., Nejentsev, S., Intemann, C.D., Browne, E.N., Chinbuah, M.A., Gyapong, J., Osei, I., Owusu-Dabo, E., Zeitels, L.R., Herb, F., Horstmann, R.D., Meyer, C.G., 2009. MCP-1 promoter variant -362C associated with protection from pulmonary tuberculosis in Ghana, West Africa. Hum Mol Genet 18, 381-388.

Thye, T., Owusu-Dabo, E., Vannberg, F.O., van Crevel, R., Curtis, J., Sahiratmadja, E., Balabanova, Y., Ehmen, C., Muntau, B., Ruge, G., Sievertsen, J., Gyapong, J., Nikolayevskyy, V., Hill, P.C., Sirugo, G., Drobniewski, F., van de Vosse, E., Newport, M., Alisjahbana, B., Nejentsev, S., Ottenhoff, T.H., Hill, A.V., Horstmann, R.D., Meyer, C.G., 2012. Common variants at 11p13 are associated with susceptibility to tuberculosis. Nat Genet 44, 257-259.

Thye, T., Vannberg, F.O., Wong, S.H., Owusu-Dabo, E., Osei, I., Gyapong, J., Sirugo, G., Sisay-Joof, F., Enimil, A., Chinbuah, M.A., Floyd, S., Warndorff, D.K., Sichali, L., Malema, S., Crampin, A.C., Ngwira, B., Teo, Y.Y., Small, K., Rockett, K., Kwiatkowski, D., Fine, P.E., Hill, P.C., Newport, M., Lienhardt, C., Adegbola, R.A., Corrah, T., Ziegler, A., Morris, A.P., Meyer, C.G., Horstmann, R.D., Hill, A.V., 2010. Genome-wide association analyses identifies a susceptibility locus for tuberculosis on chromosome 18q11.2. Nat Genet 42, 739-741.

Tigno-Aranjuez, J.T., Asara, J.M., Abbott, D.W., 2010. Inhibition of RIP2's tyrosine kinase activity limits NOD2-driven cytokine responses. Genes Dev 24, 2666-2677.

Tishkoff, S.A., Williams, S.M., 2002. Genetic analysis of African populations: human evolution and complex disease. Nat Rev Genet 3, 611-621.

Torrelles, J.B., Azad, A.K., Schlesinger, L.S., 2006. Fine discrimination in the recognition of individual species of phosphatidyl-myo-inositol mannosides from Mycobacterium tuberculosis by C-type lectin pattern recognition receptors. J Immunol 177, 1805-1816.

Torrelles, J.B., Schlesinger, L.S., 2010. Diversity in Mycobacterium tuberculosis mannosylated cell wall determinants impacts adaptation to the host. Tuberculosis (Edinb) 90, 84-93.

Travassos, L.H., Carneiro, L.A., Ramjeet, M., Hussey, S., Kim, Y.G., Magalhaes, J.G., Yuan, L., Soares, F., Chea, E., Le Bourhis, L., Boneca, I.G., Allaoui, A., Jones, N.L., Nunez, G., Girardin, S.E., Philpott, D.J., 2010. Nod1 and Nod2 direct autophagy by recruiting ATG16L1 to the plasma membrane at the site of bacterial entry. Nat Immunol 11, 55-62.

Tso, H.W., Ip, W.K., Chong, W.P., Tam, C.M., Chiang, A.K., Lau, Y.L., 2005. Association of interferon gamma and interleukin 10 genes with tuberculosis in Hong Kong Chinese. Genes Immun 6, 358-363.

Tsuchiya, S., Kobayashi, Y., Goto, Y., Okumura, H., Nakae, S., Konno, T., Tada, K., 1982. Induction of maturation in cultured human monocytic leukemia cells by a phorbol diester. Cancer Res 42, 1530-1536.

Tsuchiya, S., Yamabe, M., Yamaguchi, Y., Kobayashi, Y., Konno, T., Tada, K., 1980. Establishment and characterization of a human acute monocytic leukemia cell line (THP-1). Int J Cancer 26, 171-176.

Turner, R.D., Bothamley, G.H., 2014. Cough and the Transmission of Tuberculosis. J Infect Dis.

Uehara, A., Yang, S., Fujimoto, Y., Fukase, K., Kusumoto, S., Shibata, K., Sugawara, S., Takada, H., 2005. Muramyldipeptide and diaminopimelic acid-containing desmuramylpeptides in combination with chemically synthesized Toll-like receptor agonists synergistically induced production of interleukin-8 in a NOD2- and NOD1-dependent manner, respectively, in human monocytic cells in culture. Cell Microbiol 7, 53-61.

Umemura, M., Yahagi, A., Hamada, S., Begum, M.D., Watanabe, H., Kawakami, K., Suda, T., Sudo, K., Nakae, S., Iwakura, Y., Matsuzaki, G., 2007. IL-17-mediated regulation of innate and acquired immune response against pulmonary Mycobacterium bovis bacille Calmette-Guerin infection. J Immunol 178, 3786-3796.

Underhill, D.M., Ozinsky, A., Smith, K.D., Aderem, A., 1999. Toll-like receptor-2 mediates mycobacteria-induced proinflammatory signaling in macrophages. Proc Natl Acad Sci U S A 96, 14459-14463.

Unterholzner, L., Keating, S.E., Baran, M., Horan, K.A., Jensen, S.B., Sharma, S., Sirois, C.M., Jin, T., Latz, E., Xiao, T.S., Fitzgerald, K.A., Paludan, S.R., Bowie, A.G., 2010. IFI16 is an innate immune sensor for intracellular DNA. Nat Immunol 11, 997-1004.

van Buuren, N., Burles, K., Schriewer, J., Mehta, N., Parker, S., Buller, R.M., Barry, M., 2014. EVM005: an ectromelia-encoded protein with dual roles in NF-kappaB inhibition and virulence. PLoS Pathog 10, e1004326.

van de Veerdonk, F.L., Teirlinck, A.C., Kleinnijenhuis, J., Kullberg, B.J., van Crevel, R., van der Meer, J.W., Joosten, L.A., Netea, M.G., 2010. Mycobacterium tuberculosis induces IL-17A responses through TLR4 and dectin-1 and is critically dependent on endogenous IL-1. J Leukoc Biol 88, 227-232.

van der Wel, N., Hava, D., Houben, D., Fluitsma, D., van Zon, M., Pierson, J., Brenner, M., Peters, P.J., 2007. M. tuberculosis and M. leprae translocate from the phagolysosome to the cytosol in myeloid cells. Cell 129, 1287-1298.

Velez, D.R., Hulme, W.F., Myers, J.L., Weinberg, J.B., Levesque, M.C., Stryjewski, M.E., Abbate, E., Estevan, R., Patillo, S.G., Gilbert, J.R., Hamilton, C.D., Scott, W.K., 2009. NOS2A, TLR4, and IFNGR1 interactions influence pulmonary tuberculosis susceptibility in African-Americans. Hum Genet 126, 643-653.

Vergne, I., Chua, J., Deretic, V., 2003. Tuberculosis toxin blocking phagosome maturation inhibits a novel Ca2+/calmodulin-PI3K hVPS34 cascade. J Exp Med 198, 653-659.

Vergne, I., Fratti, R.A., Hill, P.J., Chua, J., Belisle, J., Deretic, V., 2004. Mycobacterium tuberculosis phagosome maturation arrest: mycobacterial phosphatidylinositol analog phosphatidylinositol mannoside stimulates early endosomal fusion. Mol Biol Cell 15, 751-760.

Vervoort, R., Buist, N.R., Kleijer, W.J., Wevers, R., Fryns, J.P., Liebaers, I., Lissens, W., 1997. Molecular analysis of the beta-glucuronidase gene: novel mutations in mucopolysaccharidosis type VII and heterogeneity of the polyadenylation region. Hum Genet 99, 462-468.

Vidal, S.M., Malo, D., Vogan, K., Skamene, E., Gros, P., 1993. Natural resistance to infection with intracellular parasites: isolation of a candidate for Bcg. Cell 73, 469-485.

Vukmanovic-Stejic, M., Reed, J.R., Lacy, K.E., Rustin, M.H., Akbar, A.N., 2006. Mantoux Test as a model for a secondary immune response in humans. Immunol Lett 107, 93-101.

Wang, W., Alpert, E., 1995. Downregulation of phorbol 12-myristate 13-acetate-induced tumor necrosis factor-alpha and interleukin-1 beta production and gene expression in human monocytic cells by human alpha-fetoprotein. Hepatology 22, 921-928.

Watson, R.O., Manzanillo, P.S., Cox, J.S., 2012. Extracellular M. tuberculosis DNA targets bacteria for autophagy by activating the host DNA-sensing pathway. Cell 150, 803-815.

Werninghaus, K., Babiak, A., Gross, O., Holscher, C., Dietrich, H., Agger, E.M., Mages, J., Mocsai, A., Schoenen, H., Finger, K., Nimmerjahn, F., Brown, G.D., Kirschning, C., Heit, A., Andersen, P., Wagner, H., Ruland, J., Lang, R., 2009. Adjuvanticity of a synthetic cord factor analogue for subunit Mycobacterium tuberculosis vaccination requires FcRgamma-Syk-Card9-dependent innate immune activation. J Exp Med 206, 89-97.

Wheeler, E., Miller, E.N., Peacock, C.S., Donaldson, I.J., Shaw, M.A., Jamieson, S.E., Blackwell, J.M., Cordell, H.J., 2006. Genome-wide scan for loci influencing quantitative immune response traits in the Belem family study: comparison of methods and summary of results. Ann Hum Genet 70, 78-97.

WHO, 2010. Treatment of tuberculosis guidelines 4th edition.

WHO, 2011. Leprosy prevalence rates, data reported to WHO as of January 2011. WHO publications.

WHO, 2014. Global Tuberculosis Report 2014. WHO publications.

Winau, F., Weber, S., Sad, S., de Diego, J., Hoops, S.L., Breiden, B., Sandhoff, K., Brinkmann, V., Kaufmann, S.H., Schaible, U.E., 2006. Apoptotic vesicles crossprime CD8 T cells and protect against tuberculosis. Immunity 24, 105-117.

Windheim, M., Lang, C., Peggie, M., Plater, L.A., Cohen, P., 2007. Molecular mechanisms involved in the regulation of cytokine production by muramyl dipeptide. Biochem J 404, 179-190.

Winston, J.T., Strack, P., Beer-Romero, P., Chu, C.Y., Elledge, S.J., Harper, J.W., 1999. The SCFbeta-TRCP-ubiquitin ligase complex associates specifically with phosphorylated destruction motifs in IkappaBalpha and beta-catenin and stimulates IkappaBalpha ubiquitination in vitro. Genes Dev 13, 270-283.

Wolf, A.J., Linas, B., Trevejo-Nunez, G.J., Kincaid, E., Tamura, T., Takatsu, K., Ernst, J.D., 2007. Mycobacterium tuberculosis infects dendritic cells with high frequency and impairs their function in vivo. J Immunol 179, 2509-2519.

Wong, K.W., Jacobs, W.R., Jr., 2011. Critical role for NLRP3 in necrotic death triggered by Mycobacterium tuberculosis. Cell Microbiol 13, 1371-1384.

Wright, S.D., Silverstein, S.C., 1983. Receptors for C3b and C3bi promote phagocytosis but not the release of toxic oxygen from human phagocytes. J Exp Med 158, 2016-2023.

Xue, Y., Zhao, Z.Q., Hong, D., Zhao, M.Y., Zhang, Y.X., Wang, H.J., Wang, Y., Li, J.C., 2010. Lack of association between MD-2 promoter gene variants and tuberculosis. Genet Mol Res 9, 1584-1590.

Yang, H., Young, D.W., Gusovsky, F., Chow, J.C., 2000. Cellular events mediated by lipopolysaccharide-stimulated toll-like receptor 4. MD-2 is required for activation of mitogen-activated protein kinases and Elk-1. J Biol Chem 275, 20861-20866.

Yang, Q., Doublie, S., 2011. Structural biology of poly(A) site definition. Wiley Interdiscip Rev RNA 2, 732-747.

Yang, S., Tamai, R., Akashi, S., Takeuchi, O., Akira, S., Sugawara, S., Takada, H., 2001. Synergistic effect of muramyldipeptide with lipopolysaccharide or lipoteichoic acid to induce inflammatory cytokines in human monocytic cells in culture. Infect Immun 69, 2045-2053.

Yang, S., Wang, B., Humphries, F., Jackson, R., Healy, M.E., Bergin, R., Aviello, G., Hall, B., McNamara, D., Darby, T., Quinlan, A., Shanahan, F., Melgar, S., Fallon, P.G., Moynagh, P.N., 2013. Pellino3 ubiquitinates RIP2 and mediates Nod2-induced signaling and protective effects in colitis. Nat Immunol 14, 927-936.

Yang, Y., Yin, C., Pandey, A., Abbott, D., Sassetti, C., Kelliher, M.A., 2007. NOD2 pathway activation by MDP or Mycobacterium tuberculosis infection involves the stable polyubiquitination of Rip2. J Biol Chem 282, 36223-36229.

Yaron, A., Hatzubai, A., Davis, M., Lavon, I., Amit, S., Manning, A.M., Andersen, J.S., Mann, M., Mercurio, F., Ben-Neriah, Y., 1998. Identification of the receptor component of the IkappaBalpha-ubiquitin ligase. Nature 396, 590-594.

Zhang, F., Liu, H., Chen, S., Low, H., Sun, L., Cui, Y., Chu, T., Li, Y., Fu, X., Yu, Y., Yu, G., Shi, B., Tian, H., Liu, D., Yu, X., Li, J., Lu, N., Bao, F., Yuan, C., Liu, J., Zhang, L., Sun, Y., Chen, M., Yang, Q., Yang, H., Yang, R., Wang, Q., Zuo, F., Zhang, H., Khor, C.C., Hibberd, M.L., Yang, S., Zhang, X., 2011. Identification of two new loci at IL23R and RAB32 that influence susceptibility to leprosy. Nat Genet 43, 1247-1251.

Zhang, F.R., Huang, W., Chen, S.M., Sun, L.D., Liu, H., Li, Y., Cui, Y., Yan, X.X., Yang, H.T., Yang, R.D., Chu, T.S., Zhang, C., Zhang, L., Han, J.W., Yu, G.Q., Quan, C., Yu, Y.X., Zhang, Z., Shi, B.Q., Zhang, L.H., Cheng, H., Wang, C.Y., Lin, Y., Zheng, H.F., Fu, X.A., Zuo, X.B., Wang, Q., Long, H., Sun, Y.P., Cheng, Y.L., Tian, H.Q., Zhou, F.S., Liu, H.X., Lu, W.S., He, S.M., Du, W.L., Shen, M., Jin, Q.Y., Wang, Y., Low, H.Q., Erwin, T., Yang, N.H., Li, J.Y., Zhao, X., Jiao, Y.L., Mao, L.G., Yin, G., Jiang, Z.X., Wang, X.D., Yu, J.P., Hu, Z.H., Gong, C.H., Liu, Y.Q., Liu, R.Y., Wang, D.M., Wei, D., Liu, J.X., Cao, W.K., Cao, H.Z., Li, Y.P., Yan, W.G., Wei, S.Y., Wang, K.J., Hibberd, M.L., Yang, S., Zhang, X.J., Liu, J.J., 2009. Genomewide association study of leprosy. N Engl J Med 361, 2609-2618.

Zhang, X., Bogunovic, D., Payelle-Brogard, B., Francois-Newton, V., Speer, S.D., Yuan, C., Volpi, S., Li, Z., Sanal, O., Mansouri, D., Tezcan, I., Rice, G.I., Chen, C., Mansouri, N., Mahdaviani, S.A., Itan, Y., Boisson, B., Okada, S., Zeng, L., Wang, X., Jiang, H., Liu, W., Han, T., Liu, D., Ma, T., Wang, B., Liu, M., Liu, J.Y., Wang, Q.K., Yalnizoglu, D., Radoshevich, L., Uze, G., Gros, P., Rozenberg, F., Zhang, S.Y., Jouanguy, E., Bustamante, J., Garcia-Sastre, A., Abel, L., Lebon, P., Notarangelo, L.D., Crow, Y.J., Boisson-Dupuis, S., Casanova, J.L., Pellegrini, S., 2015. Human intracellular ISG15 prevents interferon-alpha/beta over-amplification and auto-inflammation. Nature 517, 89-93.

9. Appendix

9.1. Plasmid maps

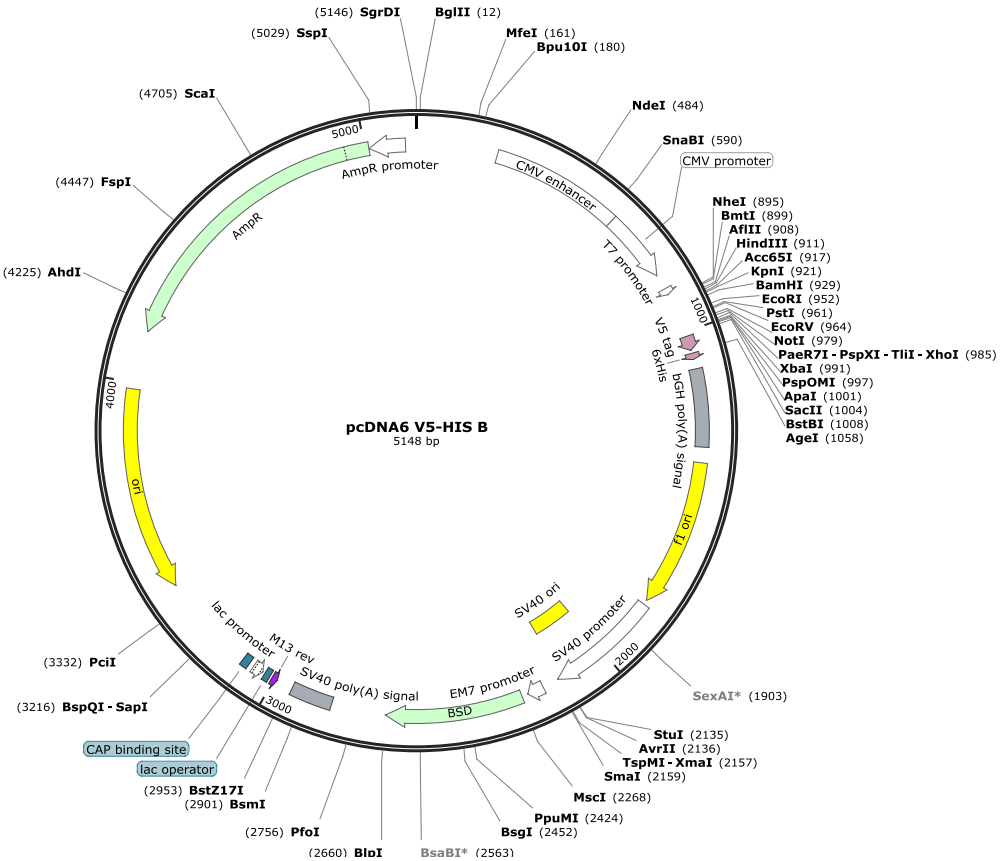

Figure 9.1 Schematic representation of pcDNA™6/V5-HIS B

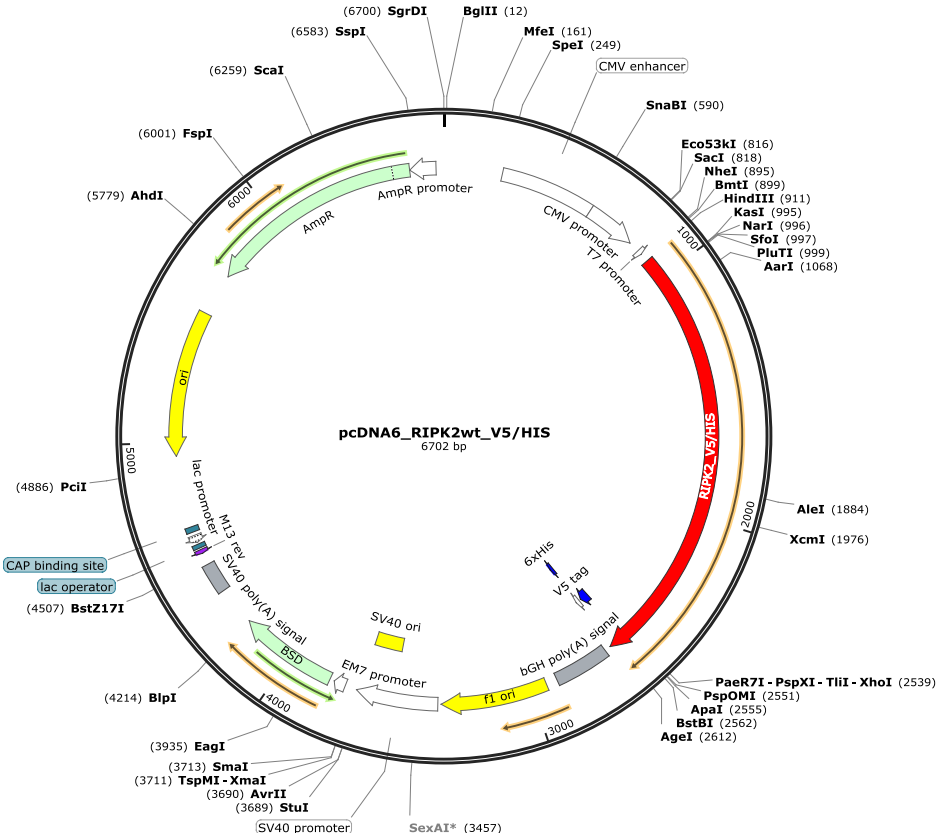

Figure 9.2 Schematic representation of pcDNA6_*RIPK2*wt_V5/HIS

Open reading frame encoding *RIPK2* and V5 epitope and HIS-tag is indicated in red. V5 epitope tag and HIS tag are shown in blue.

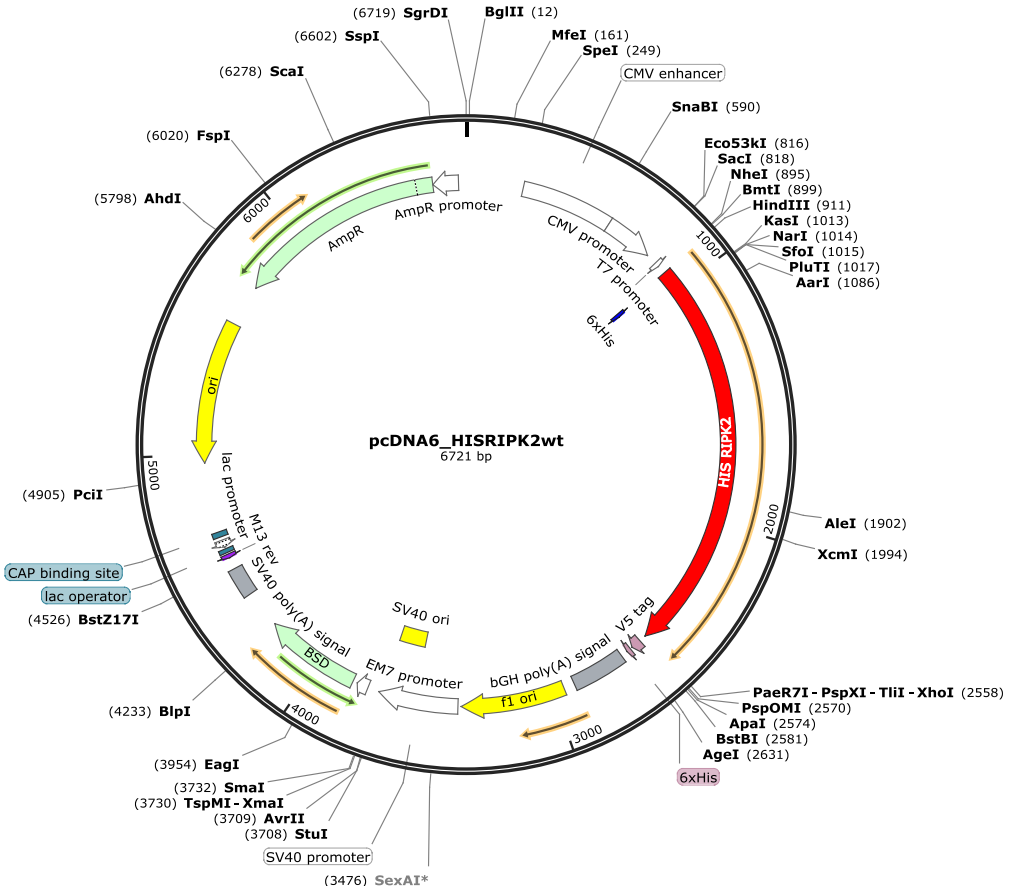

Figure 9.3 Schematic representation of pcDNA6_HIS*RIPK2*wt

Open reading frame encoding *RIPK2* and HIS-tag is indicated in red. HIS-tag is shown in blue.

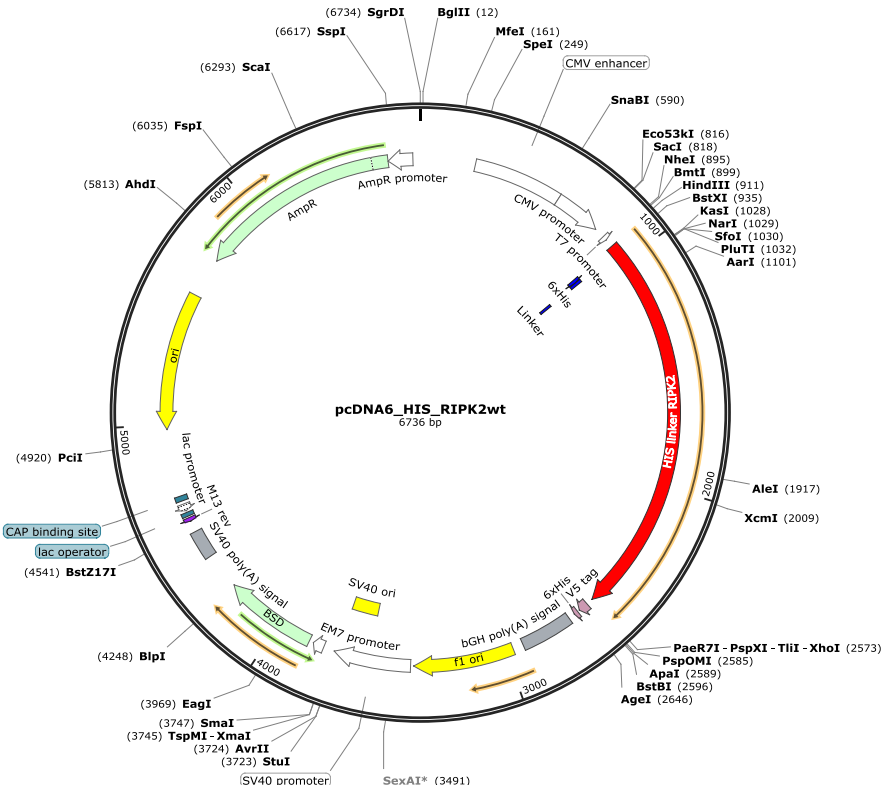

Figure 9.4 Schematic representation of pcDNA6_HIS_*RIPK2*wt

Open reading frame encoding *RIPK2* and HIS-tag is indicated in red. HIS-tag and a 15bp linker connecting the HIS-tag and the *RIPK2* coding sequence are shown in blue.

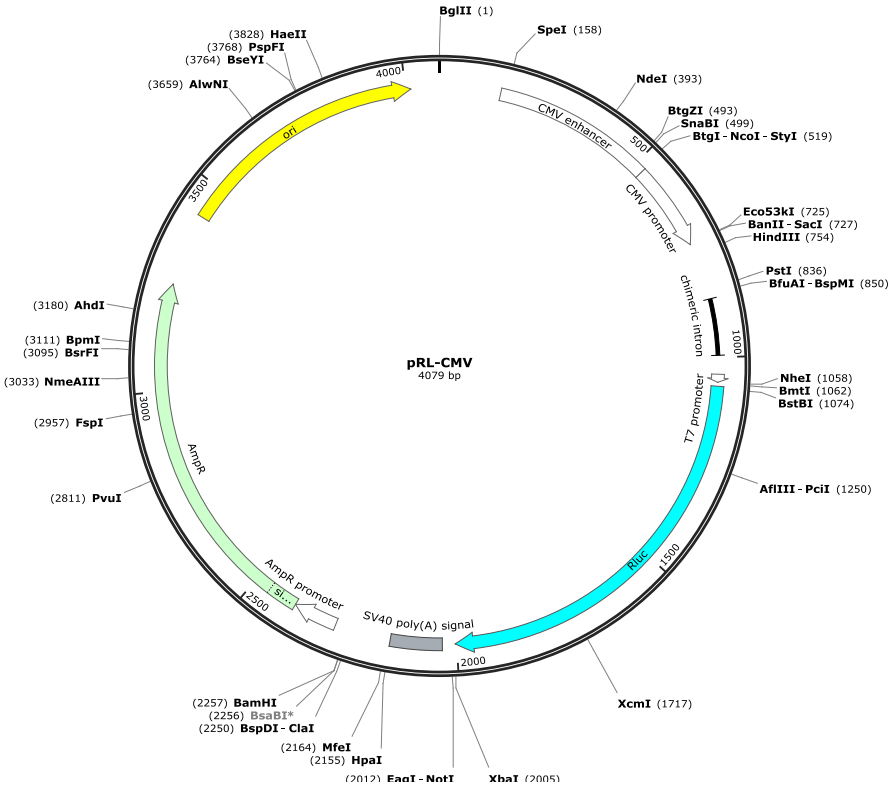

Figure 9.5 Schematic representation of pRL-CMV

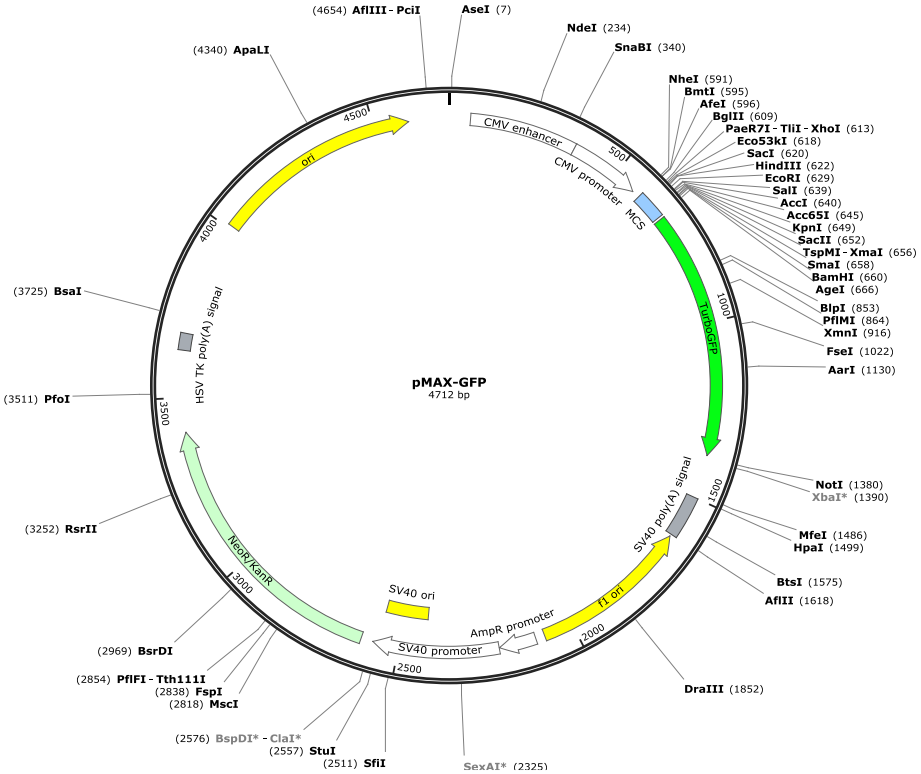

Figure 9.6 Schematic representation of pMAX-GFP

9.2 Plasmid inserts

pcDNA6B_*RIPK2*wt _V5/HIS

The bases altered in the *RIPK2* variants rs2230801 and rs35004667 are indicated in yellow.

>SEQUENCE_*RIPK2*

ATGAACGGGGAGGCCATCTGCAGCGCCCTGCCCACCATTCCCTACCACAAACTCGCC
GACCTGCGCTACCTGAGCCGCGGCGCCTCTGGCACTGTGTCGTCCGCCCGCCACGCA
GACTGGCGCGTCCAGGTGGCCGTGAAGCACCTGCACATCCACACTCCGCTGCTCGAC
AGTGAAAGAAAGGATGTCTTAAGAGAAGCTGAAATTTTACACAAAGCTAGATTTAGTTAC
ATTCTTCCAATTTTGGGAATTTGCAATGAGCCTGAATTTTTGGGAATAGTTACTGAATAC
ATGCCAAATGGATCATTAAATGAACTCCTACATAGGAAAACTGAATATCCTGATGTTGCT
TGGCCATTGAGATTTCGCATCCTGCATGAAATTGCCCTTGGTGTAAATTACCTGCACAA
TATGACTCCTCCTTTACTTCATCATGACTTGAAGACTCAGAATATCTTATTGGACAATGA
ATTTCATGTTAAGATTGCAGATTTTGGTTTATCAAAGTGGCGCATGATGTCCCTCTCACA
GTCACGAAGTAGCAAATCTGCACCAGAAGGAGGGACAATTATCTATATGCCACCTGAAA
ACTATGAACCTGGACAAAAATCAAGGGCCAGTATCAAGCACGATATATATAGCTATGCA
GTTATCACATGGGAAGTGTTATCCAGAAAACAGCCTTTTGAAGATGTCACCAATCCTTT
GCAGATAATGTATAGTGTGTCACAAGGACATCGACCTGTTATTAATGAAGAAAGTTTGC
CATATGATATACCTCACCGAGCACGTATGATCTCTCTAATAGAAAGTGGATGGGCACAA
AATCCAGATGAAAGACCATCTTTCTTAAAATGTTTAATAGAACTTGAACCAGTTTTGAGA
ACATTTGAAGAGATAACTTTTCTTGAAGCTGTTATTCAGCTAAAGAAAACAAAGTTACAG
AGTGTTTCAAGTGCCATTCACCTATGTGACAAGAAGAAAATGGAATTATCTCTGAACATA
CCTGTAAATCATGGTCCACAAGAGGAATCATGTGGATCCTCTCAGCTCCATGAAAATAG
TGGTTCTCCTGAAACTTCAAGGTCCCTGCCAGCTCCTCAAGACAATGATTTTTTATCTAG
AAAAGCTCAAGACTGTTATTTTATGAAGCTGCATCACTGTCCTGGAAATCACAGTTGGG
ATAGCACCATTTCTGGATCTCAAAGGGCTGCATTCTGTGATCACAAGACCACTCCATGC
TCTTCAGCAATAATAAATCCACTCTCAACTGCAGGAAACTCAGAACGTCTGCAGCCTGG
TATAGCCCAGCAGTGGATCCAGAGCAAAAGGGAAGACATTGTGAACCAAATGACAGAA
GCCTGCCTTAACCAGTCGCTAGATGCCCTTCTGTCCAGGGACTTGATCATGAAAGAGG
ACTATGAACTTGTTAGTACCAAGCCTACAAGGACCTCAAAAGTCAGACAATTACTAGAC
ACTACTGACATCCAAGGAGAAGAATTTGCCAAAGTTATAGTACAAAAATTGAAAGATAAC
AAACAAATGGGTCTTCAGCCTTACCCGGAAATACTTGTGGTTTCTAGATCACCATCTTTA
AATTTACTTCAAAATAAAAGCATG

pcDNA6B_*RIPK2*I259T_V5/HIS

The polymorphism rs2230801 is highlighted in red.

>SEQUENCE_*RIPK2* rs2230801

ATGAACGGGGAGGCCATCTGCAGCGCCCTGCCCACCATTCCCTACCACAAACTCGCC
GACCTGCGCTACCTGAGCCGCGGCGCCTCTGGCACTGTGTCGTCCGCCCGCCACGCA
GACTGGCGCGTCCAGGTGGCCGTGAAGCACCTGCACATCCACACTCCGCTGCTCGAC
AGTGAAAGAAAGGATGTCTTAAGAGAAGCTGAAATTTTACACAAAGCTAGATTTAGTTAC
ATTCTTCCAATTTTGGGAATTTGCAATGAGCCTGAATTTTTGGGAATAGTTACTGAATAC
ATGCCAAATGGATCATTAAATGAACTCCTACATAGGAAAACTGAATATCCTGATGTTGCT
TGGCCATTGAGATTTCGCATCCTGCATGAAATTGCCCTTGGTGTAAATTACCTGCACAA
TATGACTCCTCCTTTACTTCATCATGACTTGAAGACTCAGAATATCTTATTGGACAATGA
ATTTCATGTTAAGATTGCAGATTTTGGTTTATCAAAGTGGCGCATGATGTCCCTCTCACA
GTCACGAAGTAGCAAATCTGCACCAGAAGGAGGGACAATTATCTATATGCCACCTGAAA
ACTATGAACCTGGACAAAAATCAAGGGCCAGTATCAAGCACGATATATATAGCTATGCA
GTTATCACATGGGAAGTGTTATCCAGAAAACAGCCTTTTGAAGATGTCACCAATCCTTT
GCAGATAATGTATAGTGTGTCACAAGGACATCGACCTGTTATTAATGAAGAAAGTTTGC
CATATGATACACCTCACCGAGCACGTATGATCTCTCTAATAGAAAGTGGATGGGCACAA
AATCCAGATGAAAGACCATCTTTCTTAAAATGTTTAATAGAACTTGAACCAGTTTTGAGA
ACATTTGAAGAGATAACTTTTCTTGAAGCTGTTATTCAGCTAAAGAAAACAAAGTTACAG
AGTGTTTCAAGTGCCATTCACCTATGTGACAAGAAGAAAATGGAATTATCTCTGAACATA
CCTGTAAATCATGGTCCACAAGAGGAATCATGTGGATCCTCTCAGCTCCATGAAAATAG
TGGTTCTCCTGAAACTTCAAGGTCCCTGCCAGCTCCTCAAGACAATGATTTTTTATCTAG
AAAAGCTCAAGACTGTTATTTTATGAAGCTGCATCACTGTCCTGGAAATCACAGTTGGG
ATAGCACCATTTCTGGATCTCAAAGGGCTGCATTCTGTGATCACAAGACCACTCCATGC
TCTTCAGCAATAATAAATCCACTCTCAACTGCAGGAAACTCAGAACGTCTGCAGCCTGG
TATAGCCCAGCAGTGGATCCAGAGCAAAAGGGAAGACATTGTGAACCAAATGACAGAA
GCCTGCCTTAACCAGTCGCTAGATGCCCTTCTGTCCAGGGACTTGATCATGAAAGAGG
ACTATGAACTTGTTAGTACCAAGCCTACAAGGACCTCAAAAGTCAGACAATTACTAGAC
ACTACTGACATCCAAGGAGAAGAATTTGCCAAAGTTATAGTACAAAAATTGAAAGATAAC
AAACAAATGGGTCTTCAGCCTTACCCGGAAATACTTGTGGTTTCTAGATCACCATCTTTA
AATTTACTTCAAAATAAAAGCATG

pcDNA6B_*RIPK2*L268V_V5/HIS

The polymorphism rs35004667 is highlighted in red.

>SEQUENCE_*RIPK2* rs35004667

ATGAACGGGGAGGCCATCTGCAGCGCCCTGCCCACCATTCCCTACCACAAACTCGCC
GACCTGCGCTACCTGAGCCGCGGCGCCTCTGGCACTGTGTCGTCCGCCCGCCACGCA
GACTGGCGCGTCCAGGTGGCCGTGAAGCACCTGCACATCCACACTCCGCTGCTCGAC
AGTGAAAGAAAGGATGTCTTAAGAGAAGCTGAAATTTTACACAAAGCTAGATTTAGTTAC
ATTCTTCCAATTTTGGGAATTTGCAATGAGCCTGAATTTTTGGGAATAGTTACTGAATAC
ATGCCAAATGGATCATTAAATGAACTCCTACATAGGAAAACTGAATATCCTGATGTTGCT
TGGCCATTGAGATTTCGCATCCTGCATGAAATTGCCCTTGGTGTAAATTACCTGCACAA
TATGACTCCTCCTTTACTTCATCATGACTTGAAGACTCAGAATATCTTATTGGACAATGA
ATTTCATGTTAAGATTGCAGATTTTGGTTTATCAAAGTGGCGCATGATGTCCCTCTCACA
GTCACGAAGTAGCAAATCTGCACCAGAAGGAGGGACAATTATCTATATGCCACCTGAAA
ACTATGAACCTGGACAAAAATCAAGGGCCAGTATCAAGCACGATATATATAGCTATGCA
GTTATCACATGGGAAGTGTTATCCAGAAAACAGCCTTTTGAAGATGTCACCAATCCTTT
GCAGATAATGTATAGTGTGTCACAAGGACATCGACCTGTTATTAATGAAGAAAGTTTGC
CATATGATATACCTCACCGAGCACGTATGATCTCTGTAATAGAAAGTGGATGGGCACAA
AATCCAGATGAAAGACCATCTTTCTTAAAATGTTTAATAGAACTTGAACCAGTTTTGAGA
ACATTTGAAGAGATAACTTTTCTTGAAGCTGTTATTCAGCTAAAGAAAACAAAGTTACAG
AGTGTTTCAAGTGCCATTCACCTATGTGACAAGAAGAAAATGGAATTATCTCTGAACATA
CCTGTAAATCATGGTCCACAAGAGGAATCATGTGGATCCTCTCAGCTCCATGAAAATAG
TGGTTCTCCTGAAACTTCAAGGTCCCTGCCAGCTCCTCAAGACAATGATTTTTTATCTAG
AAAAGCTCAAGACTGTTATTTTATGAAGCTGCATCACTGTCCTGGAAATCACAGTTGGG
ATAGCACCATTTCTGGATCTCAAAGGGCTGCATTCTGTGATCACAAGACCACTCCATGC
TCTTCAGCAATAATAAATCCACTCTCAACTGCAGGAAACTCAGAACGTCTGCAGCCTGG
TATAGCCCAGCAGTGGATCCAGAGCAAAAGGGAAGACATTGTGAACCAAATGACAGAA
GCCTGCCTTAACCAGTCGCTAGATGCCCTTCTGTCCAGGGACTTGATCATGAAAGAGG
ACTATGAACTTGTTAGTACCAAGCCTACAAGGACCTCAAAAGTCAGACAATTACTAGAC
ACTACTGACATCCAAGGAGAAGAATTTGCCAAAGTTATAGTACAAAAATTGAAAGATAAC
AAACAAATGGGTCTTCAGCCTTACCCGGAAATACTTGTGGTTTCTAGATCACCATCTTTA
AATTTACTTCAAAATAAAAGCATG

pcDNA6B_HIS*RIPK2*wt_V5/HIS

The bases altered in the *RIPK2* polymorphisms rs2230801 and rs235004667 are highlighted in yellow, the HIS-tag is highlighted in blue.

>SEQUENCE_HIS*RIPK2*

ATGCATCATCACCATCACCATAACGGGGAGGCCATCTGCAAACGGGGAGGCCATCTGC
AGCGCCCTGCCCACCATTCCCTACCACAAACTCGCCGACCTGCGCTACCTGAGCCGC
GGCGCCTCTGGCACTGTGTCGTCCGCCCGCCACGCAGACTGGCGCGTCCAGGTGGC
CGTGAAGCACCTGCACATCCACACTCCGCTGCTCGACAGTGAAAGAAAGGATGTCTTA
AGAGAAGCTGAAATTTTACACAAAGCTAGATTTAGTTACATTCTTCCAATTTTGGGAATT
TGCAATGAGCCTGAATTTTTGGGAATAGTTACTGAATACATGCCAAATGGATCATTAAAT
GAACTCCTACATAGGAAAACTGAATATCCTGATGTTGCTTGGCCATTGAGATTTCGCAT
CCTGCATGAAATTGCCCTTGGTGTAAATTACCTGCACAATATGACTCCTCCTTTACTTCA
TCATGACTTGAAGACTCAGAATATCTTATTGGACAATGAATTTCATGTTAAGATTGCAGA
TTTTGGTTTATCAAAGTGGCGCATGATGTCCCTCTCACAGTCACGAAGTAGCAAATCTG
CACCAGAAGGAGGGACAATTATCTATATGCCACCTGAAAACTATGAACCTGGACAAAAA
TCAAGGGCCAGTATCAAGCACGATATATATAGCTATGCAGTTATCACATGGGAAGTGTT
ATCCAGAAAACAGCCTTTTGAAGATGTCACCAATCCTTTGCAGATAATGTATAGTGTGTC
ACAAGGACATCGACCTGTTATTAATGAAGAAAGTTTGCCATATGATATACCTCACCGAG
CACGTATGATCTCTCTAATAGAAAGTGGATGGGCACAAAATCCAGATGAAAGACCATCT
TTCTTAAAATGTTTAATAGAACTTGAACCAGTTTTGAGAACATTTGAAGAGATAACTTTTC
TTGAAGCTGTTATTCAGCTAAAGAAAACAAAGTTACAGAGTGTTTCAAGTGCCATTCACC
TATGTGACAAGAAGAAAATGGAATTATCTCTGAACATACCTGTAAATCATGGTCCACAAG
AGGAATCATGTGGATCCTCTCAGCTCCATGAAAATAGTGGTTCTCCTGAAACTTCAAGG
TCCCTGCCAGCTCCTCAAGACAATGATTTTTTATCTAGAAAAGCTCAAGACTGTTATTTT
ATGAAGCTGCATCACTGTCCTGGAAATCACAGTTGGGATAGCACCATTTCTGGATCTCA
AAGGGCTGCATTCTGTGATCACAAGACCACTCCATGCTCTTCAGCAATAATAAATCCAC
TCTCAACTGCAGGAAACTCAGAACGTCTGCAGCCTGGTATAGCCCAGCAGTGGATCCA
GAGCAAAAGGGAAGACATTGTGAACCAAATGACAGAAGCCTGCCTTAACCAGTCGCTA
GATGCCCTTCTGTCCAGGGACTTGATCATGAAAGAGGACTATGAACTTGTTAGTACCAA
GCCTACAAGGACCTCAAAAGTCAGACAATTACTAGACACTACTGACATCCAAGGAGAAG
AATTTGCCAAAGTTATAGTACAAAAATTGAAAGATAACAAACAAATGGGTCTTCAGCCTT
ACCCGGAAATACTTGTGGTTTCTAGATCACCATCTTTAAATTTACTTCAAAATAAAAGCA
TGTAA

pcDNA6B_*RIPK2*I259T_V5/HIS

The polymorphism rs2230801 is highlighted in red; the HIS-tag is highlighted in blue.

>SEQUENCE_HIS*RIPK2* rs2230801

ATGCATCATCACCATCACCATAACGGGGAGGCCATCTGCAAACGGGGAGGCCATCTGC
AGCGCCCTGCCCACCATTCCCTACCACAAACTCGCCGACCTGCGCTACCTGAGCCGC
GGCGCCTCTGGCACTGTGTCGTCCGCCCGCCACGCAGACTGGCGCGTCCAGGTGGC
CGTGAAGCACCTGCACATCCACACTCCGCTGCTCGACAGTGAAAGAAAGGATGTCTTA
AGAGAAGCTGAAATTTTACACAAAGCTAGATTTAGTTACATTCTTCCAATTTTGGGAATT
TGCAATGAGCCTGAATTTTTGGGAATAGTTACTGAATACATGCCAAATGGATCATTAAAT
GAACTCCTACATAGGAAAACTGAATATCCTGATGTTGCTTGGCCATTGAGATTTCGCAT
CCTGCATGAAATTGCCCTTGGTGTAAATTACCTGCACAATATGACTCCTCCTTTACTTCA
TCATGACTTGAAGACTCAGAATATCTTATTGGACAATGAATTTCATGTTAAGATTGCAGA
TTTTGGTTTATCAAAGTGGCGCATGATGTCCCTCTCACAGTCACGAAGTAGCAAATCTG
CACCAGAAGGAGGGACAATTATCTATATGCCACCTGAAAACTATGAACCTGGACAAAAA
TCAAGGGCCAGTATCAAGCACGATATATATAGCTATGCAGTTATCACATGGGAAGTGTT
ATCCAGAAAACAGCCTTTTGAAGATGTCACCAATCCTTTGCAGATAATGTATAGTGTGTC
ACAAGGACATCGACCTGTTATTAATGAAGAAAGTTTGCCATATGATACACCTCACCGAG
CACGTATGATCTCTCTAATAGAAAGTGGATGGGCACAAAATCCAGATGAAAGACCATCT
TTCTTAAAATGTTTAATAGAACTTGAACCAGTTTTGAGAACATTTGAAGAGATAACTTTTC
TTGAAGCTGTTATTCAGCTAAAGAAAACAAAGTTACAGAGTGTTTCAAGTGCCATTCACC
TATGTGACAAGAAGAAAATGGAATTATCTCTGAACATACCTGTAAATCATGGTCCACAAG
AGGAATCATGTGGATCCTCTCAGCTCCATGAAAATAGTGGTTCTCCTGAAACTTCAAGG
TCCCTGCCAGCTCCTCAAGACAATGATTTTTTATCTAGAAAAGCTCAAGACTGTTATTTT
ATGAAGCTGCATCACTGTCCTGGAAATCACAGTTGGGATAGCACCATTTCTGGATCTCA
AAGGGCTGCATTCTGTGATCACAAGACCACTCCATGCTCTTCAGCAATAATAAATCCAC
TCTCAACTGCAGGAAACTCAGAACGTCTGCAGCCTGGTATAGCCCAGCAGTGGATCCA
GAGCAAAAGGGAAGACATTGTGAACCAAATGACAGAAGCCTGCCTTAACCAGTCGCTA
GATGCCCTTCTGTCCAGGGACTTGATCATGAAAGAGGACTATGAACTTGTTAGTACCAA
GCCTACAAGGACCTCAAAAGTCAGACAATTACTAGACACTACTGACATCCAAGGAGAAG
AATTTGCCAAAGTTATAGTACAAAAATTGAAAGATAACAAACAAATGGGTCTTCAGCCTT
ACCCGGAAATACTTGTGGTTTCTAGATCACCATCTTTAAATTTACTTCAAAATAAAAGCA
TGTAA

pcDNA6B_*RIPK2*L268V_V5/HIS

The polymorphism rs35004667 is highlighted in red; the HIS-tag is highlighted in blue.

>SEQUENCE_HIS*RIPK2* rs35004667

ATGCATCATCACCATCACCATAACGGGGAGGCCATCTGCAAACGGGGAGGCCATCTGC
AGCGCCCTGCCCACCATTCCCTACCACAAACTCGCCGACCTGCGCTACCTGAGCCGC
GGCGCCTCTGGCACTGTGTCGTCCGCCCGCCACGCAGACTGGCGCGTCCAGGTGGC
CGTGAAGCACCTGCACATCCACACTCCGCTGCTCGACAGTGAAAGAAAGGATGTCTTA
AGAGAAGCTGAAATTTTACACAAAGCTAGATTTAGTTACATTCTTCCAATTTTGGGAATT
TGCAATGAGCCTGAATTTTTGGGAATAGTTACTGAATACATGCCAAATGGATCATTAAAT
GAACTCCTACATAGGAAAACTGAATATCCTGATGTTGCTTGGCCATTGAGATTTCGCAT
CCTGCATGAAATTGCCCTTGGTGTAAATTACCTGCACAATATGACTCCTCCTTTACTTCA
TCATGACTTGAAGACTCAGAATATCTTATTGGACAATGAATTTCATGTTAAGATTGCAGA
TTTTGGTTTATCAAAGTGGCGCATGATGTCCCTCTCACAGTCACGAAGTAGCAAATCTG
CACCAGAAGGAGGGACAATTATCTATATGCCACCTGAAAACTATGAACCTGGACAAAAA
TCAAGGGCCAGTATCAAGCACGATATATATAGCTATGCAGTTATCACATGGGAAGTGTT
ATCCAGAAAACAGCCTTTTGAAGATGTCACCAATCCTTTGCAGATAATGTATAGTGTGTC
ACAAGGACATCGACCTGTTATTAATGAAGAAAGTTTGCCATATGATATACCTCACCGAG
CACGTATGATCTCTGTAATAGAAAGTGGATGGGCACAAAATCCAGATGAAAGACCATCT
TTCTTAAAATGTTTAATAGAACTTGAACCAGTTTTGAGAACATTTGAAGAGATAACTTTTC
TTGAAGCTGTTATTCAGCTAAAGAAAACAAAGTTACAGAGTGTTTCAAGTGCCATTCACC
TATGTGACAAGAAGAAAATGGAATTATCTCTGAACATACCTGTAAATCATGGTCCACAAG
AGGAATCATGTGGATCCTCTCAGCTCCATGAAAATAGTGGTTCTCCTGAAACTTCAAGG
TCCCTGCCAGCTCCTCAAGACAATGATTTTTTATCTAGAAAAGCTCAAGACTGTTATTTT
ATGAAGCTGCATCACTGTCCTGGAAATCACAGTTGGGATAGCACCATTTCTGGATCTCA
AAGGGCTGCATTCTGTGATCACAAGACCACTCCATGCTCTTCAGCAATAATAAATCCAC
TCTCAACTGCAGGAAACTCAGAACGTCTGCAGCCTGGTATAGCCCAGCAGTGGATCCA
GAGCAAAAGGGAAGACATTGTGAACCAAATGACAGAAGCCTGCCTTAACCAGTCGCTA
GATGCCCTTCTGTCCAGGGACTTGATCATGAAAGAGGACTATGAACTTGTTAGTACCAA
GCCTACAAGGACCTCAAAAGTCAGACAATTACTAGACACTACTGACATCCAAGGAGAAG
AATTTGCCAAAGTTATAGTACAAAAATTGAAAGATAACAAACAAATGGGTCTTCAGCCTT
ACCCGGAAATACTTGTGGTTTCTAGATCACCATCTTTAAATTTACTTCAAAATAAAAGCA
TGTAA

9.2. Polymorphisms identified in *RIPK2, LY96* and *NFKB2*

SNP/ indel id	Number of isolates identified with SNP (Homozygous /heterozygous)	Chromosome: Base pair[1]	Location	Frequency	SNP	Substitution	Transcript position	Codon/ Amino acid	CDS position	Comment
rs5893110	30 (24/6)	8: 89757568 - 89757569	5'UTR	-	-/ GCGCCT CTG	Upstream gene variant	-	-	-	Predicted promoter region
rs201500893	2 (0/2)	8:89757784	Exon 1	-	G/C	5' UTR variant	38	-	-	Predicted promoter region
rs115517126	13 (0/13)	8:89757804	Exon 1	0.02 (T)	A/T	5' UTR variant	58	-	-	Predicted promoter region
rs140020615	1 (0/1)	8:89757914	Exon 1	0.01 (T)	C/T	5' UTR variant	168	-	-	Predicted promoter region
rs2293809	5 (1/4)	8:89758087	Exon 1	0.09 (T)	C/T	Synonymous variant	351	GCC/GCT A9	27	Predicted promoter region
rs39499	30 (8/22)	8:89758381	Intron 1-2	0.44 (A)	A/G	Intron variant	-	-	-	Predicted promoter region
rs431264	30 (8/22)	8:89765282	Intron 2-3	0.43 (G)	G/A	Intron variant	-	-	-	Predicted promoter flanking region

Table 9.1 Polymorphisms identified in *RIPK2*[a]

[a]Based on Esembl release 78; [b]SIFT score: Substitution predicted to be damaging to protein function (<= 0.05), substitution predicted to be tolerated (>0.05); [c]Polyphen score: Probability that substitution is damaging – the closer the value is to 1 the higher the probability that the substitution is deleteriou

SNP/ indel id	Number of isolates identified with SNP (Homozygous [illegible])	Chromosome: Base pair[1]	Location	Frequency	SNP	Substitution	Transcript position	Codon/ Amino acid	CDS position	Comment
rs78006650	3 (1/2)	8:89765510	Intron 3-4	0.01 (A)	T/A	Intron variant	-	-	-	-
rs16900484	16 (0/16)	8:89769704	Intron 3-4	0.08 (C)	A/C	Intron variant	-	-	-	-
rs40377	30 (9/21)	8:89769725	Intron 3-4	0.43 (C)	C /T	Intron variant	-	-	-	-
rs56257721	2 (0/2)	8:89769900	Exon 4	0.01 (T)	A/T	Synonymous variant	926	TCA/TCT S204	612	-
rs28565967	16 (5/11)	8:89769998	Intron 4-5	0.19 (A)	G/A	Intron variant	-	-	-	-
rs74306229	5 (1/4)	8:89770129	Intron 4-5	0.09 (G)	C/G	Intron variant	-	-	-	-
rs28657795	15 (4/11)	8:89770154	Intron 4-5	0.19 (C)	T/C	Intron variant	-	-	-	-

Table 9.1 Polymorphisms identified in *RIPK2* continued[a]

[a]Based on Esembl release 78; [b]SIFT score: Substitution predicted to be damaging to protein function (<= 0.05), substitution predicted to be tolerated (>0.05); [c]Polyphen score: Probability that substitution is damaging – the closer the value is to 1 the higher the probability that the substitution is deleteriou

SNP/ indel id	Number of isolates identified with SNP (Homozygous /heterozygous)	Chromosome: Base pair[1]	Location	Frequency	SNP	Substitution	Transcript position	Codon/ Amino acid	CDS position	Comment
rs141513755	3 (1/2)	8:89771955	Intron 5-6	<0.01 (G)	C/G	Intron variant	-	-	-	-
rs2230801	7 (0/7)	8:89772751	Exon 6	0.08 (C)	T/C	Non-synonymous variant	1090	ATA/ACA I259T	776	SIFT Score[b]: 0.09 PolyPhen Score[c]: 0.654
rs35004667	2 (0/2)	8:89772777	Exon 6	<0.01 (G)	C/G	Non-synonymous variant	1116	CTA/GTA L268V	802	SIFT Score[b]: 0 PolyPhen Score[c]: 0.999
rs113551662	1 (1/0)	8:89779777	Intron 6-7	0.02 (C)	A/C	Intron variant	-	-	-	-
rs56017098	15 (4/11)	8:89779803	Intron 6-7	0.19 (A)	G/A	Intron variant	-	-	-	-
rs39505	30 (24/6)	8:89779838	Intron 6-7	0.358 (A)	C/A	Intron variant	-	-	-	-

Table 9.1 Polymorphisms identified in *RIPK2* continued[a]

[a]Based on Esembl release 78; [b]SIFT score: Substitution predicted to be damaging to protein function (<= 0.05), substitution predicted to be tolerated (>0.05); [c]Polyphen score: Probability that substitution is damaging – the closer the value is to 1 the higher the probability that the substitution is deleterious.

SNP/ indel id	Number of isolates identified with SNP (Homozygous [illegible])	Chromosome: Base pair[1]	Location	Frequency	SNP	Substitution	Transcript position	Codon/ Amino acid	CDS position	Comment
rs39506	30 (24/6)	8:89779899	Intron 6-7	0.358 (A)	C/A	Intron variant	-	-	-	-
rs55945927	17 (1/16)	8:89779939	Intron 6-7	0.08 (C)	T/C	Intron variant	-	-	-	-
rs73694485	17 (1/16)	8:89780374	Intron 7-8	0.08 (C)	T/C	Intron variant	-	-	-	-
rs73694486	17 (1/16)	8:89780385	Intron 7-8	0.08 (G)	T/G	Intron variant	-	-	-	-
rs115148476	1 (0/1)	8:89783770	Intron 7-8	<0.01 (C)	T/C	Intron variant	-	-	-	-
rs55881928	16 (1/15)	8:89783976	Intron 7-8	0.08 (G)	A/G	Intron variant	-	-	-	-
rs55697113	16 (1/15)	8:89783980	Intron 7-8	0.08 (C)	T/C	Intron variant	-	-	-	-

Table 9.1 Polymorphisms identified in *RIPK2* continued[a]

[a]Based on Esembl release 78; [b]SIFT score: Substitution predicted to be damaging to protein function (<= 0.05), substitution predicted to be tolerated (>0.05); [c]Polyphen score: Probability that substitution is damaging – the closer the value is to 1 the higher the probability that the substitution is deleterious.

SNP/ indel id	Number of isolates identified with SNP (Homozygous [illegible])	Chromosome: Base pair[1]	Location	Frequency	SNP	Substitution	Transcript position	Codon/ Amino acid	CDS position	Comment
rs199850869	1 (0/1)	8:89784119	Exon 8	-	G/A	Non-synonymous variant	1323	GTA/ATA V337I	1009	SIFT Score[b]: 0.39 PolyPhen Scorec: 0.003
rs11995005	2 (0/2)	8:89786771	Intron 9-10	0.09 (G)	A/G	Intron variant	-	-	-	-
rs61258433	9 (0/9)	8:89786892	Intron 9-10	0.08 (A)	G/A	Intron variant	-	-	-	-
rs80091185	2 (0/2)	8:89786908	Intron 9-10	0.09 (C)	A/C	Intron variant	-	-	-	-
rs74786374	2 (0/2)	8:89789708	Intron 10-11	0.01 (G)	A/G	Intron variant	-	-	-	Predicted promoter flanking region
rs40247	30 (24/6)	8:89789744	Intron 10-11	0.37 (A)	A/C	Intron variant	-	-	-	Predicted promoter flanking region
rs40453	28 (23/5)	8:89789817	Intron 10-11	0.37 (A)	A/G	Intron variant	-	-	-	Predicted promoter flanking region

Table 9.1 Polymorphisms identified in *RIPK2* continued[a]

[a]Based on Esembl release 78; [2]SIFT score: Substitution predicted to be damaging to protein function (<= 0.05), substitution predicted to be tolerated (>0.05); [3]Polyphen score: Probability that substitution is damaging – the closer the value is to 1 the higher the probability that the substitution is deleterious.

SNP/ indel id	Number of isolates identified with SNP (Homozygous	Chromosome: Base pair[1]	Location	Frequency	SNP	Substitution	Transcript position	Codon/ Amino acid	CDS position	Comment
rs16900617	16 (0/16)	8:89790263	Exon 11	0.08 (G)	A/G	Synonymous variant	1784	TTA/TTG L490	1470	Predicted promoter flanking region
rs16900627	16 (5/11)	8:89790767	Exon 11	0.17 (G)	A/G	3'UTR variant	2288	-	-	Predicted promoter flanking region
rs59258471	16 (0/16)	8:89790942-89790946	3'UTR	-	AACAA/-	3'UTR variant	2463-2467	-	-	-
rs10504883	16 (0/16)	8:89791184	3'UTR	0.08 (T)	G/T	Downstream gene variant	-	-	-	-

Table 9.1 Polymorphisms identified in *RIPK2* continued[a]

[a]Based on Esembl release 78; [b]SIFT score: Substitution predicted to be damaging to protein function (<= 0.05), substitution predicted to be tolerated (>0.05); [c]Polyphen score: Probability that substitution is damaging – the closer the value is to 1 the higher the probability that the substitution is deleterious.

SNP/ indel id	Number of isolates identified with SNP (Homozygous /heterozygous)	Chromosome: Base pair[1]	Location	Frequency	SNP	Substitution	Transcript position	Codon/ Amino acid	CDS position	Comment
rs11466001	7(0/7)	8:74004993	Intron 2-3	0.22 (G)	A/G	Intron variant	-	-	-	-
rs11466002	4(0/4)	8:74010200	Intron 3-4	0.02 (G)	A/G	Intron variant	-	-	-	-
rs183250931	1(0/1)	8:74027024	Intron 4-5	<0.01 (C)	G/C	Intron variant	-	-	-	-
rs2891354	24 (9/15)	8:74028771	Intron 4-5	0.29 (C)	T/C	Intron variant	-	-	-	-
rs11466003	2 (0/2)	8:74028948	Intron 4-5	0.03 (T)	C/T	Intron variant Splice region variant	-	-	-	-
rs10282832	11 (4/9)	8:74029071	Exon 5	0.48 (C)	A/C	3'UTR variant	427/591	-	-	-

Table 9.2 Polymorphisms identified in *LY96*[a]

[a]Based on Esembl release 78

SNP/ indel id	Number of isolates identified with SNP (Homozygous /heterozygous)	Chromosome: Base pair[1]	Location	Frequency	SNP	Substitution	Transcript position	Codon/ Amino acid	CDS position	Comment
-	1 (0/1)	10:102395596	5'UTR	-	Upstream gene variant, Intron variant	G/A	-	-	-	Predicted promoter region
rs45502493	1 (0/1)	10:102395673	5'UTR	-	Upstream gene variant, Intron variant	T/C	-	-	-	Predicted promoter region
-	2 (0/2)	10:102395843	Intron 1-2	-	Upstream gene variant, Intron variant	A/C	-	-	-	Predicted promoter region
rs45526132	1 (0/1)	10:102396210	Intron 2-3	<0.01 (C)	Intron variant	G/C	-	-	-	Predicted promoter region
rs11574845	14 (2/12)	10:102396626	Intron 4-5	0.080 (G)	Intron variant, Downstream gene variant	T/G	-	-	-	-
rs138364110	3	10:102396633 - 102396634	Intron 4-5	0.27 (T)	Intron variant, Downstream gene variant	-/T	-	-	-	-
rs116607432	1 (1/0)	10:102397500	Intron 7-8	0.01 (C)	Intron variant, Downstream gene variant	G/C	-	-	-	-

Table 9.3 Polymorphisms identified in *NFKB2*[a]

[a]Based on Esembl release 78

SNP/ indel id	Number of isolates identified with SNP (Homozygous /heterozygous)	Chromosome: Base pair[1]	Location	Frequency	SNP	Substitution	Transcript position	Codon/ Amino acid	CDS position	Comment
rs7897947	17 (4/13)	10:102397954	Intron 8-9	0.28 (G)	Intron variant, Downstream gene variant	T/G	-	-	-	-
rs4919632	11 (0/11)	10:102397970	Intron 8-9	0.05 (C)	Intron variant, Downstream gene variant	T/C	-	-	-	-
rs3740418	4 (3/1)	10:102399176	Intron 12-13	0.26 (G)	Intron variant, 3'UTR variant, Downstream gene variant	C/G	1589	-	-	Predicted promoter flanking region
rs60282371	5 (0/5)	10:102399233 - 102399234	Intron 12-13	-	Intron variant, Downstream gene variant	-/A	-	-	-	Predicted promoter flanking region
rs137919911	6 (1/5)	10:102399237	Intron 12-13	0.05 (-)	Intron variant, Downstream gene variant	G/-	-	-	-	Predicted promoter flanking region

Table 9.3 Polymorphisms identified in *NFKB2*[a] continued

[a]Based on Esembl release 78

SNP/ indel id	Number of isolates identified with SNP (Homozygous /heterozygous)	Chromosome: Base pair[1]	Location	Frequency	SNP	Substitution	Transcript	Codon/ Amino acid	CDS position	Comment
rs4919633	2 (0/2)	10:102399439	Exon 13	0.01 (A)	Synonymous variation	G/A	1519, 1832, 1432	CCG/CCA P423	1269	Predicted CTCF binding site, Predicted promoter flanking region
rs11574849	9 (1/8)	10:102399939	Intron 14-15	0.07 (A)	Intron variant, Downstream gene variant	G/A	-	-	-	Predicted promoter flanking region
-	1 (0/1)	10:102400280	Exon 16	-	Synonymous variant, Downstream gene variant	G/A	1750, 1837, 2150	ACG/ACA T529	1587	-
rs45627832	1 (0/1)	10:102400893	Intron 17-18	0.01 (T)	Intron variant, Downstream gene variant	G/T	-	-	-	-

Table 9.3 Polymorphisms identified in *NFKB2*[a]

[a]Based on Esembl release 78

SNP/ indel id	Number of isolates identified with SNP (Homozygous /heterozygous)	Chromosome: Base pair[1]	Location	Frequency	SNP	Substitution	Transcript position	Codon/ Amino acid	CDS position	Comment
rs41287457	9 (1/8)	10:102401967	Intron 21-22	0.08 (G)	Intron variant, Downstream gene variant	A/G	-	-	-	Predicted promoter flanking region
rs11574853	8 (0/8)	10:102402039	Intron 21-22	0.03 (A)	Intron variant, Downstream gene variant	T/A	-	-	-	Predicted promoter flanking region
rs7077329	6 (0/6)	10:102402210	Intron 22-23	0.27 (T)	Intron variant, Downstream gene variant	C/T	-	-	-	Predicted promoter flanking region
rs41371753	7 (0/7)	10:102402608	3'UTR	0.03 (C)	Downstream gene variant	A/C	-	-	-	-

Table 9.3 Polymorphisms identified in *NFKB2*[a]
[a]Based on Esembl release 78